8306714

Alcocer Alarcon, Carlos Felipe

A LABORATORY STUDY WITH A LIGHT CRUDE OIL TO DETERMINE THE EFFECT OF HIGH-PRESSURE NITROGEN INJECTION ON ENHANCED OIL RECOVERY

The University of Oklahoma PH.D. 1982

University
Microfilms
International 300 N. Zeeb Road, Ann Arbor, MI 48106

PLEASE NOTE:

In all cases this material has been filmed in the best possible way from the available copy. Problems encountered with this document have been identified here with a check mark ✓.

1. Glossy photographs or pages _____
2. Colored illustrations, paper or print _____
3. Photographs with dark background _____
4. Illustrations are poor copy _____
5. Pages with black marks, not original copy ✓
6. Print shows through as there is text on both sides of page _____
7. Indistinct, broken or small print on several pages _____.
8. Print exceeds margin requirements _____
9. Tightly bound copy with print lost in spine _____
10. Computer printout pages with indistinct print ✓
11. Page(s) _____ lacking when material received, and not available from school or author.
12. Page(s) _____ seem to be missing in numbering only as text follows.
13. Two pages numbered _____. Text follows.
14. Curling and wrinkled pages _____
15. Other _____

THE UNIVERSITY OF OKLAHOMA

GRADUATE COLLEGE

A LABORATORY STUDY WITH A LIGHT CRUDE OIL TO DETERMINE THE EFFECT OF HIGH-PRESSURE NITROGEN INJECTION ON ENHANCED OIL RECOVERY

A DISSERTATION

SUBMITTED TO THE GRADUATE FACULTY

in partial fulfillment of the requirements for the

degree of

DOCTOR OF PHILOSOPHY

BY

CARLOS ALCOCER ALARCON

Norman, Oklahoma

1982

A LABORATORY STUDY WITH A LIGHT CRUDE OIL TO

DETERMINE THE EFFECT OF HIGH-PRESSURE

NITROGEN INJECTION ON ENHANCED

OIL RECOVERY

A DISSERTATION

APPROVED FOR THE SCHOOL OF PETROLEUM ENGINEERING

APPROVED BY

D. E. Menzie

DISSERTATION COMMITTEE

ACKNOWLEDGMENTS

The author wishes to thank Dr. Donald Menzie for his invaluable and continuous assistance which made this research possible. Also, the author strongly feels that Dr. Donald Menzie shares any credit that this study may receive as a contribution to Petroleum Engineering.

The author wishes to extend his sincere appreciation to the members of his Doctoral Committee, Doctors R. Knapp, R. Du Bois, F. Townsend and F. Civan.

Special recognition is due to my sponsors FONINVES and INTEVEP for their continued financial assistance and encouragement. This study was financed by Tenneco Oil Co. and the University of Oklahoma.

I would like to express my indebtedness to Subijoy Dutta, G.D. Maddox and N.S. Knight for their time, help and invaluable suggestions during this research.

Finally, I would like to express my appreciation to my wife and my sons who were with me during this extraordinary adventure.

ABSTRACT

Laboratory research was conducted to study displacements of crude oil by high-pressure nitrogen injection. The objectives of this research were to study the effect of temperature and gas-oil ratio in solution on crude oil recovery and miscibility process in high-pressure nitrogen injection; to study nitrogen effectiveness in crude oil recovery after waterflooding and to investigate the effect on oil recovery of nitrogen-driven propane slugs. Nine experimental tests were performed using crude oil of 42.3° API recombined with natural gas. The experimental tests were made using two temperatures (70°F and 120°F) and three gas-oil ratios in solution (575 SCF/STB, 400 SCF/STB and 200 SCF/STB). The reservoir model was a stainless steel tube 125 feet long and 0.435 inches in diameter, packed with sand consolidated to give an average permeability of 930 md. The model was provided with five sampling valves to collect vapor samples. The vapor samples were analyzed by using a chromatograph. A temperature control system was built based on the results obtained from a heat transfer mathematical model specifically prepared for this research. The results obtained in this study suggested very strongly that crude oil recovery and miscibility depend on temperature and gas-oil ratio in solution. A multiple-regression equation to predict crude oil recovery using temperature and gas-oil ratio in solution was developed based on the experimental data. Another multiple-regression equation was developed and presented to predict crude oil recovery using temperature, gas-oil ratio in solution and injection pressure as predictors. High-pressure nitrogen displacement after waterflooding yielded low oil recovery. However, the results suggest that high crude oil recovery may be expected from displacement using nitrogen-driven propane slugs. Recommendations are made for future research projects continuing the studies on secondary recovery by nitrogen-driven propane slugs and on tertiary recovery by high-pressure nitrogen injection after waterflooding.

TABLE OF CONTENTS

LIST OF TABLES

LIST OF FIGURES

Figure		Page

Figure		Page

Figure		Page

Figure		Page

A LABORATORY STUDY WITH A LIGHT CRUDE OIL TO DETERMINE THE EFFECT OF HIGH-PRESSURE NITROGEN INJECTION ON ENHANCED OIL RECOVERY

CHAPTER I

INTRODUCTION

Statement of the Problem

A relatively new process of vaporization gas drive designed to increase ultimate production by the application of high-pressure nitrogen(N_2)injection has been receiving special attention because of the high cost and limited supply of natural gas.

The main goal of injection of N_2 is to achieve miscibility with the reservoir fluid. When miscibility is reached all the capillary forces would disappear and displacement efficiency woudl approach 100% in the swept zone.

The miscibility obtained by nitrogen injection in a light crude oil reservoir is a conditional miscibility, where the fluids are not miscible on first contact but form two phases, with one of the fluids absorbing components from the other. After sufficient contacts and exchange of components,

the system becomes miscible. This N_2-light crude oil miscibility phenomenom is complex and depends on composition of the reservoir fluid, temperature, pressure and also involving other factors such as interphase mass transfer, effect of relative permeability, capillary pressure and gravity. The most important advantages presented by using N_2 instead of natural gas for enhanced oil recovery purposes are: Reliability of supply, control of corrosion in subsurface and surface production equipment, no adverse phase behavior effect, ease of gas processing and clean-up and non-polluting. The most serious disadvantages are the cost of separation of N_2 from air, and that N_2 has to be compressed at high-pressure to be used effectively. However, this is an economical factor that requires evaluation in each particular case.

This research is the continuation of an investigation conducted by Tarek Ahmed (1) (1980). This previous researcher studied the displacement of light crude oil by nitrogen at different injection pressures at room temperature and using a constant gas-oil-ratio in solution into a low permeability-reservoir physical model which consisted of a consolidated sand-packed stainless steel tube 125 feet long and .435 inches in diameter. Sampling points were located at equal intervals along the length of the linear core. These sampling points facilitated the taking of vapor samples for analysis by means of a gas chromatograph. This analysis permits the study of the compositional changes taking place in

the reservoir physical model during displacements.

The primary objectives of the present research are as follows:

a) To physically modify the laboratory equipment used by the previous researcher to control and simulate reservoir temperatures;

b) to investigate the effect of temperature on oil recovery and miscibility in high-pressure injection;

c) to study the effect of gas-oil ratio in solution on oil recovery and the mechanism of displacement of crude oil by nitrogen injection;

d) to study nitrogen effectiveness on oil recovery after waterflooding the reservoir;

e) to investigate the effect on miscibility and oil recovery by nitrogen-driven propane slug; and,

f) to compare results with the previous research to determine reproducibility and validity of the results as well as effectiveness of the laboratory equipment to do this type of research.

Because of the nature of this research, the experimental data obtained is the most important part of this work.

Review of Previous Investigations

Since natural gas has been used as a displacement fluid in miscible and immiscible displacements in enhanced oil recovery techniques throughout the world during many years, there is abundant literature about experimental and field

applications of natural gas. Due to that, the review of all of those researches has been well done by different researchers (11,12,71), consequently, the literature review in the work will only deal with experimental and field applications related to the use of N_2 as a displacement fluid on enhanced oil recovery techniques.

Air injection was the earliest enhanced oil recovery method in the petroleum industry, due to the fact that air was the most abundant and readily available gas in nature. Air injection usually increases production for a short time but soon leads to severe operational problems. Most of the problems with the use of air as a displacement fluid are con-concerned with oxygen content in the air. Because the oxygen is highly reactive it causes problems on the surface and in the reservoir. Some of the major problems are: Spontaneous ignition in the reservoir, corrosion, formation of explosive mixtures, alteration of reservoir oil (64).

By 1928, Power (48) stated that "the relative merits of air and natural gas as propulsive agents in pressure drive operations have been discussed for a number of years." Power (48) (1928) performed a laboratory study to determine whether air is superior to natural gas as a driving medium or vice versa. His laboratory work started at the laboratory of the University of California in January, 1927, and finished in a private laboratory in Tulsa, Oklahoma, in February, 1928. The apparatus used was designed especially for his work. For

historical reasons and comparison purposes, the apparatus is shown in figure 1. The most interesting thing in Power's work was that he used nitrogen in his experiments. From the experimental work performed, it is concluded:

1. that the solubility of natural gas in oil is much greater than that of nitrogen in oil at equal temperatures and pressures; and that the solubility of nitrogen in oil closely approaches that of air in oil, as it is shown in figure 2:
2. that increments of dissolved natural gas lower the absolute viscosity of oil progressively; and that up to a certain critical point increments of dissolved nitrogen in oil lower the absolute viscosity to a minimum, beyond which additional dissolved nitrogen tends to increase the viscosity of the oil.
3. Volume for volume, nitrogen is superior to natural gas as a propulsive agent at all pressures.

In 1958, Koch and Hutchinson (36) conducted a laboratory study on miscible displacement using flue gas. The results of those experiments confirmed that the composition of the displacement gas is relatively unimportant in order to establish the miscibility pressure for a given reservoir fluid. They also reported that above the miscibility pressure the breakthrough recovery is a constant, (see figure 3).

In Table 1 are shown some results obtained by Koch and Hutchinson during their experiments. These results suggested

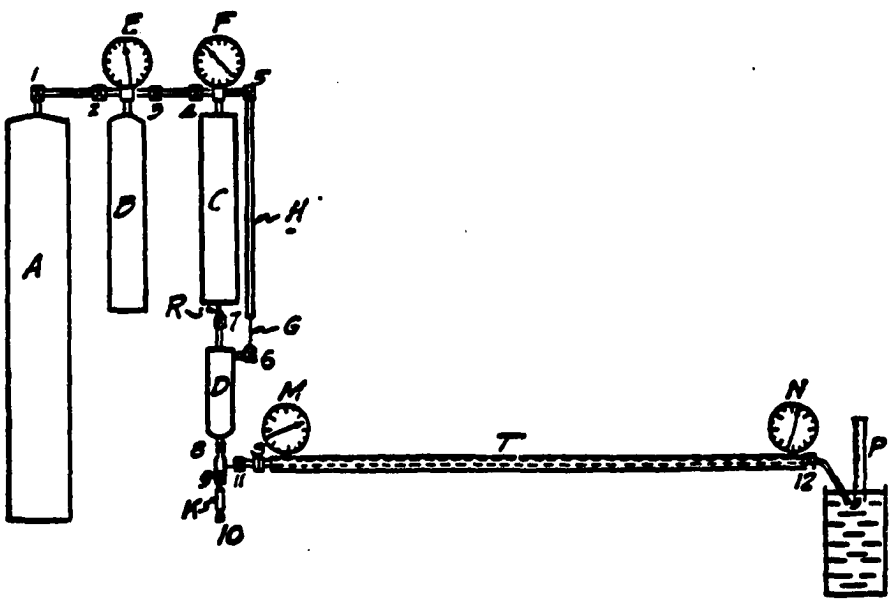

FIG. 1.—APPARATUS USED FOR EXPERIMENTAL WORK WITH DISSOLVED GAS IN OIL

(AFTER POWER (48) 1928)

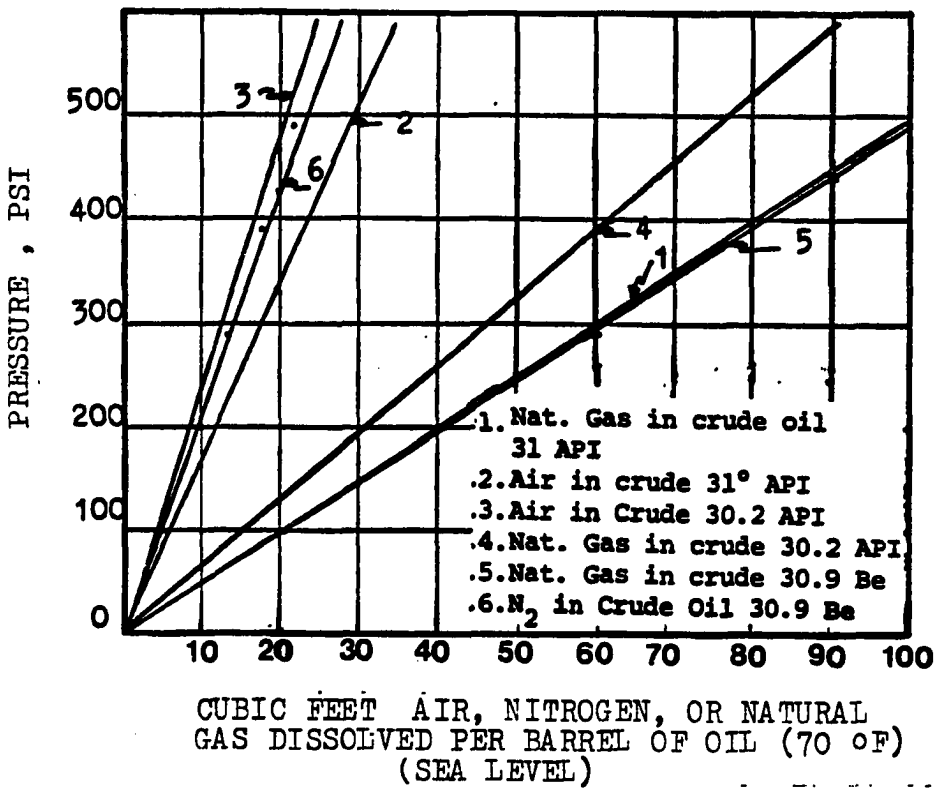

FIGURE 2. SOLUBILITY OF VARIOUS GASES IN CRUDE OIL
(After Power (48) 1928)

TABLE 1

THE EXPERIMENTAL RESULTS AFTER KOCH ET AL (36)
OIL GRAVITY: 40.5° API
TEMPERATURE: 140°F

Run No.	Injection Gas Composition % N_2	Injection Pressure PSI	Stock Tank Oil Recovery % of OIP Initially At Breakthrough
L-44	15	3500	68.0
L-45	15	3600	74.0
L-46	15	3700	80.4
L-42	66	3500	67.3
L-41	66	3700	77.9
L-40	100	2900	49.2
L-38	100	3500	67.2
L-37	100	3800	77.6
L-39	100	4000	80.6
L-32	100	4300	80.6

FIGURE 3

STOCK TANK OIL PRODUCED PRIOR TO GAS BREAKTHROUGH AS A FUNCTION OF RESERVOIR PRESSURE AND INJECTION GAS COMPOSITION.

(AFTER KOCH AND HUTCHINSON [36]).

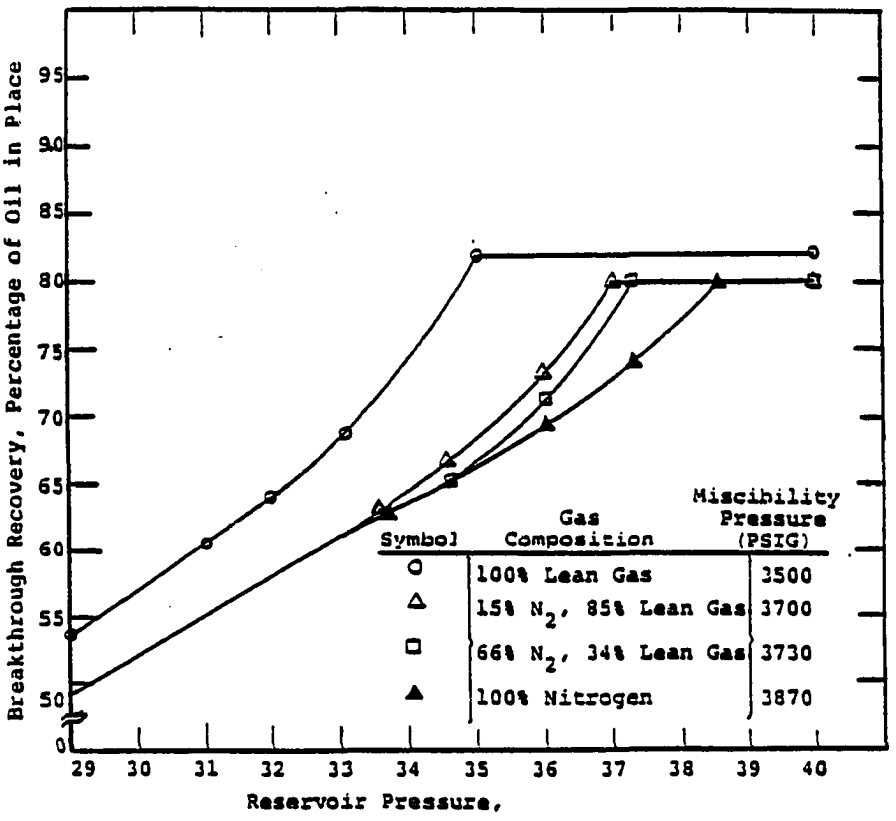

that dilution of nitrogen with relatively small amounts of hydrocarbon gas can be helpful in reducing the miscible pressure. The authors finally suggested that in cases where miscibility can be achieved between the flue gas and a miscible slug, use of flue gas should be considered.

A laboratory work was reported by McNeese (64) in April, 1963. After performing four tests on a physical reservoir model 143 feet long, he concluded that miscibility can be obtained by using nitrogen in the same way as it is obtained by using a lean hydrocarbon gas. He observed that "the leading edge of the transition zone will finally contain the same components that would have been present if the displacing gas had been pure hydrocarbon."

Between 1976 and 1977, Rushing et al, (51,52,53) conducted experimental work using a reservoir physical model 40 feet long of stainless steel with 140-200 mesh sieve manufactured glass beads. In their work they illustrated the high-pressure nitrogen phase relations with crude oil during multiple contact of nitrogen and oil to reach miscibility. They explained how nitrogen works by using ternary diagrams. Figure 4 shows oil recovery by high-pressure nitrogen injection at 150°F. and a pressure range of from 3000 to 5000 psi obtained by the authors. Tests were made on a 54.4° API gravity crude oil containing 700 scf/bbl. They mainly studied the effect of N_2 injection pressure on oil recovery. In their work, they concluded that "the lighter crudes, with

FIGURE 4

OIL RECOVERY IS HIGHER AT HIGHER PRESSURES (MODIFIED AFTER RUSHING et al (50,51,52) 1977)

TEMPERATURE: 150°F.
54.4° API GRAVITY
GAS TO OIL RATIO: 700 SCF/BBL

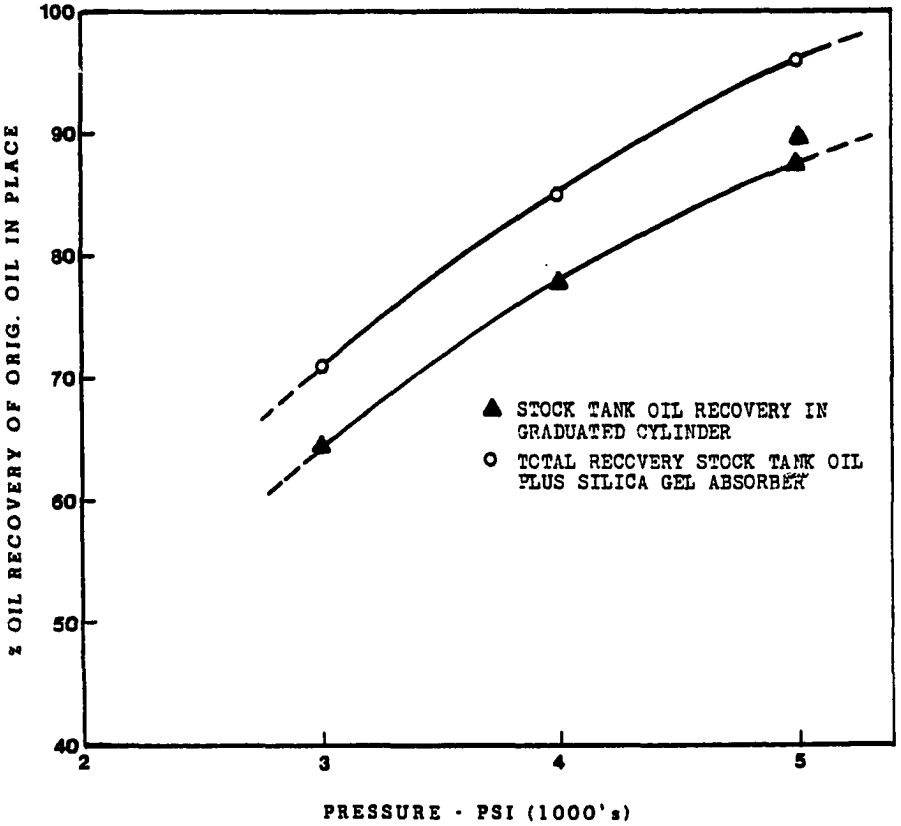

some gas in solution, have been more responsive to high-pressure nitrogen injection," and finally they suggested that "experimental or laboratory tests are required to confirm the applicability of this process for a particular oil."

In 1978, Peterson (47), conducted a laboratory work using crude oil from the Painter field-Wyoming, to determine miscibility pressure by multiple contacts with nitrogen. The author used a reservoir physical model, a 56 ft. long tube. The model was saturated with oil and displaced with N_2 at 4280 psi at reservoir temperature. Results showed that miscibility was obtained after multiple contacts and 90% of oil recovered after injection of about 90% PV of N_2.

In 1975, Hardy and Robertson (25) reported a field case history in Block 31 field, Texas. That was reported as the world's first large-scale miscible displacement project by high-pressure gas injection. Originally, in 1949, produced gas was reinjected for partial pressure maintenance. In 1952, the reservoir was unified and research concluded that high-pressure injection will improve recovery by miscible displacement. In 1966, the hydrocarbon lean gas injection was switched to Flue Gas Injection (87% nitrogen, 12% CO_2 and 1% CO). In Block 31, the miscibility pressure for flue gas was practically identical to miscibility pressure for hydrocarbon injection gas. Block 31 is considered a typical example of miscible displacement, started with hydrocarbon lean gas injection and later changing to flue gas injection.

Moses and Wilson (44)(1978) conducted a laboratory work using nitrogen to displace condensate in a packed column at 4000 PSIG and 200° F. Their tests lead the authors to conclude that nitrogen is an effective displacing gas for condensate reservoir cycling. Also, they observed that the increase in dew point resulting from mixing with nitrogen is much greater than that resulting from mixing with lean gas.

In 1979, Calvin and Vogel (9) reported an evaluation of Nitrogen Injection as a method of increasing gas cap reserves and accelerating depletion in the Byckman Creek Field, Uinta County, Wyoming. The reservoir under consideration has a thick gas cap and it was very important to prevent oil migration into the gas cap during depletion or oil will be trapped and reserves reduced. Six main recovery processes were evaluated for the oil zone with a reservoir simulator and/or an economic model. The study reports "that N_2 was chosen as the cap replacement for both technical and economic reasons. These include:

1. "favorable physical properties: density, viscosity and volume factors;
2. relatively pure and therefore corrosion free;
3. is readily and dependably available;
4. non-polluting;
5. has no adverse phase behavior effects;
6. ease of gas processing and cleanup; and,

7. (Lower) price."

The author concluded that nitrogen injection project at Ryckman Creek will increase gas reserves and provide gas to the public more than 25 years earlier than would be the case under historical type techniques.

In 1980, Vogel and Yarborough(71) conducted laboratory tests in which gas condensate and black oil were contacted by nitrogen at reservoir conditions. Based on the results of their study, the authors concluded that:

a. "The injection of nitrogen into gas condensate reservoir fluid will significantly increase the dew point pressure and may cause retrograde liquid condensation.

b. When black oil is contacted with nitrogen the light and intermediate components will be reduced drastically in the oil. The effect is to decrease oil formation volume factor and solution gas-oil ratio, and to increase the oil density and viscosity."

Eckles et al(21), reported in 1980, one of the most important N_2 injection field projects under way concerned with nitrogen as a enhanced oil recovery method. They reported the injection of a mixture of 30% of Nitrogen with 70% of methane into the hot, high-pressured and multilayered Wilcox Sands in the Fardoche Field, Pt. Coupee Parish, Lousiana. They stated that "nitrogen was selected as a

substitute make-up gas based primarily on pioneer work reported by Koch & Hutchinson in October, 1957, on miscible displacements of reservoir oil using flue gas."

The layers have different types of oils. Reservoir simulation studies predicted oil recovery as high as 89% at breakthrough. This project is a very expensive and complex project that demands high technology and the interdisciplinary work of many high level professionals related to petroleum engineering.

In 1980, Ahmed(1) conducted a laboratory work using nitrogen injection at high-pressure and room temperature. All the researcher's experiments were done using the reservoir physical model represented by a loop of stainless steel tube packed with consolidated sand. The dimensions of the model were 125 feet long and .435 inches in diameter. The average porosity reported was 29% and the average permeability to nitrogen was 930 md. The reservoir physical model has five sampling valves (Fig. 5) located at equal intervals along the length of the reservoir physical model. The sampling points were used to obtain vapor samples to track the phase compositional changes in the porous media during each displacement by means of chromatographic analysis. The porous medium was Oklahoma sand number 1 with 100 mesh size and the oil used was 43° API gravity. The author reported six (6) tests using nitrogen which are presented in table 2. As it can be seen from the data, the solution gas-oil ratio was kept constant at 575 SCF/STB

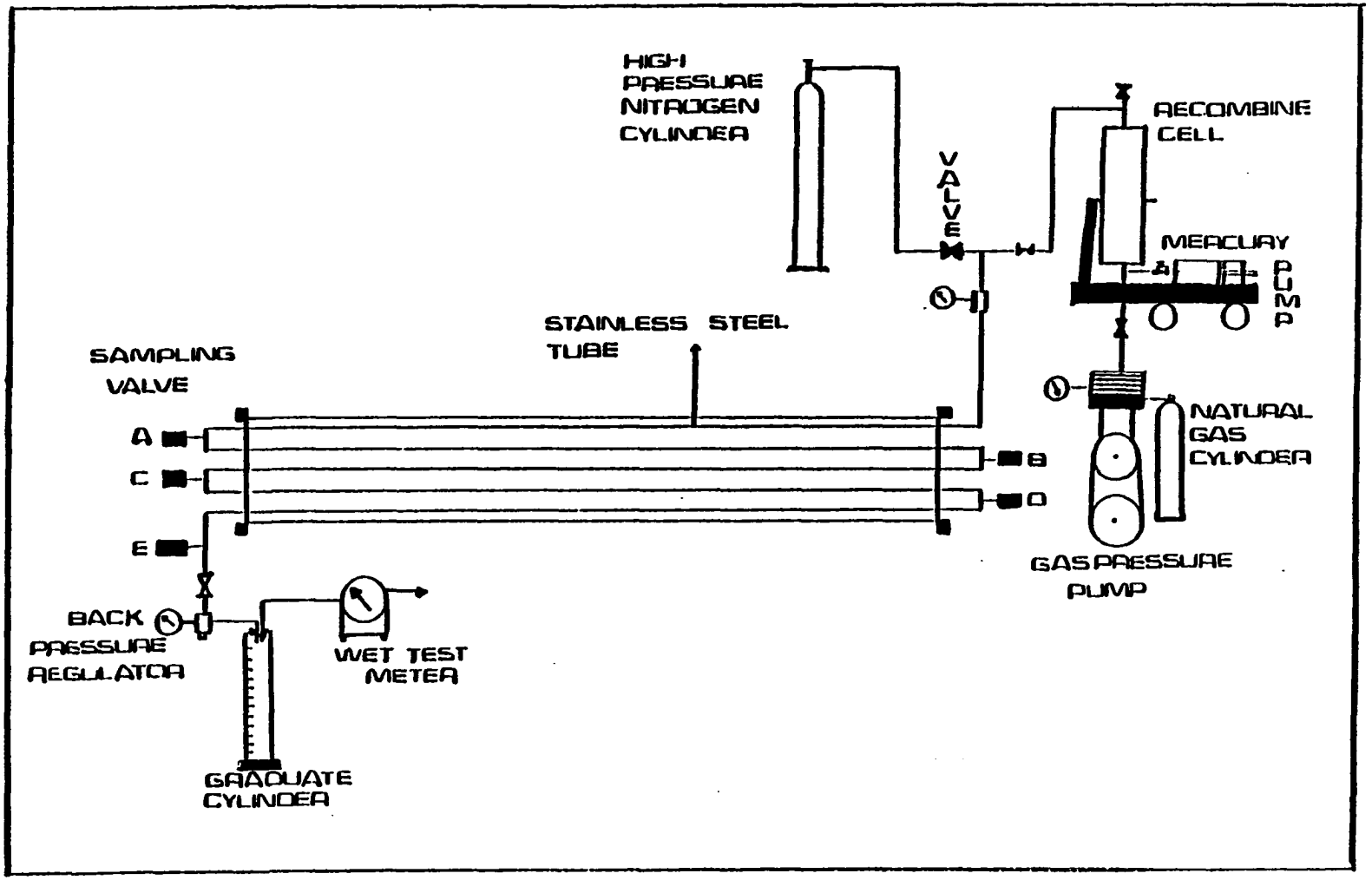

FIGURE 5: SCHEMATIC OF DISPLACEMENT APPARATUS
AFTER AHMED (1)

TABLE 2

RESULTS OF OIL DISPLACEMENT BY NITROGEN AND WATER INJECTION AFTER T. Ahmed (1).

Run No.	Type of Displ. Fluid	Injection Pressure, Psi.	Solution G.O.R. SCFISTB	Initial Oil Saturation	Initial Water Saturation	Initial Stock Tank Oil in Place CC	Oil Recovery at B.T., % of Stock Tank I.O.I.P.
1	N_2	4000	575	.756	.244	698	80
2	N_2	5000	575	.75	.25	692	86
3	N_2	3000	575	.732	.268	676	54
4	N_2	3700	575	.743	.257	686	72
5	H_2O	variable	575	.76	.24	702	65
6	N_2	4000	575	.266	.734	246	13
7	N_2	5000	0	.75	.25	900	59

for all the tests. The most important accomplishment of the author was to obtain the miscibility pressure for the systems under consideration (Figure 6). Also, the study of compositional changes taking place during the displacements of crude oil by nitrogen injection were done successfully. Ahmed[1] concluded that:

1. The minimum miscibility pressure for the system under study was greater than 3800 Psi. At that pressure and above, a rich gas slug, followed by a transition zone, will develop in the reservoir physical model.
2. the size of the formed slug decreases when pressure increases.
3. the oil saturation and solution gas-oil ratio are important parameters in obtaining miscibility.
4. A practical criterion to determine miscibility is observing the compositional profiles of the displacing phase in the reservoir physical model. A plateau section of the compositional profiles indicates miscibility.

Finally, Ahmed[1] recommended that it is important to investigate the effect of solution gas-oil ratio and the temperature on the behavior of miscible displacement by nitrogen injection.

In 1981, Clancy and Kroll[16] published a paper. They pointed out that there are at least six or more applications

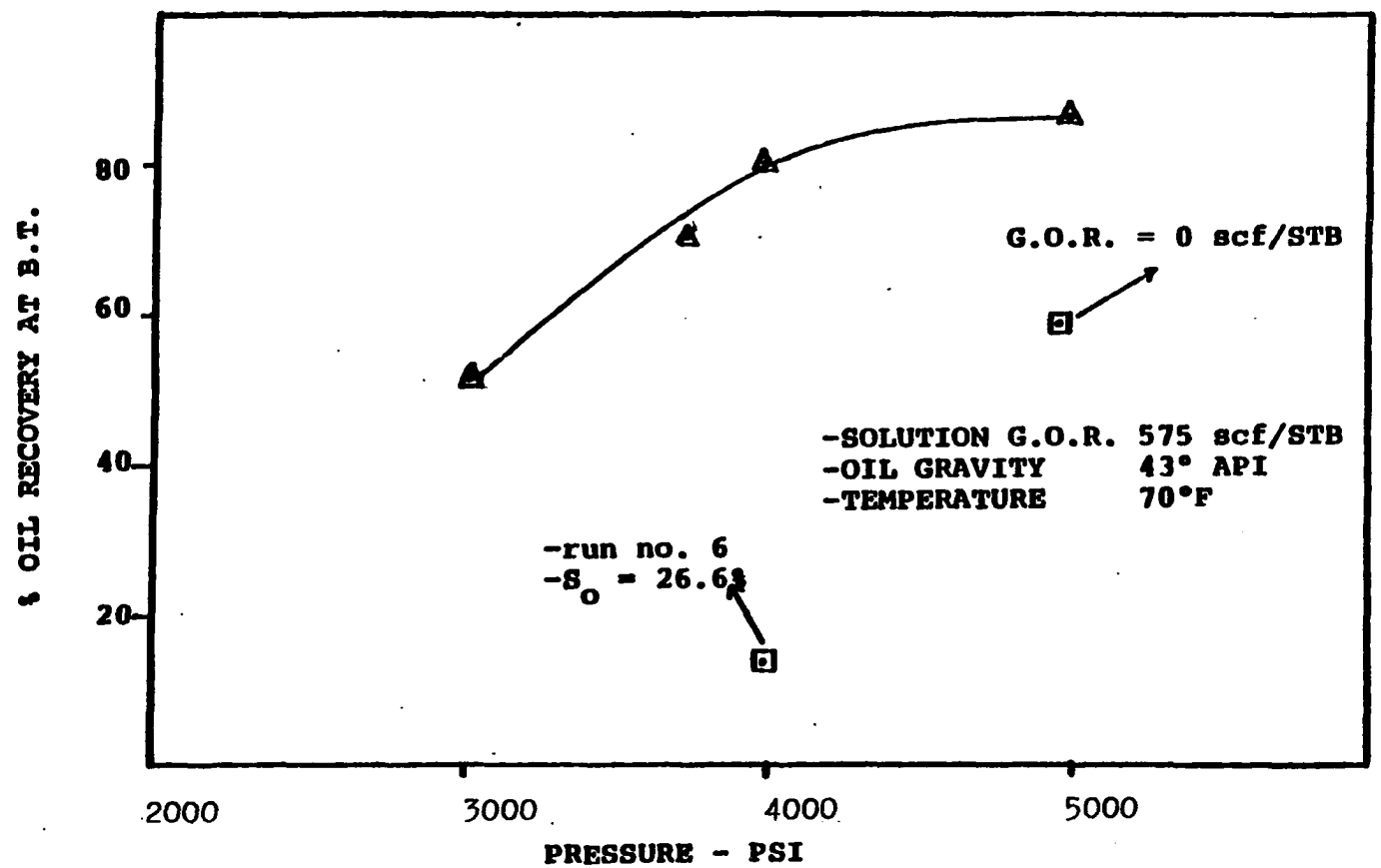

Figure 6: **Effect of pressure on oil recovery**
(After Ahmed(1) 1980)

for nitrogen in the enhanced recovery of oil, and nitrogen is the natural substitute for natural gas or carbon dioxide. After explaining and discussing different methods and sources of nitrogen they concluded that "the ultimate source of nitrogen is the air and cryogenic air separation or combustion gas clean-up (inert gas), generating nitrogen. Twelve of the fourteen nitrogen projects started or committed to in the last four years use air separation nitrogen."

Also, they observed that the air separation technology is more than 75 years old and very well-known even though it is new for the petroleum industry; consequently, the existing process and equipment for air separation is quite applicable to oil field needs.

In March, 1981, Batycky et al(4), reported an experimental study. They investigated the use of nitrogen injection to stabilize water encroachment and to improve gas recovery from carbonate reservoir cores. They concluded after a very extensive laboratory work the following:

1. The recovery of gas methane after injection of nitrogen in carbonate cores is inferior to the recovery obtained using consolidated sandstone.
2. In most carbonate cores, the highest recovery efficiency occured at lower rates, because mass transfer from poorly connected pores controlled the recovery.
3. "In a carbonate reservoir, the injection of a

miscible fluid (nitrogen) following waterflooding may not necessarily lead to reconnection and total recovery of the trapped hydrocarbon phase".

4. The methane recovery ranged from 91.8 to 97% of the original methane in place.

In December, 1981, Carlisle and Crawford (10) reported a laboratory investigation. They conducted an experimental work on oil recovery by nitrogen-driven propane slugs. They reviewed the most important publications about gas pushing propane slugs and considered that it would appear that propane slugs can be pushed economically by nitrogen for some selected reservoirs.

The reservoir physical model they used was a coiled sand back 40 feet long and packed with an unconsolidated sand. "The coiled sand pack was immersed in a constant temperature". They used an oil of 34.5° API at 112° F. and 3000 Psi injection pressure. The oil was not recombined with gas. The results obtained by the authors in six runs are presented in figure 7.

Finally, they concluded as follows:

"The data appear to fit for slug concentrations ranging between 0.2 and 0.8 fraction of propane, which for many conditions is sufficient for miscibility of propane with crude oil";

"The reservoir displacement pressure appears to have considerable effect on the oil recovery using the propane

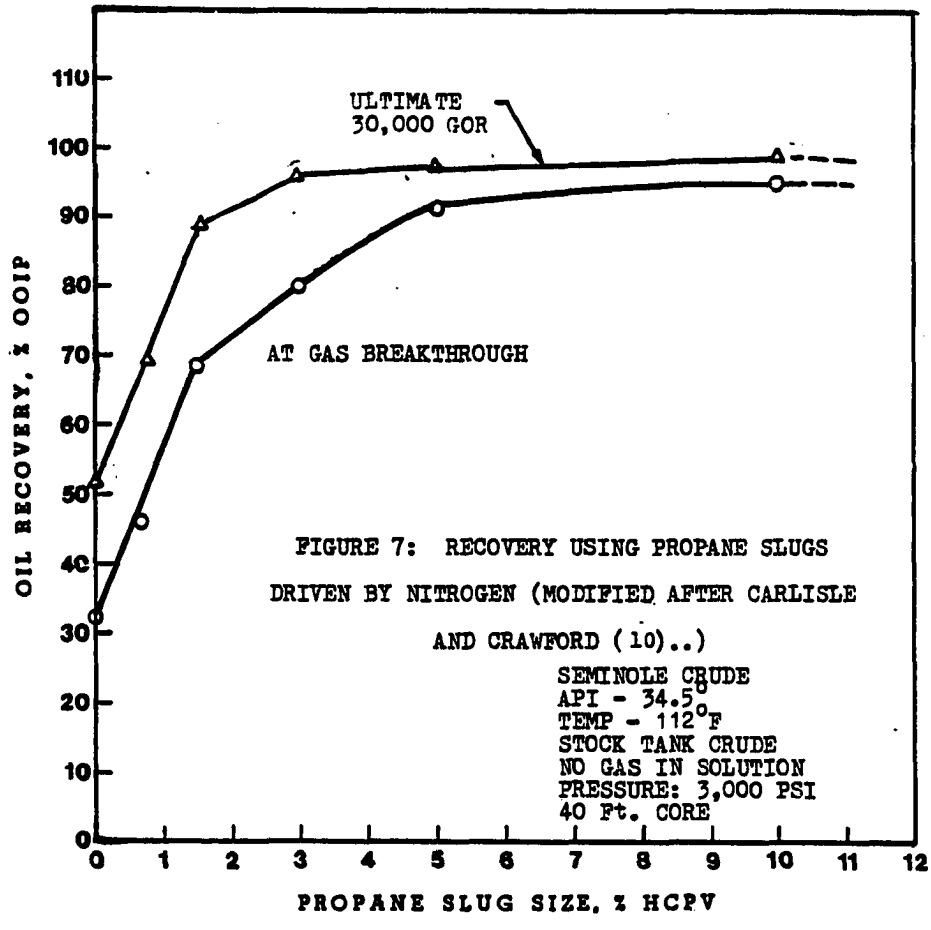

FIGURE 7: RECOVERY USING PROPANE SLUGS DRIVEN BY NITROGEN (MODIFIED AFTER CARLISLE AND CRAWFORD (10)..)

slug;" and,

"Laboratory data indicate that nitrogen-driven propane slugs can be very effective in producing oil."

The authors used neither gas in solution in the 34.5° API oil nor compositional analysis of the changes taking place during the displacements.

In February, 1982, Greenwalt et al(23), reported a field test of nitrogen WAG (water alternating gas) injectivity at the Jay/LEC Field in Florida and Alabama. They pointed out that the test was done because some miscible WAG projects have encountered a reduction in water injectivity after gas injection. The operators speculated that either the precipitation of asphaltenes, trapped residual gas saturation, or movement of fine granules of reservoir rock caused declines in injectivity. The author said: "In nitrogen WAG project, the low solubility of nitrogen in water will prevent the trapped gas saturation from changing significantly during the water injection phases of WAG injection. They concluded that the results from the field experiment they performed were very inconsistent." Changing rock wettability and movement of formation fine grains may have contributed to the inconsistent results." However, they reported that a substantial decline (40%) in well water injectivity indices would occur after nitrogen injection, first. Secondly, disappearance of trapped nitrogen saturation due to solution in injected water will increase

the water injectivity index. Finally, they observed a typical WAG test cycle is not long enough for increasing water injectivity because of solution of nitrogen in water.

Scope and Limitation of the Study

Since this research is involved with many items that would be significant each by itself for a research, it is convenient to specify what this research is attempting to do:

1. Formulation and preparation of a computer program to simulate the heat transfer process in the physical model and to specify the type of heater to use to simulate the reservoir temperature.
2. To confirm the validity of the data obtained by previous research using the available laboratory equipment at Oklahoma University.
3. Develop and test a new method for cleaning and preparation of the reservoir physical model used by Ahmed (1) in order to make more representative tests.
4. Injection of nitrogen into the reservoir physical model at one pressure and different temperatures to study the effect of temperature on recovery, miscibility and track the phase compositional change taking place during displacements.
5. Injection of nitrogen into the reservoir physical model at one pressure above the miscibility pressure and different solution gas-oil ratio to

study the effect of solution gas-oil ratio on oil recovery, miscibility and track the compositional changes taking place during displacements.

6. Run a regular waterflood and then displace nitrogen to study if miscibility is obtained under those conditions. Compare with results of previous researches.

7. Run a nitrogen-driven propane slug test to study the possibility for future investigation using the same laboratory equipment.

Because of the experimental nature of this work, the most important part of this research is the obtained laboratory data.

CHAPTER II

EXPERIMENTAL EQUIPMENT AND PROCEDURE OF INVESTIGATION

A. Equipment

The experimental equipment available at Oklahoma University shown in Figure 5 was modified to perform this laboratory research. A schematic diagram of the modified experimental equipment used in this work is shown in Figure 8.

This equipment has been redesigned to study the following aspects related to high pressure nitrogen injection:

a. Effect of temperature on oil recovery and miscibility.

b. Effect of solution gas-oil ratio on oil recovery and miscibility.

c. Effect of high water saturation in tertiary nitrogen injection.

d. Effect of using a propane slug driven by nitrogen on oil recovery and miscibility.

e. Compare results with previous researches to determine if the experimental equipment is suitable for this type of experiments.

The experimental equipment is divided into the following parts:

1. PVT-Injection System
2. Reservoir Physical Model
3. Temperature Control System
4. Production and analytical System.

1. PVT-Injection System

This system consisted of a high pressure constant volumetric rate positive displacement mercury pump, visual PVT cell, windowed PVT condensate cell, high pressure variable volumetric rate positive displacement pump, gas compressor, low pressure variable volumetric rate centrifuge pump, high pressure nitrogen supply cylinder, medium pressure nitrogen supply cylinder, medium pressure propane supply cylinder and vacuum pump.

1-1. Constant Volumetric Rate Positive Displacement Mercury Pump:

This mercury pump is a Ruska Model 2261 Bench-mounted motorized pump. This pump is equipped with an electric motor drive. The pump is provided with adjustable travel-limited switches to stop the motor when the plunger reaches a preset point in either direction of travel. This pump has a single cylinder with a capacity of 100 cc and is able to inject a maximum pressure of 25000 psi. The dial resolution is .01 cc and the resolution of the scale is 1 cc. The pump is provided with 5 outlets with a 1/8" NPT thread. As is shown in Figure 8, the mercury pump is connected to a PTV windowed cell, a mercury container and a pressure gauge.

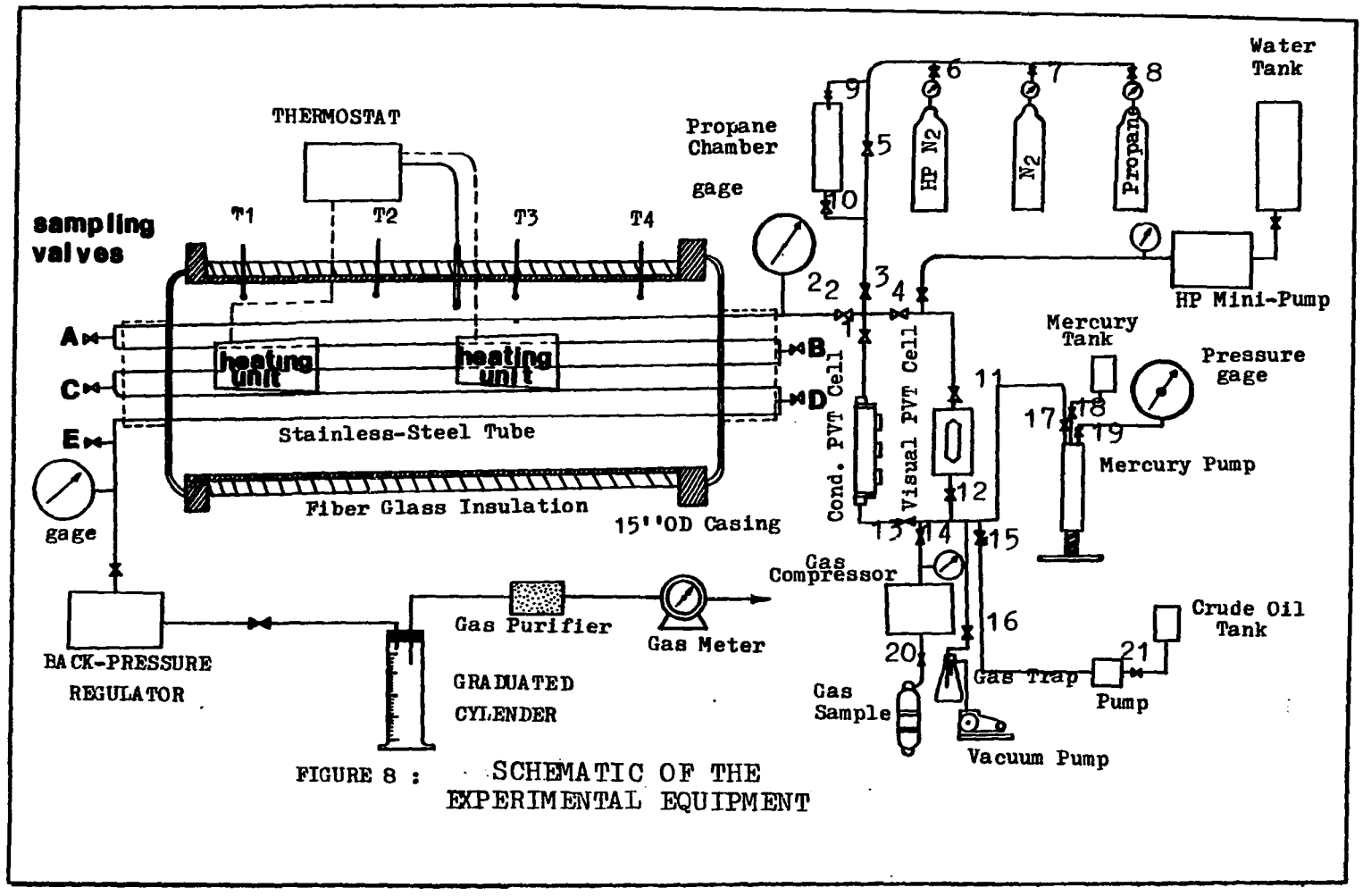

FIGURE 8 : SCHEMATIC OF THE EXPERIMENTAL EQUIPMENT

1-2. Visual PVT Cell

The visual PVT Cell (Figure 9) is basically a cylindrical container which was used in this work to measure bubble-point pressure of a hydrocarbon reservoir fluid at high temperatures and pressures, and to recombine gas and liquid fluids to reproduce actual reservoir conditions in the laboratory. The Cell has a glass window for observing when the first bubble of gas is liberated from the liquid. The visual PVT Cell has a standard volume of 650 cc and a pressure rating of 10,000 Psi at 350°F. The Visual PVT Cell is mounted on a base that allows one to shake the cell. The cell is connected to: The mercury pump, the reservoir physical model, windowed PVT cell, gas compressor, vacuum pump and the centrifuge pump. All the connections are 1/8" stainless steel tubing.

1-3. The Windowed PVT Condensate Cell

The windowed PVT condensate cell used in this work is a Ruska Cell Model No. 2306. The cell is a cylinder with a volume of 400 cc. This cell has three windows arranged in the face of the cell so any liquid level can be determined visually. If the fluid level disappears between windows, it can be made visual by inverting the cell. The cell is supported by a metallic base mounted in the mercury pump table. Three shallow holes are drilled into the cell wall for inserting thermocouples to determine when temperature equilibrium has been obtained.

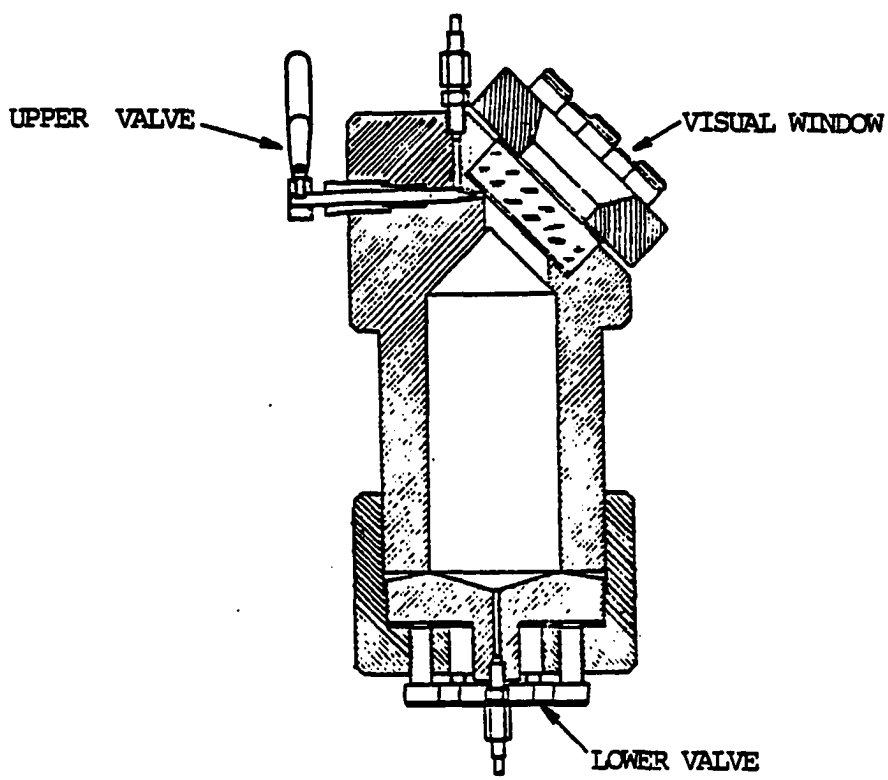

Figure NO.9 VISUAL PVT CELL

1-4. High Pressure Variable Volumetric Rate Positive Displacement Type Pump

This pump was an "LDG" minipump duplex model 2396-57 with a maximum capacity 580 ml/hr. The capacity is proportional to motor speed. The pump's working pressure is 6,000 Psi. The weight of this duplex pump is 24 lbs. net and its dimensions are: 10-1/8" W., 8-3/4" D., and 7-3/8" H. The maximum working temperature is 122° F. This LDG minipump should be protected from liquid contact and not operated in a potentially explosive environment. The pump is equipped with compression type tube fittings built into suction and discharge cartridges of the pump. The suction side accepts only 1/8" outside diameter tube; the discharge only accepts 1/16" outside diameter tube. Calibration of the pump is shown in Appendix A.

1-5. Gas Compressor

A gas compressor manufactured by C.A. Mathey Machine Works and available at Oklahoma University, was used in this work with the purpose of injecting with enough pressure the field natural gas into the visual PVT cell. In this way, it is possible to perform a proper recombination between the natural gas and oil. The inlet of the compressor is connected to a small natural gas supply cylinder with ¼" stainless steel tubing. The outlet is connected to the visual PVT Cell and the windowed PVT condensate cell by 1/8" stainless steel tubing.

1-6. Low Pressure Variable Rate Centrifugal Pump

A small centrifugal pump manufactured by March Mfg. Inc., model 112 was used to charge with oil the visual PVT pump.

1-7. Nitrogen and Propane Cylinders

A Matheson high pressure nitrogen cylinder was used in these experiments. The capacity of this cylinder is 494 cf at 6000 psi and 70°F. By means of a stainless steel high pressure regulator, manufactured by Matheson, it was possible to control the injection pressure very closely and with high sensitivity, into the reservoir physical model. The connections were done through 1/4" stainless steel tubing.

A conventional medium pressure nitrogen cylinder provided by the University of Oklahoma was also used in these experiments. The capacity was 494 of at 2500 psi and 70°F. The connections were done through 1/8" stainless steel tubing.

The purity of nitrogen in both cylinders was 99.99%. A conventional low pressure propane cylinder was used in this experiment. The propane was under 100 psi pressure and 70°F. temperature.

The cylinders are shown in Figure 8.

1-8. Vacuum Pump

A vacuum pump manufactured by Cenco Megavar Pump was used in this experiment. The position of the vacuum pump in

the system is shown in figure 8.

2. Reservoir Physical Model

The reservoir physical model used in this experiment was available at the Oklahoma University. This reservoir physical model is represented by a linear artificial core constructed by putting consolidated sand packed inside of a stainless steel tube 125' long and .435" internal diameter.(figure 8). The model is provided with five sampling valves along the length of the tube to facilitate the taking of vapor samples during the displacement test for chromatograph analysis.

The properties of the reservoir physical model were recalculated. The average porosity was .32 and the absolute permeability result was 910 md. The absolute permeability was obtained by nitrogen displacements. Several displacements of nitrogen at different rates were done and a computer program was written to obtain the liquid absolute permeability. The program and graph calculation of absolute permeability are shown in Appendix E.

Under the safety conditions in this reservoir physical model, reservoir conditions under 7000 Psi at 160°F. can be simulated.

A description of the temperature control system for the reservoir physical model follows.

3. Temperature Control System

One of the primary objectives of this work was to

design and specify a heating system to control the temperature and simulate with minimum variation the reservoir temperature. A computer program was developed to simulate heat transfer in the reservoir physical model. The computer program and results are given in Appendix B.

The temperature control system used in this work consisted of: heating units, thermostat, insulation blanket and thermometers. (As shown in figure 8.)

Two commercial heating units manufactured by Arvin Industries, Inc., model 29H60-3, were used in these experiments. Each heating unit has a heating capacity of 1500 BTU/Hr. The two heaters were used to independently supply heat to the annulus between the stainless steel tube containing the consolidated sandpack and the 15" diameter pipe. A Chromalox Industrial Thermostat-type AR-2524 was used to automatically control the heat requirements in the annulus between the stainless steel tube and 15" diameter pipe. The Chromalox thermostat used has a temperature range: 50°-250°F. The electricity rating is 25 amps and 120 volts. The source temperature is read by means of a sensitive bulb with .250" diameter and 5½" length. Thermostats are tested and calibrated at the factory to the temperature of the sensing bulb. However, they should be calibrated to the actual working temperature. It was calibrated to work according to the 4 reading thermometers provided in the 15" casing pipe. Figure 10 illustrates the relationship among thermometers, thermostat

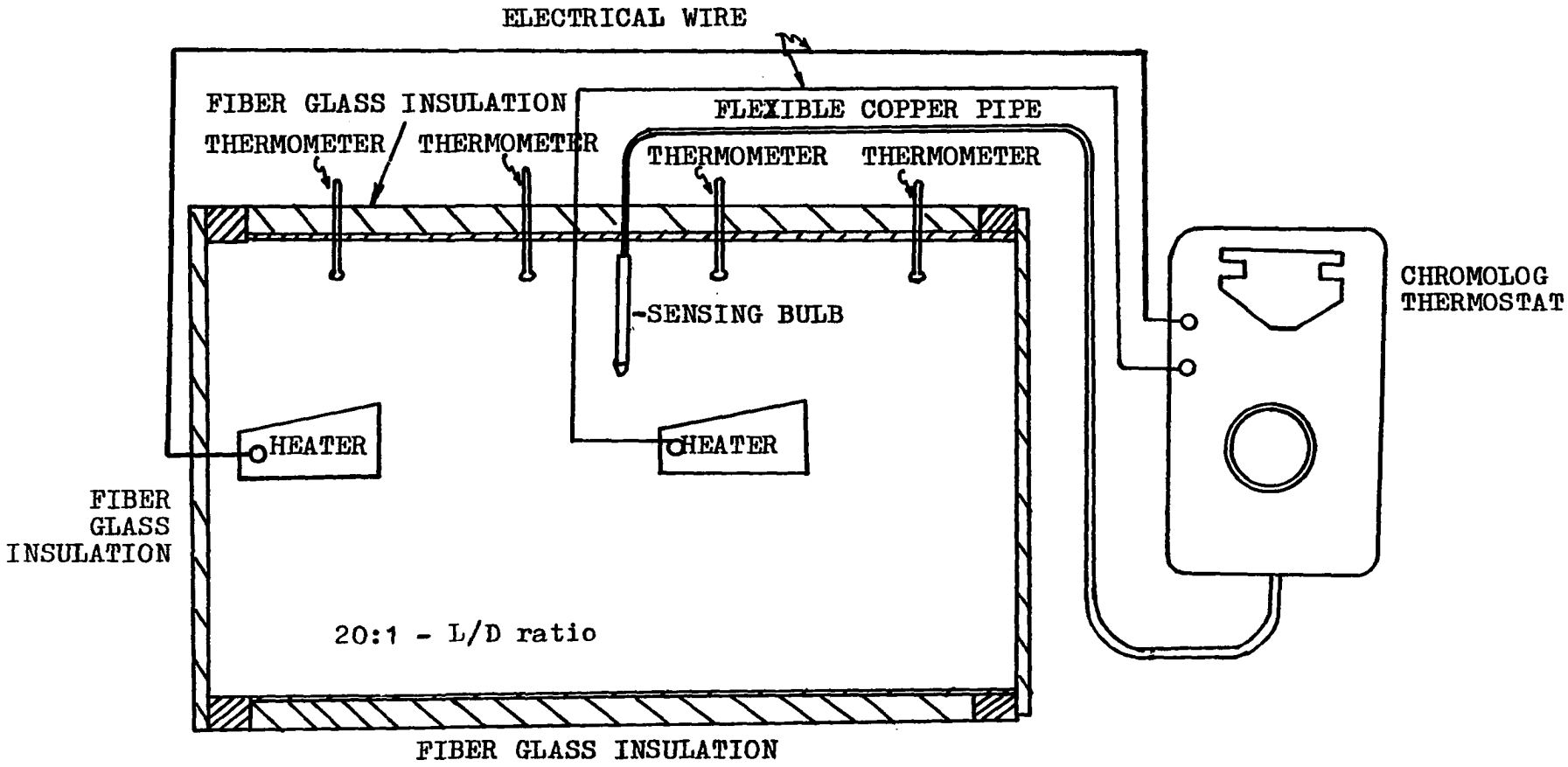

FIGURE 10: DETAILS OF THE HEATING SYSTEM

and heaters. Also in that figure is shown the insulating material.

A thermo-saver fiberglass insulation blanket faced with white vinyl (twice as dense as normal water heater or home type insulation) was used to insulate the model. Several blankets were used, each blanket having these dimensions: 2" x 48" x 87". This insulation material meets ASTM E84 25/50 requirements.

As is shown in figure 10 , the temperature system was provided by four regular thermometers to monitor temperatures in the reservoir physical model.

4. Production and Analytical System

The production and analytical system (Figure 8) consisted of:

1. Back-pressure regulator;
2. Graduated cylinder;
3. Gas filter;
4. Gas-metering apparatus
5. Chromatograph; and
6. Refractometer.

4-1. Back Pressure Regulator

The direct operating pressure reducing valve type DR10D originally installed in the equipment shown in figure 5 was changed because this valve was unsuitable for this investigation. A back-pressure regualtor, manufactured by TESCOM Corporation, with handknob adjustments, model 26-3220-24 was

installed. The maximum setting back-pressure was 5,000 Psi. The working temperature was between -4.0 to +160°F. The back pressure of the system was held constant at 2,000 Psi for all the tests performed in this work.

4-2. Graduated Cylinder

A graduated cylinder with 1,000 cc. of capacity and previously modified to work as liquid-gas separator was used in this work.

4-3. Gas Filter

A filter made of silica gel was used immediately after the graduated cylinder.

4-4. Gas-Metering Apparatus

As is shown in figure 8, a Sargent wet test meter, manufactured by Precision Scientific Co. was used to determine the amount of gas produced during displacements. The scale resolution is 0.001 SCF.

4-5. Chromatograph

A GOW-MAC 550P series chromatograph was used to analyze the vapor samples collected during the tests performed in this research. The GOW-MAC series 550P is a compact dual column thermal conductivity gas chromatograph with temperature programming capability. The basic principle and components of a gas chromatographic system as is shown in figure 11. In that figure the microprocessor (CPU) that GOW-MAC chromato-

graph has, is not shown. This microprocessor (CPU) allows the operator to write programs to control initial temperature, final temperature, rate of temperature rise and time held before automatic shutdown. Also, it is possible to set up the detector temperature, bridge current and inlet temperature.

Vapor samples were analyzed, using helium as a carrier gas, in a 30' x 1/8" column packed with 30% DC-200/500 on chromosorb PAW 60-80.

The chromatograph run conditions were as follows:

Sample: 2 cc. of vapor sample.

Temperature program: Isothermal conditions.

Parameters: 65-00-00-65-10 (temp-time-Ramp-final temp-time).

Inlet temperature: 65°F.

Detector temperature: 200°F.

Bridge current: 160 ma.

run time: 10 minutes.

In order to control the flow of the carrier gas (Helium) an automatic Flowmeter was used.

In order to perform gas analysis with a chromatograph it is necessary to go through a theoretical and practical training beforehand. It is necessary to know the equipment and its limitations before attempting any gas analysis. An entire chapter was devoted in Ahmed's[1] dissertation to assist any researcher who needs to use techniques of chromatograph analysis in his work. It is also necessary to use very carefully all the information available in the chromatograph

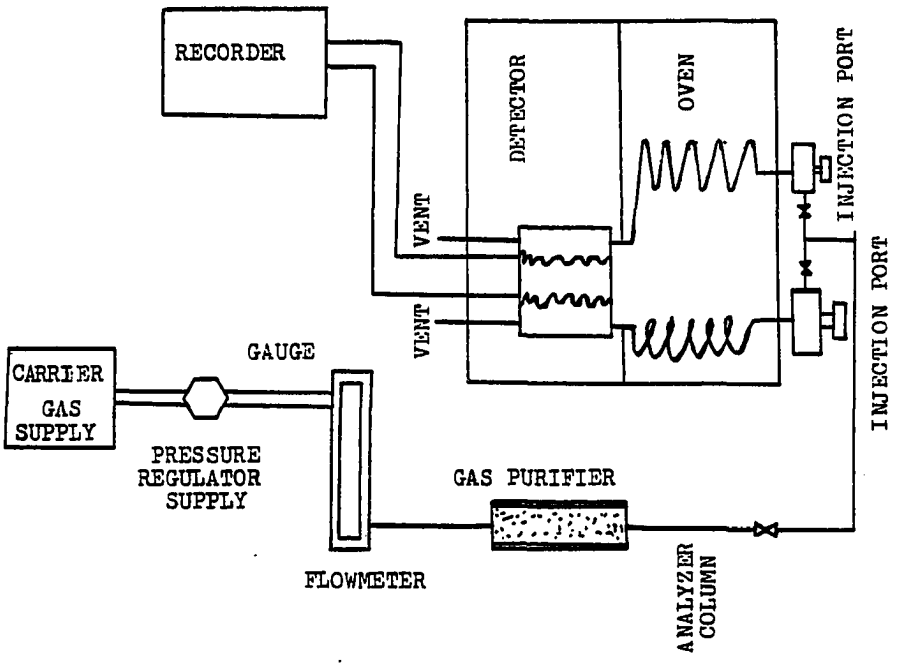

FIGURE 11

SCHEMATIC GAS CHROMATOGRAPHIC SYSTEM

operating manuals.

4-6. Refractometer

An Abbe Refractometer, available at Oklahoma University was used in this experiment to analyze optically a mixture of oil-naphtha. Before using this instrument it was necessary to calibrate it. Data and curve of Refractive Indexes versus percentage of oil-naphtha in mixture is presented in Appendix D.

5. Additional Equipment

In order to determine fluid properties other instruments were used. The instruments used were: Fann viscosimeter, KIMRAY Gas Gravitometer, Hydrometers, etc.

Materials

The materials used in these experiments were: Insulation material, medium material, light oil, natural gas and standard gas samples.

The outside insulation material used in this investigation to cover the 15" O.D. casing was a Thermo Saver Commercial fiberglass insulation blanket. This material has a thermal conductivity of 0.12 BTU/ft^2-hr-^{o}F, The section of the stainless steel tube containing the porous medium was insulated using commercial urethane. This material has a density of 1.9 Lb/ft^3 and a thermal conductivity of 0.15 BTU/ft^2 hr-^{o}F.

The porous medium used in this investigation was artificial, consolidated sand packed. The sand used was clean

Oklahoma sand, number 1 with 100 mesh size. Data and calculation of absolute permeability for this porous medium are shown in Appendix E.

The oil selected for this study was Tenneco's South Lone Elm Field light oil. This field is located in Noble County, Oklahoma. Table 3 shows the oil properties and some PVT characteristics.

The natural gas used in these experiments was a field natural gas sampled at South Lone Elm Field, Noble County, Oklahoma. The natural gas was collected at 70 PSI in a small gas cylinder. For safety's sake, it was necessary to collect a limited number of natural gas samples and consequently several field trips for this purpose were needed. The natural gas was analyzed by means of the chromatograph. The analysis results are shown in Table 4.

Several standard gas samples were used in this investigation to calibrate the chromatograph.

Samples of analyzed Scott Gas, distributed by Alltech Associates, was used. The Gases have the following compositions:

Methane, cathalog #G0124. . . . . 10%

Ethane, Cathalog #G 0224. . . . . 10%

Propane, Cathalog #G0524. . . . . 10%

Butane, Cathalog #G0924 . . . . . 10%

All these gas samples were in 90% of nitrogen.

TABLE 3

SOUTH ELM UNIT OIL PROPERTIES

Avg. stock tank ^{o}API Gravity at 60°F.....	42.4
Specific Gravity at 60°F.....	0.814
Oil viscosity at 70°F. (Cp).....	3.2
Formation Volume Factor at pressure 2,000 PSI: (With Natural Gas)	
At GOR = 200 SCF/STB.....	1.1 $\frac{Bbl}{STB}$
At GOR = 400 SCF/STB.....	1.2 $\frac{Bbl}{STB}$
At GOR = 575 SCF/STB.....	1.29 $\frac{Bbl}{STB}$
Bubble Point Pressure at 70°F.	
At GOR = 200 SCF/STB.....	750 PSI
At GOR = 400 SCF/STB.....	1550 PSI
At GOR = 575 SCF/STB.....	1790 PSI

TABLE 4

CHROMATOGRAPHIC ANALYSIS OF FIELD NATURAL GAS

Sample collected at: South Lone Elm Field
Noble County, Oklahoma

Sampled and run by: CAA

Chromatograph run conditions

2cc of sample

65-00-00-65-10

65-200-160

Carrier Gas: Helium, 55 cc/min.

Paper Speed: 4 cm/min.

COMPOSITION	MOL%
C_1	78.32
C_2	11.32
C_3	4.96
i-C_4	.75
N-C_4	2.49
i-C_5	.79
N-C_5	.98
C_6+	.36
	99.99

Also, was used a Analyzed Natural Gas sample Hewlett Packard P/N 5080-8756. The composition was as follows:

N_2 ..... 6%

CO_2 ..... 1%

C_1 ..... 69%

C_2 ..... 9%

C_3 ..... 6%

i-C_4 ..... 3%

n-C_4 ..... 3%

i-C_5 ..... 1%

n-C_5 ..... 1%

C_6^+ 5%

O_2 ..... .5%

The last standard gas sample used in this investigation was an ALTECH Associated can with C_1- C6 N-paraffins, 1000 ppm in N_2.

Other Materials

Throughout the experiments, tap water, naphtha and mercury were used.

Procedure of Investigation and Techniques

Separate experimental procedures and techniques were required in this investigation. The procedures involved in these experiments were as follows:

1. Procedure for recombination process.
2. Procedure for PVT analysis.
3. Procedure for saturation of the reservoir physical model.
4. Procedure for oil recovery by nitrogen displacement.
5. Procedure for oil recovery by waterflooding.
6. Procedure for oil recovery by propane slug driven by nitrogen.

1. Procedure for Recombination Process

The procedure of recombination used by the previous researcher was changed in this work. Ahmed (1) used the windowed PVT condensate cell with a capacity of 400 cc to recombine oil and gas. In this work, a visual PVT cell with a capacity of 650 cc. was used for the same purpose. The two advantages are that 1) visual PVT Cell can be shaken and, 2) the amount of recombinations during a test are reduced.

The windowed PVT Condensate Cell was used to discharge high-pressure mercury and undesirable high-pressure oil and gas mixtures. This kind of mixture is frequently found when it is necessary to recombine oil-gas with a different GOR in solution.

Based on figure 12 which represents the recombination system, the visual PVT Cell was connected to the inlet of the

reservoir physical model through a 1/8" stainless steel tube. The bottom of the visual PVT Cell is connected to the gas compressor, vacuum pump, oil-feed pump, windowed PVT condensate cell and to the mercury pump. All these connections were made through 1/8" stainless steel tube. All the sections were provided with suitable 1/8" choke needle valves.

The following steps will describe the recombination procedure:

Step 1: Selection of the GOR in solution to work with.

Step 2: Calculation to determine the maximum amount of oil that can be recombined depending on the GOR in the solution selected and the pressure range of the compressor.

For a GOR = 575 SCF/STB the oil volume was 200 cc.
For a GOR = 400 SCF/STB the oil volume was 260 cc.
For a GOR = 200 SCF/STB the oil volume was 360 cc.

Step 3: Vacuum the visual PVT Cell for 2 hrs.

Step 4: By using the vacuum in the cell charge oil into the cell according to step 2. If the flow is too slow the oil feed pump is used.

Step 5: By using the gas compressor inject natural gas into the cell. The amount of gas and the required injection pressure is determined mathematically by using an equation of state for real gases.

Step 6: By using the mercury pump inject mercury into the cell up to 2000 Psi. At that pressure the content of the cell was always one phase fluid.

After step 5, the recombined oil was ready to be injected into the reservoir physical model for saturation.

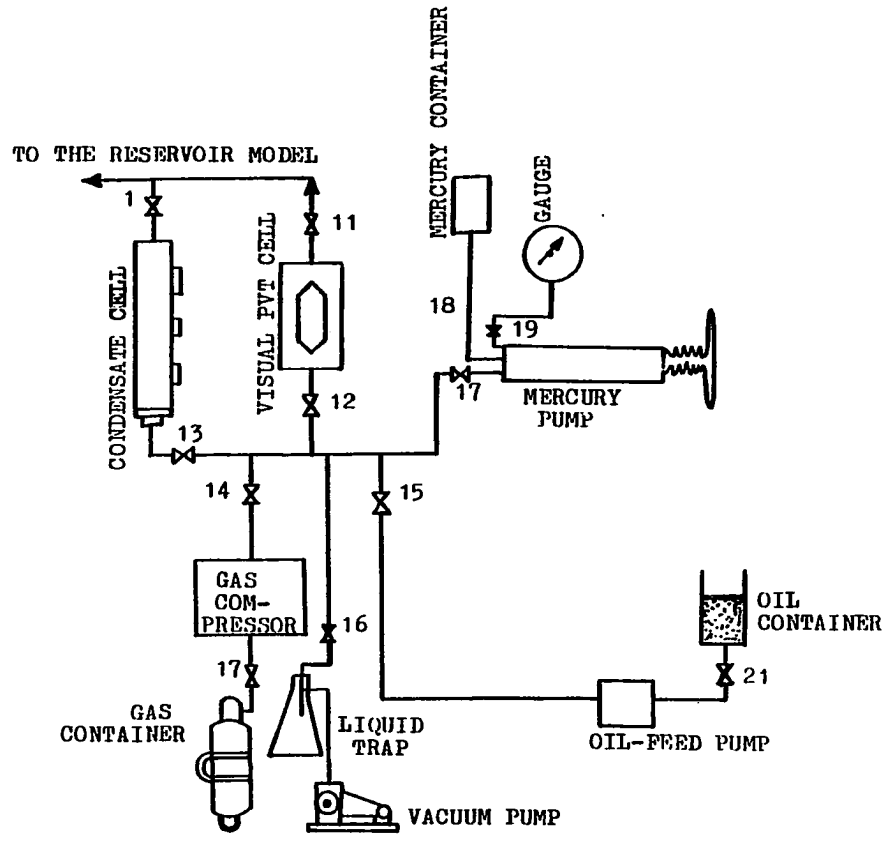

FIGURE 12: RECOMBINATION SYSTEM

2. Procedure for PVT Analysis

The bubble-point pressure of a hydrocarbon reservoir fluid is defined as the pressure at which the first bubble of gas is separated from the liquid hydrocarbon. This bubble-point pressure is determined in the laboratory by means of the visual PVT Cell (pressure-volume-temperature cell) and the formation volumetric factor as well. In order to obtain bubble-point pressure (also saturation pressure) and formation volumetric factor in the laboratory, the following steps must be followed:

Step 1: Follow all the first five steps for recombination process.

Step 2: After step 1, the cell is already charged. Then shake the visual PVT Cell for 5 minutes, and open the bottom valve which communicates with the mercury pump and raise the pressure to a value above the average pressure of the reservoir. This value has to be known before hand.

Step 3: Close the bottom valve of the cell and take the first gauge reading. Shake for 5 minutes and reduce the pressure 10 Psi.

Step 4: Look through the glass window in order to check if there is gas in the cell which is the indication that the first bubble appeared.

Step 5: Repeat the above procedure for several pressures until the first bubble of gas appears in the visual PVT cell. When the bubble-point pressure is detected, go to step 6.

Step 6: Go several times below and above the saturation

pressure to be sure the gauge pressure reading of the bubble point is right.

Note: The reading of the volume of mercury removed from the cell has to be done at one reference pressure to avoid corrections due to expansion of the mercury and equipment.

The results obtained by using this method are given in figures 13, 14 and 15.

Different in solution GOR'S generated different saturation pressures and formation volumetric factors as well. All the analyzed gas-oil mixtures represent different reservoir fluids and consequently they behave differently from each other.

3. Procedure for Saturation of the Reservoir Physical Model

Before each displacement with nitrogen or water it is necessary to saturate the reservoir physical model with connate water and original oil with gas in solution. Due to the great length and low permeability of the model this procedure was the most time-consuming one in all the investigation. The procedure used in this work was originally proposed by Rushing et al[52], then modified by Ahmed[1] in 1980, and finally modified again by the author of this work.

This procedure used has the following steps:

Step 1: Set up the heating system to increase the temperature to the desired working temperature. Go to second step when temperature becomes steady.

Step 2: After a run, the reservoir physical model was flooded with a solvent(naphtha). Naphtha was displaced until

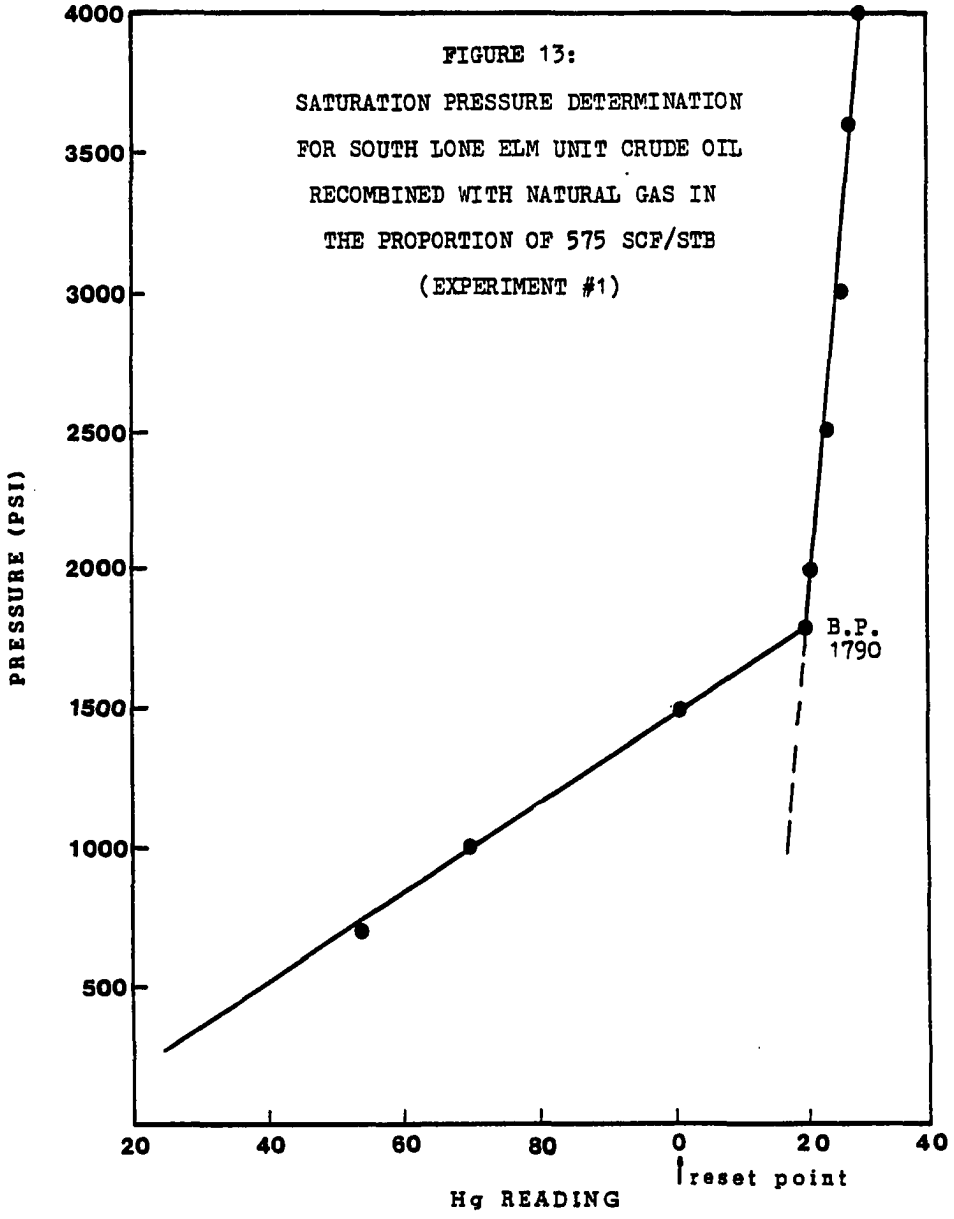

BUBBLE POINT: 1790 PSI

FIGURE 14: SATURATION PRESSURE DETERMINATION FOR SOUTH LONE ELM UNIT CRUDE OIL WITH NATURAL GAS IN THE PROPORTION OF 400 SCF/STB (EXPERIMENT #3)

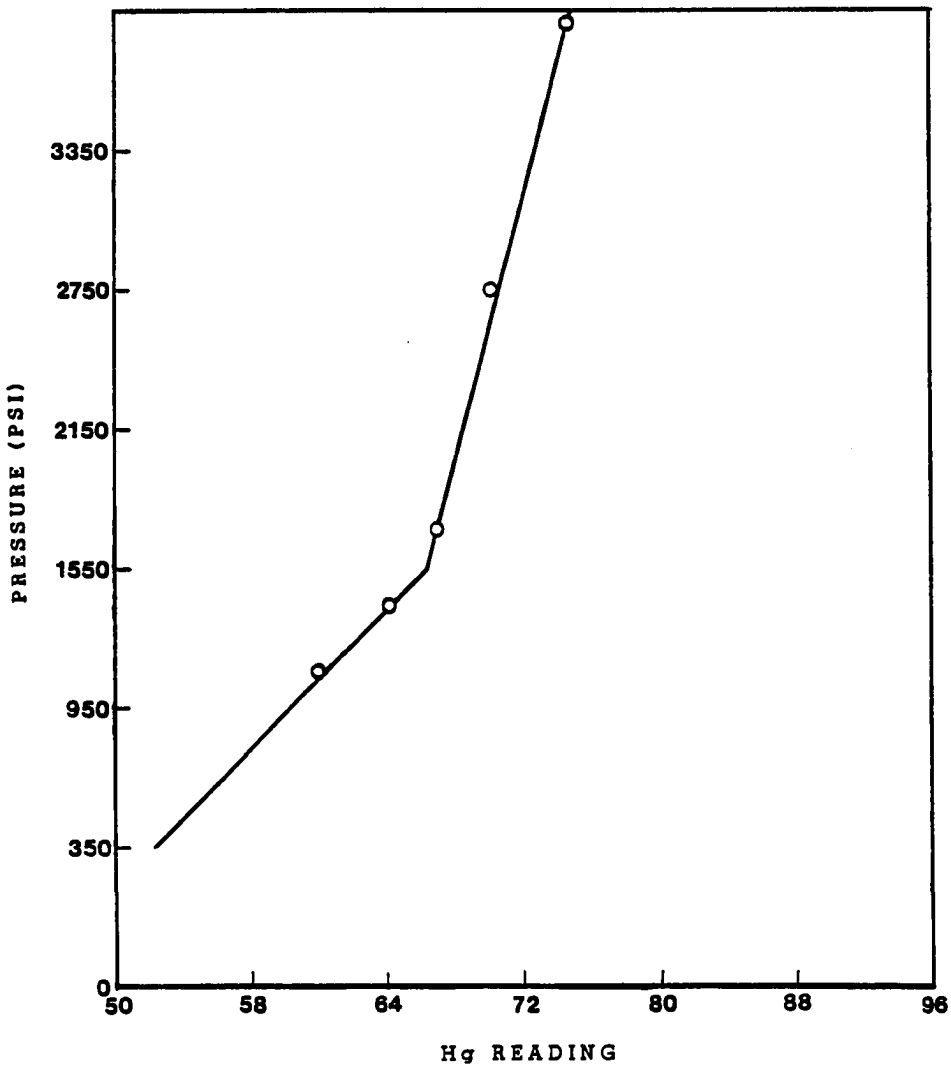

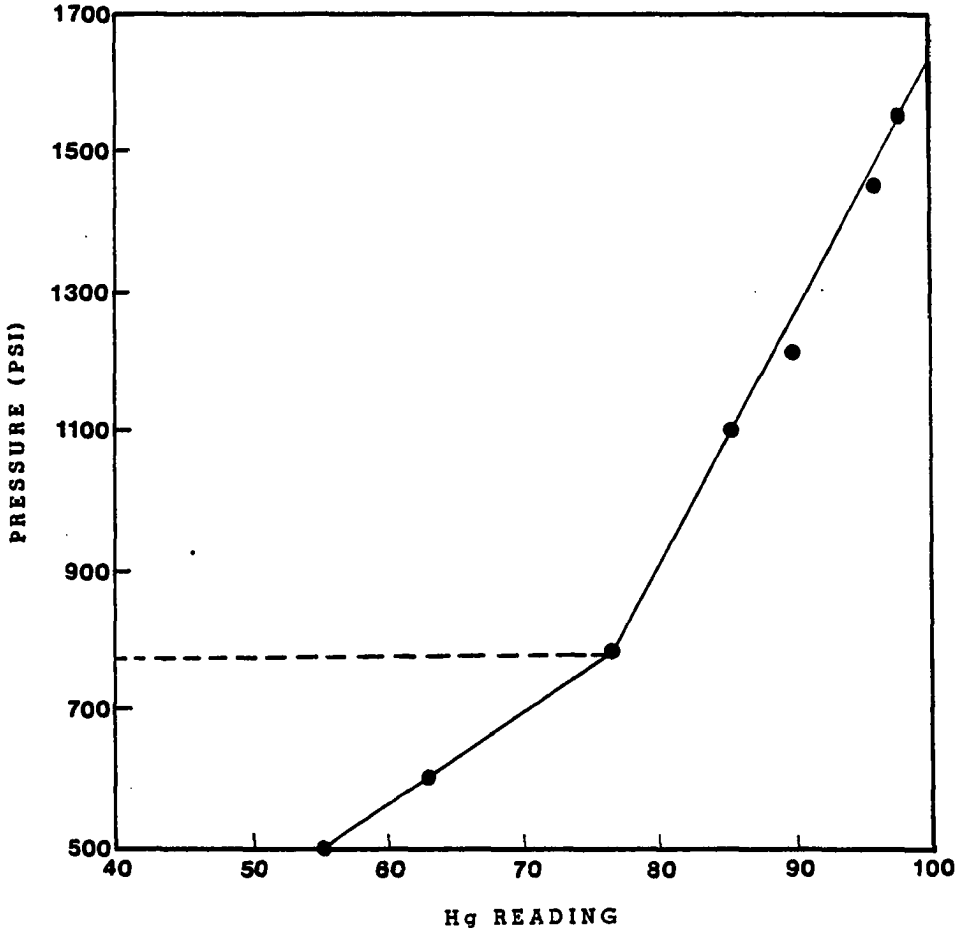

FIGURE 15: SATURATION PRESSURE DETERMINATION FOR SOUTH LONE ELM UNIT CRUDE OIL RECOMBINED WITH NATURAL GAS IN THE PROPORTION OF 200 SCF/STB (EXPERIMENT #4)

all the residual oil was recovered. The recovery of residual oil was monitored by using optical methods. A refractometer previously calibrated to determine percentage of oil fraction in the recovery naphtha-oil mixture was used. The data and calibration curve are shown in Appendix D. The advantage of using optical technique is that it is not necessary to make the assumption that the porous medium is cleaned after injecting a certain amount of naphtha.

Step 3: The naphtha was displaced by nitrogen injection. The effluent gas was analyzed in the chromatograph till 100% of the N_2 was produced. The model was vacuumed for 24 hours.

Step 4: Then the remaining nitrogen was displaced by water. Water was displaced till no more gas was flowing from the core.

Step 5: The water was displaced into the reservoir physical model by means of the high-pressure variable volumetric rate positive displacement. The LDG minipump was added to the laboratory equipment in order to make the saturation process more versatile and cleaner. Doing this step with the mercury pump takes too long and there is the possibility of injecting mercury into the core. By doing a volumetric balance, the porous volume is calculated.

Step 6: The recombined oil, contained in the visual PVT Cell, was injected into the core by means of the mercury pump. The maximum pressure to inject was 600 Psi, then it is necessary to wait till the oil is squeezed into the core and the pressure drops enough to continue the resaturation process.

Step 7: The saturation of the reservoir physical model continues until breakthrough of oil is obtained in the outlet of the model. By volumetric comparison the amount of oil at reservoir conditions in the reservoir physical model is determined by measuring the difference between initial and final water saturation in the model. Data of oil and water saturation for all the runs done in this investigation are presented in table 16.

4. Procedure for Oil Recovery by Nitrogen Displacement

After the reservoir physical model has been saturated with water and recombined oil and the temperature of the system is at the desired test temperature, the equipment is ready to run a displacement by nitrogen. In reference to figure 8 the following steps are followed:

Step 1: Close valves 2 and 3 and open valves 1 and 4 and set up the desired injection pressure by using the highly sensitive Matheson Regulator. Set up the pressure (2000 Psi) at the back-pressure regulator at the outlet of the model. Make sure all the sampling valves are closed.

Step 2: Take the first wet gas meter reading at zero time. Check for leaks.

Step 3: Collect oil in graduated cylinder and take oil and gas reading every 15 minutes at least.

Step 4: At intervals of time fixed beforehand, take samples of vapor, starting by sampling point A. Before taking the sample, the special sampling valve has to be vacuumed. Open the sampling valve for one minute. Open the lower section and bleed the oil

till only gas is in the valve. By using an Alltech high-pressure gas syringe Series A, size 10cc. take 3 cc. of gas sample. Throw away one cc. of gas and keep two cc of gas for chromatographic analysis by locking the syringe.

Step 5: Stop displacement at N_2 breakthrough. A rapid movement of the arrow of the wet test meter is one indication of N_2 breakthrough. A sharp reduction in the oil production rate is another indication. Chromatograph analysis to determine almost 100% N_2 is the ultimate indication.

The most important parameters that were recorded were:

1. Temperature at 4 points along the model (°F).
2. Barometric Pressure (mmHg)
3. Injection Pressure (Psi)
4. Outlet pressure (psi)
5. Time (min)
6. Oil recovery (cc)
7. Gas Produced (SCF)
8. Water saturation at initial condition (fraction)
9. Oil saturation at initial condition (fraction)
10. Pore volume (fraction)
11. GOR in solution in oil (Scf/stb)
12. Formation volumetric factor (Bbl/stb)
13. Oil Gravity (^{o}API)
14. Room temperature (^{o}F)
15. Time and crude oil recovery when the vapor samples are collected.

5. Procedure for Oil Recovery by Waterflooding

The procedure is similar to the displacement by Nitrogen except Step 1. In this case, Valves 3 and 4 in figure 8 are open and valve 5 must be open as well. The additional parameters that have to be recorded are: water injection and pressure drop. Because the injection rate of water was constant, the pressure drop is changing continuously.

6. Procedure for Oil Recovery by Propane Slug Drive by N_2

After the reservoir model is ready for displacements, a pre-calculated amount of low pressure liquid propane is transferred to a chamber which is able to withstand high pressure. By handling the appropriate valves, the propane chamber can be put in series in the injection line to the reservoir physical model. Then the propane is pushed into the reservoir model by nitrogen at high pressure. In general, the procedures are the same as described in section 5 and 6 for pure nitrogen and waterflooding but the only difference is the use of the propane chamber.

CHAPTER III

HEAT TRANSFER SIMULATION

In an effort to select a proper heating system for this research in order to keep the Reservoir Physical Model at constant desired temperature, a computer program was developed to simulate the heat transfer. A listing of the computer program and its subroutines are given in Appendix B. Also given is a listing of a sample output.

The transient heat transfer problem was solved in the simulation by considering steady state condition for an infinitesimal time increment. The program computes the total heat requirement for the system shown in Figure 10. The amount of heat is an essential factor in determining the heater size to be used according to the level of desired temperature and the insulation condition of the system under consideration.

Theoretical and Mathematical Basis of the Model

Two different options of heating method were studied and stimulated. Open flame heating was considered to be the first option where radiation plays the key role in heat transfer mechanism. As a second option the system was considered where forced convection heating plays the predominant role.

It may be noted that in the later option, when the thermo- statically controlled heater is cut-off, in that period, period, free convection and radiation become the dominant modes of heat transfer. Each of these modes of heat transfer was taken into consideration in detail in the computer model prepared for this investigation.

At the very outset of the program, the heating option is clearly specified for the program and the corresponding mode of heat is selected by the program to calculate the requirement may be observed frequently in the computer program.

Recurrence of the major heat transfer equations involved are observed frequently in the computer program.

Convection and radiation were found to be the significant modes of heat transfer within the Reservoir Physical mechanisms and used in the computer model are listed hereunder.

Radiation Mode:

The following equations are used for the radiant heat transfer mechanism (35).

$$Q_{rt} = A_f\ F_{ft}\ \sigma(T_f^4 - T_t^4)(\Delta\zeta) - Q_{\ell t} - Q_{\ell a} - Q_{tp} \qquad (1)$$

$$Q_{rp} = A_f\ F_{fp}\ \sigma(T_f^4 - T_p^4) - Q_{\ell p} \qquad (2)$$

Where:

$\Delta\zeta$ = Infinitesimal time increment (taken as 0.01 hour)

F_{ft} = View factor from flame to tube

F_{fp} = View factor from flame to pipe

A_f = Flame area

σ = Stefan-Boltzman constant = 0.1714×10^{-8} Btu/hr ft^2 °R^4

T = absolute temperature in °R

Q = heat loss during infinitesimal time increment

Subscripts:

a = ambient

rt = radiation from tube

rp = radiation from pipe

f = flame

t = tube

p = pipe

ℓt = loss from tube

ℓa = loss from air

tp = loss from tube to pipe

ℓp = loss from pipe

m = mean

pt = pipe to tube

The heat loss terms used in the right hand side of equation (1) and (2) are further defined as follows:

$$Q_{\ell t} = h_c A_t \ (t_t - t_m) \ (\Delta\zeta) \tag{3}$$

$$Q_{\ell a} = A_t \ \sigma(T_f^4 - T_a^4) \ (\Delta\zeta) \tag{4}$$

$$Q_{tp} = A_t F_{pt} \ (T_t^4 - T_p^4) \ (\Delta\zeta) \tag{5}$$

$$Q_{\ell p} = h_c \ A_p (T_p - T_a) \ (\Delta\zeta) \tag{6}$$

Where:

h_c = free heat transfer coefficient and mathematically is defined as:

$$h_c = (Nu)\ (k)/D \tag{6A}$$

Where:

k = Thermal conductivity of air

Nu = Nusselt number

$$Nu = 0.152\ Gr^{0.281} \tag{6B}$$

Gr = Grashof number

$$Gr = \rho^2 g\ \beta \Delta T\ D^3/\ \mu^2 \tag{6C}$$

Where:

g = gravitational constant

ρ = density of air

β = Temperature coefficient of volumetric expansion

μ = Viscosity of the air

Δt = Temperature differential

The above listed equations are used for purely radiant mode of heat transfer using an open flame heater.

As it was mentioned earlier, a second option of heating by using forced convection mode was also included in the computer model. In this second option, radiant heat transfer is also partly associated and given by the equation:

$$Q_{\ell t} = A_t\ \sigma(T_t^4 - T_a^4)\ (\Delta\zeta) \tag{7}$$

<u>Forced Convection</u>

The basic equation for heat transfer by forced convection is given by:

$$Q = h_{cf} A\Delta t \quad (8)$$

Where:

h_{cf} = forced convection heat transfer coefficient

Δt = temperature differential

The parameter "h_{cf}" in equation (8) is the most predominant factor in heat loss computa on, and to evaluate that factor the following correlation between Nusselt, Prandtl and Grashof numbers were used (35):

For turbulent flow:

$$N_u = 0.023\ [1.0 + (D/L)^{0.7}]\ R_e^{0.8}\ P_r^{0.33} \quad (9)$$

For Laminar flow:

$$h_{cf} = 0.229\ (k)\ (R_e^{.632}) \quad (10)$$

Where:

R_e = Reynold number

k = Thermal conductivity of the air.

Pipe and Tube Temperature Distribution

Equation used for calculating the current pipe and tube temperature are basic heat/energy balance equations given by:

Total Heat loss/Gain = (Mass)(Sp. Heat)(Temperature change) (11)

or

$$\Delta_t = \frac{Q}{mC_p} \quad (12)$$

$$T_{new} = T_{old} + \Delta T \quad (13)$$

Fundamental Definitions

Total heat required = Total heat loss + (MASS)(Sp. heat)*

(temperature rise of pipe, tube and core)

Total heat supplied = Total heat required + heat lost to the air in forced convection.

The block diagram of the main computer program for heat transfer simulation is shown in Figure 16. The subroutines are shown in Figure 17. As it was mentioned before, a listing of the program is given in Appendix B, also a list of all the symbols used in the elaboration of that program is given in Appendix C.

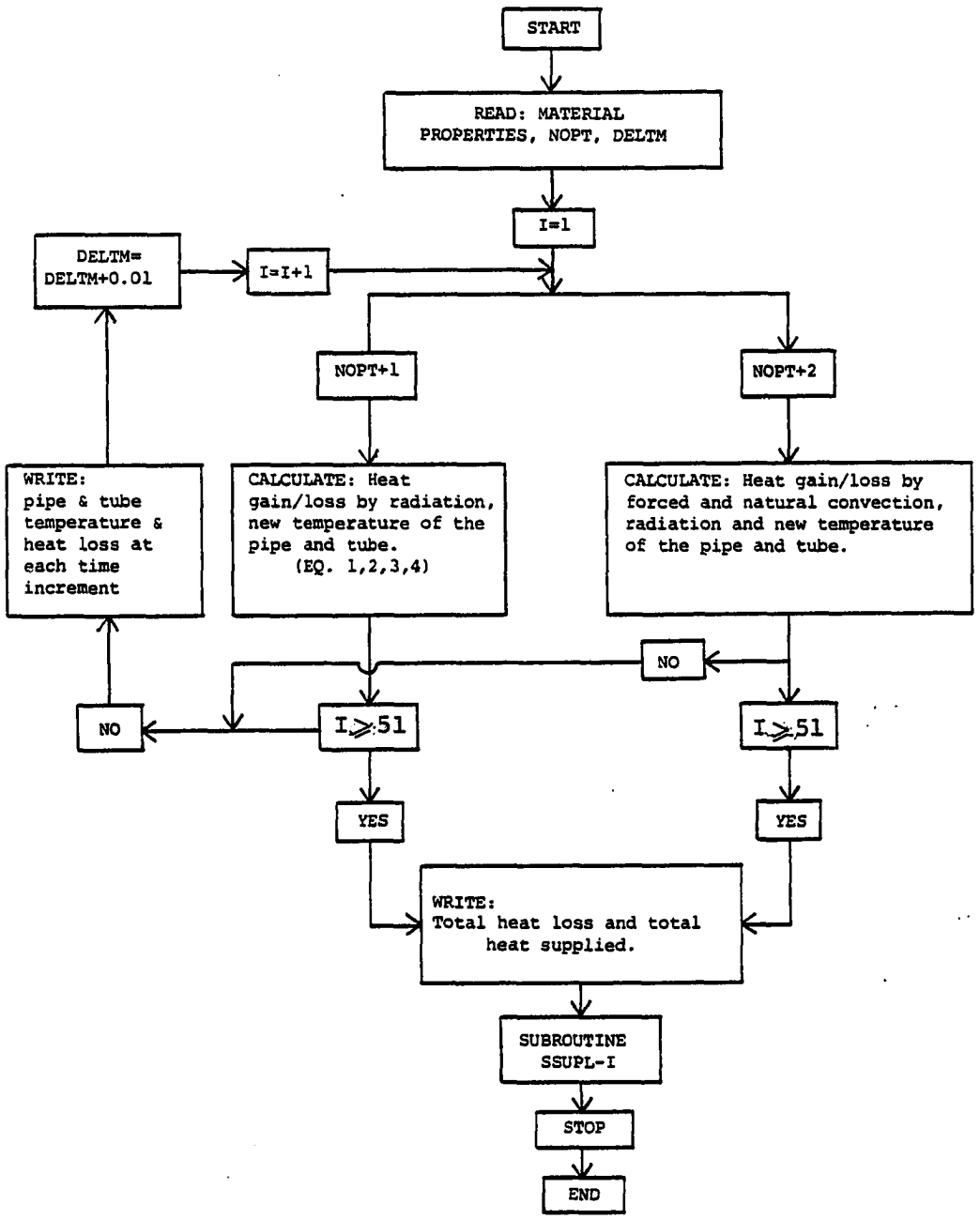

Figure 16. Block Diagram of the Main Program for Heat Transfer Simulation.

SUBROUTINE SSUPL-I

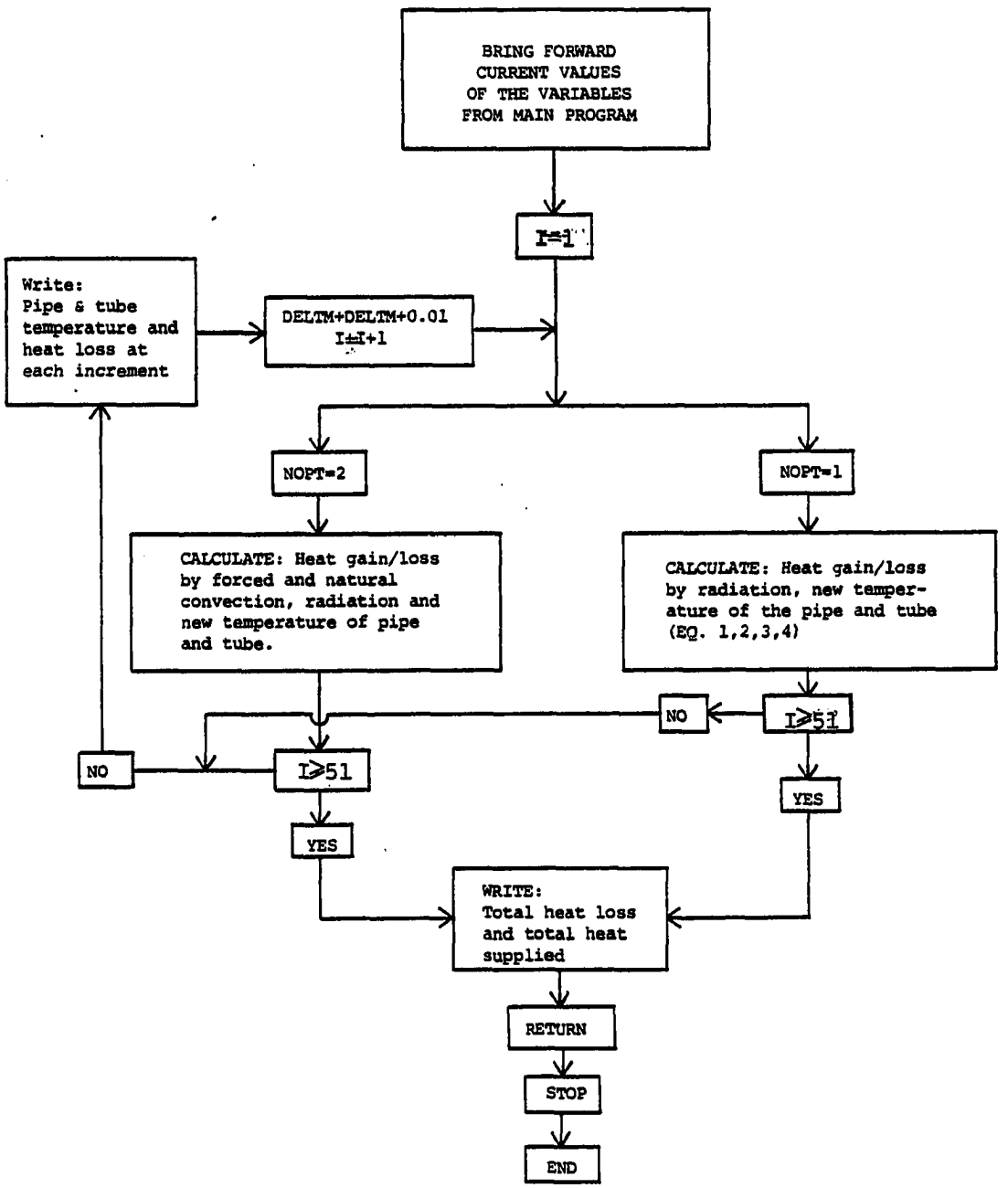

Figure 17. Block Diagram of Subroutine "SUPPL-I" for Heat Transfer Simulation.

CHAPTER IV

PRESENTATION AND DISCUSSION OF RESULTS

A. Analysis of Variables Used in this Study

This present study has been made in an effort to establish repeatibility based on the previous work (1) and to determine validity of the reservoir physical model available at Oklahoma University to perform this type of research, as well as to extend the understanding of the development of miscibility by multiple contact dynamic vaporization process when temperature and gas-oil ratio are the independent variables.

In this study, injection pressure was selected as a fixed variable because miscibility pressure or pressure effect on miscibility for a specific crude oil is a very well recognized fact in technical literature. Laboratory studies on miscibility pressure have been reported: in 1958, by Koch and Hutchinson (36) (Figure 3; in 1977, by Rushing et al (50, 51, 52) (Figure 4); in 1978, by Peterson (47); and by Ahmed (1) in 1980 (Figure 6). The miscibility pressure for the crude oil used in this study was clearly determined by Ahmed (1). For this reason, it was not practical to study and determine the miscibility pressure once more. It was considered

repetitious. The Injection pressure in all the experiments done in this study was fixed at 4000 psi. The outlet pressure was fixed at 2000 psi. Consequently, the rate of advance of the displacing front was supposed to be closely similar for all the tests. In the previous research the rate of advance of the displacement front was a dependent variable which was not taken into consideration for final evaluation of the results. In this study, for all practical purposes, this variable was considered fixed throughout all the experiments.

In general, the independent variables used in this study for all the experiments were pressures, temperature, gas-oil ratio in solution, water saturation and initial oil saturation. Pressure, temperature and GOR in solution were directly manipulated variables. The dependent variables were crude oil recovery, gas recovery and compositional changes in the second zone which will be described later.

No control or determination of relative permeabilities were made during the nitrogen displacement processes. This is a topic by itself that is worth being studied. The effect of gravity was theoretically reduced by using a very slim core with a diameter of 0.435 inches. The effect of possible spots of heterogeneities, along the core was theoretically minimized by using a long core with a length of 125 feet.

During the first six tests and test no. 9, the water saturations were immobile water. The effect of mobile water

was studied in tests no. 7 and 8. A crude oil of 42.4° API gravity recombined with natural hydrocarbon gas was used in all the tests; consequently, initial composition was a fixed variable.

B. Experimental Results

In this section, the results are presented experiment by experiment. The data analysis was focused on the displacement process based on production curves analysis, compositional vapor analysis, composition profiles, ternary diagrams and liquid and vapor intensive properties. Nine (9) dynamic displacement experiments performed in this investigation are presented. All these tests were conducted in a horizontal reservoir physical model described in the previous section and shown in Figure 8. The nine tests were distributed as follows: six (6) regular nitrogen displacement processes; one (1) regular water-flooding; one (1) tertiary recovery by nitrogen after regular water-flooding, and one (1) propane slug driven by nitrogen.

As is shown in Table 19, nine (9) experiments were conducted by using the same porous medium. This was saturated with water and crude oil with a gravity of 42.4° API. The crude oil was recombined with three different GORs in solution and two different temperatures. For practical purposes, in the discussion the low temperature (70°F), will be called cold condition and high temperature (120°F), will be called hot condition. The three GOR's used in these experiments

will be called low, medium and high GOR's for 200, 400 and 575 SCF/STB, respectively. The crude oil without recombined natural gas will be called dead oil.

B-1. First Experiment

The results obtained from the first high-pressure nitrogen injection test are presented in Table 5. All the parameters and conditions for this test are as follows:

Barometric Pressure	29.2"
Room Temperature.	72°F
Injection pressure.	4000-6000 PSI
Gas-Oil ratio in solution	575 SCF/STB
Crude Oil Saturation.	77% PV
Water saturation.	23% PV
Stock Tank oil in place	689.2 cc
Crude oil gravity	42.4° API
Volumetric Flow rate.	1.14 cc/min
Front Advance Velocity.	.237 cm/sec.
Formation Volumetric Factor	1.29 Bbl/STB

Table 5 shows the records of the time, cumulative crude oil recovery, fractional crude oil recovery, cumulative produced gas and outlet pressure. The total crude oil recovery was 83% of the stock tank oil in place.

This test was designed to check the statement that no significant additional recovery would be obtained above the miscibility pressure. The nitrogen injection pressure was varied from 4000 to 6000 psi in periods of 30 minutes. After

TABLE 5

HIGH-PRESSURE NITROGEN INJECTION
EXPERIMENT #1 DATA
Injection Pressure: 4000 PSIG

TIME (MIN)	CUM. OIL PRODUCTION (cc)	OIL RECOVERY % OOIP	CUM. PRODUCED GAS (SCF)	CUMULATIVE PRODUCED GOR (SCF/STB)	OUTLET PRESSURE (PSIG)
0	0	--	--	--	2000
56	58	.08	.21	575.5	2005
86	86	.12	.31	573	2010
155	158	.23	.57	573	2000
233	226	.33	.82	576	2000
311	328	.48	1.19	576	2000
350	385	.55	1.39	574	2000
389	470	.68	1.70	575	2000
450	540	.78	1.95	574	2000
467	560	.81	2.03	576	2005
500	572	.83	2.07	575	2000
			BREAKTHROUGH		
545	575	.831	7.08	1957	2000

each period the pressure regulator was reset at 6000 psi. The crude oil recovery obtained seems to agree very well with that conclusion drawn by the previous researcher (1).

A plot of crude oil recovery vs. time is shown in Figure 18. The 83% oil recovery strongly suggests that miscibility was achieved during the displacement. A change in shape is noted in the curve after producing 312 cc of crude oil. There is a definite increase in the slope; then the slope decreases after nitrogen breakthrough. This increment in displacement effectiveness may be explained by proposing that the displacing front becomes miscible with the virgin crude oil after being immiscible for a long section in the core.

Unfortunately, an unexpected electrical problem in the chromatograph recorder did not permit obtaining vapor chromatograph analysis during the nitrogen displacement. However, the result suggested that the reservoir physical model produced very good repeatability when compared with Ahmed (1) results.

Figure 19 shows the produced gas versus crude oil recovery. In this figure there can be noted a similar change of shape in the curve as was noted in Figure 18.

In Figure 20 is shown the produced gas-oil ratio as a fraction of oil recovery. The shape of this curve shows that there is small variation in the produced gas-oil ratio. This is in agreement with Rushing et al (50,51,52) and Ahmed (1).

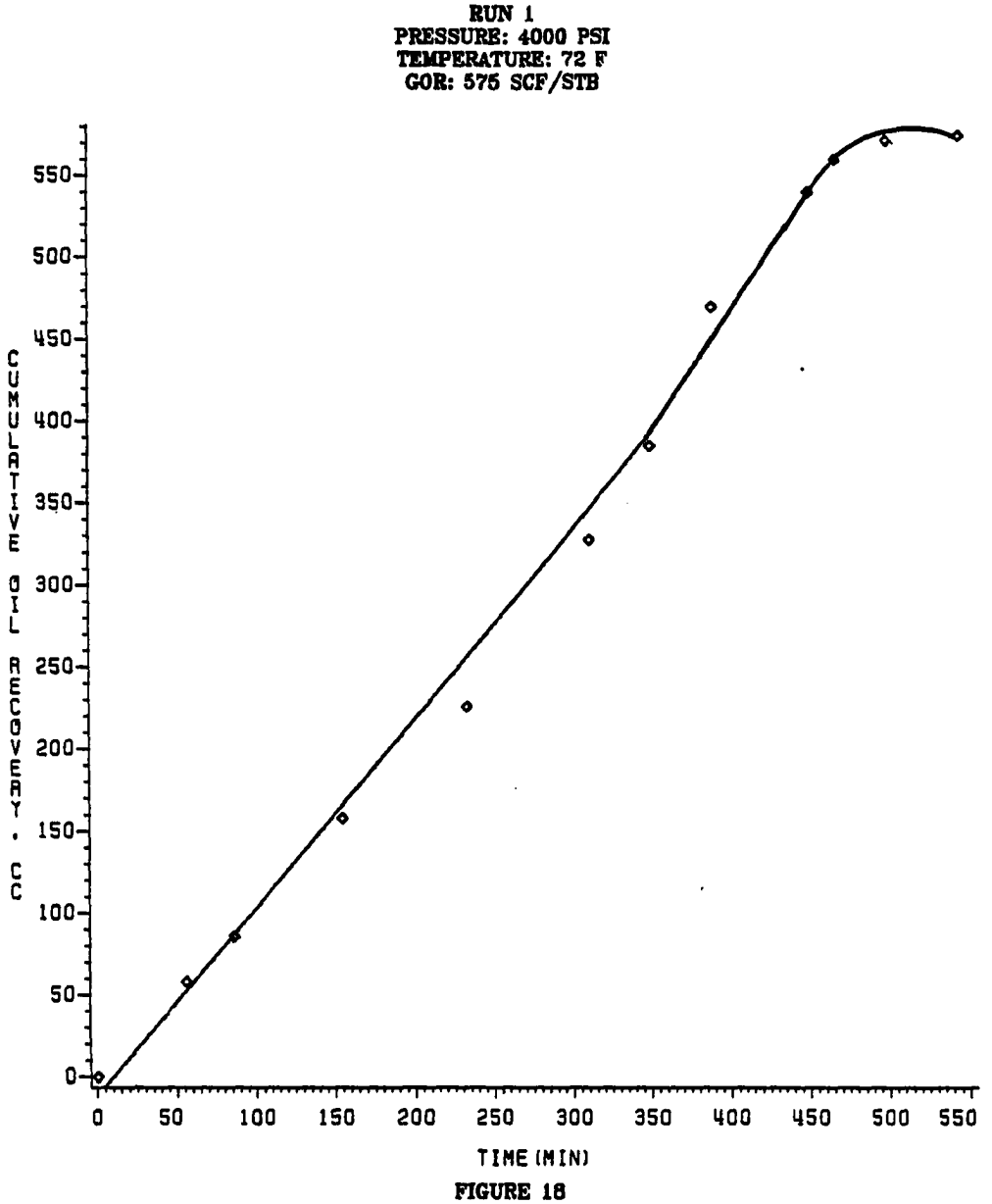

FIGURE 18

CUMULATIVE OIL RECOVERY VS TIME

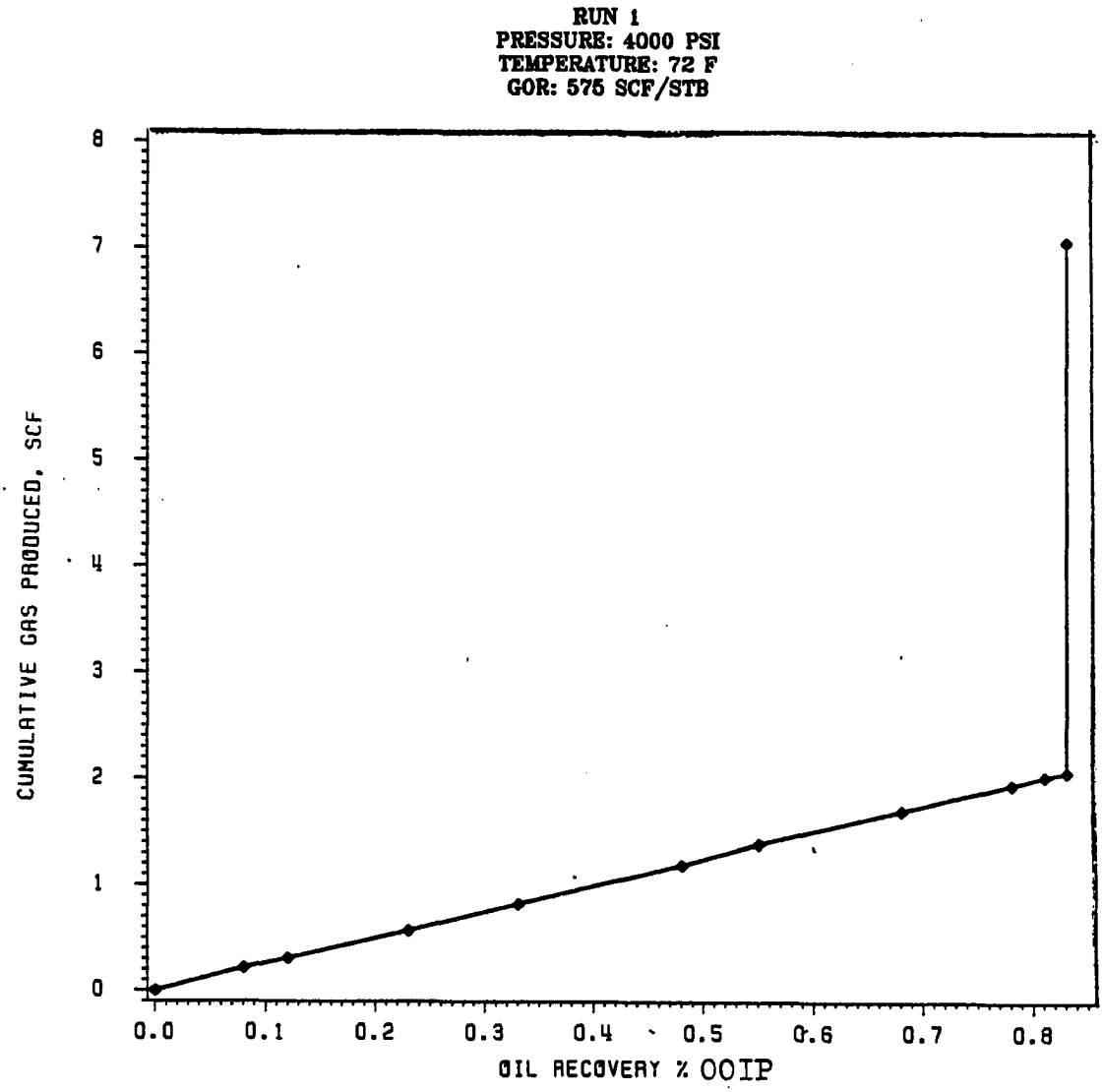

FIGURE 19
CUMULATIVE GAS PRODUCED VS OIL FRACTION RECOVERY

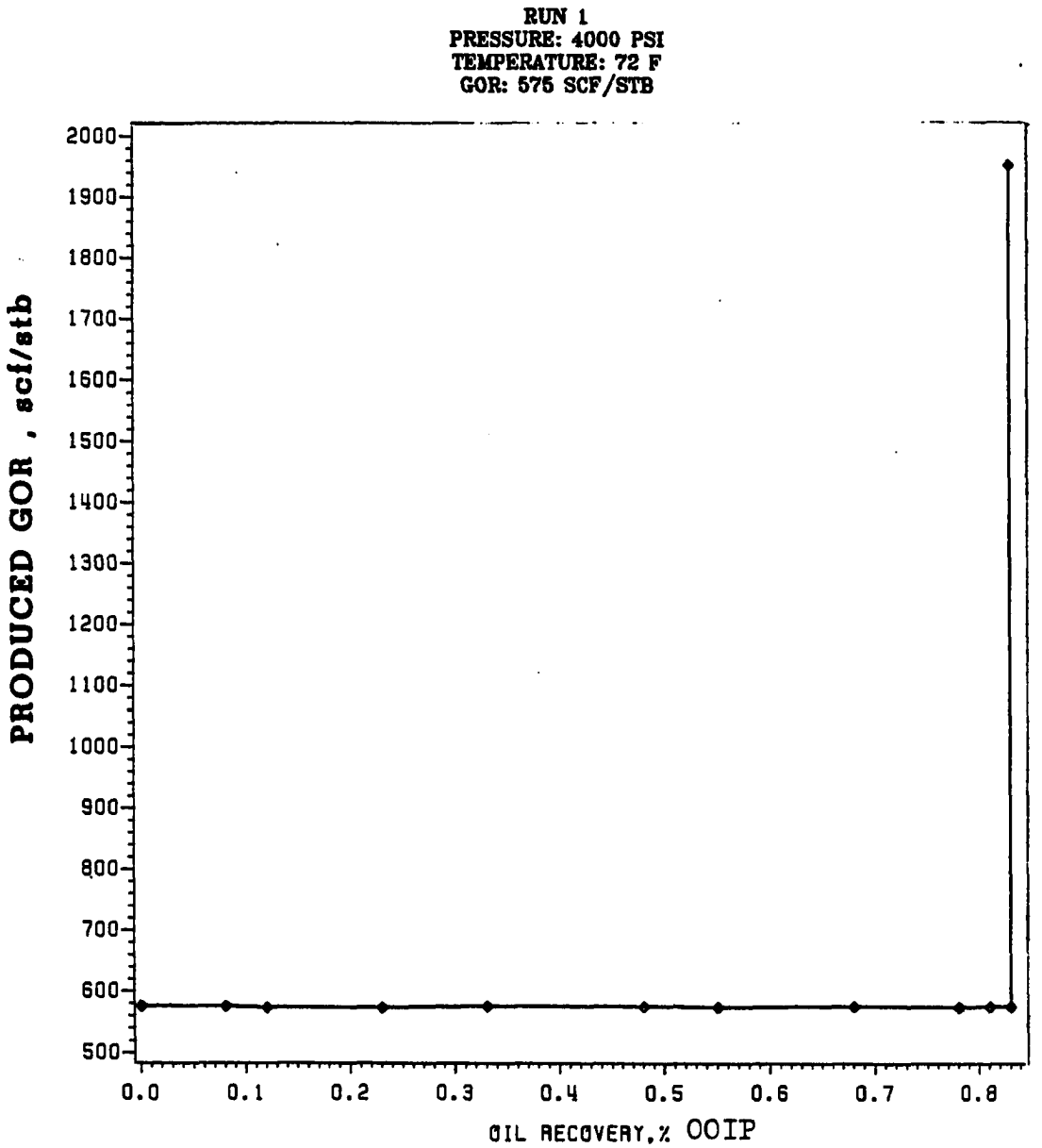

FIGURE 20
PRODUCED GOR VS OIL RECOVERY

This almost constant value of the produced GOR strongly suggests that all the oil that was recovered from this test was not affected from a compositional point of view by nitrogen injection. The °API gravity of the recovered oil was the same as before the test. This confirmed that the produced oil has not contacted with nitrogen and has not undergone any compositional change during displacement at breakthrough.

B-2. Second Experiment

This second test was designed to establish repeatability and validity of the reservoir physical model used in this study. Also, this test will be used in the comparative analysis with future tests to study the effect of temperature and gas-oil ratio in solution on crude oil recovery and the miscibility process in nitrogen injection.

During this test, the pressure regulator was set at 4000 psi. This test was a normal test where no problems were reported. The production data obtained in this test are presented in Table 6.

The greatest concern during this test was the taking of vapor samples and their chromatographic analysis. Thirteen vapor samples were taken from the different sampling points along the reservoir physical model shown in Figure 8. The results of the chromatographic analysis of vapor samples are shown in Table 7.

The test was run under the following parameters and conditions:

Barometric Pressure	28.70" Hg.
Room Temperature.	69.5°F
Injection Pressure.	4000 psi
Solution Gas-Oil Ratio.	575 SCF/STB
Crude Oil Saturation.	76.4% PV
Water Saturation.	23.6% PV
Stock Tank Oil in Place	42.4° API
Front Advance Velocity.	.115 cm/sec
Formation Volumetric Factor	1.29 Bbl/STB

During this test, the following steps were made to gather and evaluate the experimental data:

a) Vapor samples were taken from the displacing phase during the recovery process and analyzed by means of the chromatograph. Then the vapor molal fractions were plotted compound by compound as a function of Pore Volume of Nitrogen injected. Figures 24, 25, 26 and 27 show vapor molal fraction by compound as a function of PV nitrogen injected. Each figure along the reservoir physical molel.

b) Produced gas and oil were measured periodically. Production history of this test is presented in Figures 21, 22 and 23.

c) Calculation of liquid molal fraction using experimental values of vapor molal fraction.

d) Representation of the displacement process by nitrogen injection by a ternary diagram.

TABLE 6

HIGH PRESSURE NITROGEN INJECTION
- EXPERIMENT #2
Injection Pressure : 4000 PSIG

TIME (MIN)	CUMULATIVE OIL PRODUC. (CC)	OIL RECOVERY (% OOIP)	CUMULATIVE PRODUCED GAS (SCF)	OUTLET PRESSURE (PSIG)
0	--	--	--	2000
20	21	0.034	.08	2000
30	30	0.048	.11	2000
60	56	0.090	.20	2010
90	83	0.134	.30	2000
120	108	0.174	.39	2005
150	136	0.219	.49	2000
175	160	0.257	.58	2000
200	183	.294	.66	2000
240	220	.354	.80	2010
255	232	.373	.84	2000
300	272	.438	.98	2000
330	303	.487	1.10	2000
345	316	.508	1.14	2005
390	356	.573	1.29	1995
420	384	.618	1.39	2000
450	412	.663	1.49	2000
480	436	.676	1.57	2000
495	454	.730	1.64	2005
510	480	.766	1.74	2000
540	502	.798	1.87	2000
550	503	.809	1.90	2000
				N_2 BREAKTHROUGH
585	504	.811	12.5	2000

TABLE 7: CHROMATOGRAPH ANALYSIS OF VAPOR SAMPLES - EXPERIMENT #2

TEMPERATURE: 69.5°F:INJECTION PRESSURE: 4000 PSI; GOR: 575 SCF/STB

	SAMPLE$_A$ AT POINT			SAMPLE$_B$ AT POINT			SAMPLE$_C$ AT POINT			SAMPLE$_D$ AT POINT			
PV OF N2 INJECTED (%)	15	17	26	30	45	50	55	65	72	74-80	82	85	90
N_2	52.3	71.9	87.7	33.2	60.65	84.14	27	53.00	80.94	8.5	14.8	42	87.55
C_1	30.1	18.06	7.2	45.1	22.1	7.2	40.2	27.2	11.4	52.26	50.3	35	6.1
C_2	6.1	4.21	2.8	8.1	7.2	5.05	13.4	6	1.0	14.3	12.1	8.2	2.1
C_3	3.54	2.4	1.1	6.1	5.05	.27	9.5	6.0	4.5	10.8	9.5	6.2	2.3
C_4	2.17	.41	.2	1.2	.8	.05	1.6	1.1	.16	1.8	1.75	1.1	0.35
N-C_4	2.25	1.19	.5	1.4	.75	.15	1.6	1.2	.15	1.81	1.70	1.2	0.45
C_5	.58	.35	.1	.61	.25	.01	.8	.57	.00	1.42	1.1	.7	.15
N-C_5	1.05	.45	.1	.45	.15	.00	.9	.85	.00	1.32	1.25	.5	.15
C_6+	1.91	.95	.3	3.85	2.75	.65	5.1	.42	.18	7.8	7.5	5.1	.85

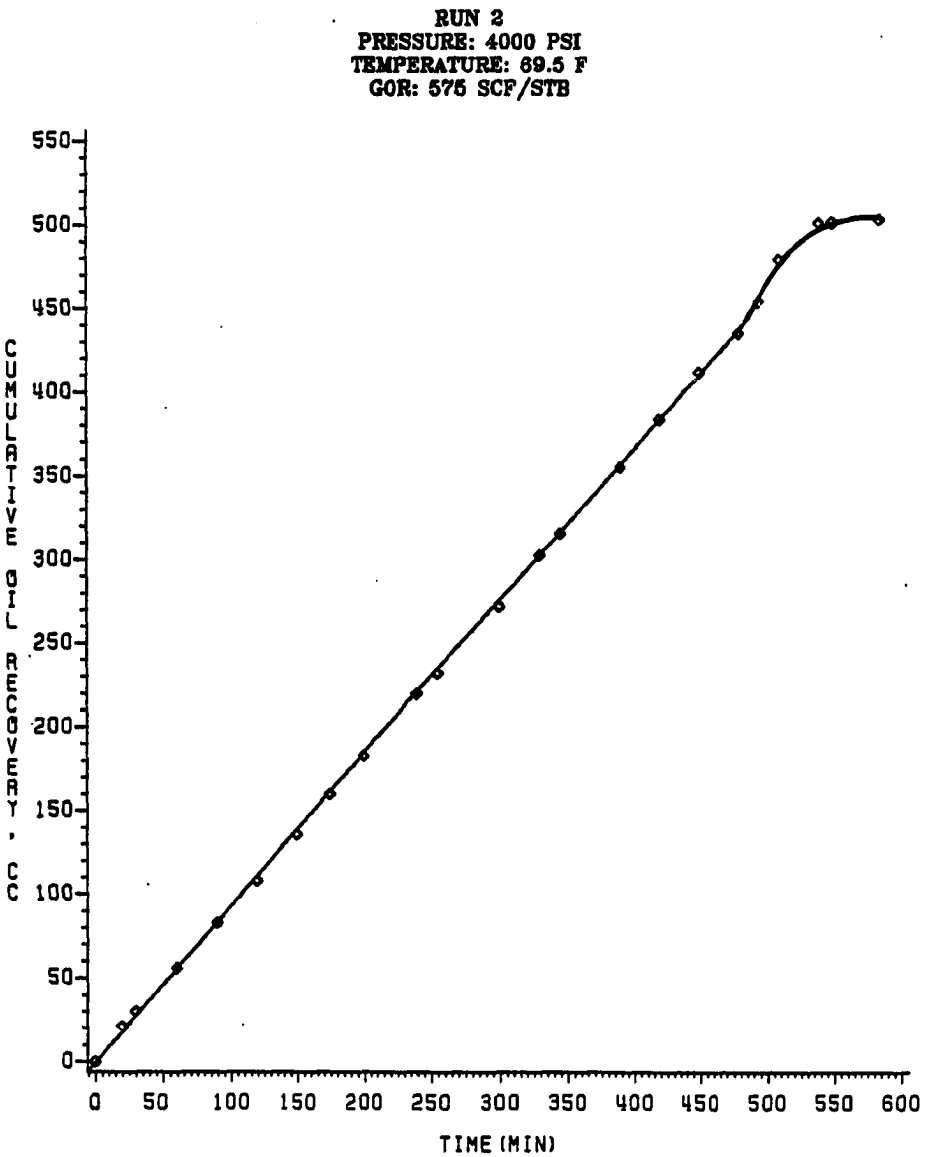

FIGURE 21
CUMULATIVE OIL RECOVERY VS TIME

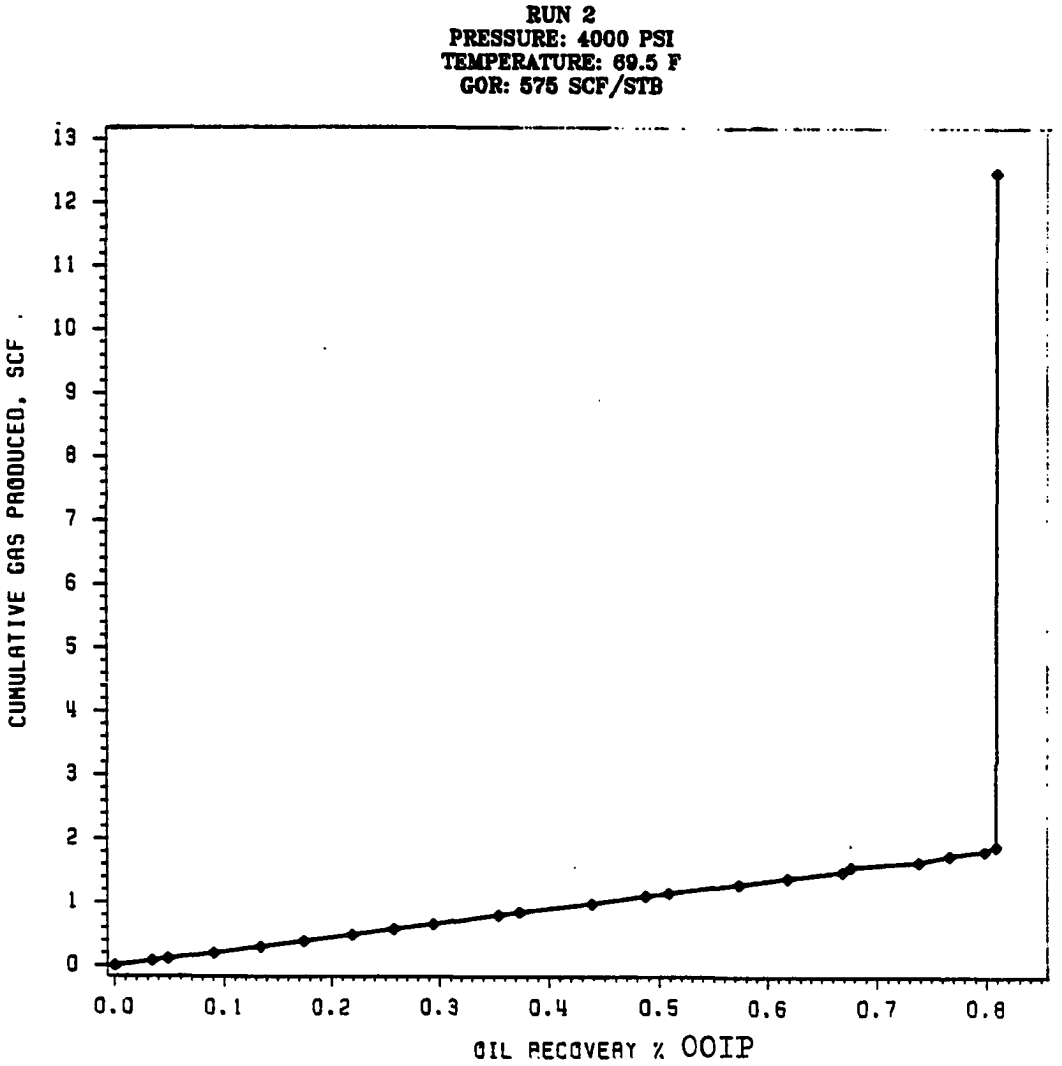

FIGURE 22
CUMULATIVE GAS PRODUCED VS OIL RECOVERY

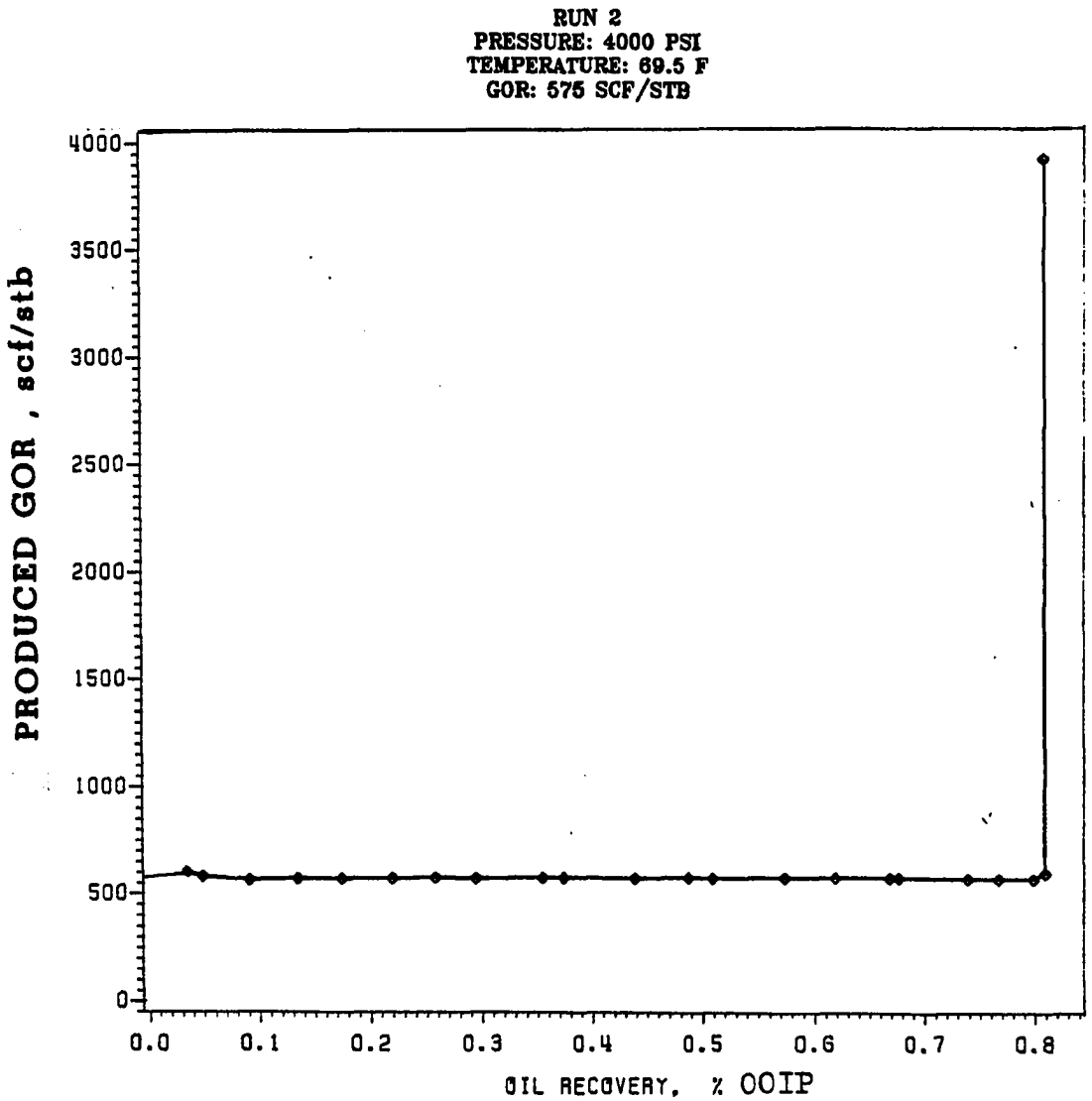

FIGURE 23
PRODUCED GOR VS OIL RECOVERY

e) Calculation of liquid and vapor phase intensive properties.

The analysis of results obtained from the proper evaluation of sections a, b, c, d and e made from the experiments in this research show very clearly that three zones exist in the displacement of reservoir light crude oil by nitrogen injection. These zones are:

1. A virgin zone which is the leading zone during the displacement.
2. The second zone which is a two-phases flowing zone.
3. The third zone which is one-phase flowing zone.

The first zone was identified in this experiment by analysing the results obtained from produced fluids, gas and liquid. Figure 23 shows that the produced GOR is almost constant during all the displacement process until nitrogen breakthrough when the curve increased sharply. The original reconstituted gas in solution of the crude oil is almost similar to the produced GOR.

The second zone identified in this test was a two-phase flowing zone. In all the experiments with injection of pure nitrogen, even though with the most favorable conditions for miscibility, this two-phase zone was detected. This zone is the result of the nitrogen being initially immiscible with the reservoir light crude oil.

Analysis of the shape of compositional profiles curves (Figures 24, 25, 26 and 27) suggested that vaporization is

very strong at the beginning of the process and at the leading edge of the second zone. The slopes of the straight lines of the compositional profiles (Figures 24, 25, 26, 27) are a direct consequence of the vaporization rate. It can be observed that at point A the slope is -5.50% Molal fraction/% PV N_2 injected. At the point B, slope is -1.00% Molal fraction/% PV N_2 injected and at point C, is -.3% Molal fraction/% PV N_2 injected. This suggests that the vaporization process decreases as long as the displacing front advanced. That suggests that the vapor will need more length after a while to strip the same amount of intermediates from the crude oil. This phenomenon suggested that providing more intermediates in the first portion of the reservoir physical model would sharply reduce the immiscible displacement length and increase displacement efficiency.

The content of C_{1-5} increases very sharply when 20% of the total available length has been covered. Then the vaporization process decreases during the rest of the displacement. That implies the initial composition of the crude oil is an important factor which affects initial equilibrium in relation with the nearness to the critical point. The critical point is defined as the point at which the vapor and liquid phases become continuously identical. In this test, miscibility was postulated after no change in the composition of the front was detected. In Figure 27 miscibility is shown when the slope of the compositional profile is zero. In this test,

miscibility was detected at the sampling point D between 76% and 82% PV N_2 injected (Figure 27). From the same figure, the size of the miscible bank can be estimated. In this test, the miscible bank was approximately 6% PV.

The miscibility process was monitored by constructing ternary diagrams. In order to construct the ternary diagrams it was necessary to calculate the liquid molal composition of the second and third zones at different intervals of time at different points along the core. In order to calculate liquid molal fraction, the convergence pressure approach was used. This method is explained step by step in Appendix F.

The ternary diagrams illustrating the building up of miscibility for this test are shown in Figures 28, 29, 30 and 31. From the results obtained at point A, it is possible to approxmiately predict the composition of the miscible bank if this were to be created during the displacement. The composition of the miscible bank is shown in the Figure 31.

The original prediction of the composition of the miscibility bank according to Figure 28 at sampling point A was different from the actual composition. This is due to the fact that this prediction is a gross approximation because the ternary diagram is not accurate from a thermodynamic point of view. On the other hand, the hydrocarbon liquid molal fraction is just a calculated approxmiation. Analyzing liquid samples taken during the displacement would improve this prediction. The ternary diagrams obtained in this test have

shown very clearly that the development of miscibility by high-pressure nitrogen injection can be visualized conceptually with ternary phase diagrams constructed from pseudo-components: Nitrogen, Methane through pentane and hexane plus. The generation of miscibility by injection of an inert gas to displace a crude oil is explained in Appendix G and discussed in this chapter by using the traditional ternary diagram approach used by different authors in the technical literature.

Theoretically, miscibility is reached when all the intensive properties such as density and viscosity in the liquid phase are similar to density and viscosity in the vapor phase respectively and surface tension is zero. The density of the liquid and vapor phases were plotted in Figures 32 to 35. By analyzing these figures it is possible to visualize the mechanisms by which oil and nitrogen change in composition; the oil becoming poorer in intermediates and increasing its viscosity, density and molecular weight; and on the other hand, the vapor increasing its viscosity and density. This type of plotting, properties vs. % PV nitrogen injected, can be used to predict miscibility. Figures 32 to 39 show how properties changed during a displacement process by high pressure nitrogen injection during different conditions in this research.

As it is shown in Figure 40, the interfacial tension never reaches the theoretical value of zero. This suggests

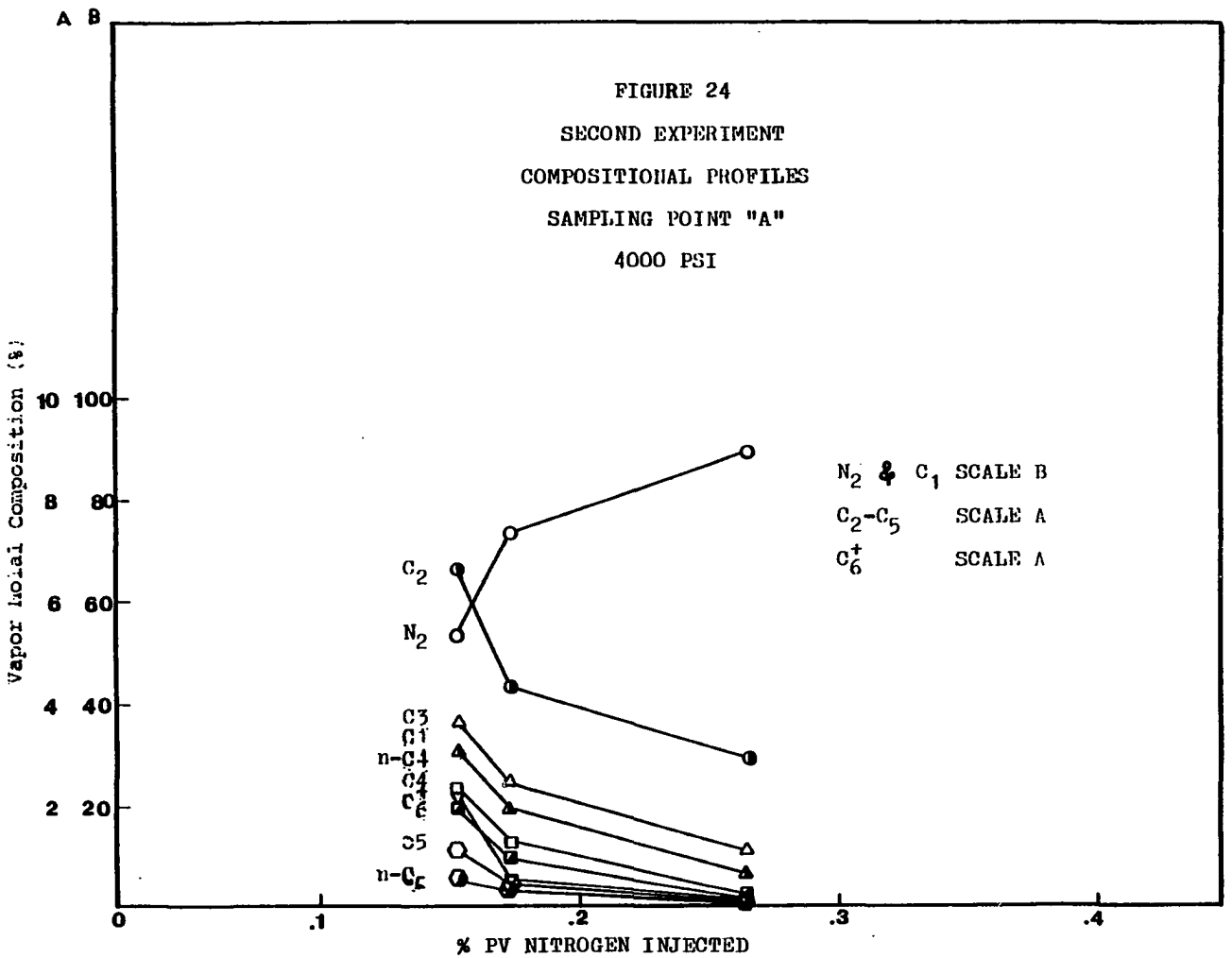

FIGURE 24

SECOND EXPERIMENT

COMPOSITIONAL PROFILES

SAMPLING POINT "A"

4000 PSI

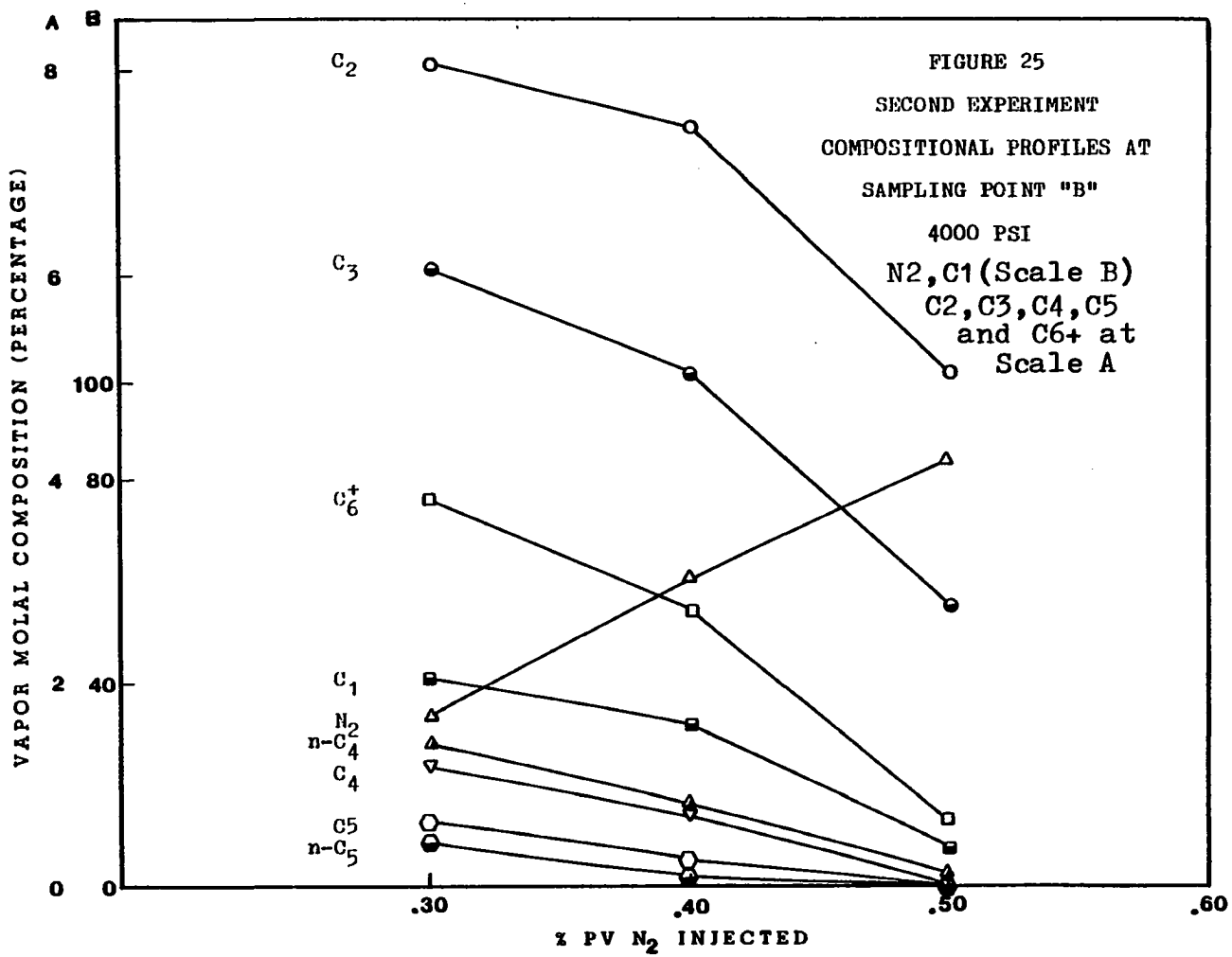
FIGURE 25
SECOND EXPERIMENT
COMPOSITIONAL PROFILES AT
SAMPLING POINT "B"
4000 PSI
N2,C1(Scale B)
C2,C3,C4,C5
and C6+ at
Scale A
A
B
8
6
100
4
80
2
40
0
0
C_2
C_3
C_6^+
C_1
N_2
n-C_4
C_4
C5
n-C_5
.30
.40
.50
.60
% PV N_2 INJECTED
VAPOR MOLAL COMPOSITION (PERCENTAGE)

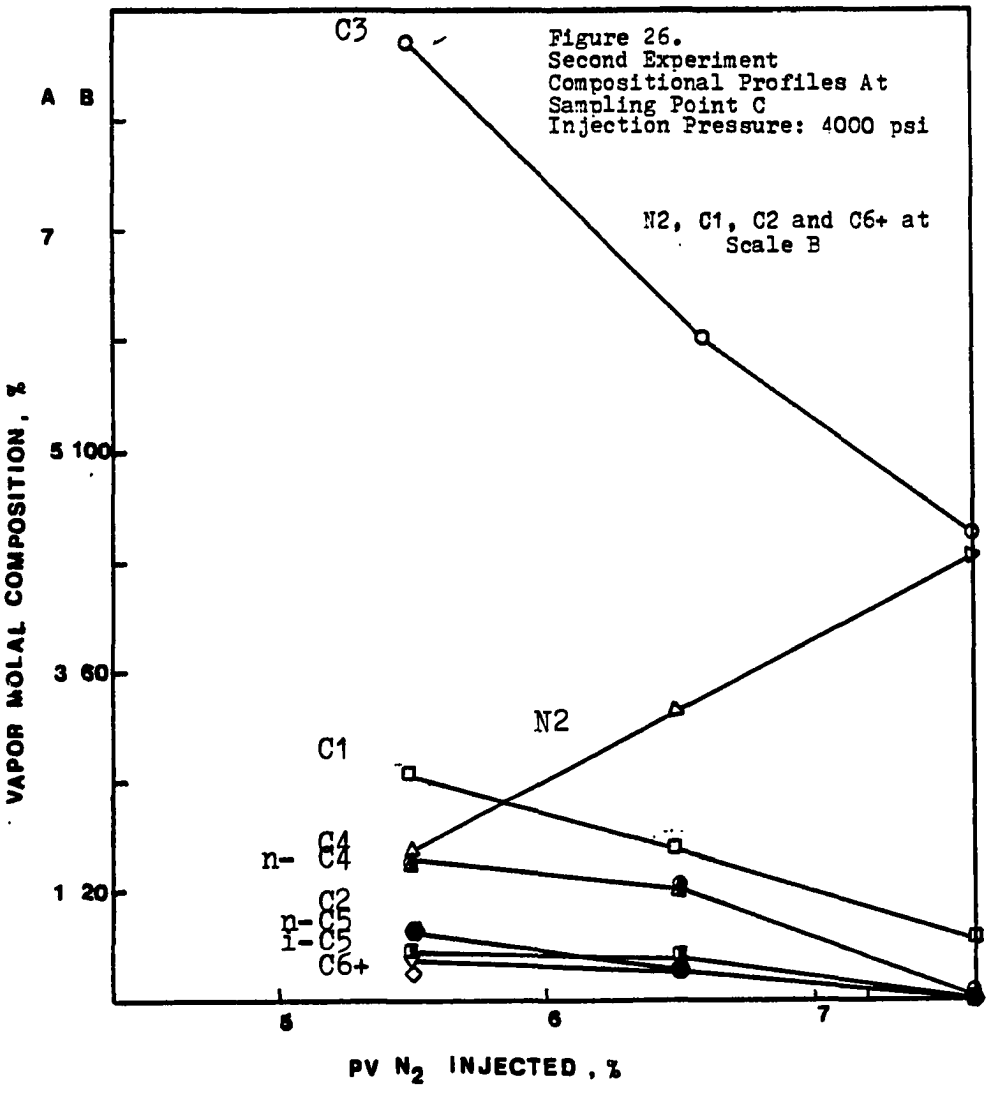

Figure 26.
Second Experiment
Compositional Profiles At
Sampling Point C
Injection Pressure: 4000 psi

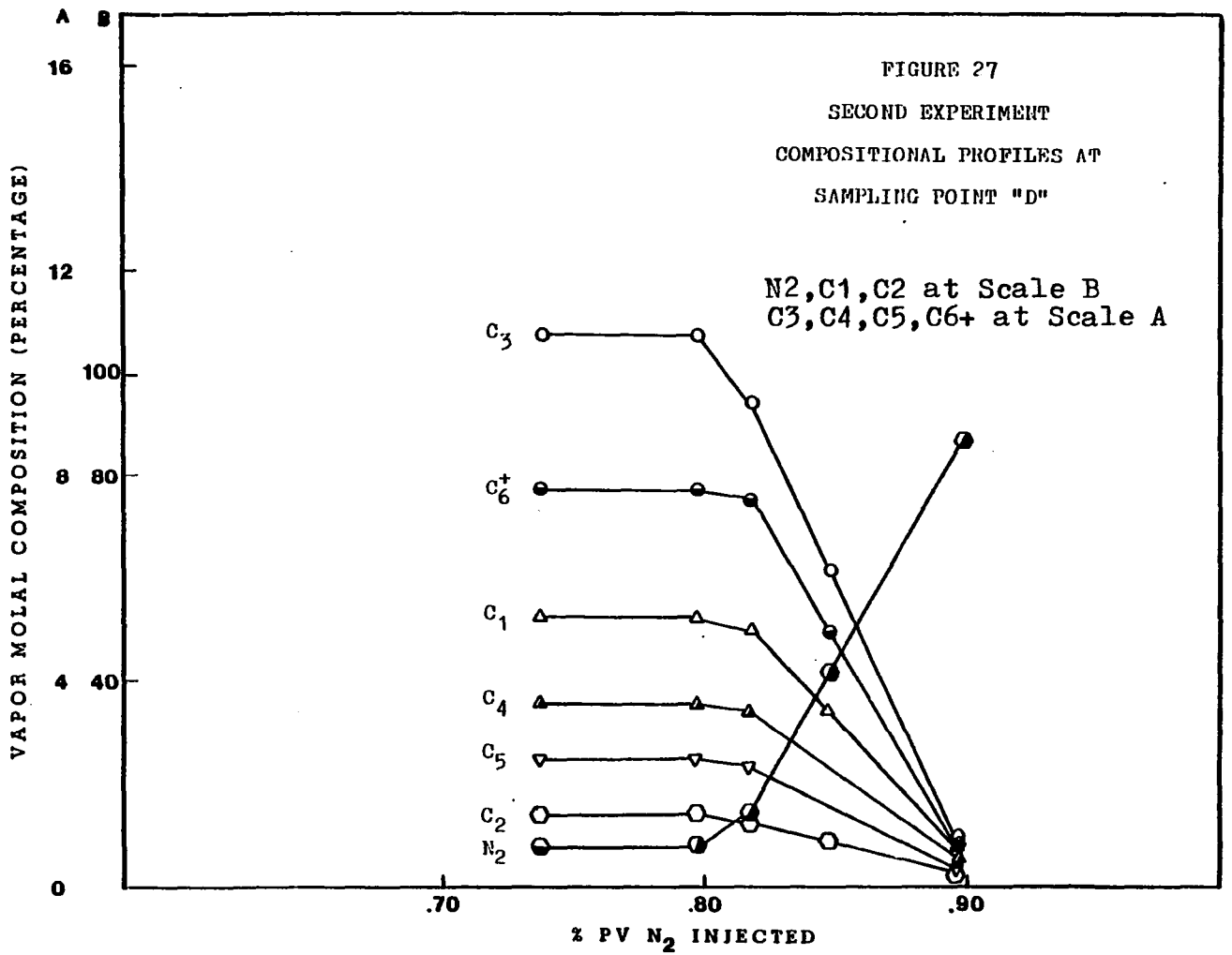

FIGURE 27

SECOND EXPERIMENT

COMPOSITIONAL PROFILES AT

SAMPLING POINT "D"

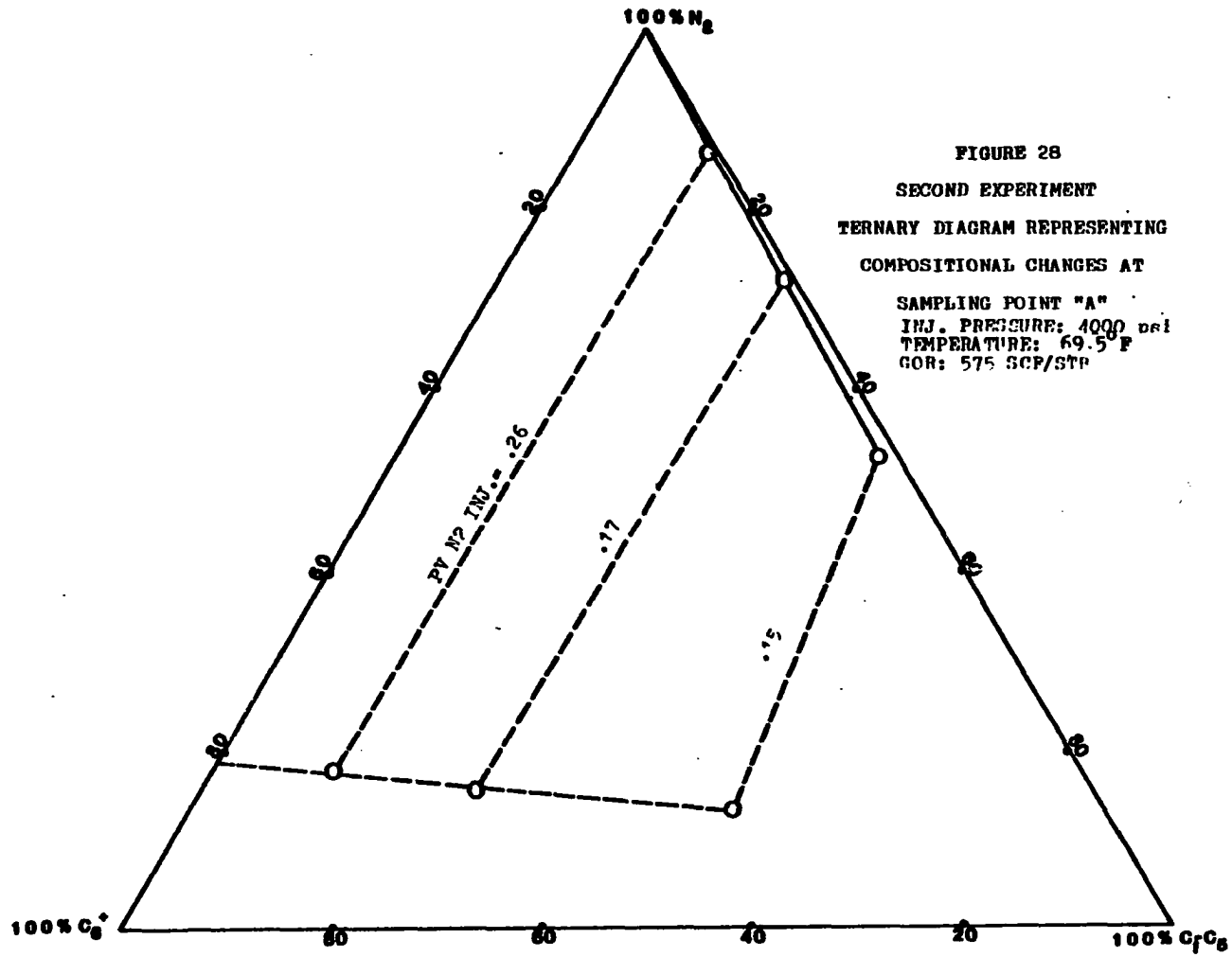

FIGURE 28

SECOND EXPERIMENT

TERNARY DIAGRAM REPRESENTING

COMPOSITIONAL CHANGES AT

SAMPLING POINT "A"

INJ. PRESSURE: 4000 psi
TEMPERATURE: 69.5°F
GOR: 575 SCF/STB

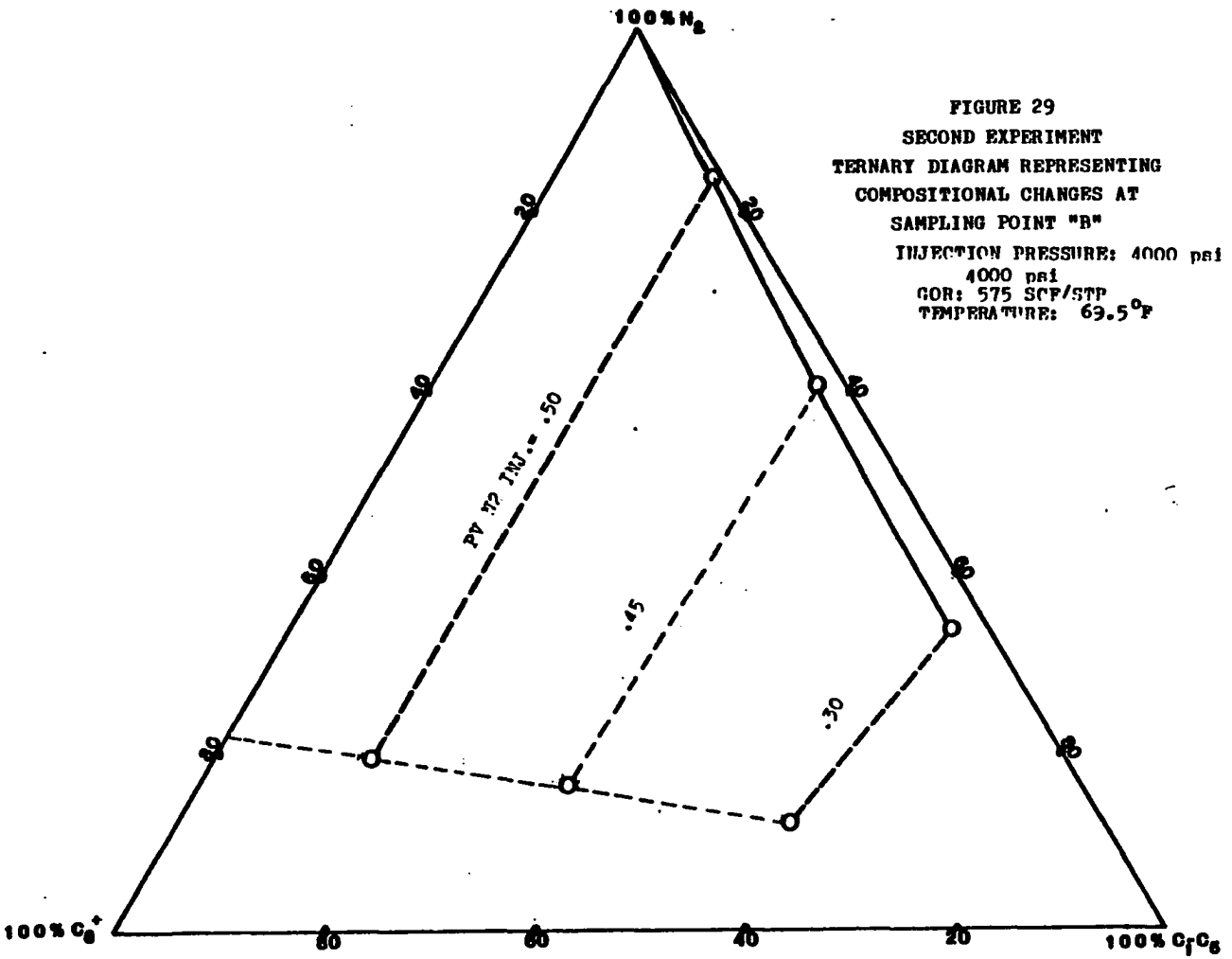

FIGURE 29
SECOND EXPERIMENT
TERNARY DIAGRAM REPRESENTING
COMPOSITIONAL CHANGES AT
SAMPLING POINT "B"
INJECTION PRESSURE: 4000 psi
4000 psi
GOR: 575 SCF/STB
TEMPERATURE: 69.5°F

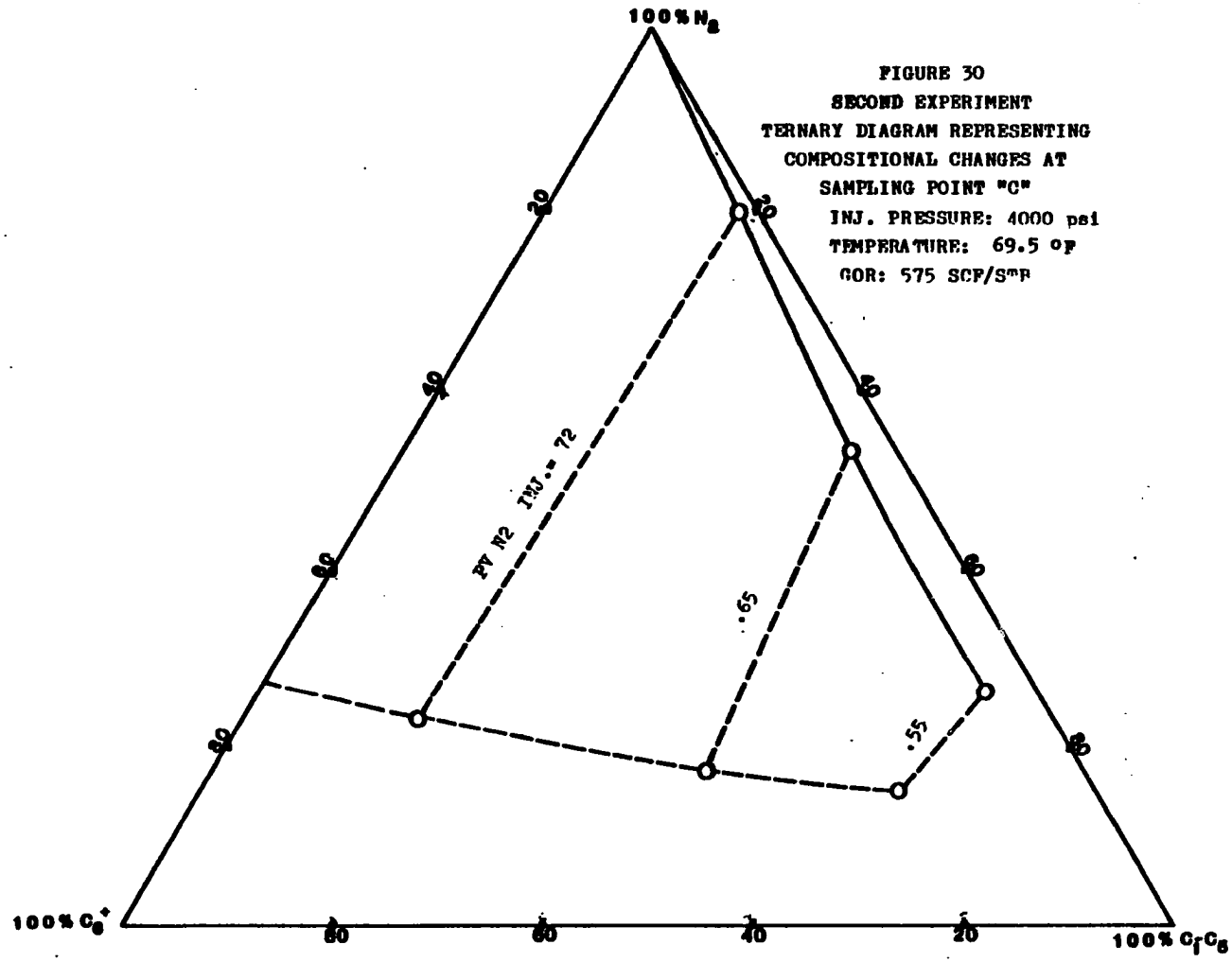

FIGURE 30
SECOND EXPERIMENT
TERNARY DIAGRAM REPRESENTING
COMPOSITIONAL CHANGES AT
SAMPLING POINT "C"
INJ. PRESSURE: 4000 psi
TEMPERATURE: 69.5 °F
GOR: 575 SCF/STB

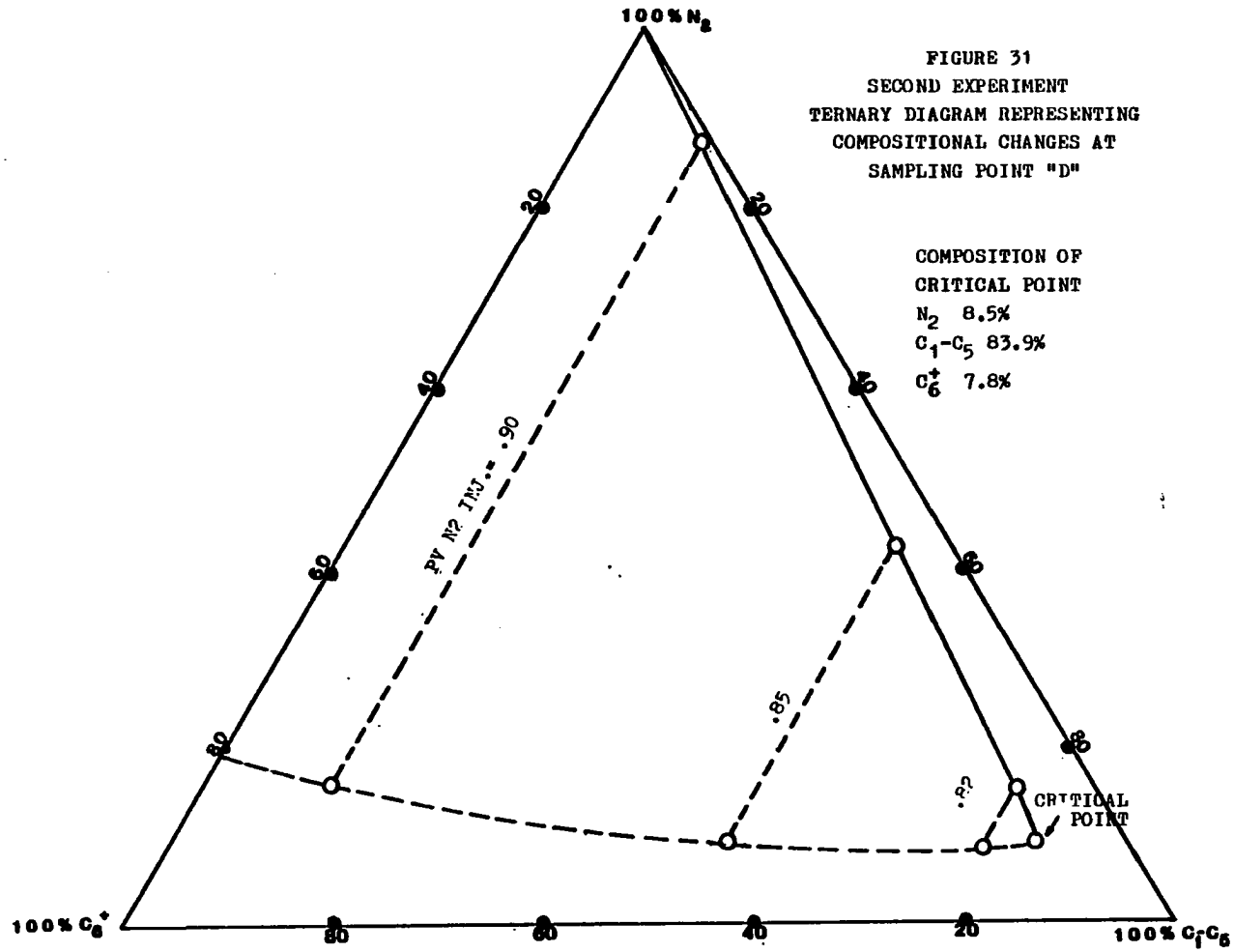

FIGURE 31
SECOND EXPERIMENT
TERNARY DIAGRAM REPRESENTING
COMPOSITIONAL CHANGES AT
SAMPLING POINT "D"

COMPOSITION OF
CRITICAL POINT
N_2 8.5%
C_1-C_5 83.9%
C_6^+ 7.8%

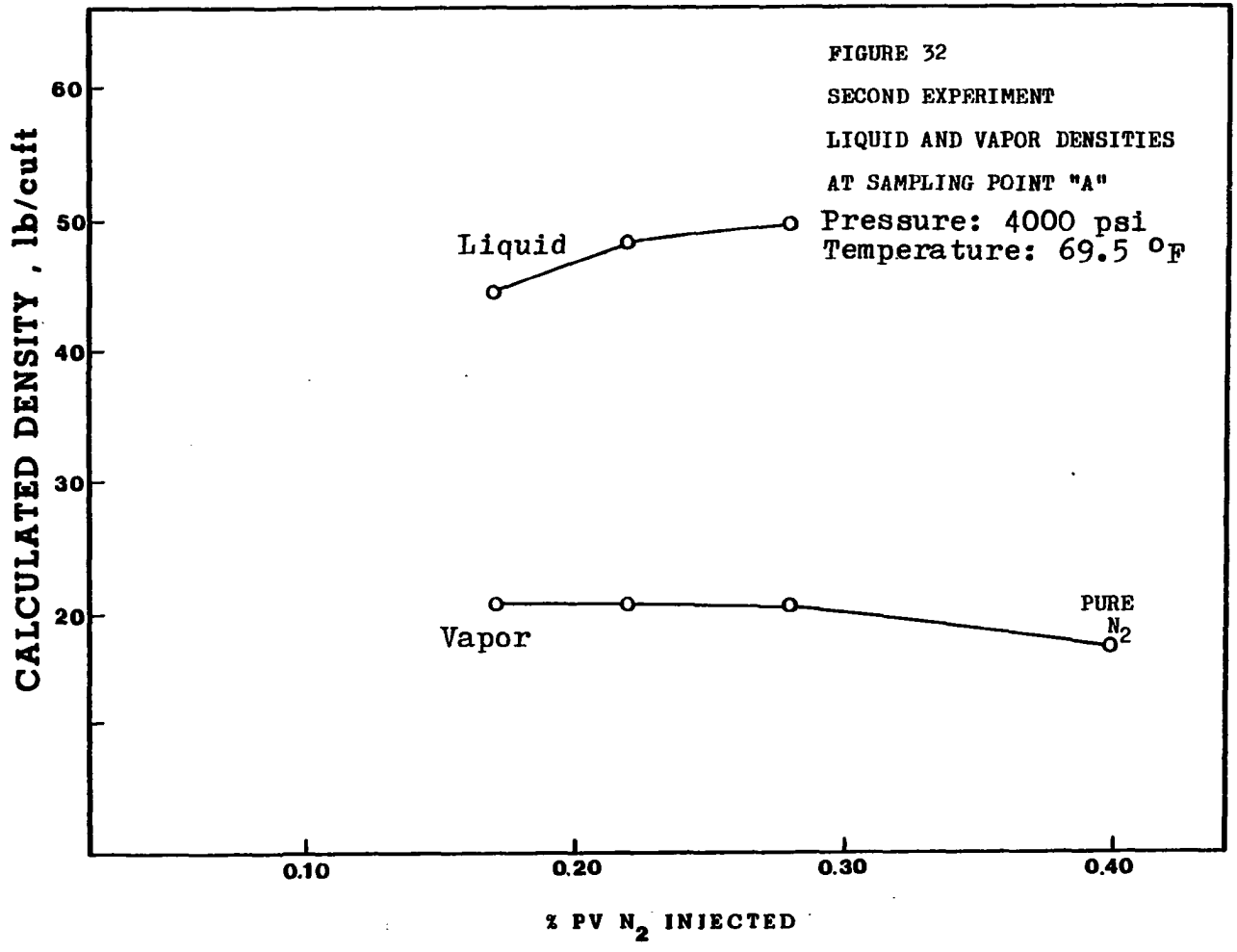
FIGURE 32
SECOND EXPERIMENT
LIQUID AND VAPOR DENSITIES
AT SAMPLING POINT "A"
Pressure: 4000 psi
Temperature: 69.5 °F
Liquid
Vapor
PURE N_2
CALCULATED DENSITY , lb/cuft
60
50
40
30
20
0.10
0.20
0.30
0.40
% PV N_2 INJECTED

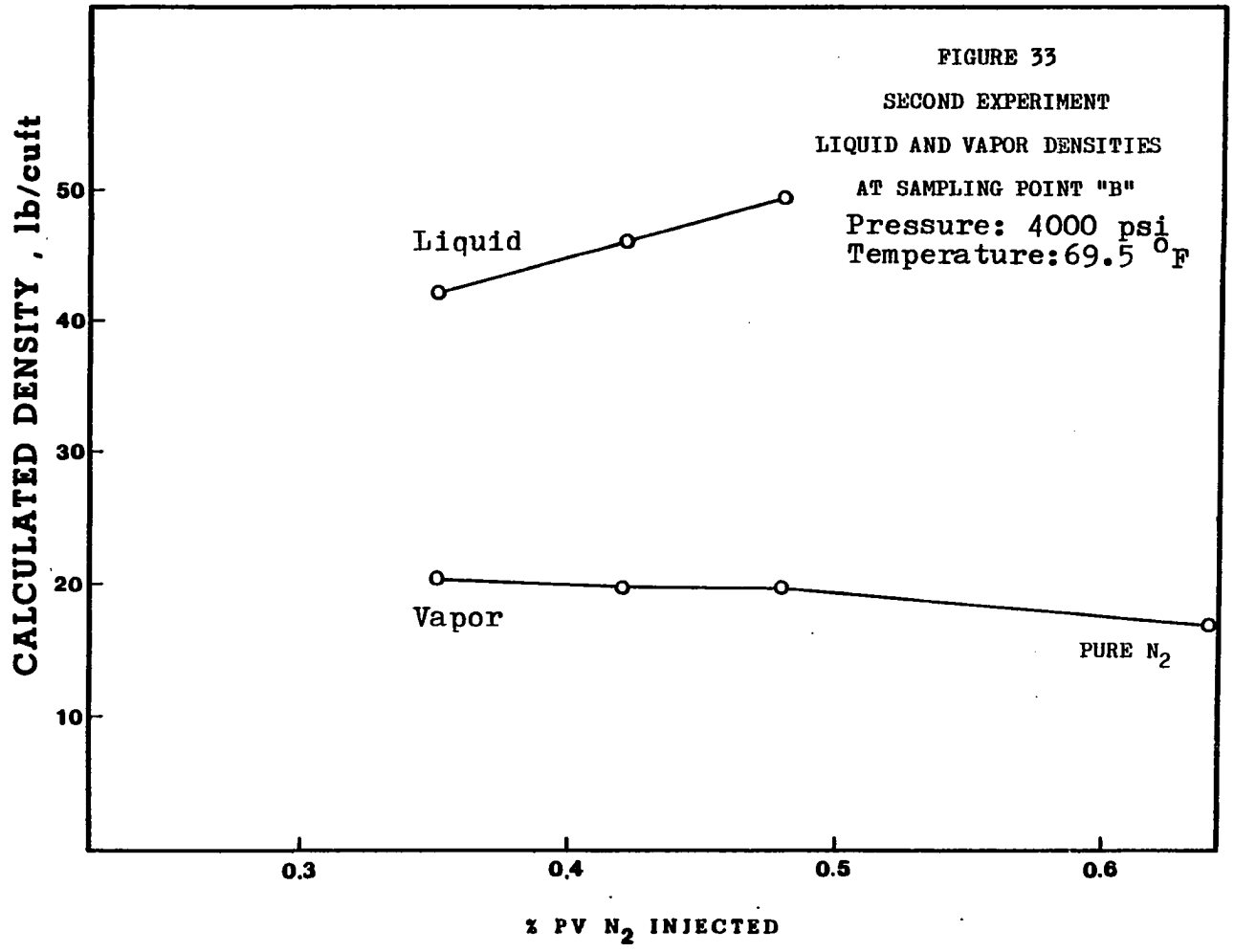
FIGURE 33
SECOND EXPERIMENT
LIQUID AND VAPOR DENSITIES
AT SAMPLING POINT "B"
Pressure: 4000 psi
Temperature: 69.5 °F
Liquid
Vapor
PURE N_2
CALCULATED DENSITY , lb/cuft
50
40
30
20
10
0.3
0.4
0.5
0.6
% PV N_2 INJECTED

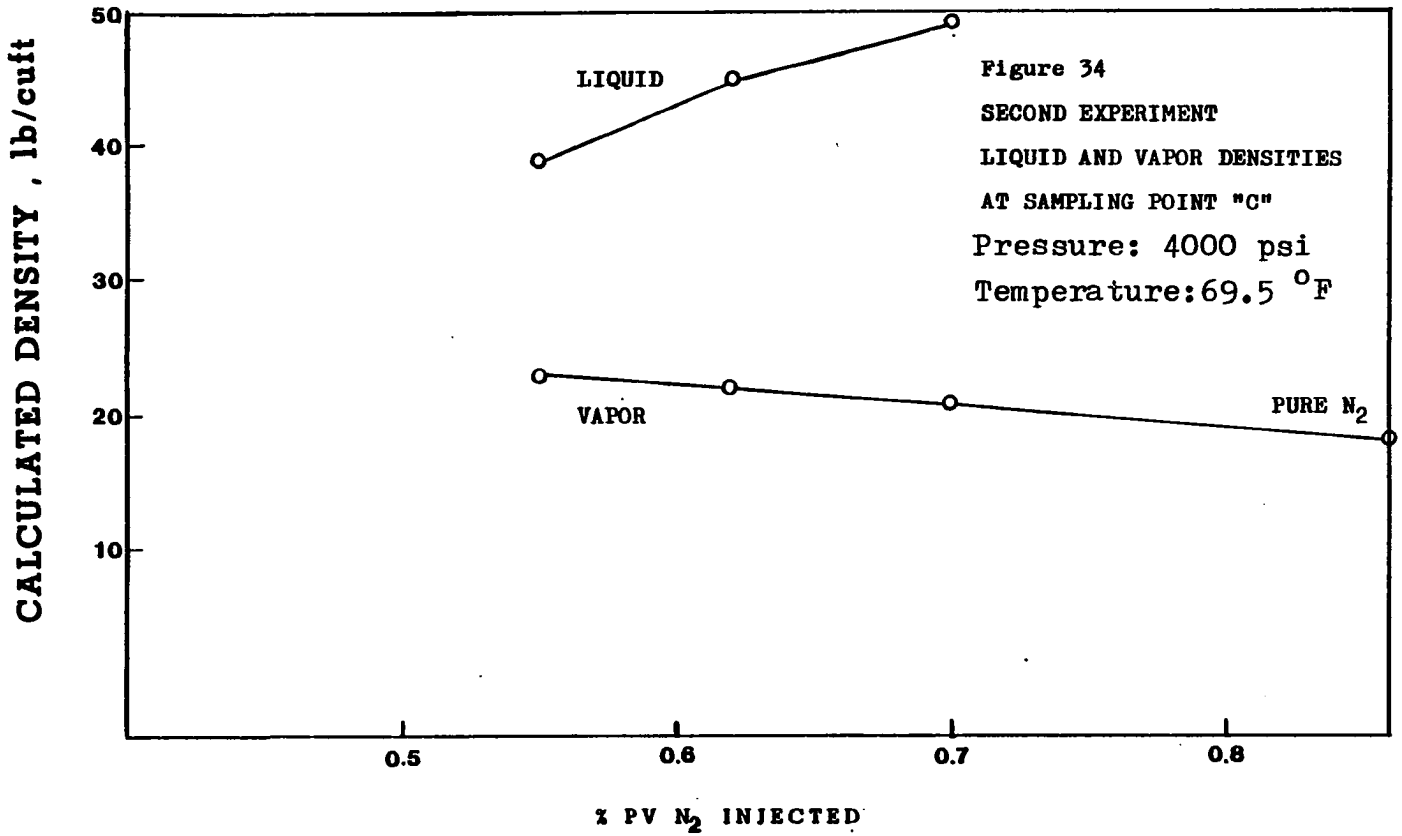

Figure 34
SECOND EXPERIMENT
LIQUID AND VAPOR DENSITIES
AT SAMPLING POINT "C"
Pressure: 4000 psi
Temperature: 69.5 °F

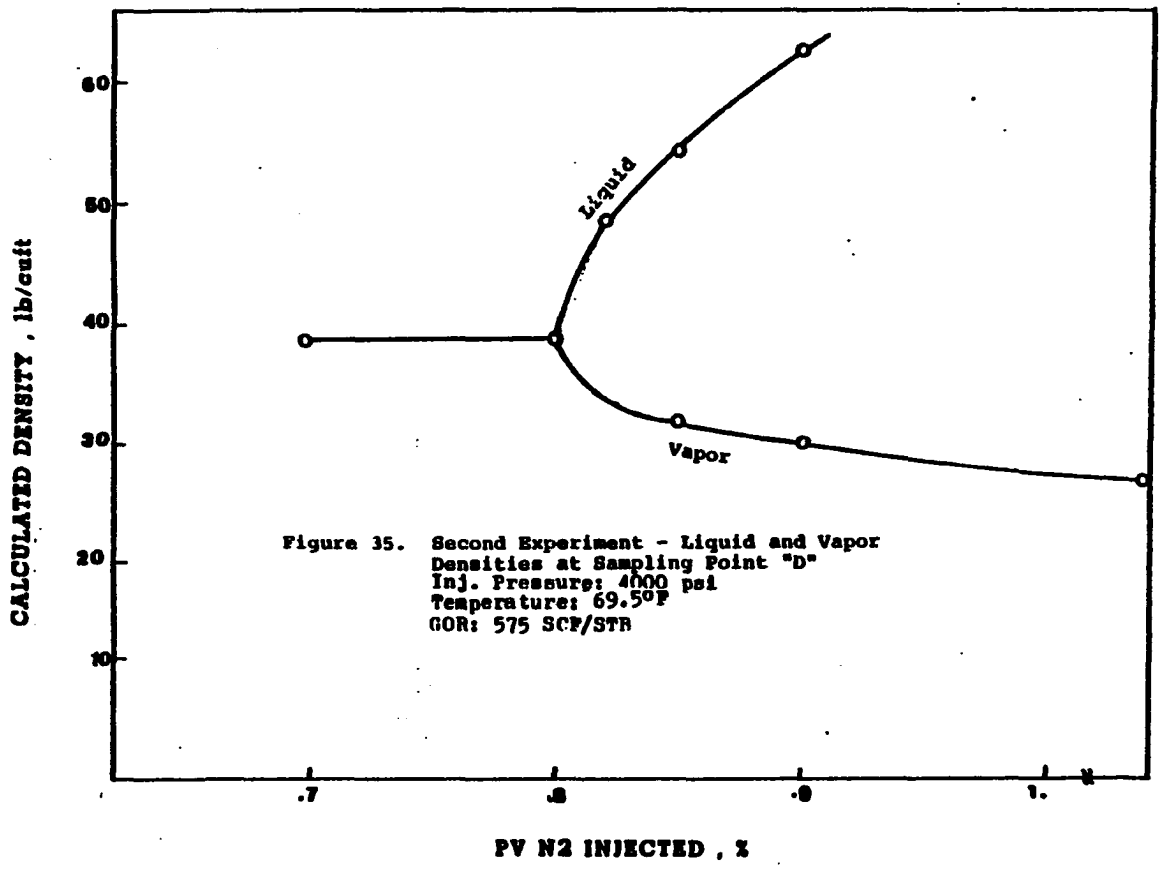

Figure 35. Second Experiment - Liquid and Vapor Densities at Sampling Point "D"
Inj. Pressure: 4000 psi
Temperature: 69.5°F
GOR: 575 SCF/STB

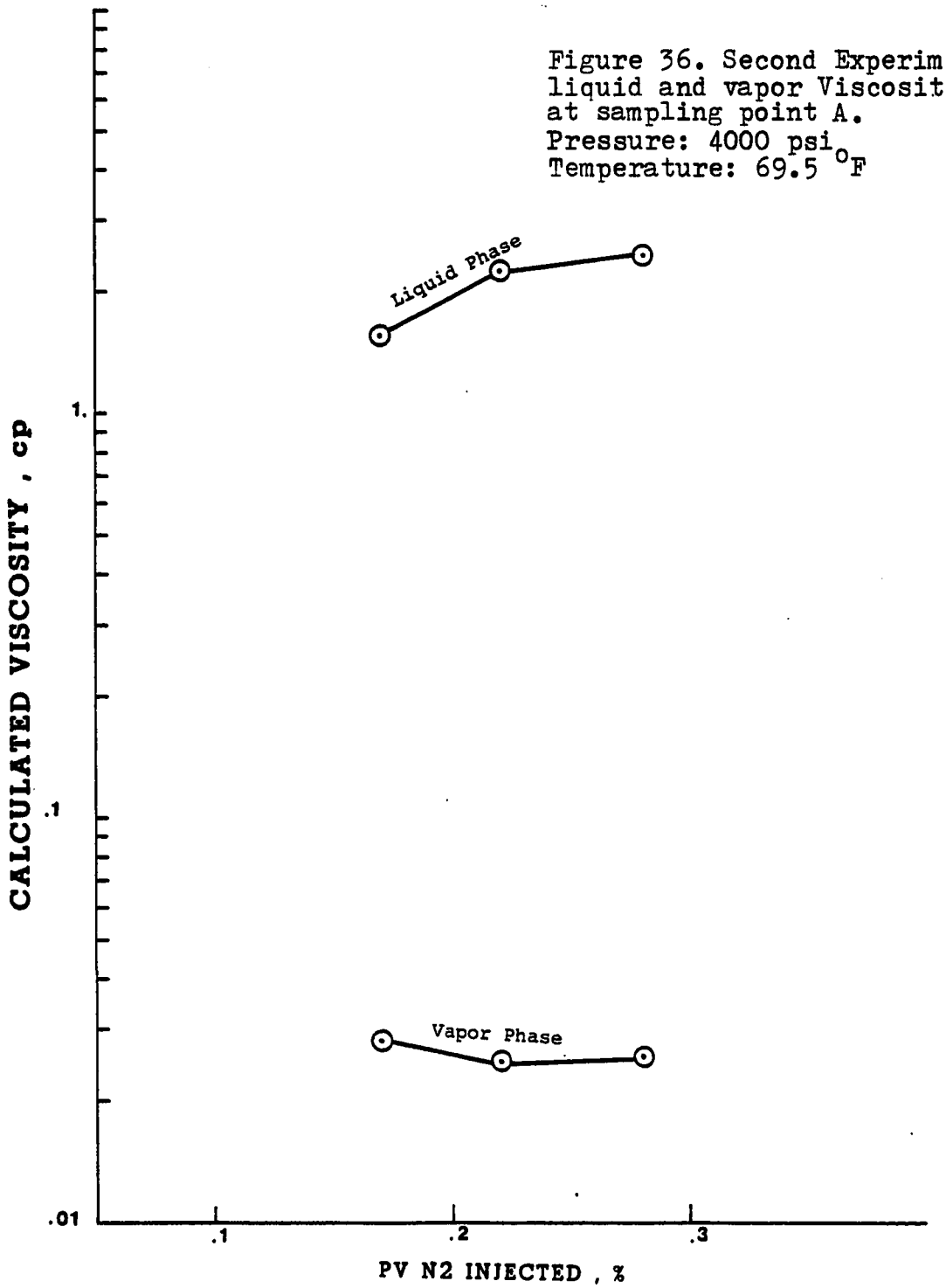

Figure 36. Second Experiment liquid and vapor Viscosities at sampling point A.
Pressure: 4000 psi
Temperature: 69.5 ^{o}F

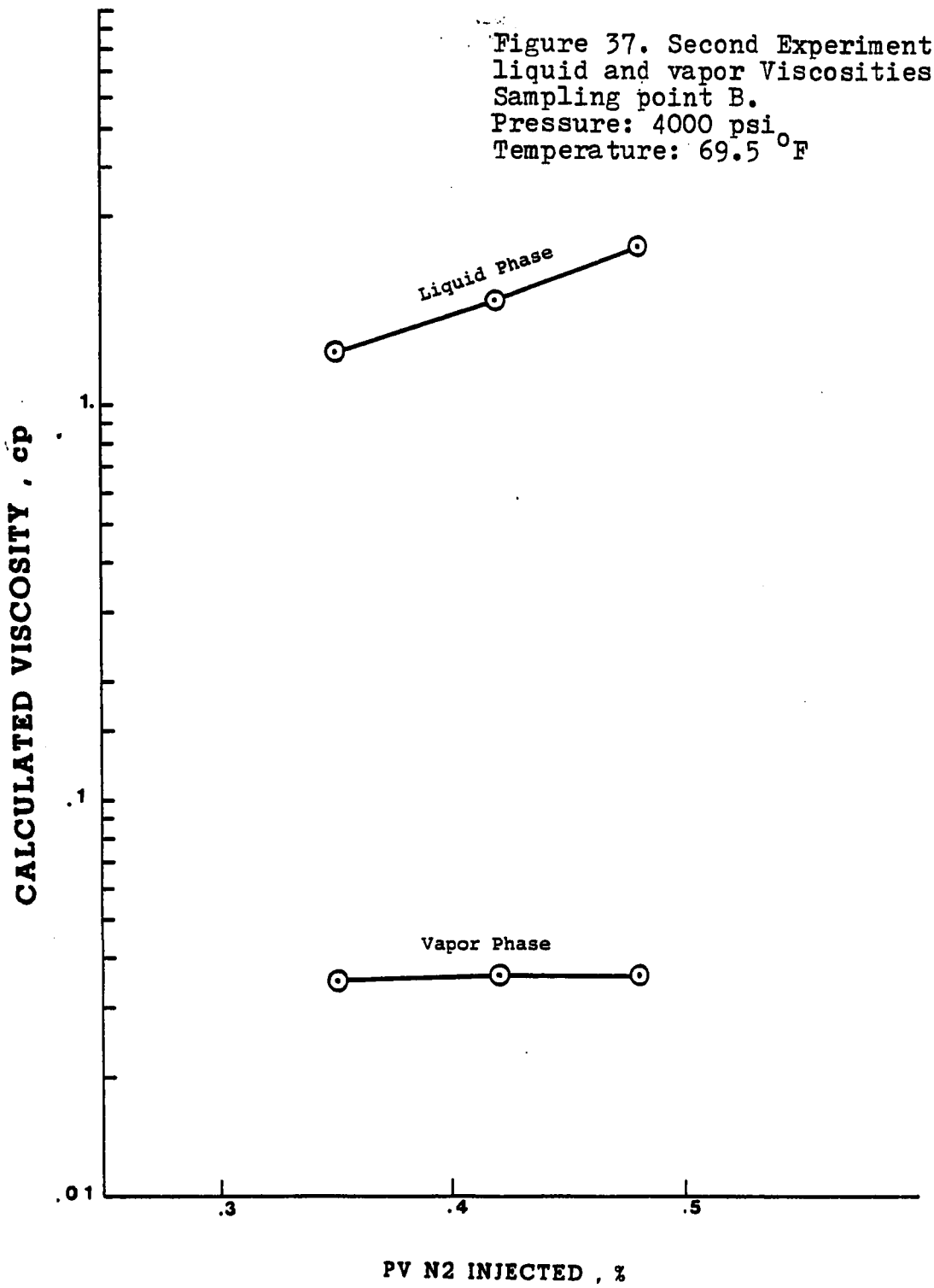

Figure 37. Second Experiment liquid and vapor Viscosities Sampling point B. Pressure: 4000 psi Temperature: 69.5 °F

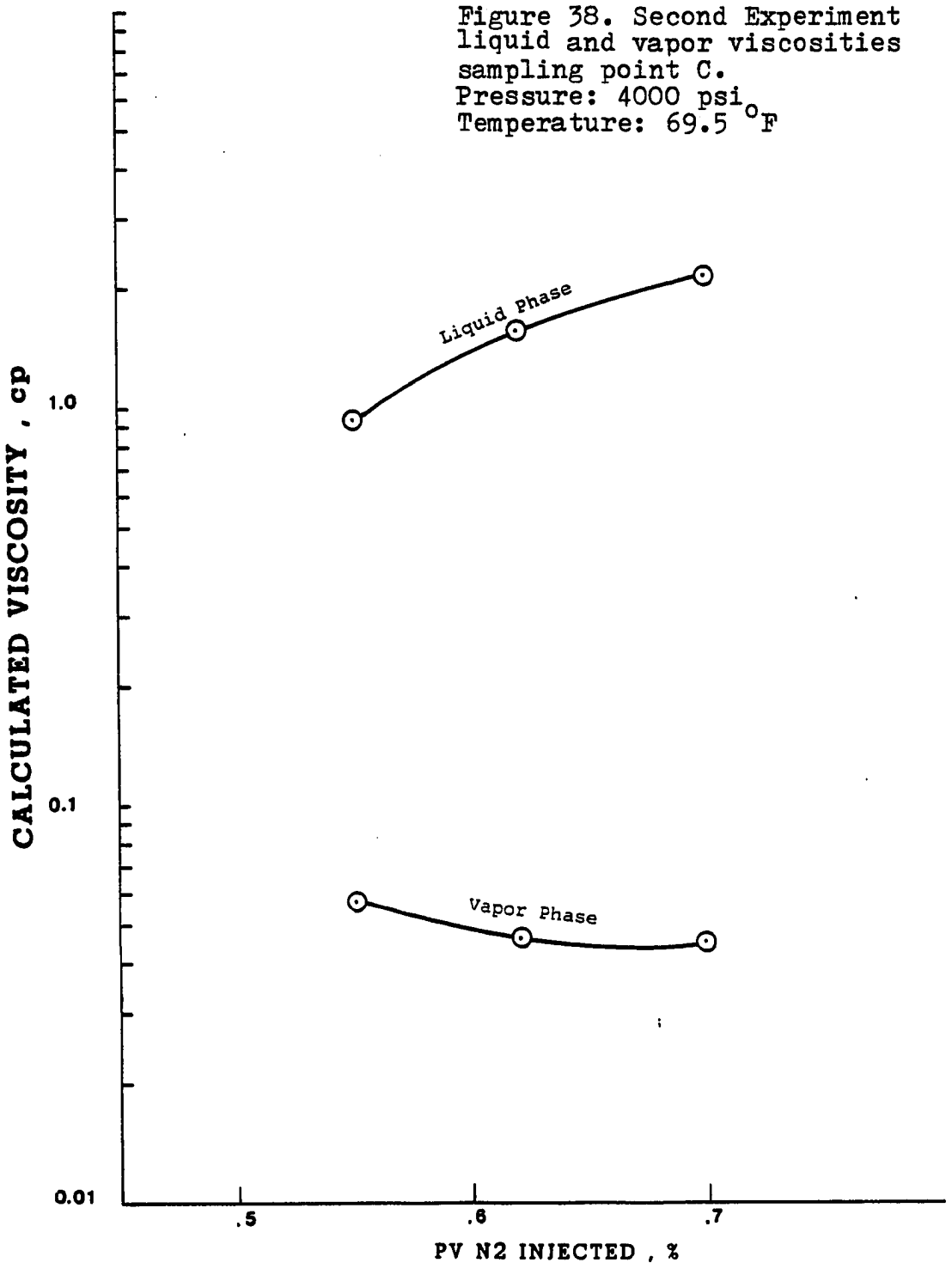

Figure 38. Second Experiment liquid and vapor viscosities sampling point C.
Pressure: 4000 psi
Temperature: 69.5 °F

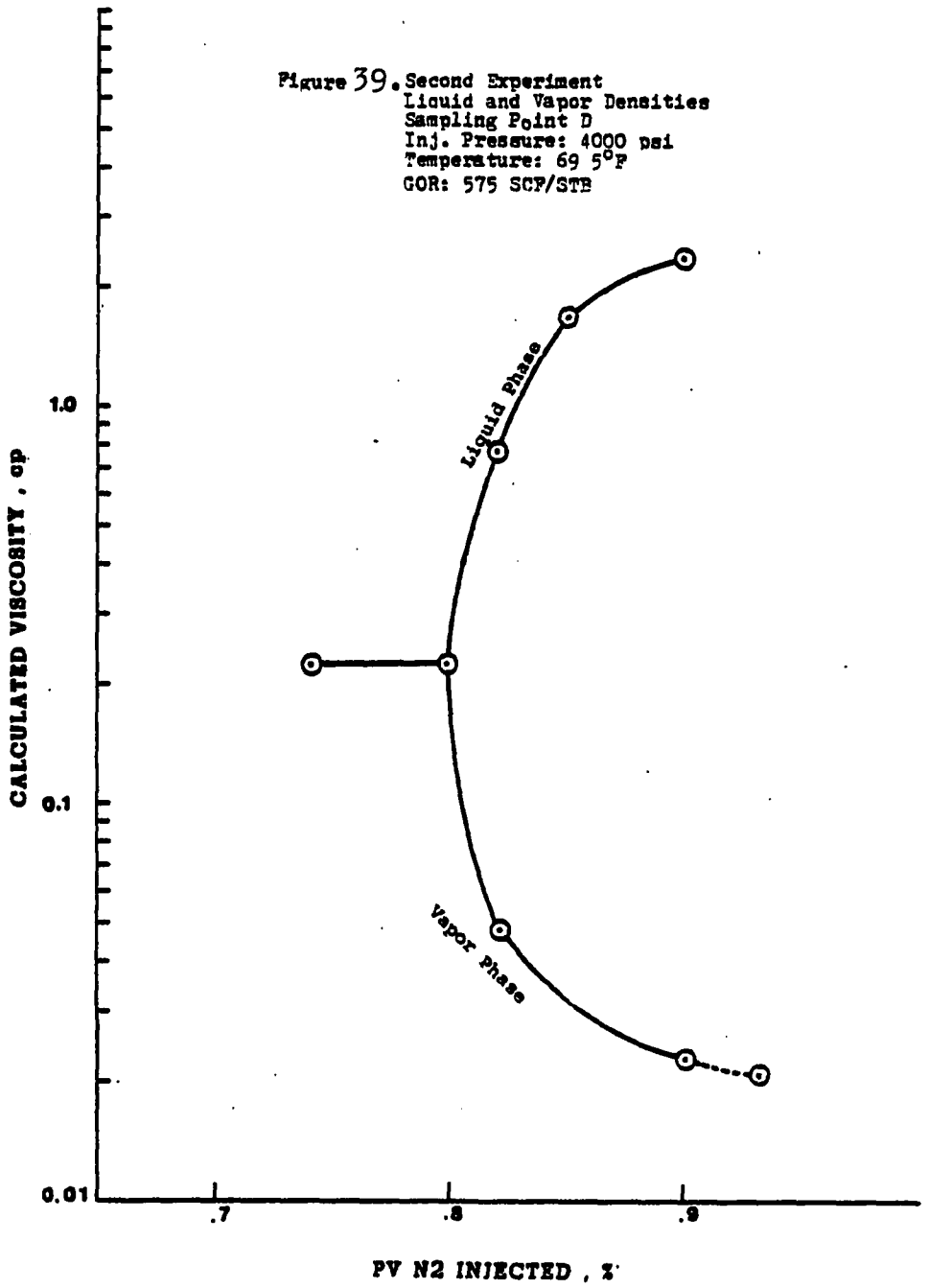
Figure 39. Second Experiment
Liquid and Vapor Densities
Sampling Point D
Inj. Pressure: 4000 psi
Temperature: 69 5°F
GOR: 575 SCF/STB
Liquid Phase
Vapor Phase
CALCULATED VISCOSITY , cp
1.0
0.1
0.01
.7
.8
.9
PV N2 INJECTED , %

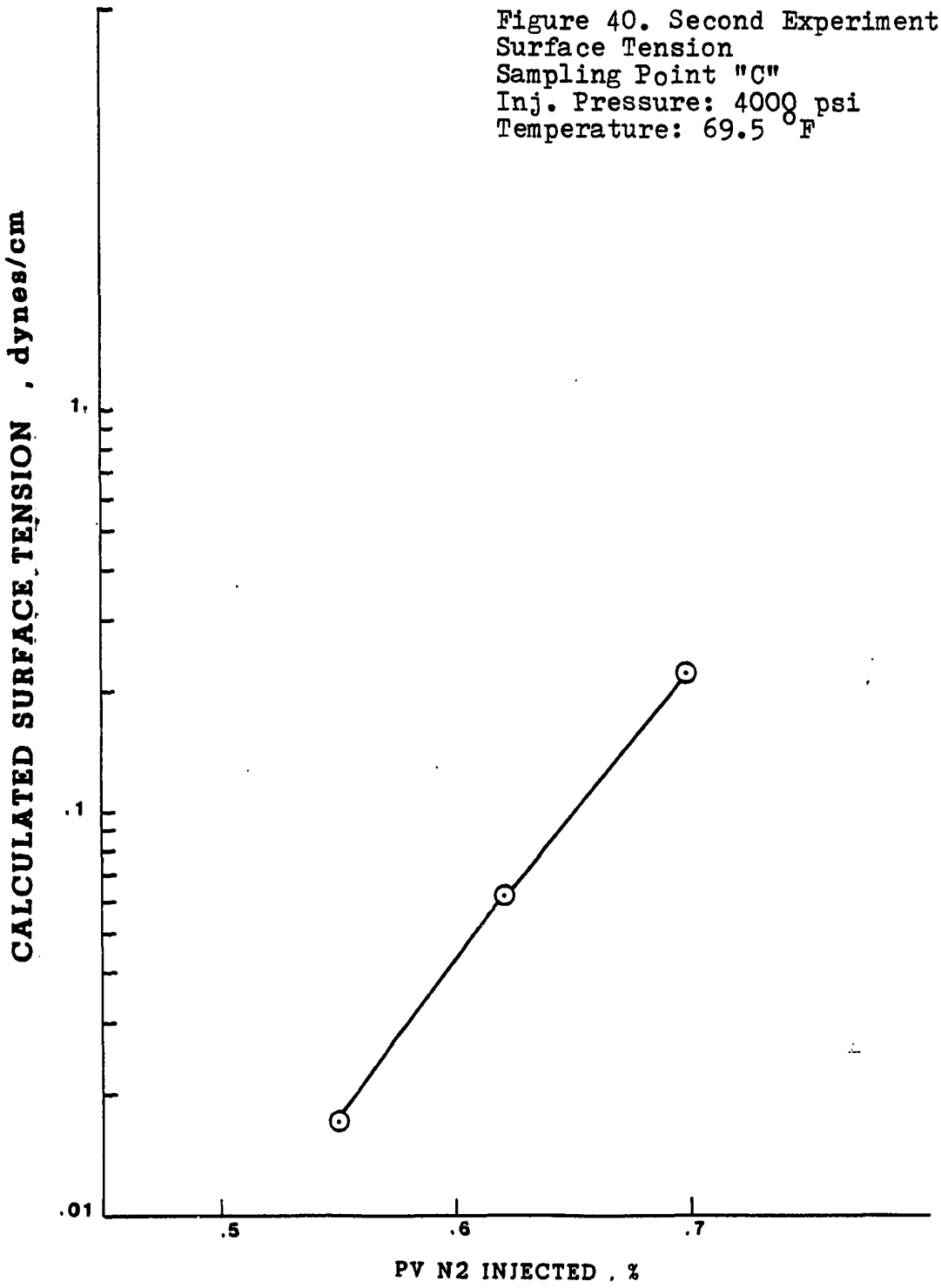

Figure 40. Second Experiment
Surface Tension
Sampling Point "C"
Inj. Pressure: 4000 psi
Temperature: 69.5 °F

that miscibility is incompleted or partial under these laboratory conditions.

The crude oil recovery of 81.1% suggests by itself that at least partial miscibility was achieved during displacement. This test result is in agreement with results reported by previous researchers ([1], 50, 51, 30, and 36).

Definitely this test shows that the reservoir physical model is reliable to conduct this type of research.

Third Experiment

The third test was a regular crude light oil displacement by high pressure nitrogen injection. The production data is presented in Table 8. Basically this test was designed to study the effect of gas-oil in solution on crude oil recovery and miscibility. The amount of natural gas to be recombined with the crude oil was reduced in this test. A gas-oil ratio of 400 SCF/STB was used, as it is shown in Figure 14. Both the calculated formation volumetric factor and the saturation pressure decreased for the reservoir crude oil.

The value of all the conditions and parameters for this test were the following:

Barometric Pressure	28.95" Hg.
Room Temperature.	69°F
Reservoir Temperature	70.5°F.
Injection Pressure.	4000 psi
Solution Gas-Oil Ragio.	400 SCF/STB
Crude Oil Saturation.	78% PV

Water Saturation.	22% PV
Stock Tank Oil in Place	762.50 cc
Oil Gravity	42.4° API
Front Advance velocity.	.107 cm/sec
Formation Volumetric Factor	1.20 Bbl/STB
Crude Oil Saturation Pressure	1550 psi

This test was a normal test with no problems reported. Samples from the displacement phase were taken during the displacement process and analyzed by means of a chromatograph. The vapor analysis results are given in Table 9.

The fractional crude oil recovery for this test was .754. The recovery under these conditions was lower than the previous test and as production history shows in Figure 41.

The compositional profile curves presented in Figure 43, 44, 45 and 46 do not present any significant change in relation with the types of curve obtained from the second test. The strong vaporization process at the beginning of the test seems to be a typical characteristic of this type of displacement.

Again miscibility was postulated when no compositional change was observed in the results of the sample analysis. This is represented by zero slope in the curves of the different compounds in the Figure 46.

Surprisingly, the miscibility was obtained almost after injected 71% PV of nitrogen. This value is slightly lower than the previous test. The miscible bank formed during this

TABLE 8

HIGH PRESSURE NITROGEN INJECTION DATA
EXPERIMENT #3
Injection Pressure: 4000 PSIG

TIME (MIN)	CUMULATIVE OIL PRODUCTION (CC)	OIL RECOVERY (% OOIP)	CUMULATIVE PRODUCED GAS (SCF)	PRESSURE OUTLET (PSIG)
0	0	0	0	2000
38	35	0.0459	.09	2005
49	46	0.0603	.12	2000
65	70	0.0918	.18	2000
87	98	0.12852	.25	2000
103	112	0.14689	.28	2000
123	132	0.1731	.33	2000
156	172	0.225	.43	2000
176	200	0.263	.50	2000
214	225	0.295	.57	2000
230	245	0.32	.62	2010
261	265	0.347	.67	1995
277	280	0.367	.71	2000
280	300	0.393	.76	2000
218	320	0.4196	.81	2000
340	350	0.459	.88	2000
362	360	0.472	.90	2000
408	400	0.524	1.01	2000
426	415	0.544	1.05	2000
467	468	0.613	1.17	2000
488	489	0.641	1.23	2000
508	520	0.681	1.31	2000
539	548	0.178	1.38	2000
580	568	0.744	1.43	2000
590	575	0.754	1.45	2000
600	575.5	--	1.88	N_2 BREAKTHROUGH

test was approximately 5% of PV.

This result suggested that higher GOR in solution make the displacement of this kind more efficient. However, the difference in compositional behavior of the second zone detected in this test and the crude oil recovery obtained do not offer a very significant and meaningful result to establish a conclusion. More tests are necessary to reach any conclusion in relation to the effect of GOR in solution on crude oil recovery and miscibility.

The same procedure used to treat the second test data was used in this test. By using the convergence pressure method (explained in Appendix F) and vapor molar composition the liquid molal composition were obtained. Ternary diagrams were constructed to check miscibility process. These ternary diagrams are shown in Figures 47, 48, 49 and 50. Here again, the prediction of miscibility from the results obtained at 24 feet in the core yielded a very poor result. The prediction improved as long as the displacement progress. The prediction made at point C still is a gross approximation. One reason for obtaining poor prediction is the fact that this diagram is very irregular because of the experimental nature of the data.

The properties of the vapor and liquid phase were calculated by using the computer program "Propert" shown in Appendix H. Graphical results of density and viscosity for vapor and liquid phase are shown in Figures 51 and 52. As it

TABLE 9: CHROMATOGRAPH ANALYSIS OF VAPOR SAMPLE

EXPERIMENT #3

Temperature: 70.5 °F ; Injection pressure: 4000 Psi; GOR: 400 SCF/STB

LIQUID COMPONENT MOL%	SAMPLING POINT A			SAMPLING POINT B			SAMPLING POINT C			SAMPLING POINT D			
	.17	.22	.28	.35	.42	.48	.55	.62	.70	71-76	.80	.85	.90
N_2	60.0	76.0	88.0	27.0	49.0	77.0	23.0	46.0	78.0	11.8	19.0	28.5	89.0
C_1	24.4	13.8	6.0	44.8	30.2	11.1	46.02	29.7	9.0	53.6	48.1	40.2	7.5
C_2	6.3	4.9	3.2	9.89	7.4	4.8	12.2	9.8	6.2	12.1	11.6	11.0	2.4
C_3	4.4	3.0	1.7	7.80	5.4	3.0	9.4	7.9	3.5	10.4	9.7	0.1	1.8
$i-C_4$	.5	.12	0.0	0.8	.4	.2	1.4	0.6	0.2	1.6	1.5	1.27	0.0
$n-C_4$	.3	.08	0.0	0.61	.3	.1	0.8	0.5	0.1	0.8	0.6	0.5	0.2
$i-C_5$	0.8	.17	0.1	1.2	0.8	.5	1.8	1.0	.4	1.1	1.5	1.5	0.2
$n-C_5$	0.4	.13	0.1	0.8	.5	.2	1.0	.5	0	1.0	.8	.7	0
C_6^+	3.1	1.8	0.9	7.1	6.2	3.02	5.1	4.0	2.5	7.0	6.1	4.5	0.95

RUN 3
PRESSURE: 4000 PSI
TEMPERATURE: 70.5 F
GOR: 400 SCF/STB

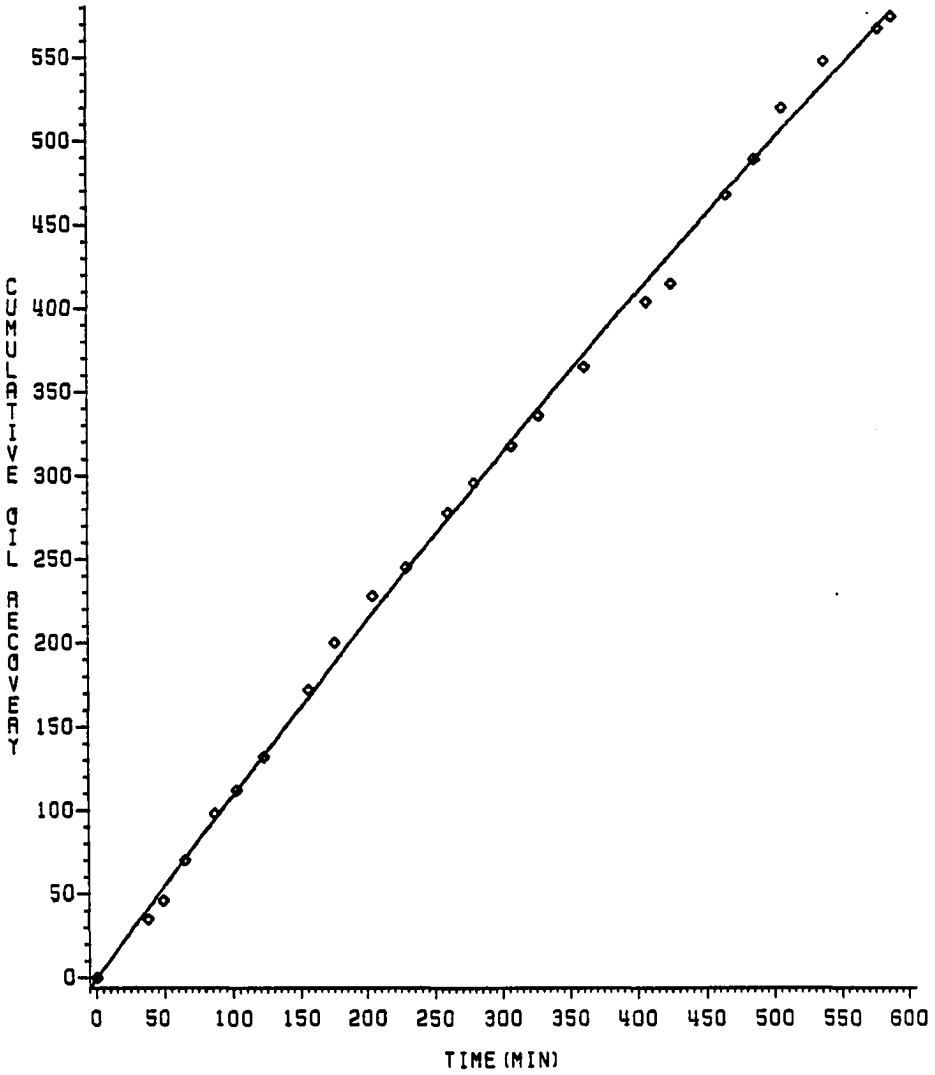

FIGURE 41
CUMULATIVE OIL RECOVERY VS TIME

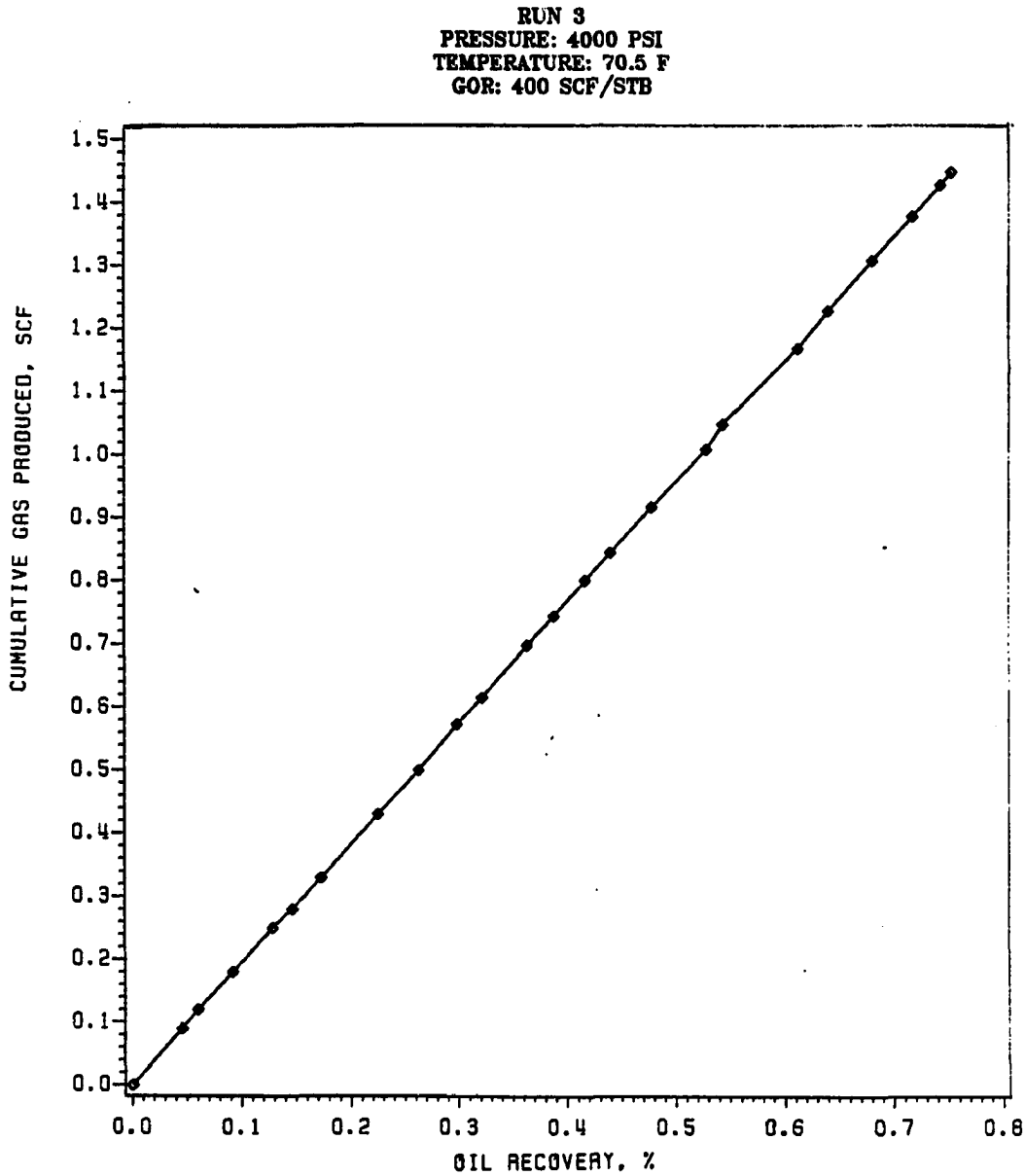

FIGURE 42

CUMULATIVE GAS PRODUCED VS OIL RECOVERY

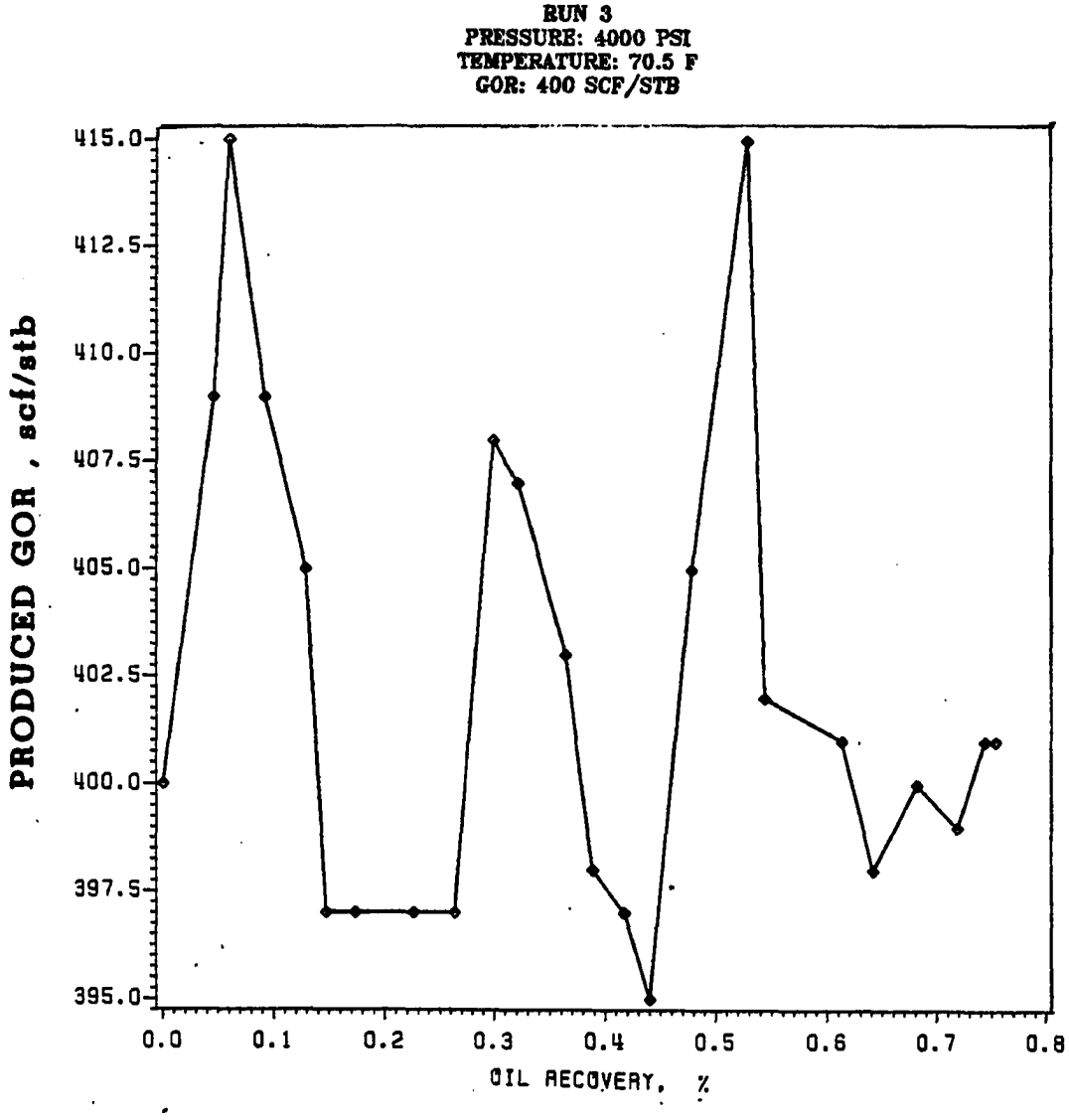

FIGURE 42A
PRODUCED GOR VS OIL RECOVERY

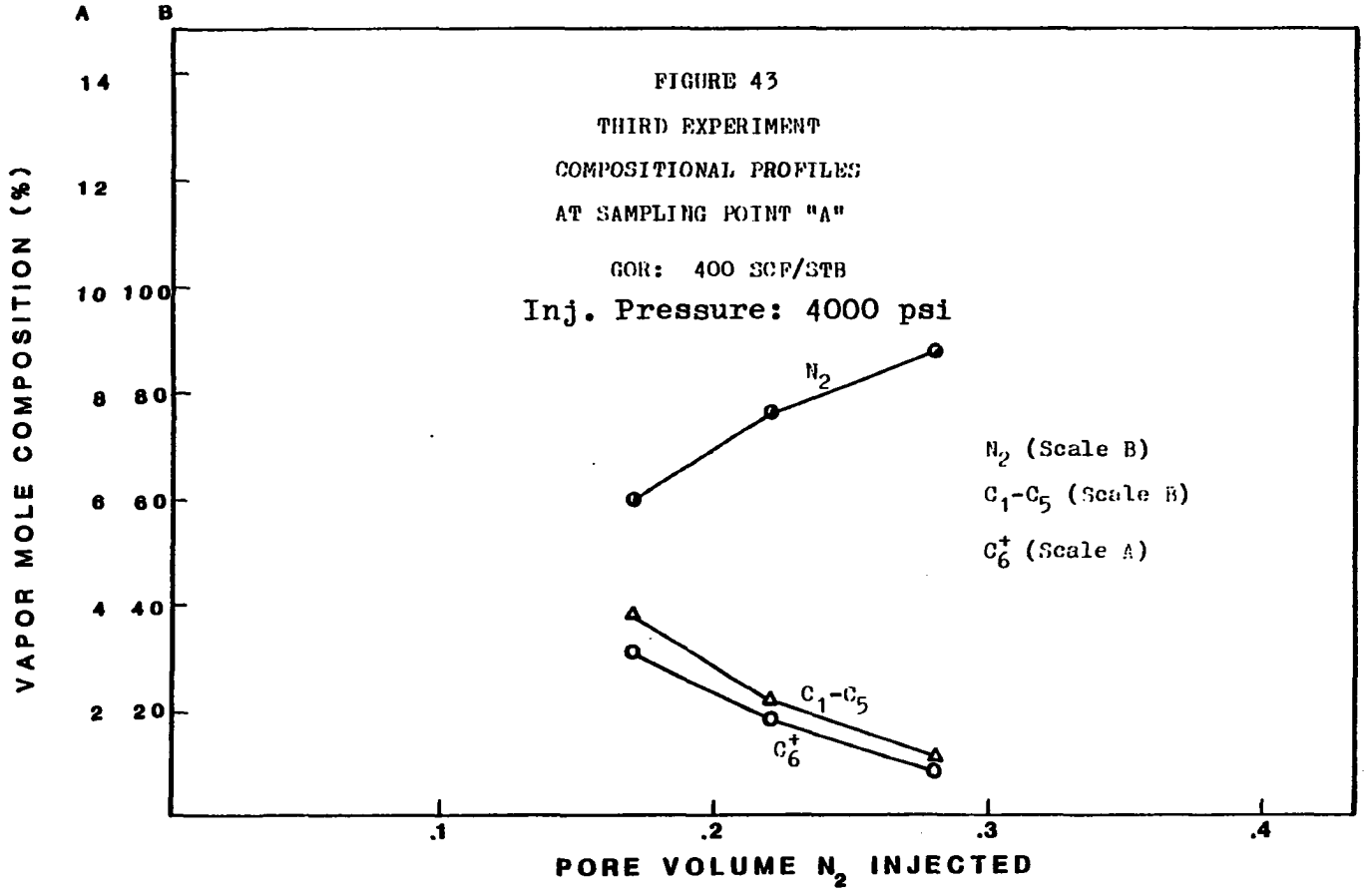

FIGURE 43

THIRD EXPERIMENT

COMPOSITIONAL PROFILES

AT SAMPLING POINT "A"

GOR: 400 SCF/STB

Inj. Pressure: 4000 psi

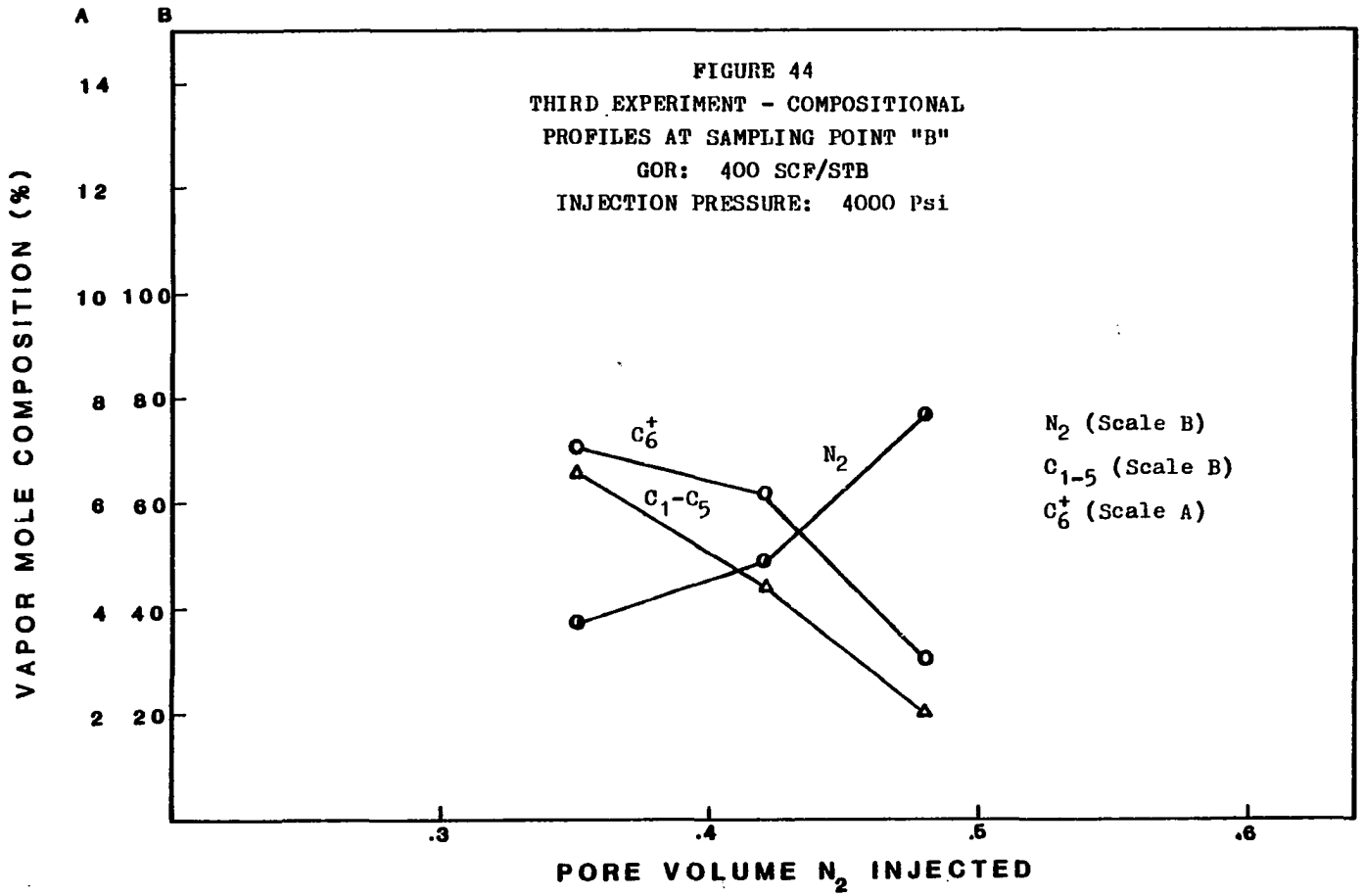

FIGURE 44
THIRD EXPERIMENT - COMPOSITIONAL
PROFILES AT SAMPLING POINT "B"
GOR: 400 SCF/STB
INJECTION PRESSURE: 4000 Psi

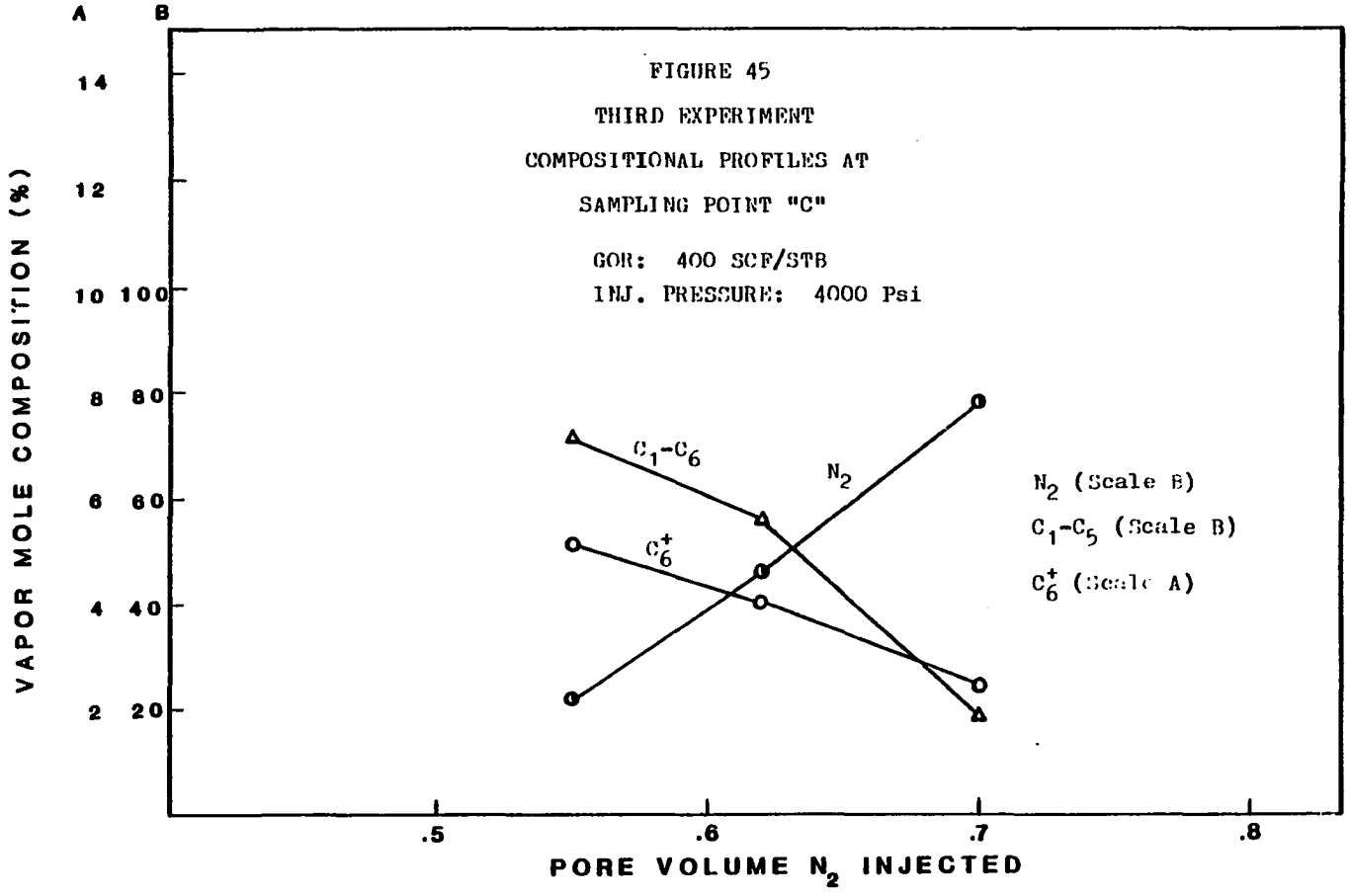

FIGURE 45

THIRD EXPERIMENT

COMPOSITIONAL PROFILES AT

SAMPLING POINT "C"

GOR: 400 SCF/STB

INJ. PRESSURE: 4000 Psi

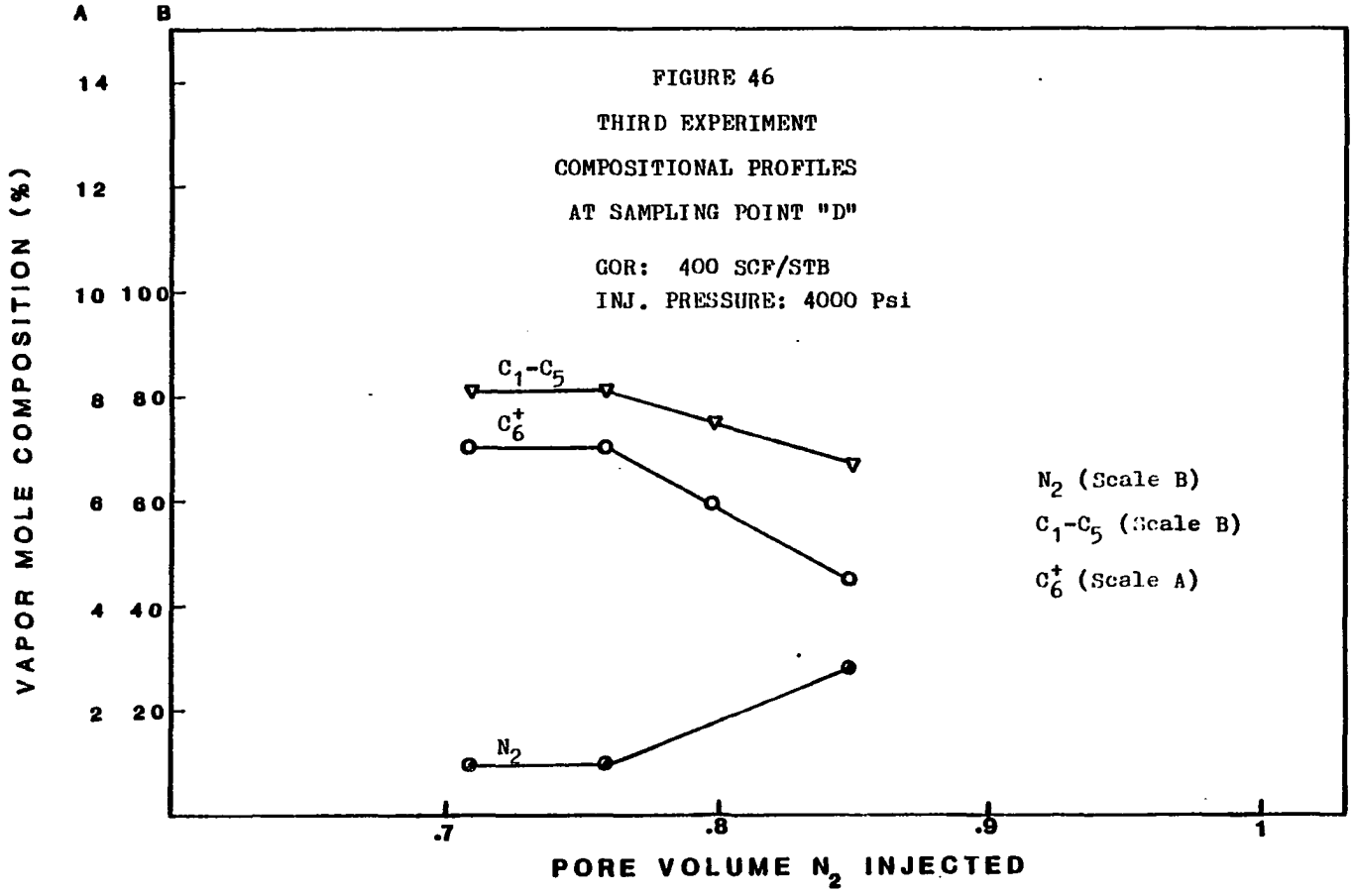

FIGURE 46

THIRD EXPERIMENT

COMPOSITIONAL PROFILES

AT SAMPLING POINT "D"

GOR: 400 SCF/STB

INJ. PRESSURE: 4000 Psi

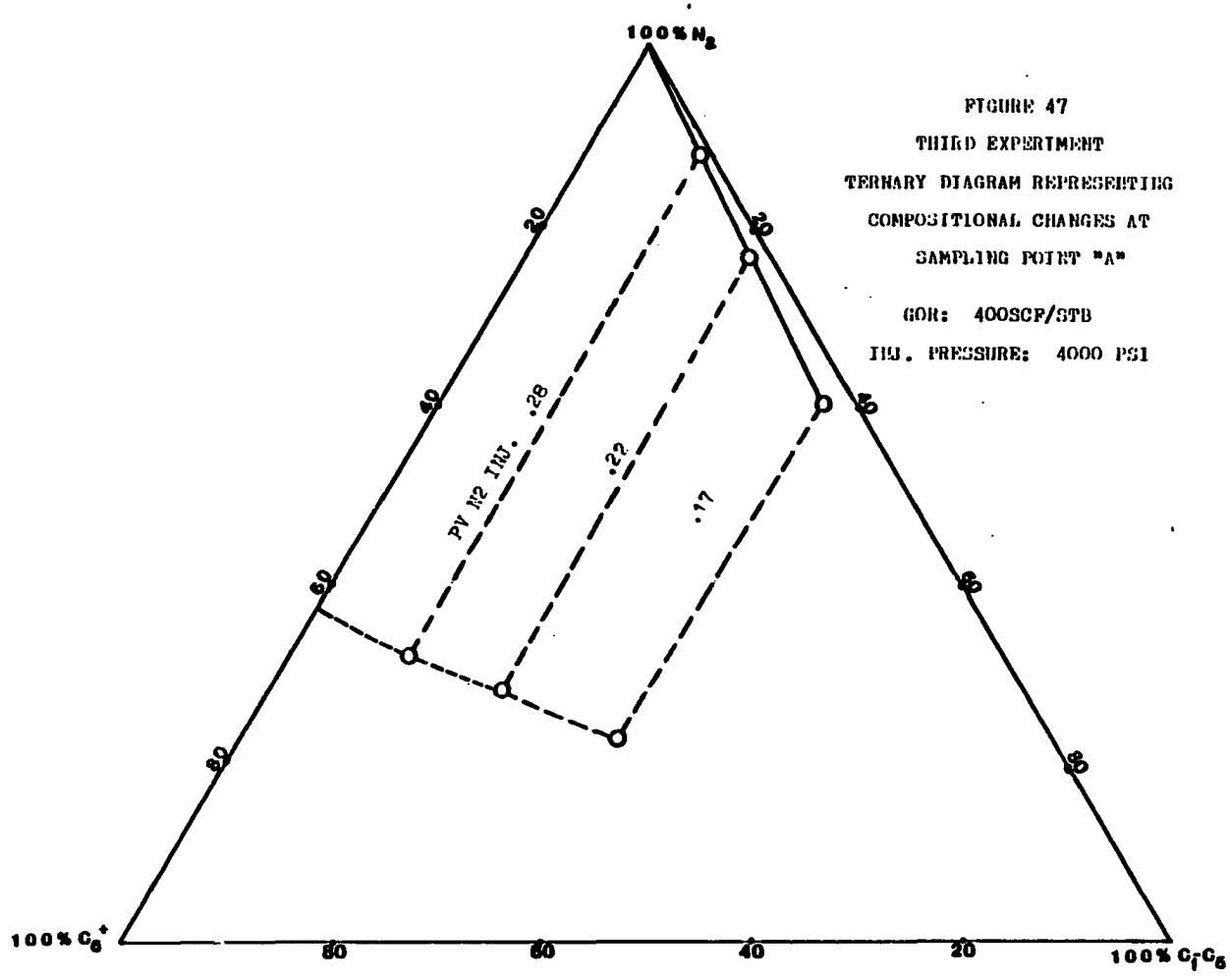

FIGURE 47
THIRD EXPERIMENT
TERNARY DIAGRAM REPRESENTING
COMPOSITIONAL CHANGES AT
SAMPLING POINT "A"

GOR: 400SCF/STB
INJ. PRESSURE: 4000 PSI

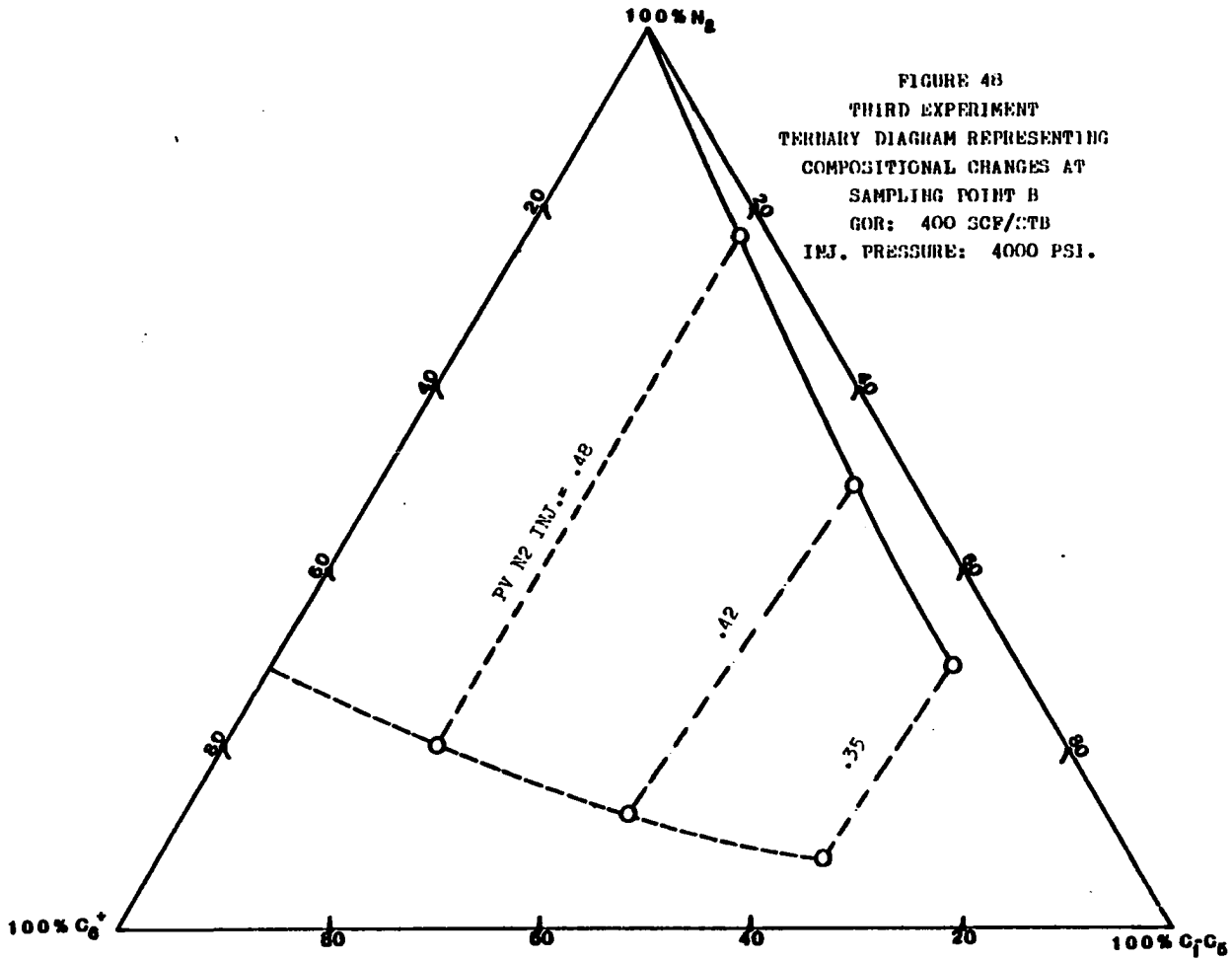

FIGURE 4B
THIRD EXPERIMENT
TERNARY DIAGRAM REPRESENTING
COMPOSITIONAL CHANGES AT
SAMPLING POINT B
GOR: 400 SCF/STB
INJ. PRESSURE: 4000 PSI.

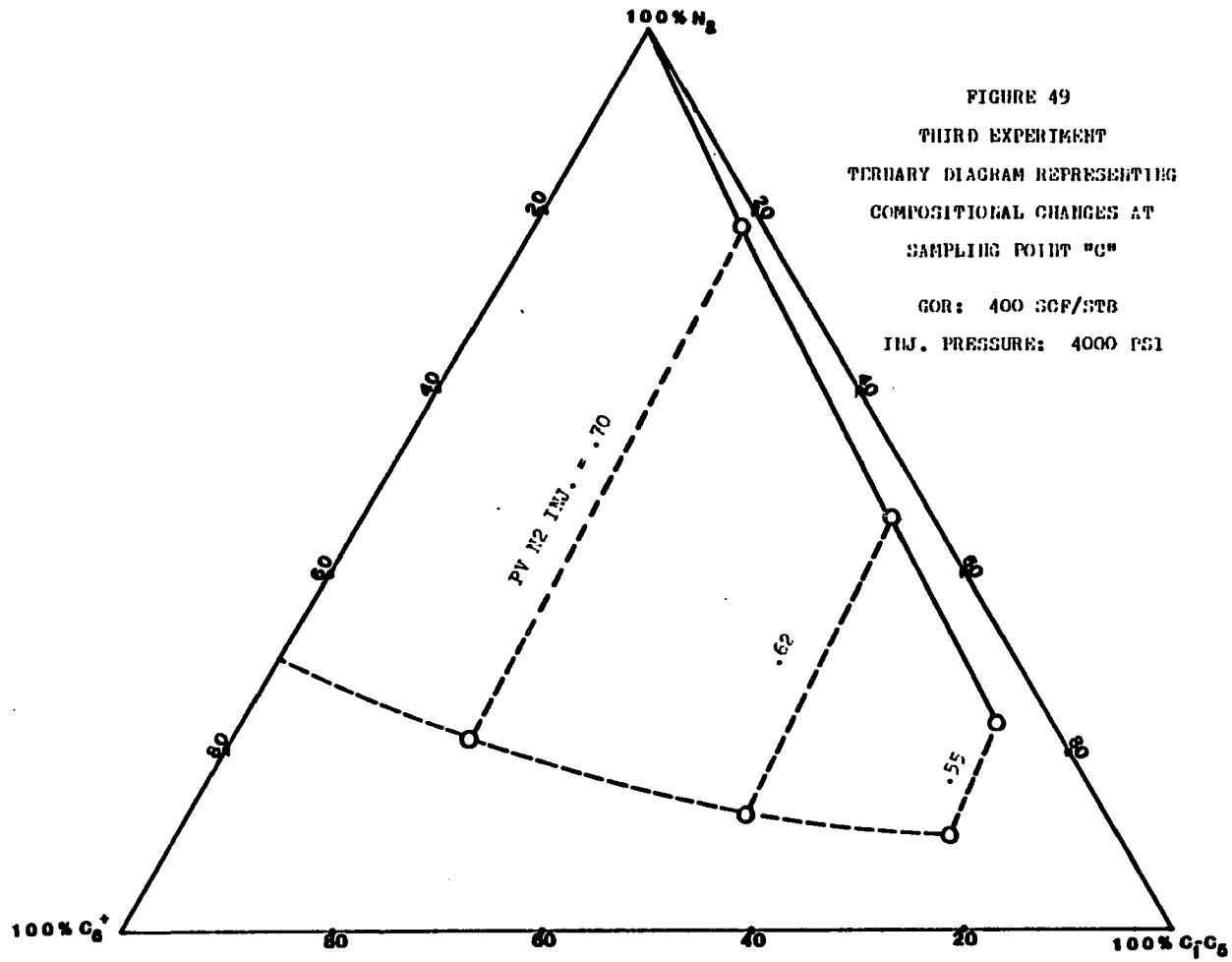

FIGURE 49

THIRD EXPERIMENT

TERNARY DIAGRAM REPRESENTING

COMPOSITIONAL CHANGES AT

SAMPLING POINT "C"

GOR: 400 SCF/STB

INJ. PRESSURE: 4000 PSI

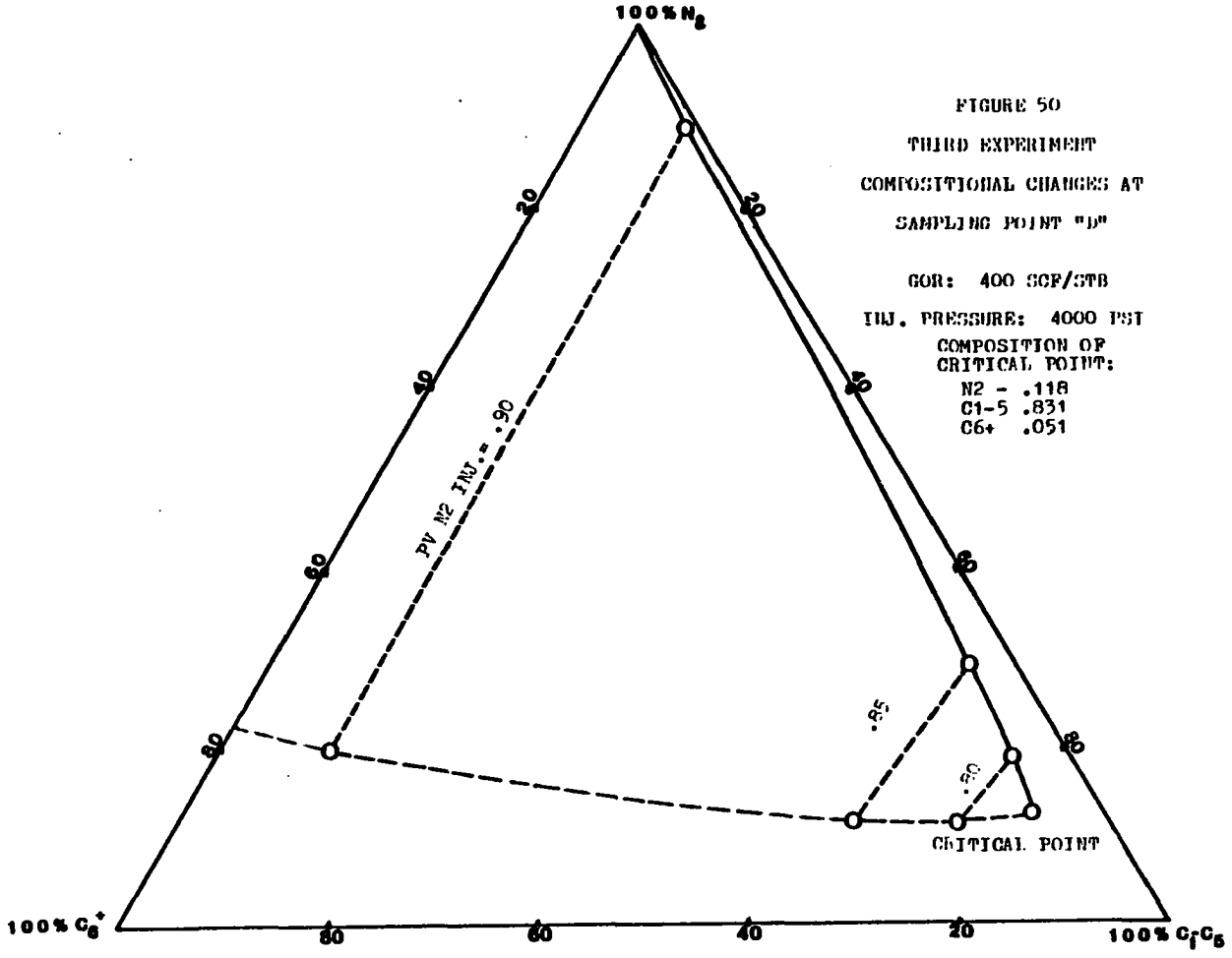

FIGURE 50

THIRD EXPERIMENT

COMPOSITIONAL CHANGES AT

SAMPLING POINT "D"

GOR: 400 SCF/STB

INJ. PRESSURE: 4000 PSI

COMPOSITION OF
CRITICAL POINT:

N2 - .118
C1-5 .831
C6+ .051

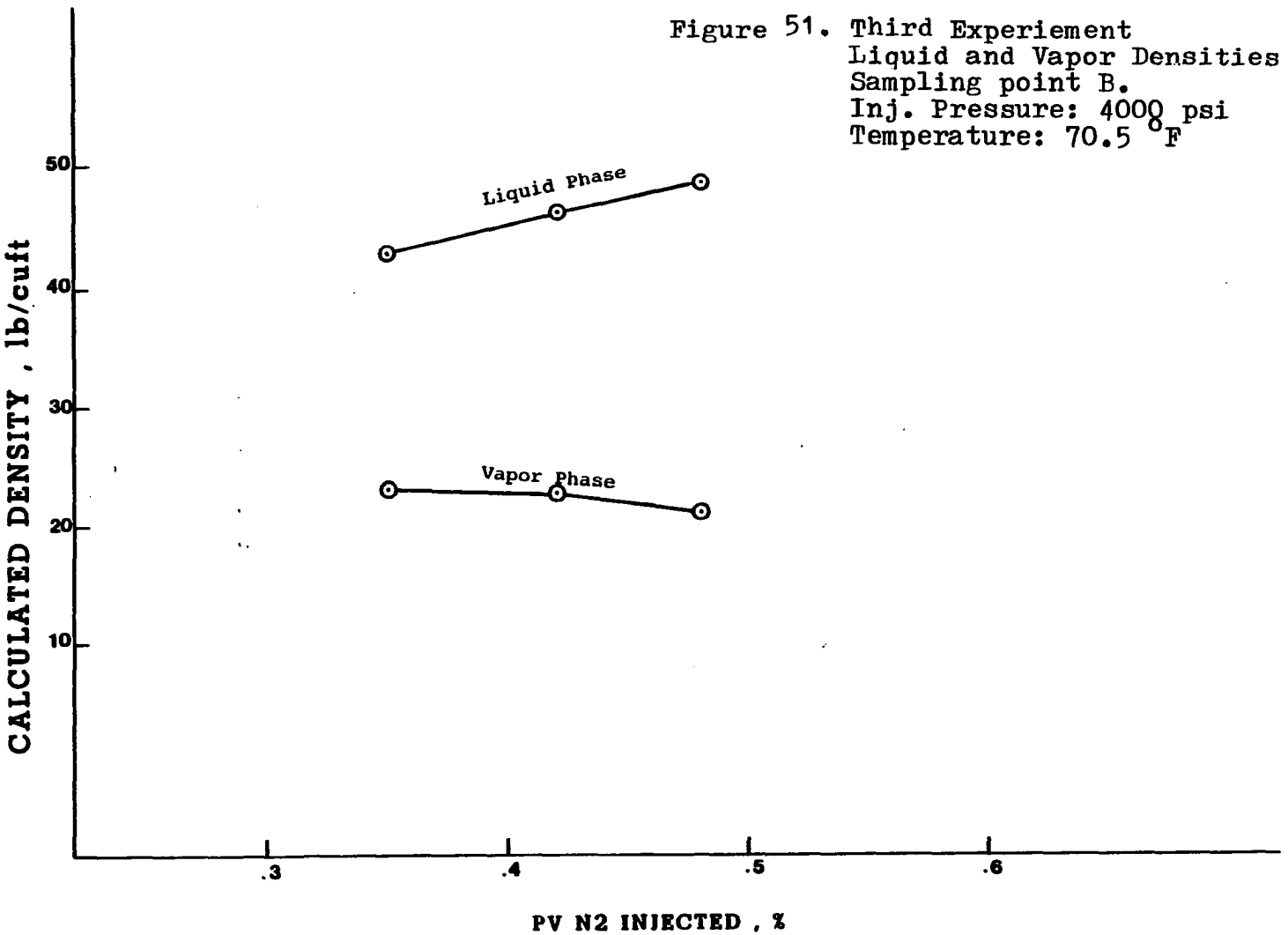

Figure 51. Third Experiement
Liquid and Vapor Densities
Sampling point B.
Inj. Pressure: 4000 psi
Temperature: 70.5 °F

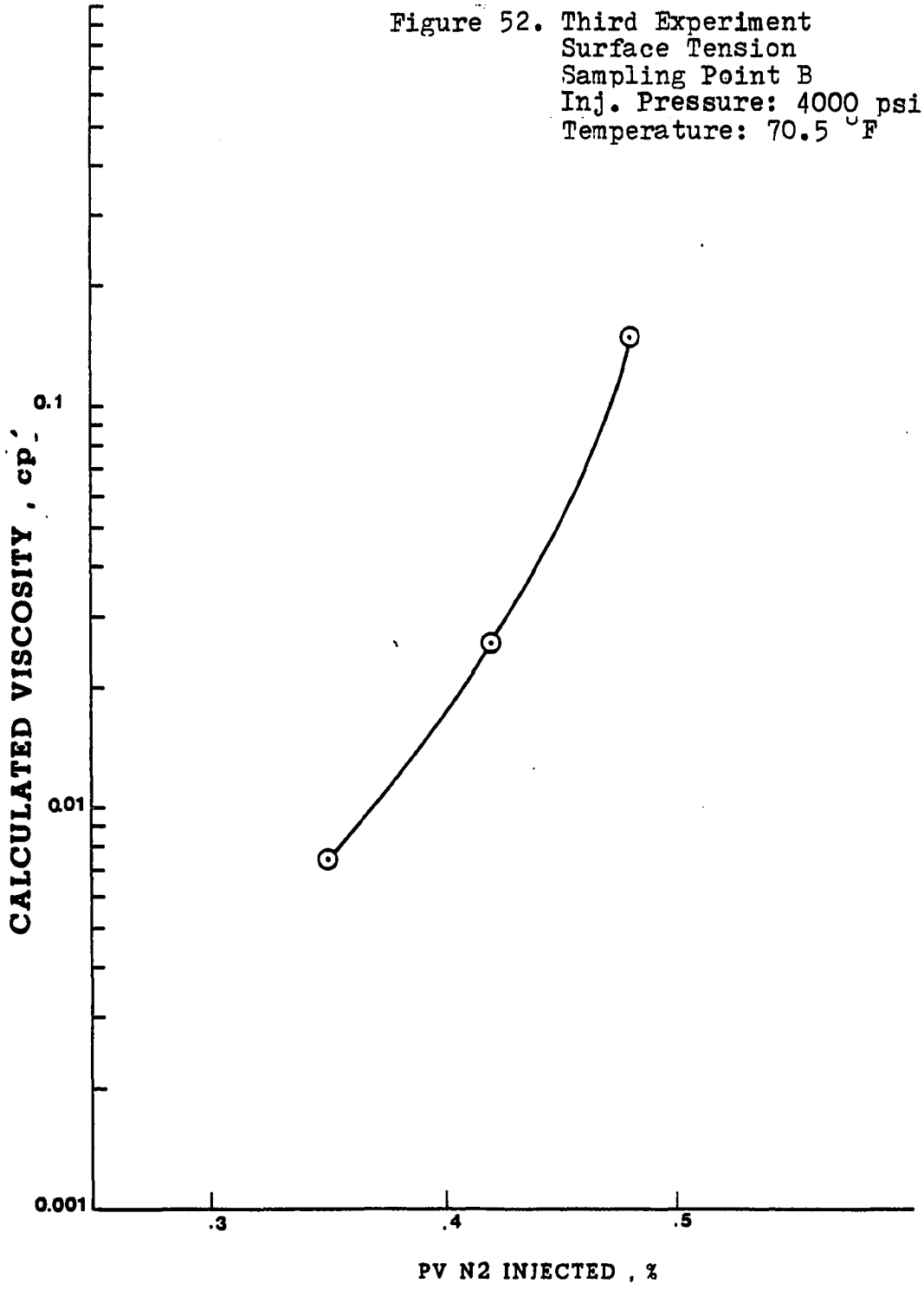

Figure 52. Third Experiment
Surface Tension
Sampling Point B
Inj. Pressure: 4000 psi
Temperature: 70.5 °F

was expected the shape of those curves resembled very much the previous test. The general aspect and meaning of these curves are in agreement with the previous research (1).

The effect of GOR in solution and temperature on crude oil recovery and miscibility will be discussed later in this chapter, after the presentation and brief analysis of all the tests performed in this study.

B-4. Fourth Experiment

This test was designed to continue the study about gas-oil ratio in solution effect on crude oil recovery and building up miscibility process. In this test the amount of natural gas dissolved in the crude oil was reduced again. The GOR in solution was reduced to 200 SCF/STB. Hence the saturation pressure and the formation volumetric factor decreased as it is shown in Figure 15.

The values of the parameters and conditions for this test are the following:

Barometric Pressure . . . . . 28.8 inches Hg.

Room Temperature. . . . . 69.5°F.

Reservoir Temperature . . . . . 70°F.

Injection Pressure. . . . . 400 psi

Solution Gas-Oil Ratio. . . . . 200 SCF/STB

Crude Oil Saturation. . . . . 77% PV

Water Saturation. . . . . 23% PV

Stock Tank Oil in Place . . . . . 809 cc

Crude Oil Gravity . . . . . 42.4° API

Front Advance Velocity. . . . . .104 cm/sec

Formation Volumetric Factor . . . . 1.1 Bbl/STB

No problems during the test were reported. The routine already established in this study, to conduct the test and evaluate data was followed in this experiment. This routine involves the following steps:

1. Collect produced crude oil and measured produced gas.

2. Collect vapor samples and analyze them by means of the chromatograph.

3. Plot composition changes in each compound to establish a compositional profile at each observation point at the reservoir.

4. Calculation of liquid molal composition by using the computer program "CALC" which is presented in Appendix F and was written for this research. The program is part of the trial and error procedure of the convergence pressure method.

5. Construction of the ternary diagram to predict and check if miscibility will be reached during the test.

6. Calculation of liquid and vapor phases properties by using the computer program "PROPER" which is shown in Appendix H.

7. Plotting both densities and viscosity as a function of N_2 injected for both liquid and vapor phases.

8. Plotting of surface tension.

9. Comparison of the results with previous researchers and discussion.

The test production history is presented in Table 10 and Figures 53 through 55. The chromatograph analysis results of the vapor samples taken during the displacement are given in Table 11. The ternary diagrams for this test are shown in Figures 60, 61, 62 and 63. The compositional profiles for this experiment are presented in Figures 56, 57, 58 and 59. Plotting of calculated properties for liquid and vapor phases are shown in Figures 64 and 65; and finally the Figure 65-A gives the interfacial tension between liquid and vapor phases at the displacement front.

The crude oil recovery obtained in this experiment was 66% of the stock tank oil in place. Compared with the recoveries obtained in previous experiments in this study it is significantly lower. Being GOR in solution, the only manipulated independent variable the author proposes that crude oil recovery is significantly affected by the initial GOR in solution of the crude oil.

Miscibility was not obtained under the conditions of this test. This can be seen in production history of the test shown in Figures 53 to 55. No significant change in the shape of the curve where crude oil recovery is plotted as a function of time.

The lower recovery by itself strongly suggests that all the displacement was a completely immiscible process. Also, a

TABLE 10

HIGH PRESSURE NITROGEN INJECTION DATA
EXPERIMENT #4
Injection Pressure: 4000 PSIG

TIME (MIN)	CUMULATIVE OIL PRODUC. (CC)	OIL RECOVERY (% OOIP)	CUMULATIVE PRODUCED GAS (SCF)	OUTLET PRESSURE (PSIG)
0	0	--	0	2000
39	20	0.02	0.05	2000
73	50	0.06	0.06	2000
97	70	0.09	0.09	2000
135	100	.12	0.13	2000
170	136	.17	0.17	2000
227	180	.22	0.23	2000
262	220	.27	0.28	2000
300	254	.31	0.32	2000
345	300	.37	0.38	2000
370	320	.40	0.40	2000
396	338	.42	0.42	2000
440	378	.47	0.48	2000
480	413	.51	0.52	2000
521	450	.56	0.56	2000
554	480	.59	0.60	2000
611	530	.66	0.66	2000
620	530.1		8.51	2000

N_2 BREAKTHROUGH

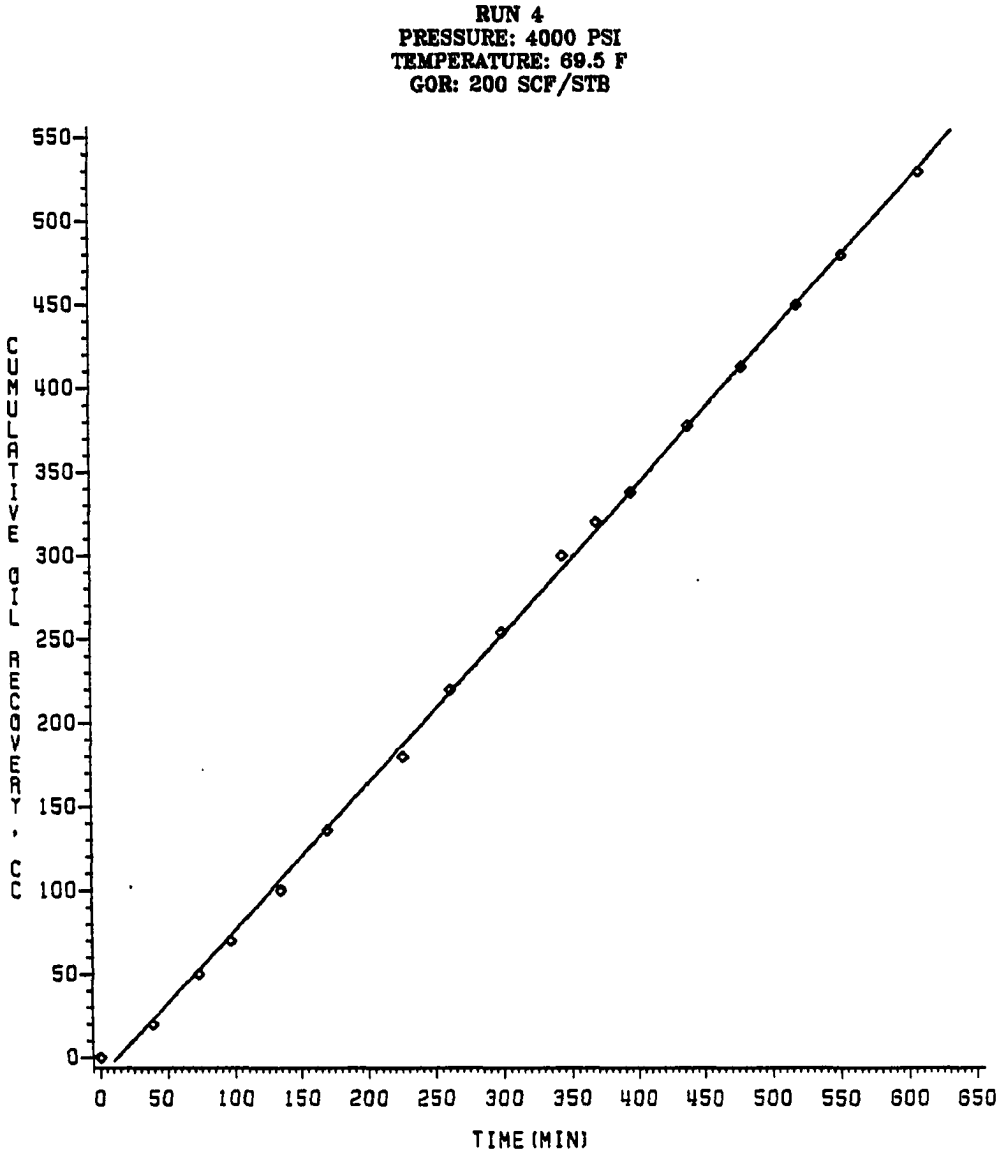

FIGURE 53
CUMULATIVE OIL RECOVERY VS TIME

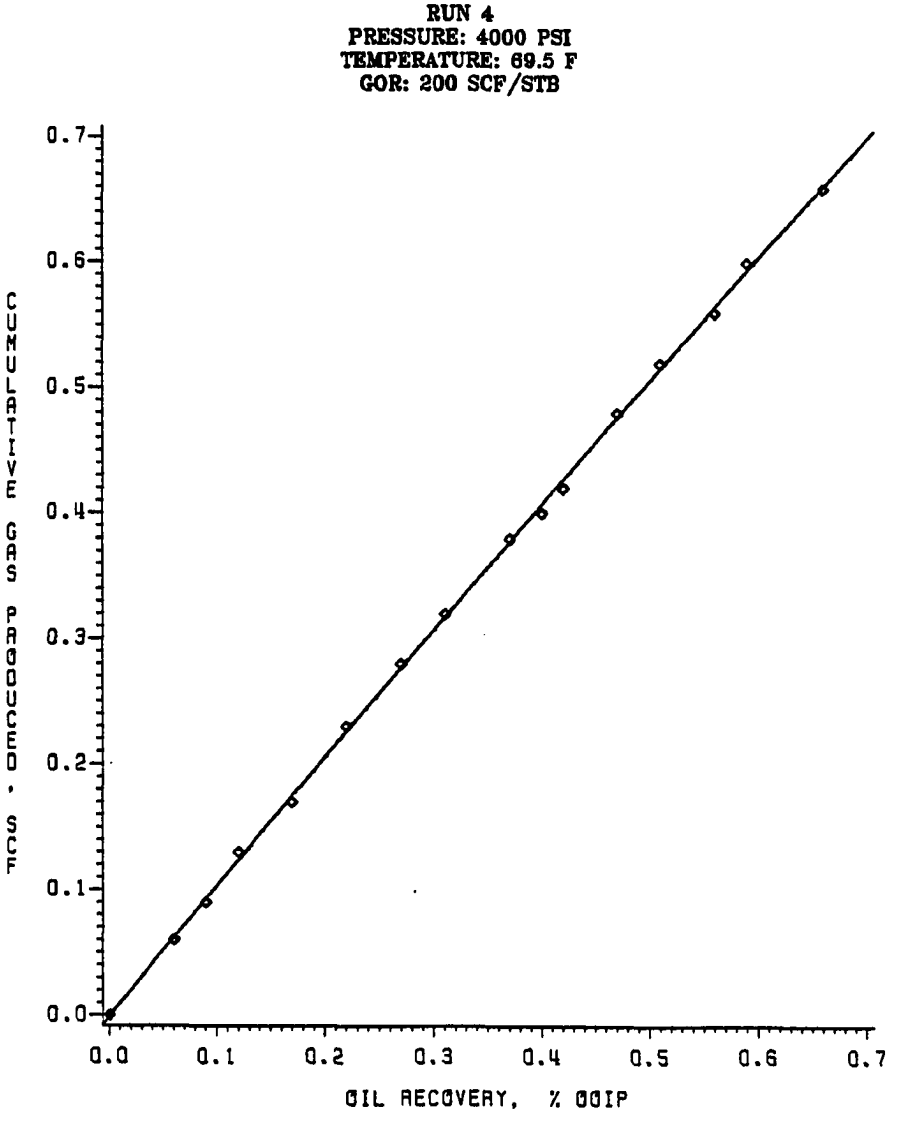

FIGURE 54
CUMULATIVE GAS PRODUCED VS OIL RECOVERY

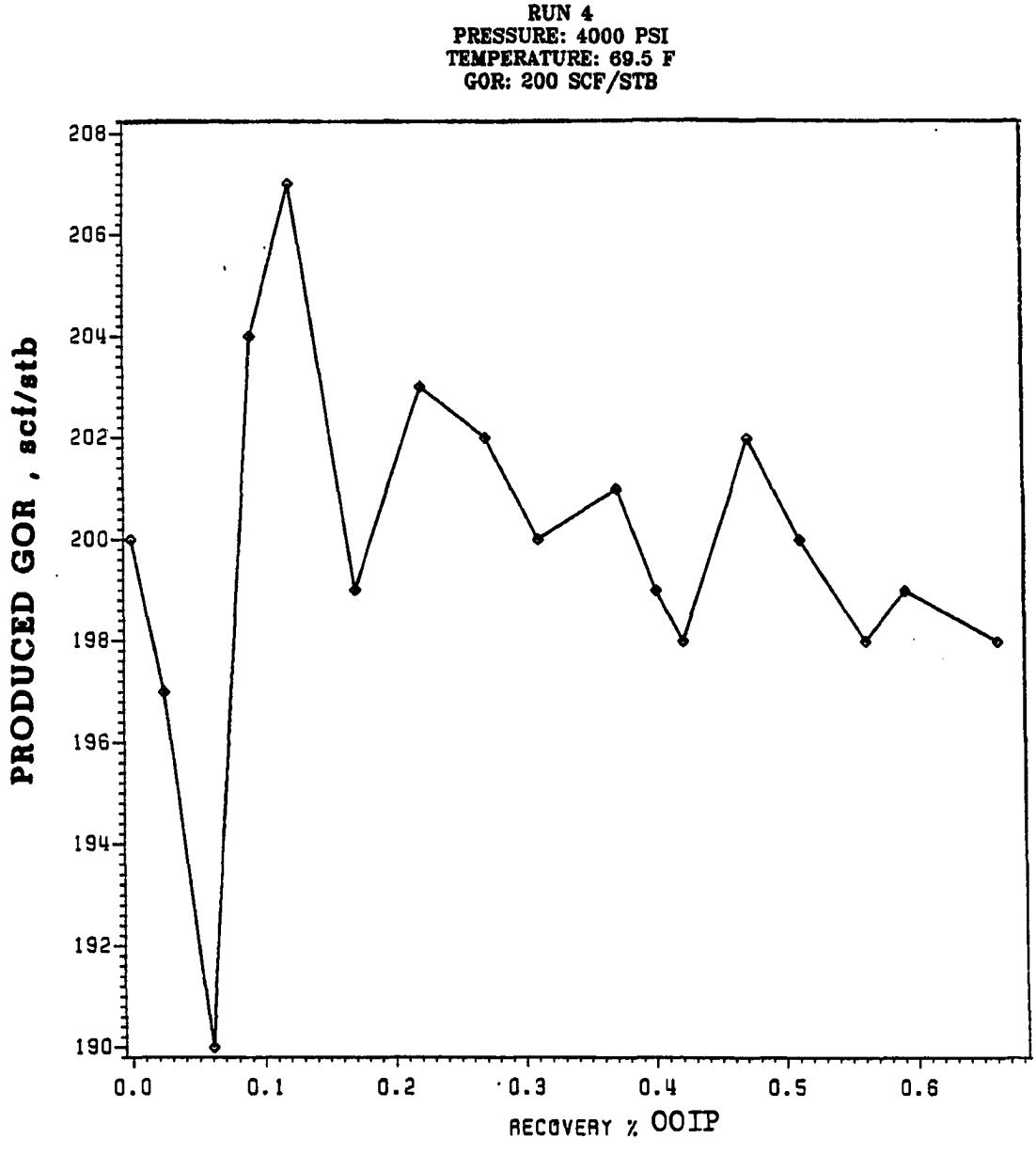

FIGURE 55

PRODUCED GOR VS OIL RECOVERY

TABLE 11: CHROMATOGRAPH ANALYSIS OF VAPOR SAMPLES

EXPERIMENT #4

Temperature: 69.5°F Injection Pressure: 4000 Psi; GOR: 200 SCF/STB

COMPONENTS	SAMPLING POINT A			SAMPLING POINT B			SAMPLING POINT C			SAMPLING POINT D		
	.17	.22	.28	.35	.42	.48	.55	.62	.70	.70	.75	.85
N_2	61.8	73.1	85.8	47.1	64.2	83.1	36.5	56.2	80.5	29.2	39.4	62.5
C_1	25.9	19.9	10.69	36.	20.	10.	35.2	26.5	13.5	42.44	37.5	27.0
C_2	4.1	2.2	1.5	9.2	6.2	2.6	9.6	7.5	3.0	10.21	9.8	4.9
C_3	2.6	1.6	.7	6.5	3.1	0.8	7.4	4.0	1.0	8.36	6.9	3.1
$i\text{-}C_4$	.4	.2	.01	.9	.85	0.8	1.31	0.8	0.1	0.80	0.5	0.4
nc_4	.3	.1	0.1	.18	.15	0	0.8	0.2	0	.49	0.2	0
$i\text{-}C_5$	.45	.3	.2	.83	.8	0.6	1.1	0.9	0	1.2	0.8	0.6
nC_5	.40	.2	.0	.80	.6	.3	.9	0.2	0	.8	0.1	0
C_6^+	4.1	2.5	1.1	7.1	3.2	1.8	7.2	3.9	1.9	6.5	4.8	1.5

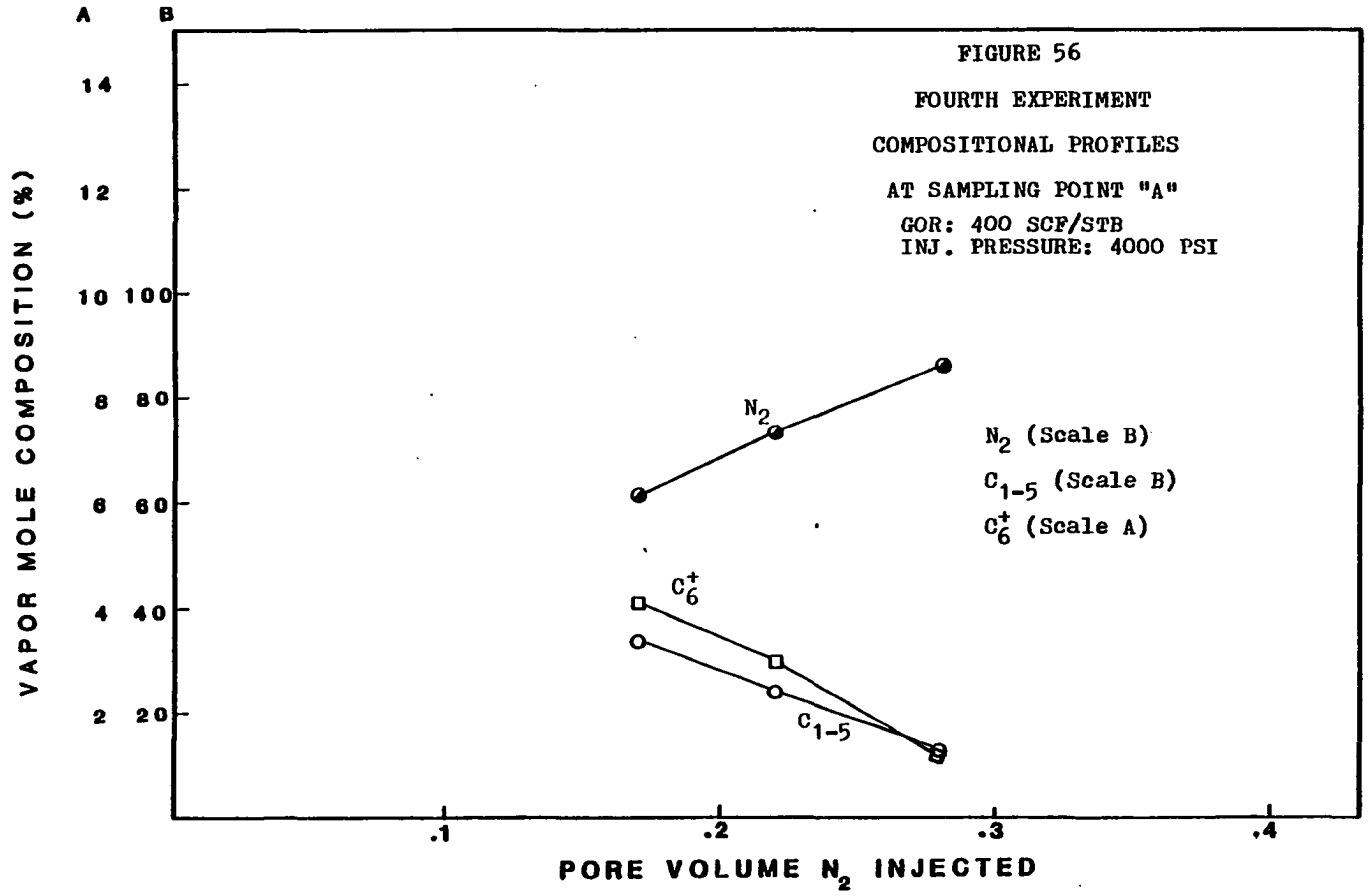

FIGURE 56

FOURTH EXPERIMENT

COMPOSITIONAL PROFILES

AT SAMPLING POINT "A"

GOR: 400 SCF/STB
INJ. PRESSURE: 4000 PSI

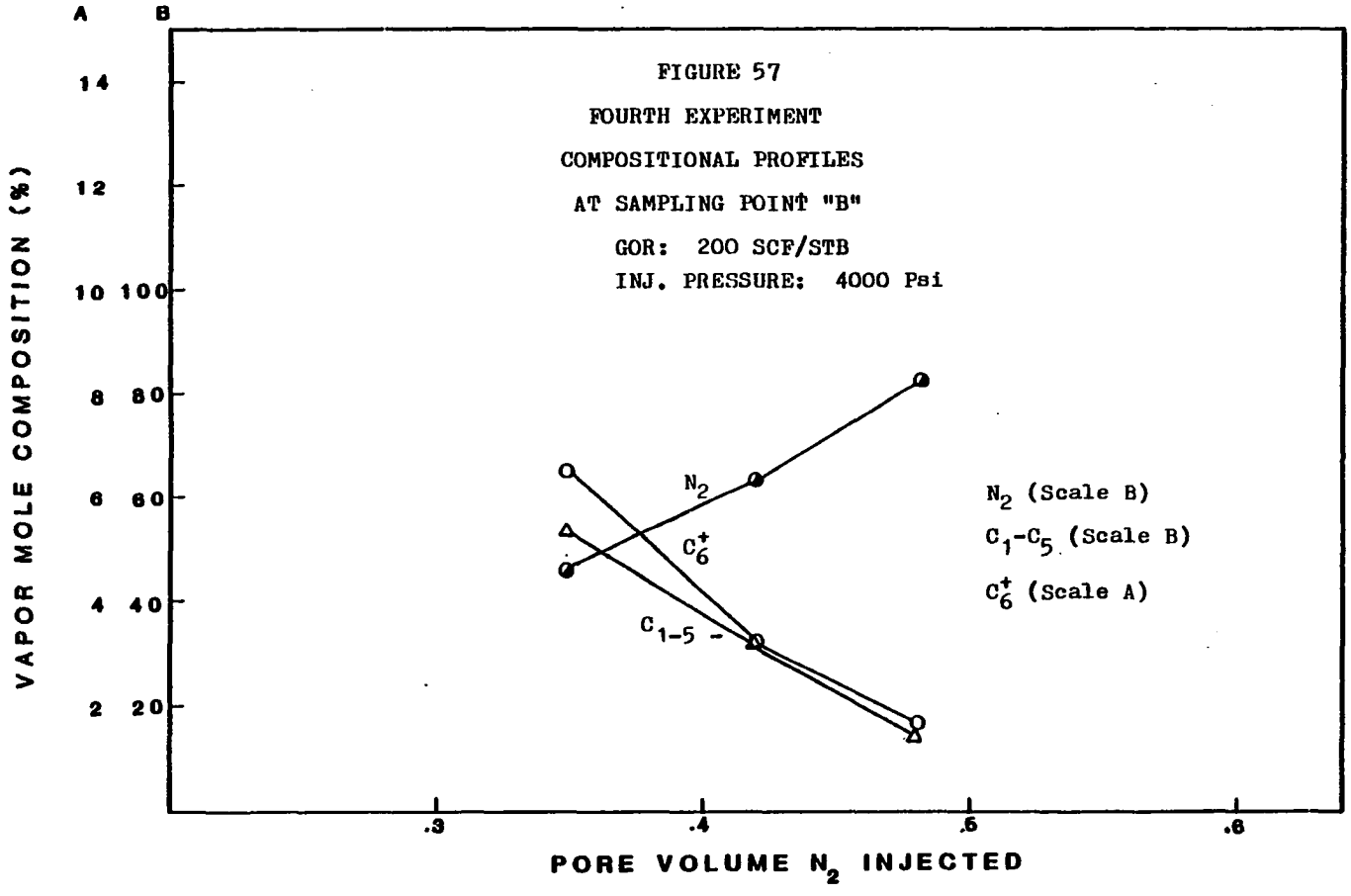

FIGURE 57

FOURTH EXPERIMENT

COMPOSITIONAL PROFILES

AT SAMPLING POINT "B"

GOR: 200 SCF/STB

INJ. PRESSURE: 4000 Psi

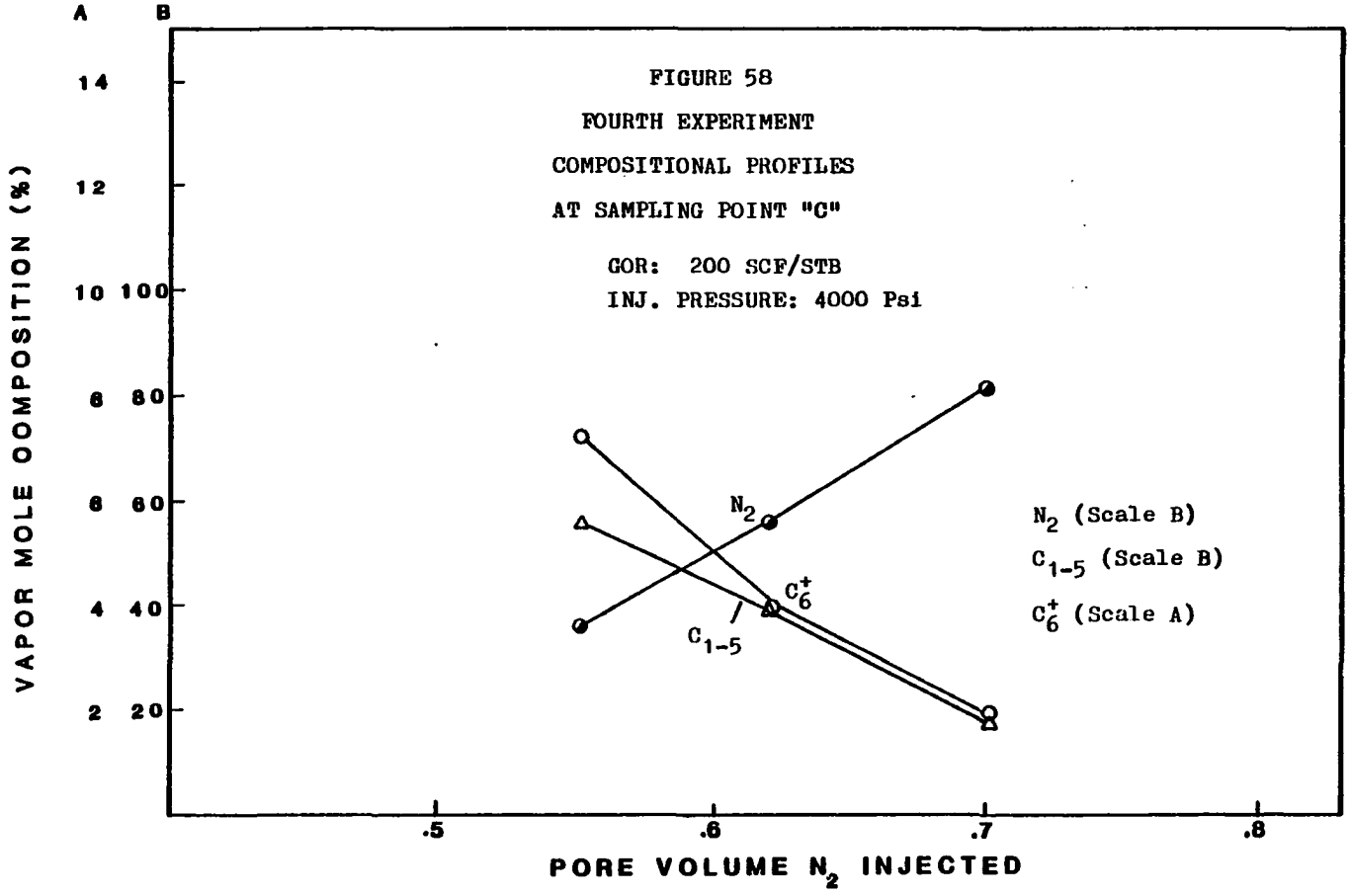

FIGURE 58

FOURTH EXPERIMENT

COMPOSITIONAL PROFILES

AT SAMPLING POINT "C"

GOR: 200 SCF/STB

INJ. PRESSURE: 4000 Psi

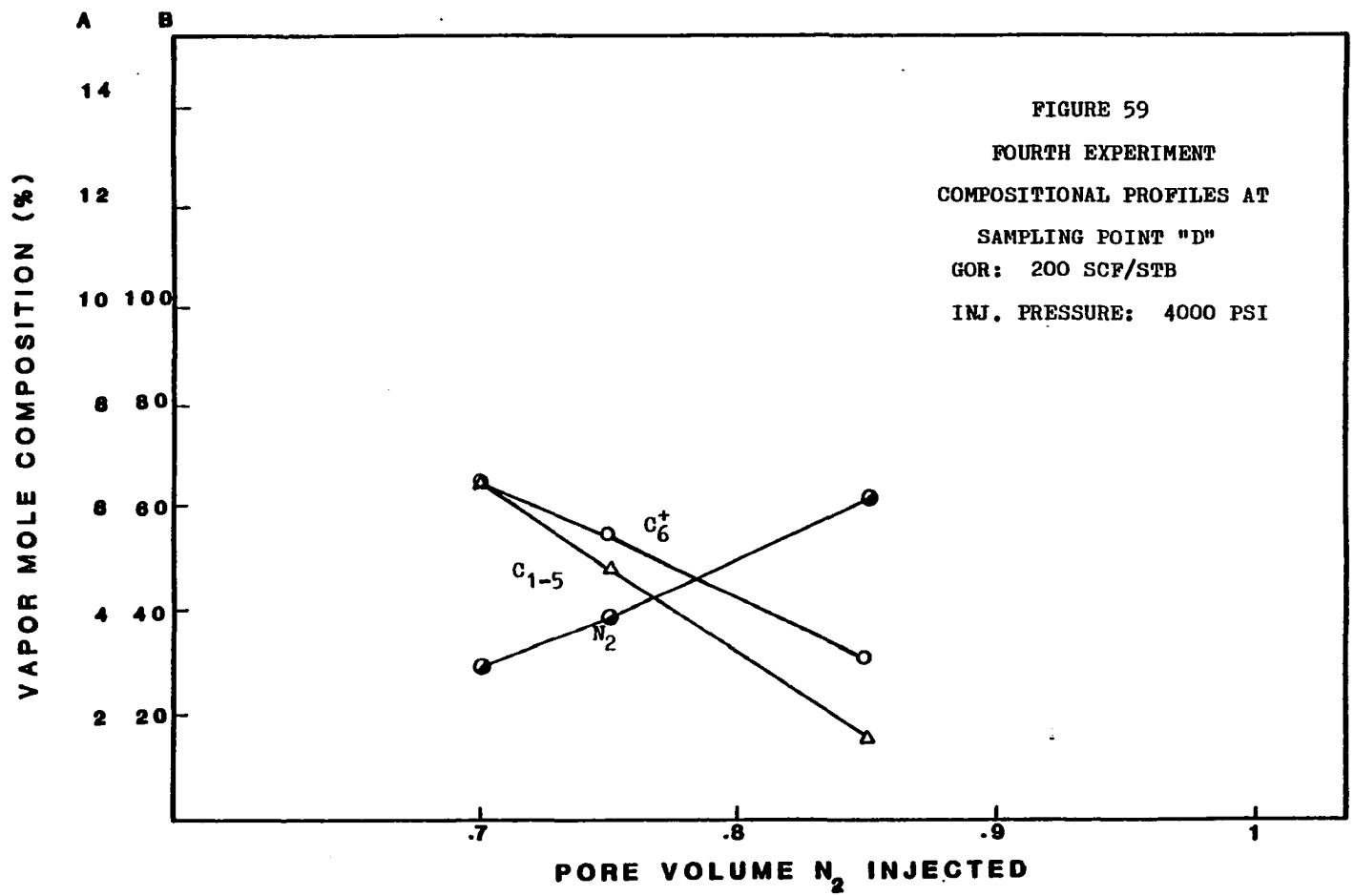

FIGURE 59

FOURTH EXPERIMENT

COMPOSITIONAL PROFILES AT

SAMPLING POINT "D"

GOR: 200 SCF/STB

INJ. PRESSURE: 4000 PSI

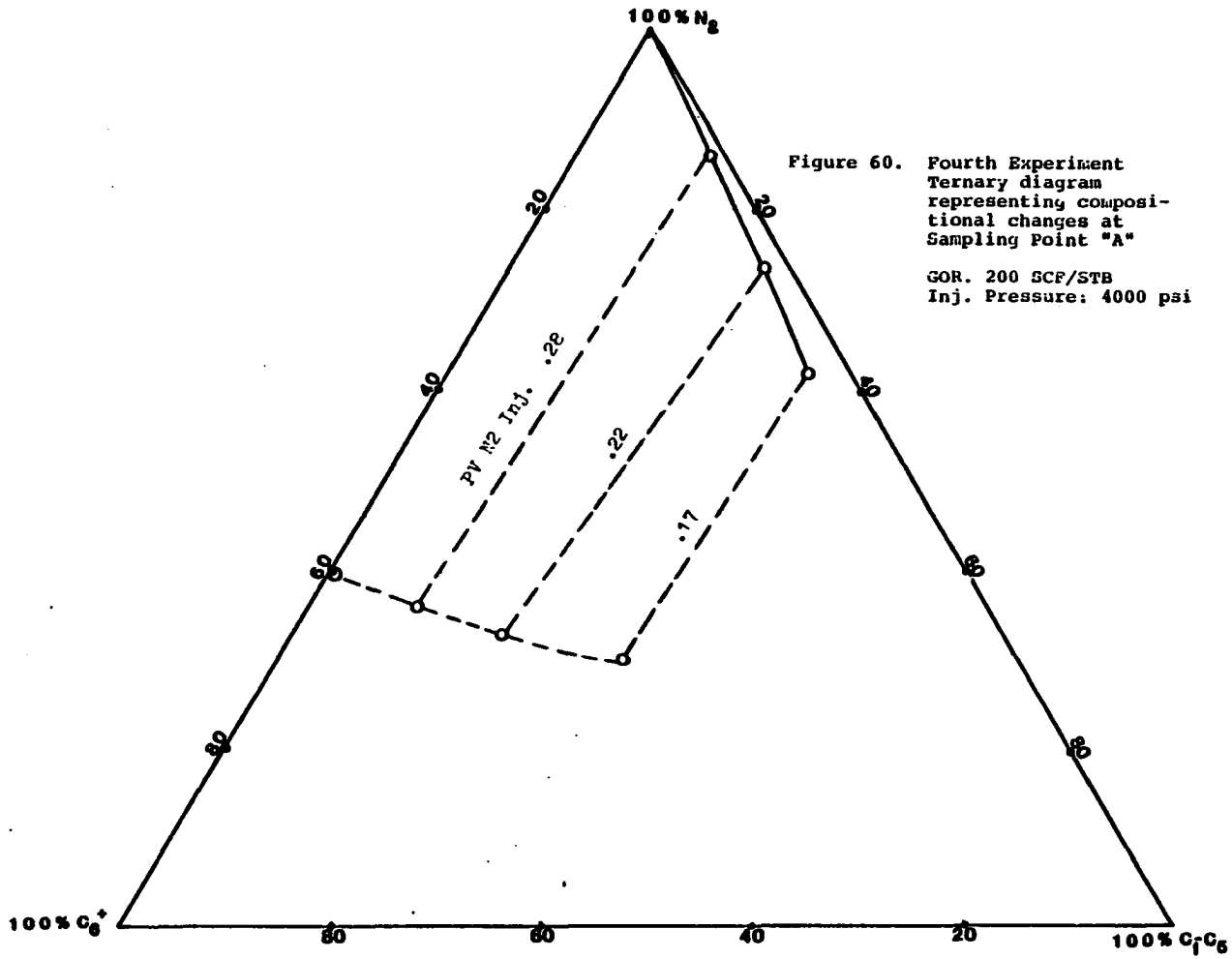

Figure 60. Fourth Experiment Ternary diagram representing compositional changes at Sampling Point "A"

GOR. 200 SCF/STB
Inj. Pressure: 4000 psi

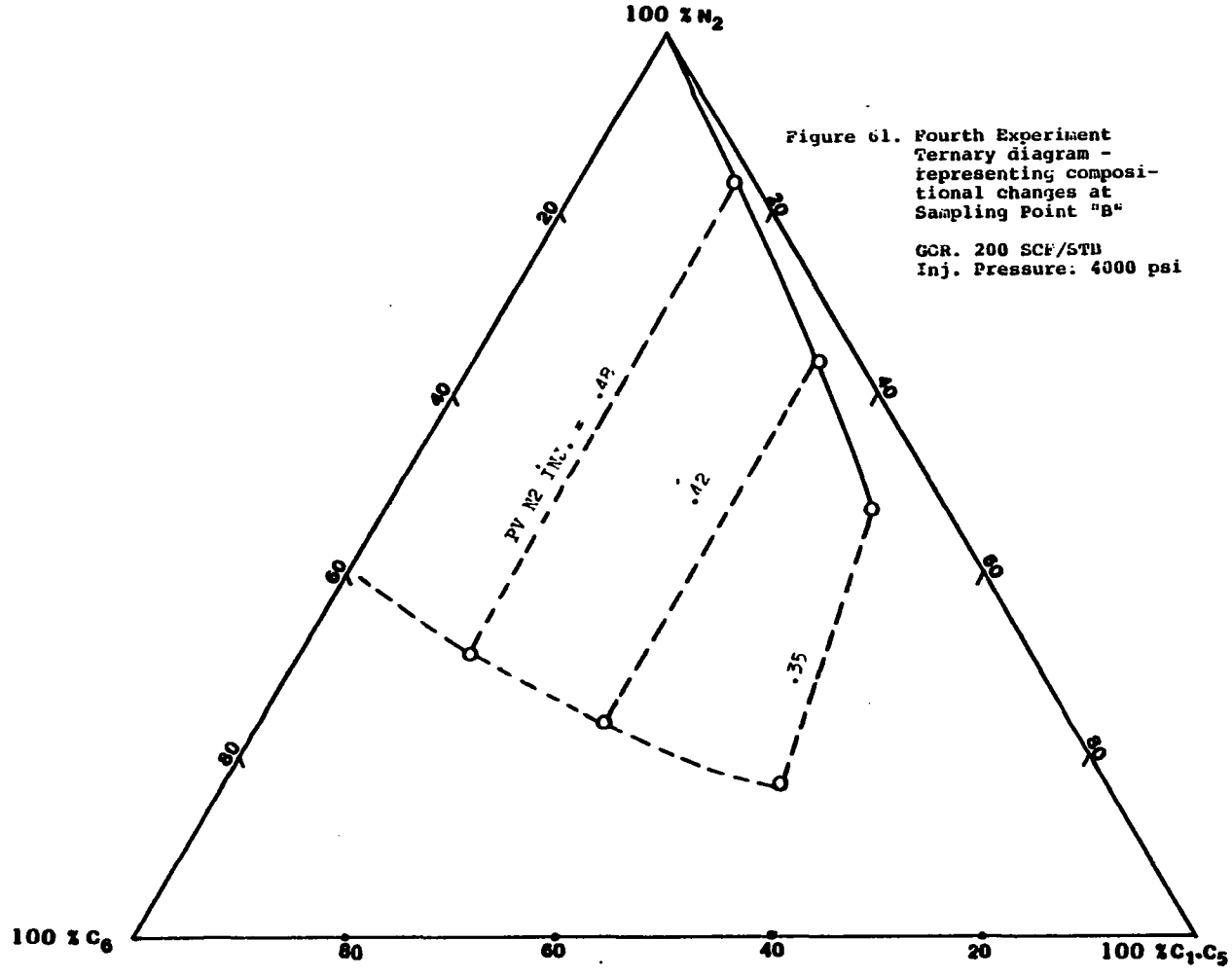

Figure 61. Fourth Experiment Ternary diagram - representing compositional changes at Sampling Point "B"

GOR. 200 SCF/STB
Inj. Pressure: 4000 psi

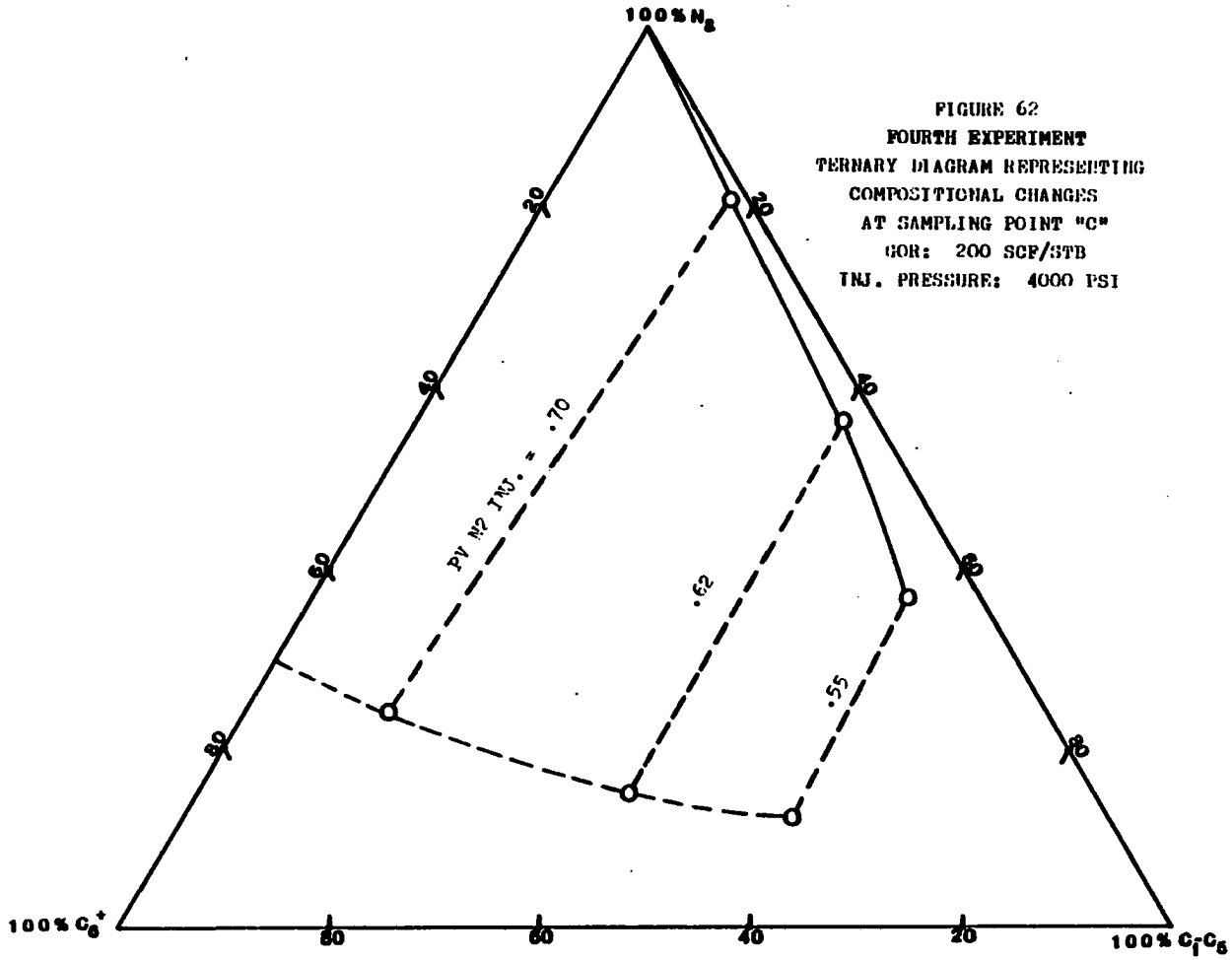

FIGURE 62
FOURTH EXPERIMENT
TERNARY DIAGRAM REPRESENTING
COMPOSITIONAL CHANGES
AT SAMPLING POINT "C"
GOR: 200 SCF/STB
INJ. PRESSURE: 4000 PSI

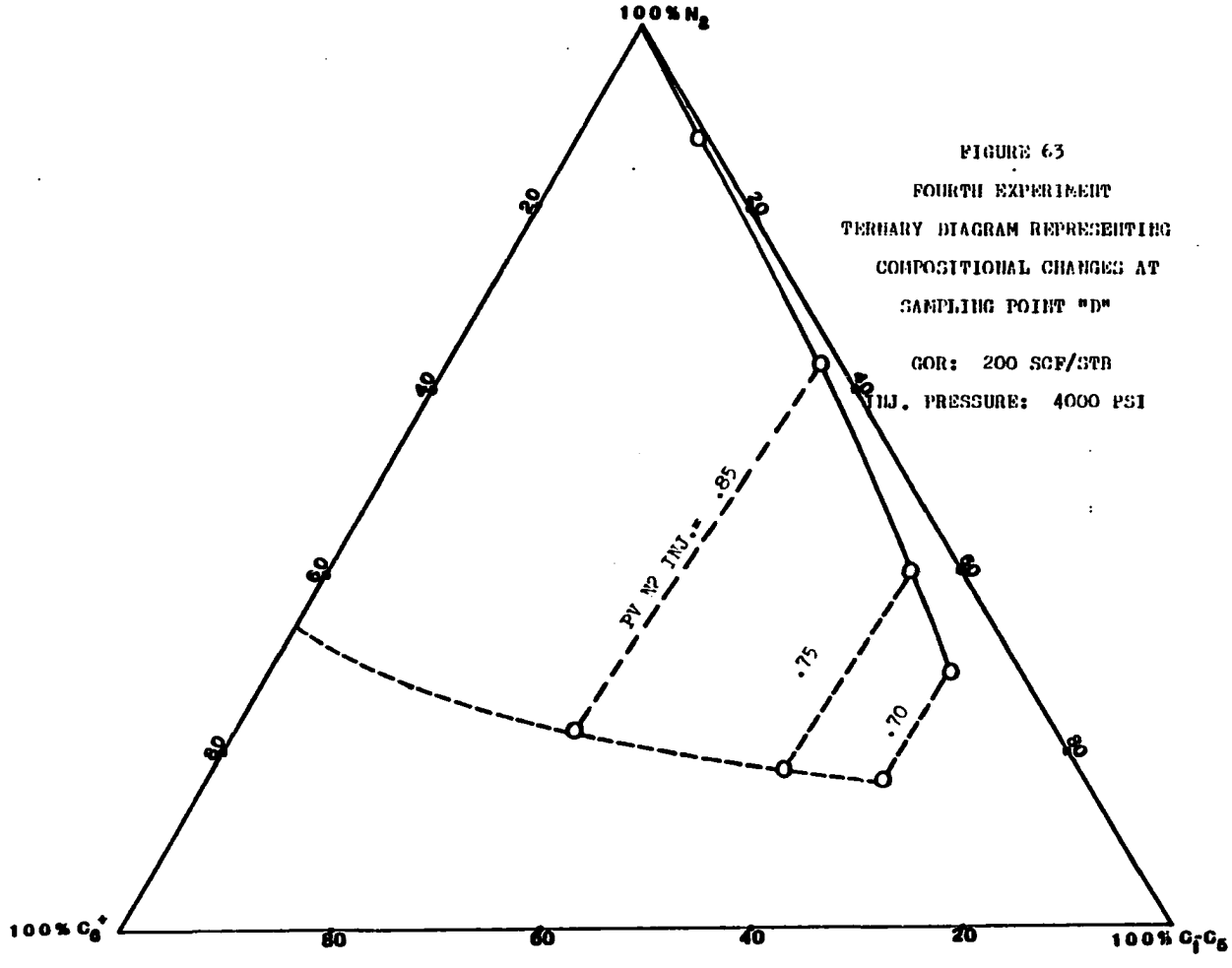

FIGURE 63

FOURTH EXPERIMENT

TERNARY DIAGRAM REPRESENTING

COMPOSITIONAL CHANGES AT

SAMPLING POINT "D"

GOR: 200 SCF/STB

INJ. PRESSURE: 4000 PSI

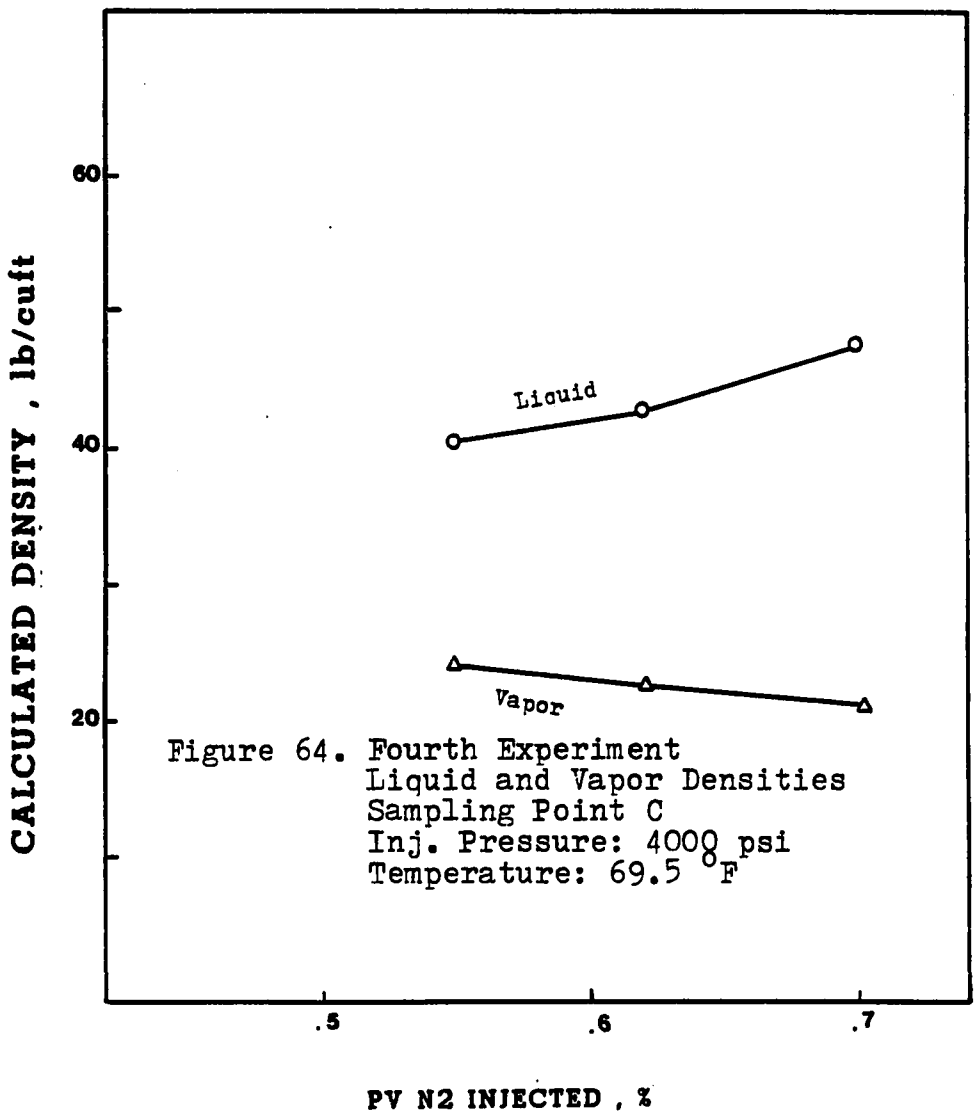

Figure 64. Fourth Experiment
Liquid and Vapor Densities
Sampling Point C
Inj. Pressure: 4000 psi
Temperature: 69.5 °F

Figure 65. Fourth Experiment
Liquid and Vapor Densities
Sampling Point "D"
Inj. Pressure: 4000 psi
Temperature: 69.5 °F

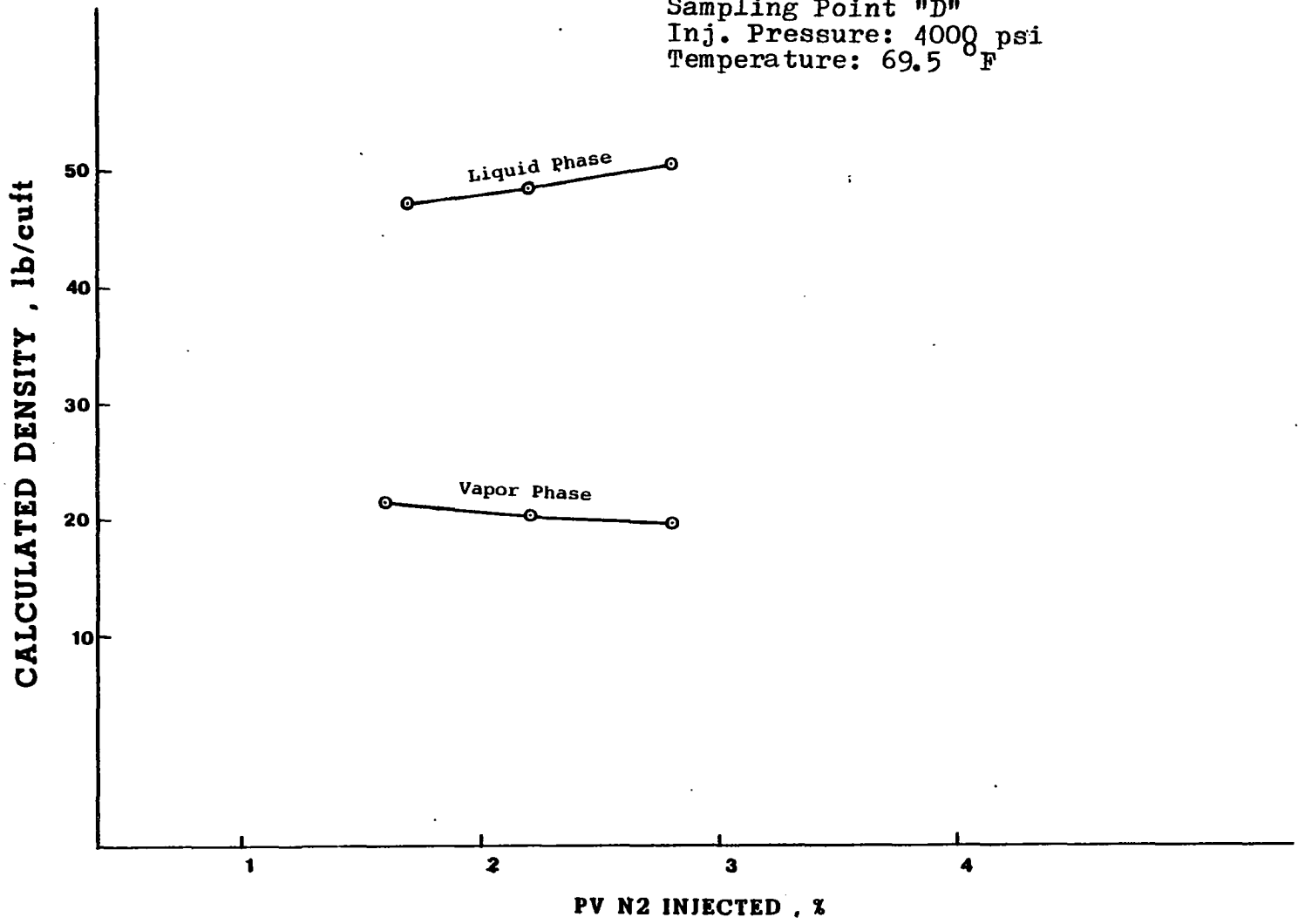

Figure 65A. Fourth Experiment
Surface Tension
Sampling Point "D"
Inj. Pressure: 4000 psi
Temperature: 69.5 °F

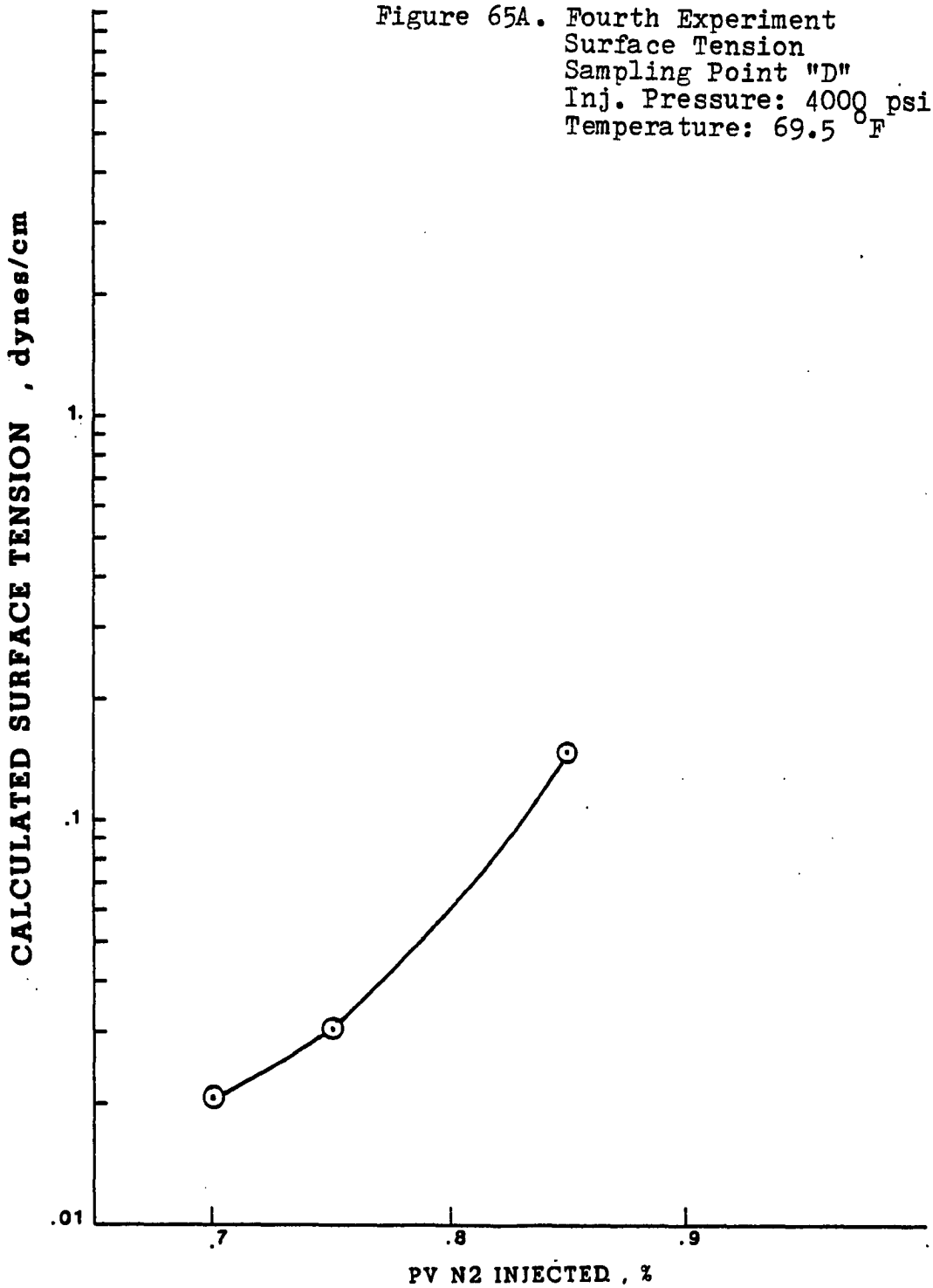

comfirmation of this fact is obtained by observing the compositional profiles and the ternary diagram, shown in Figure 56 to 59 and 60 to 63 respectively. It is obvious that the vaporization process was underway during the test but the number of contacts were not enough to create a miscible bank. This aspect will be discussed together with the results from the past and previous test. A mathematical expression will be proposed later in this chapter in the discussion of results section to related crude oil recovery and GOR in solution with validity for the reservoir physical model used in this experiment.

B-5. Fifth Experiment

In this test the reservoir physical model was maintained at isothermal conditions during all the displacement. This was the first test at hot conditions (120°F) run in this study. This test was designed to study the effect of temperature. It was decided to use the same conditions under which the first two experiments were made. Also the previous researcher (1) made a run with the same conditions but at cold conditions. These facts gave a good background for comparison.

The production history data obtained in this test are presented in Table 12. Parameters and conditions for this test are given hereunder:

Barometric Pressure . . . . . 29.8 inches Hg.

Room Temperature. . . . . 68°F.

Reservoir Physical Temperature. . .	120°F
Injection Pressure.	4000 psi
Solution Gas-Oil Ratio.	575 SCF/STB
Crude Oil Saturation.	80.2% PV
Water Saturation.	19.8% PV
Stock Tank Oil in Place	647.28 cc.
Oil Gravity	42.4° API
Front Advance Velocity.	.116 cm/sec
Formation Volumetric Factor	1.29 Bbl/STB

All the procedure followed in previous tests in this study was followed in this test too.

The chromatograph analysis in form of compositional profiles are given in Figures 69 to 72.

The crude oil fractional recovery of 84.5% is the highest obtained in this study so far. This high crude oil nign recovery suggests that miscibility was achieved during the N_2 displacement. The size of the miscible bank formed in this displacement was approximately 8% PV. In comparison with all the tests run at cold conditions this miscible bank is greater. Compositional profiles curves confirm that miscibility was achieved during this test. The history of production for this test is shown in figures 66, 67 and 68. The change in shape of figure 66 suggests miscibility.

Since in this the temperature was isolated as a manipulated independent variable, it could be proposed that temperature has a significant effect on crude oil recovery.

TABLE 12

HIGH PRESSURE NITROGEN INJECTION DATA
EXPERIMENT #5
Injection Pressure: 4000 PSIG

TIME (MIN)	CUMUL. OIL PROD. (CC)	OIL RECOVERY (% OOIP)	CUMUL. GAS (SCF)	TEMPERATURES (°F) (1)	(2)	(3)	(4)	OUTLET PRESSURE (PSIG)
0	0	0		120	120	121	120	2000
15	9	.014	.03					
30	21	.032	.07					
40	30	.046	.10	119	121	124	118	2005
60	49	.075	.17					
100	90	.139	.32	123	122	121	118	2010
125	114	.176	.41					
200	186	.287	.67	119	121	121	120	2000
260	246	.38	.88					
300	285	.44	1.03	122	120	120	120	2000
324	309	.477	1.11					
382	364	.562	1.31					
415	397	.613	1.43	118	123	122	120	2000
440	432	.667	1.56					
450	452	.704	1.63					
480	481	.743	1.74					
501	504	.778	1.82					
510	516	.797	1.86					
510	518	.815	1.90	120	120	123	119	2000
530	534	.824	1.93					
540	541	.835	1.96	119	121	120	120	2000
547	543	.845	1.97	120	121	121	120	2000
		N_2 BREAKTHROUGH						
550	543.5		2.05					
560	544		2.18					

TABLE 13: CHROMATOGRAPH ANALYSIS OF VAPOR SAMPLES - EXPERIMENT #5

TEMPERATURE: 120°F.; INJECTION PRESSURE: 4000 PSI; GOR: 575 SCF/STB

COMPONENT	SAMPLING POINT A			SAMPLING POINT B			SAMPLING POINT C			SAMPLING POINT D			
	.17	.22	.28	.35	.42	.48	.55	.62	.70	.72-.80	.83	.85	.88
N_2	48.7	69.5	84.2	32.0	58.2	81.8	23.	40.3	78.2	10.8	20.1	39.2	84.8
C_1	34.7	21	.09	40.3	19	7.4	44.1	34.4	11.9	52.7	46.6	36	6.7
C_2	5.6	3.8	.030	11.3	7.6	5.3	12.6	10.8	4.5	12.3	11.9	9.5	3.1
C_3	4.2	2.6	.020	8.2	5.7	3.5	10.7	9.1	2.4	10.4	9.0	6.9	2.1
C_4	.76	.06	0.	.52	.08	0	.8	.6	0	9	0.6	.3	0.
$N\text{-}C_4$	.14	.04	0.	.78	0.12		.8	.4	0	.7	0.5	.2	0.
C_5	.68	.20	0.	.76	.24	0	1.1	0.2	0.1	1.7	1.3	.7	.3
$N\text{-}C_5$	1.2	.30	.0	1.14	.16		1.0	0.1	0	1.5	1.2	.6	.2
C_5^+	4.0	2.5	1.8	5.	3.8	2.0	5.9	5.0	2.9	9.0	8.8	6.6	2.5

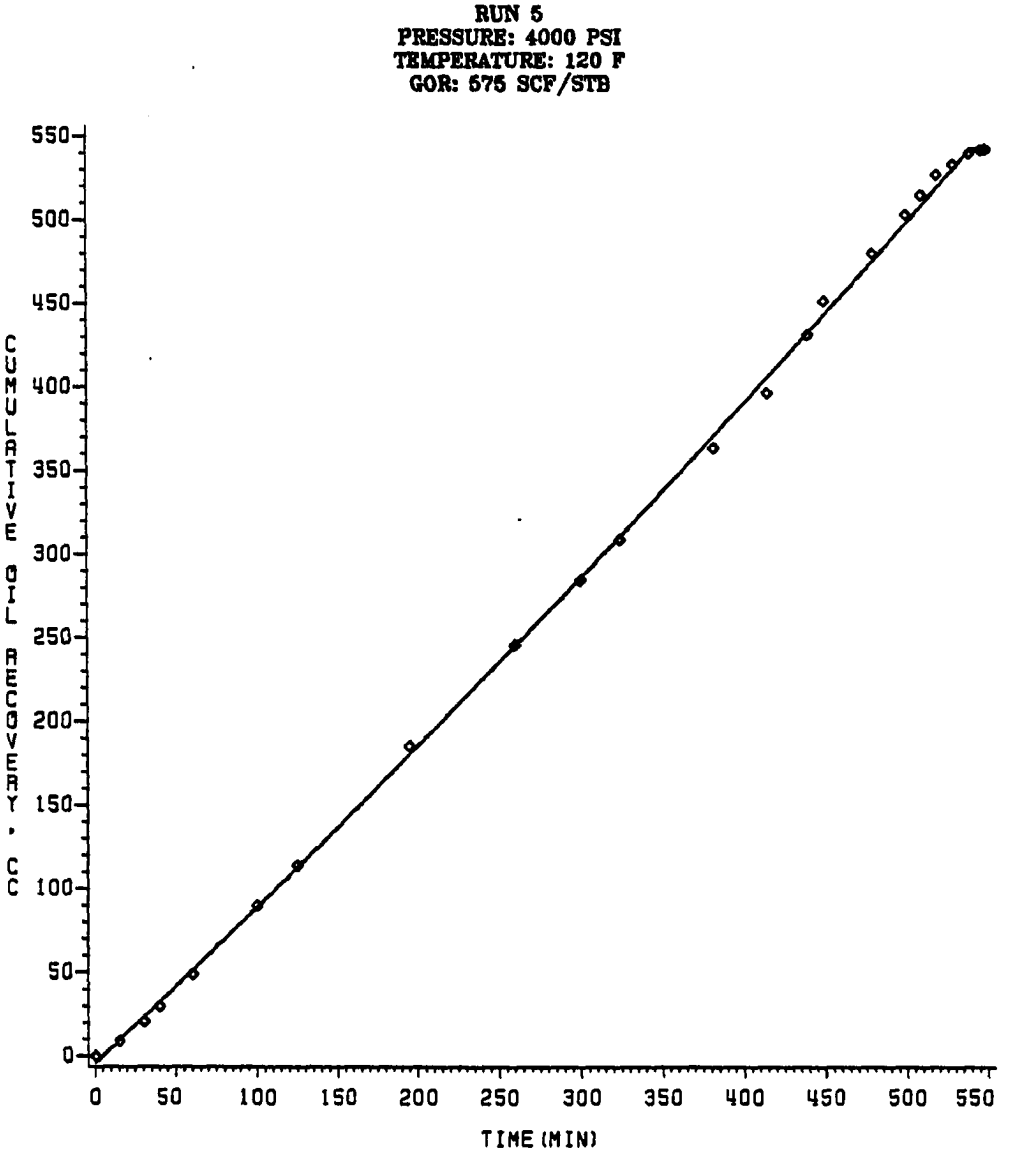

FIGURE 66
CUMULATIVE OIL RECOVERY VS TIME

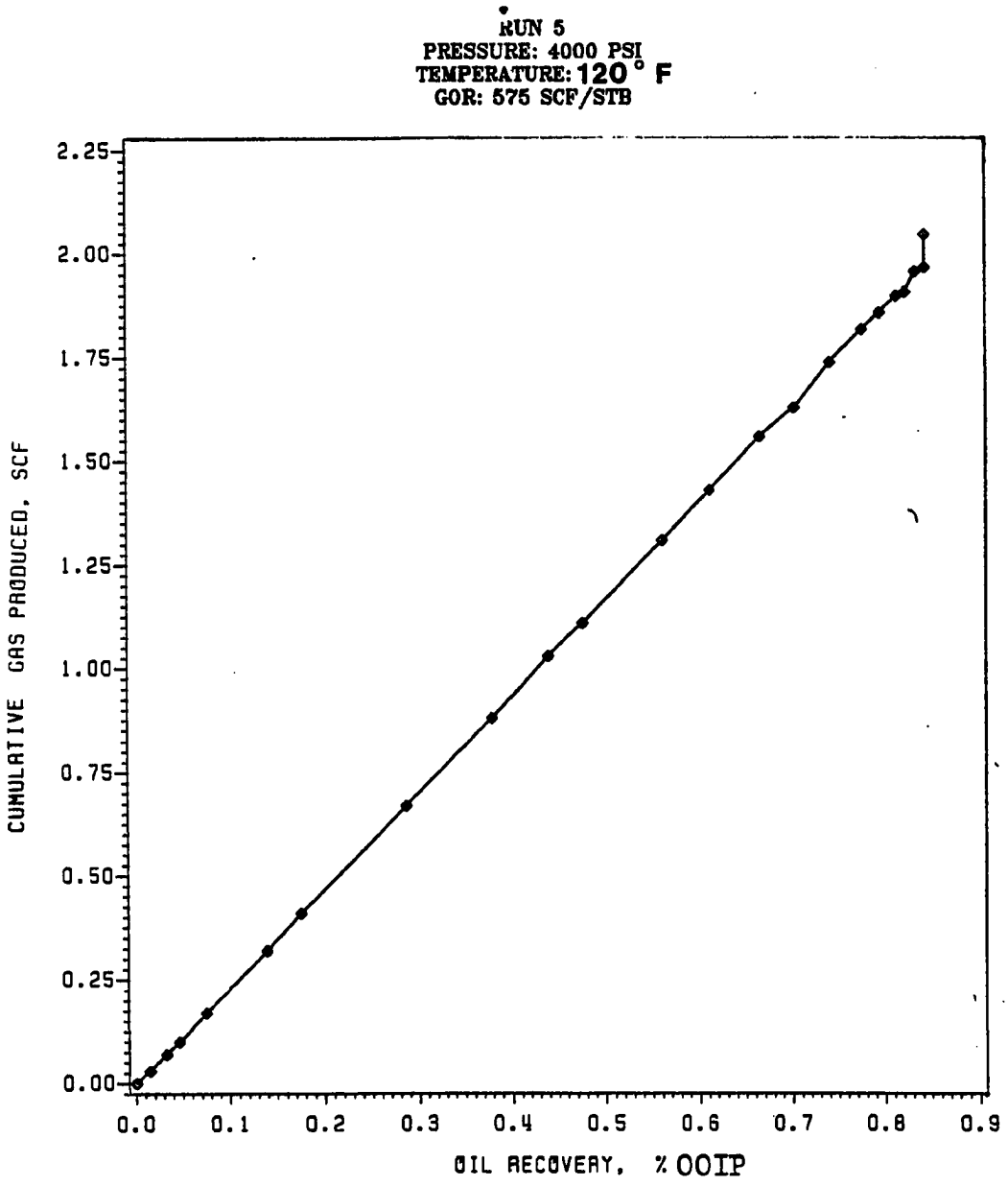

FIGURE 67
CUMULATIVE GAS PRODUCED VS OIL RECOVERY

RUN 5
PRESSURE: 4000 PSI
TEMPERATURE: 120 °F
GOR: 575 SCF/STB

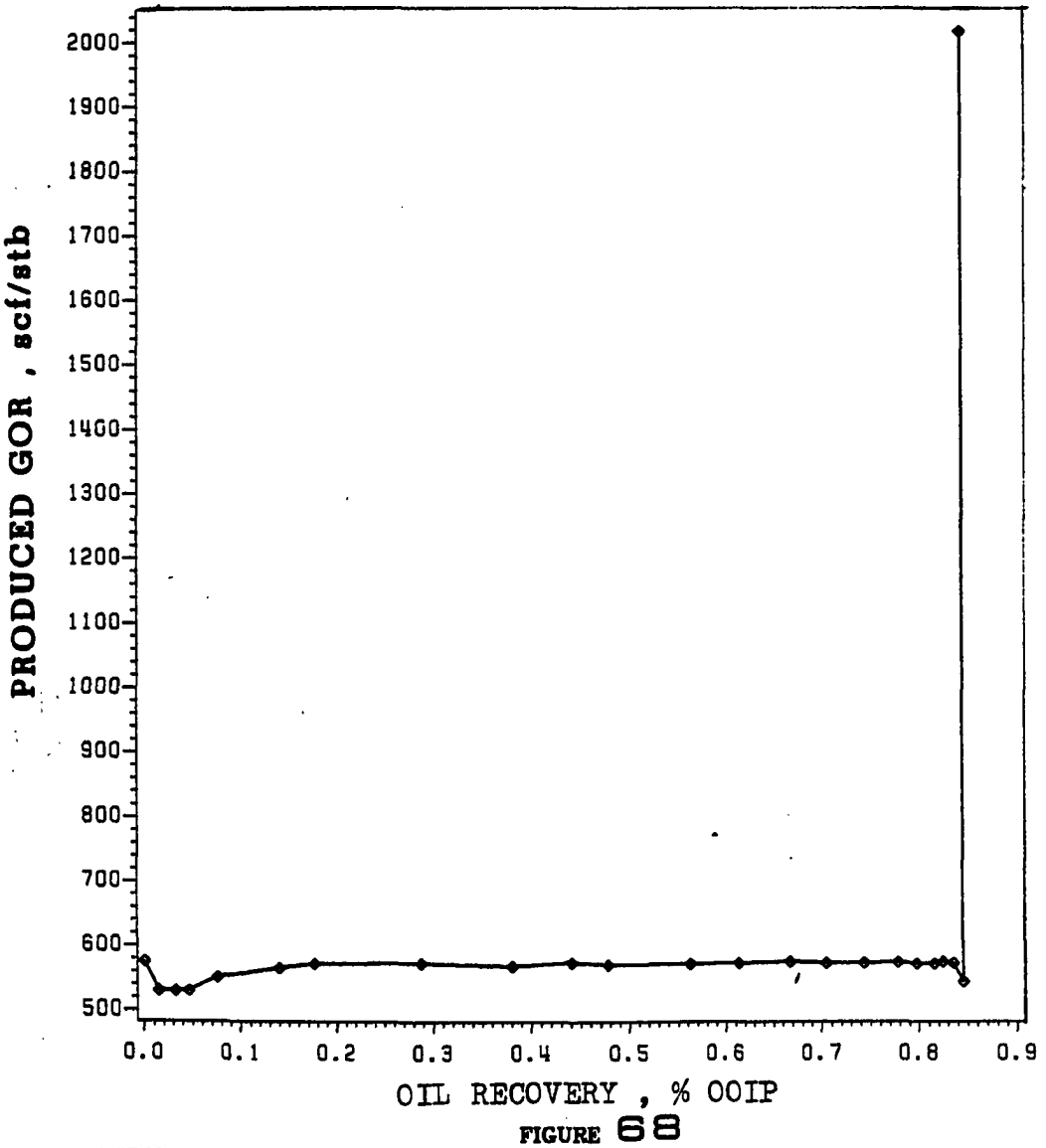

FIGURE 68

PRODUCED GOR VS OIL RECOVERY

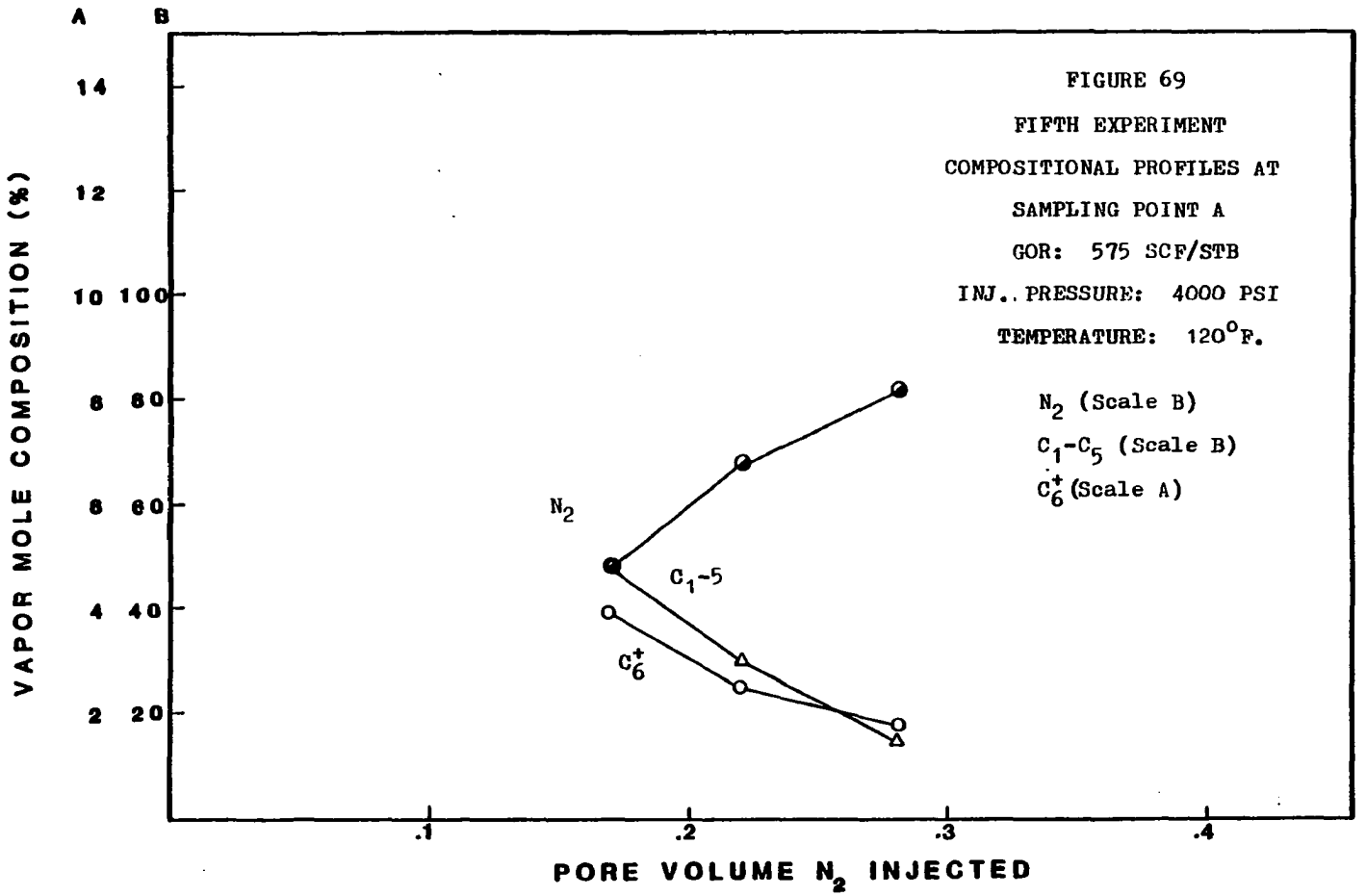

FIGURE 69
FIFTH EXPERIMENT
COMPOSITIONAL PROFILES AT
SAMPLING POINT A
GOR: 575 SCF/STB
INJ.. PRESSURE: 4000 PSI
TEMPERATURE: 120°F.

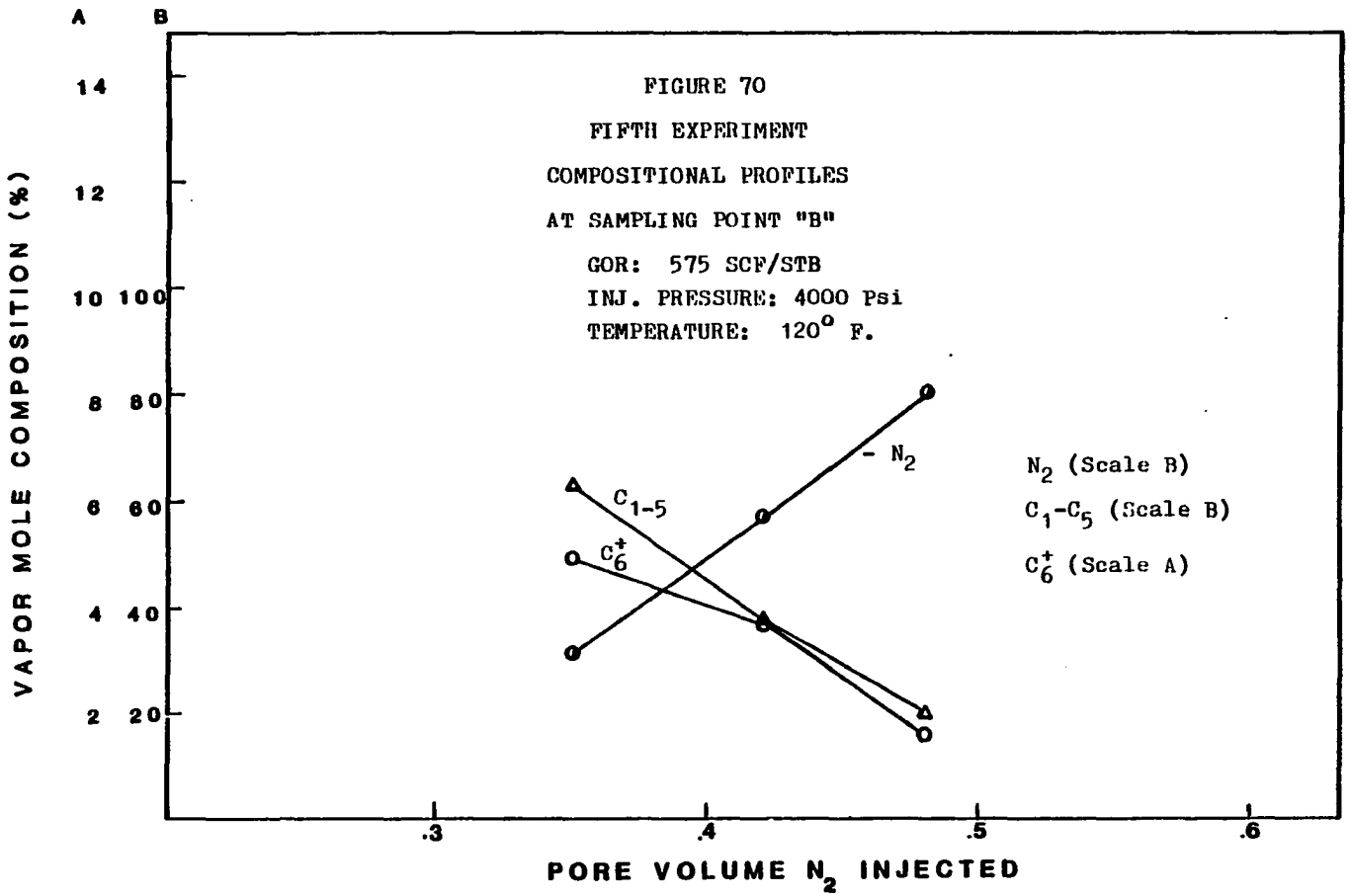

FIGURE 70

FIFTH EXPERIMENT

COMPOSITIONAL PROFILES

AT SAMPLING POINT "B"

GOR: 575 SCF/STB

INJ. PRESSURE: 4000 Psi

TEMPERATURE: 120° F.

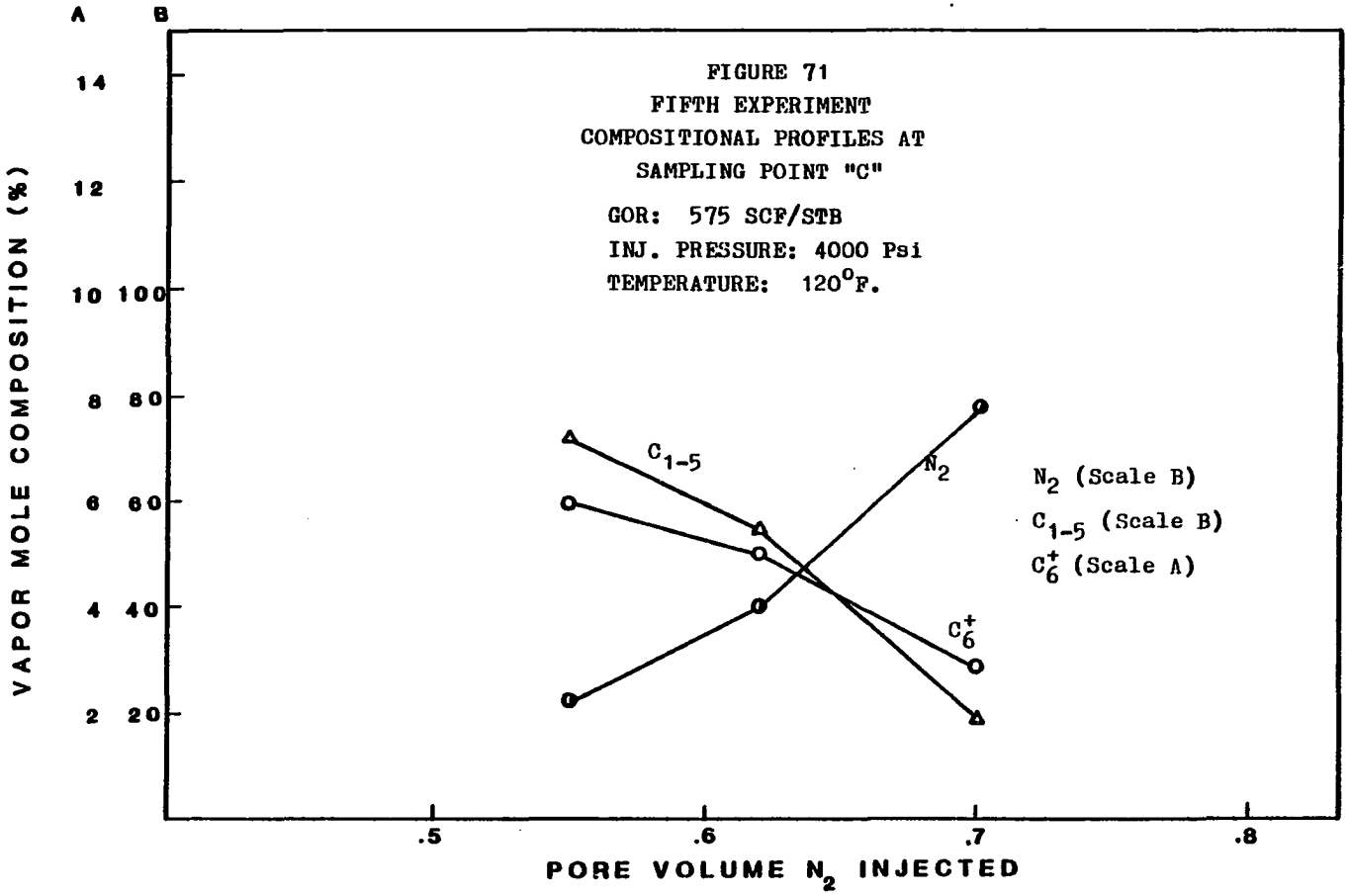

FIGURE 71
FIFTH EXPERIMENT
COMPOSITIONAL PROFILES AT
SAMPLING POINT "C"

GOR: 575 SCF/STB
INJ. PRESSURE: 4000 Psi
TEMPERATURE: 120°F.

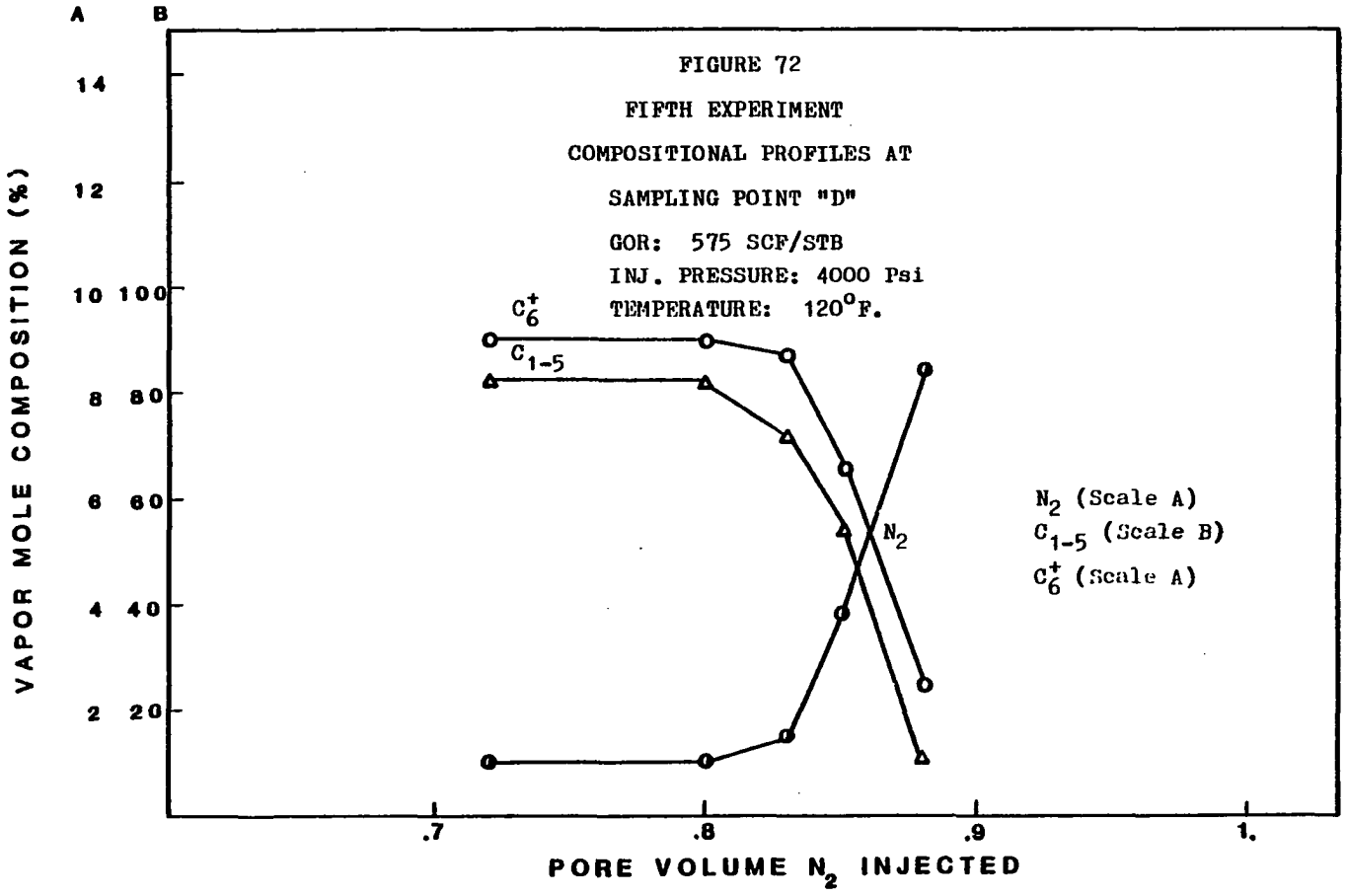

FIGURE 72

FIFTH EXPERIMENT

COMPOSITIONAL PROFILES AT

SAMPLING POINT "D"

GOR: 575 SCF/STB

INJ. PRESSURE: 4000 Psi

TEMPERATURE: 120°F.

This proposition will be discussed in detail later in this chapter.

B-6. Sixth Experiment

The sixth test was a regular nitrogen displacement in which the hot condition was kept but the amount of natural gas in solution was reduced to 200 SCF/STB.

The objective of this test was to compare with previous tests and study the combined effect of gas-oil ratio and temperature in recovery and miscibility.

Production history from this test is presented in Table 14. Parameters and conditions for this test are given below:

Barometric Pressure	28.2 inches Hg.
Room Temperature.	68°F.
Reservoir Physical Model Temperature	120°F.
Injection Pressure.	4000 psi
Solution Gas-Oil Ratio.	200 SCF/STB
Crude Oil Saturation.	81% PV
Water Saturation.	19% PV
Stock Tank oil in Place	738.18 cc.
Oil Gravity	42.4° API
Front Advance Velocity	.105 cm/sec
Formation Volumetric Factor	1.1 Bbl/STB

Samples of the displacing phase were taken and analyzed during this test. Results are shown in Table 15.

TABLE 14

HIGH PRESSURE NITROGEN INJECTION DATA
EXPERIMENT #6
Injection Pressure: 4000 PSIG

TIME (MIN)	CUMUL. OIL PROD. (CC)	OIL RECOVERY (% OOIP)	CUMUL. GAS (SCF)	TEMPERATURES (°F) (1)	(2)	(3)	(4)	OUTLET PRES-SURE (PSIG)
0	0	0	--	120	120	121	120	2000
20	8	0.011	.01	121	120	120	121	2000
40	17	0.023	.02	119	118	118	119	2005
60	38	0.051	.05	120	120	120	121	2000
81	52	0.070	.06	120	118	118	120	2000
100	70	0.095	.09	121	123	122	121	2000
120	84	0.108	.10	120	121	121	120	2000
140	104	0.141	.13	120	120	120.5		
							121	2000
161	121	0.164	.15	121	120	120	120	2000
186	140	0.190	.17	121	120	121	120	2000
210	159	.215	.20	120	120	120	120	2000
232	180	.244	.23	121	120	121	120	2000
256	200	.271	.25	120	119	120	119	2000
280	222	.301	.28	120	119	121	120	2007
300	246	.333	.31	119	118	120	119	2000
320	261	.354	.32	120	120	120	120	2001
342	280	.379	.35	121	120	121	120	2000
360	297	.402	.37	120	119	120	119	2000
400	332	.450	.42	123	121	121	119	2000
442	363	.492	.46	122	121	121	120	2000
480	410	.555	.52	121	120	120	119	2005
510	446	.604	.56	120	119	120	119	2000
541	471	.641	.60	121	120	121	120	2000
560	484	.669	.62	120	120	120	120	2000
581	500	.677	.63	119	118	119	119	2002
604	512	.694	.64	120	120	120	120	2004
	BREAKTHROUGH							
620	512.02		.75	120	120	121	120	2000

TABLE 15: CHROMATOGRAPH ANALYSIS OF VAPOR SAMPLES

EXPERIMENT #6

Temperature: 120°F.; Injection Pressure: 4000 Psi; GOR: 200 SCF/STB

COMPONENTS	SAMPLING POINT A			SAMPLING POINT B			SAMPLING POINT C			SAMPLING POINT D		
	.17	.22	.28	.35	.42	.48	.55	.62	.70	.75	.83	.88
N_2	44.0	63.5	93.90	31.70	51.9	79.4	26.4	48.9	80.10	23.1	39.5	75.7
C_1	39.3	26.8	4.35	41.96	29.5	12.6	41.6	30.4	13.9	46.7	37.1	16.2
C_2	6.2	2.9	.57	10.7	8.6	3.3	11.3	8.7	3.1	11.87	9.69	3.1
C_3	4.2	2.35	.04	7.52	4.8	1.8	8.74	4.23	1.04	9.89	6.6	1.9
i C_4	0.52	0.13	0	1.0	.8	.6	1.3	.92	.06	.71	.51	.3
nC_4	.62	.13	0	0.2	.0	.0	.66	.46	.0	.70	.2	.1
i C_5	.67	.39	.02	.94	.18	.6	1.4	.90	.0	1.41	.8	.5
nC_5	.57	.3	.02	.88	.81	.2	1.1	.49	.0	.80	.3	.1
C_6^+	4.0	3.5	1.1	5.1	3.5	1.5	7.5	5.1	1.8	6.2	5.3	2.1

No miscibility was achieved during this test. There are not evidences of miscibility from compositional profiles (Figures 76 to 79), or production history; specifically there is not visible change in shape of the curve of crude oil recovery versus time shown in Figure 73.

As can be seen in Figures 76 to 79, the vaporization process was underway from the very beginning of the displacement but miscibility never was achieved.

In comparison with Experiment No. 4, recovery at breakthrough (66%) was higher in this test at hot conditions (69.4%). Since basically all the displacement was immiscible the increase in recovery has to be attributed partially to the increase in temperature. More detail will be discussed in the next section.

B-8. Seventh and Eighth Experiments

The seventh test was a regular waterflooding at 120°F. The rate of injection was constant, hence, the pressure varied during all the test. Pressure changes are reported. At water breakthrough the water injection was stopped. An analysis of this test will be presented later in this section.

The eighth test was a tertiary oil recovery by high-pressure nitrogen injection. The gas-oil ratio in solution was 575 SCF/STB for the test. Results of the test are presented in Table 17. Samples from the displacement phase were taken and analyzed by means of the chromatograph.

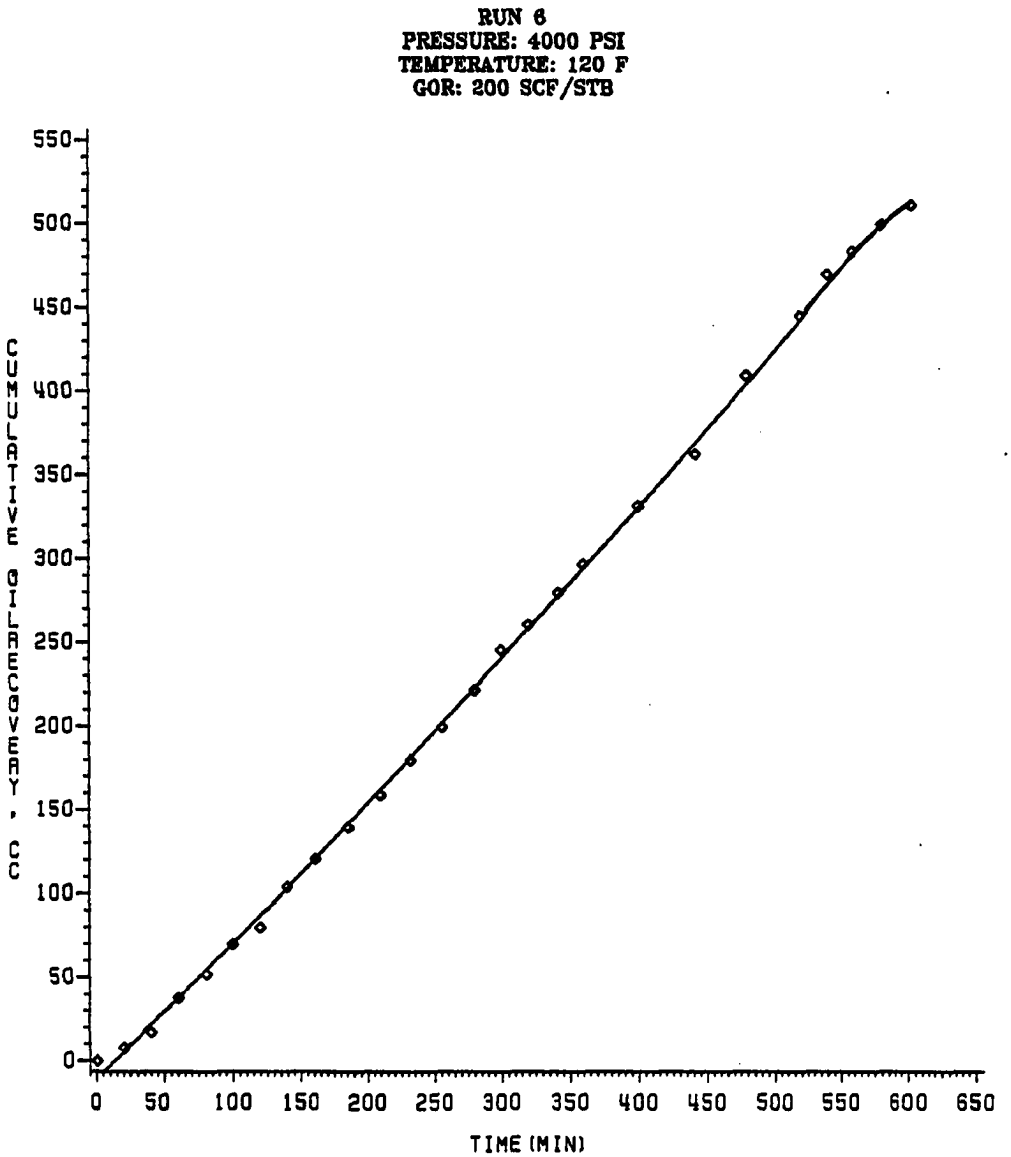

FIGURE 73
CUMULATIVE OIL RECOVERY VS TIME

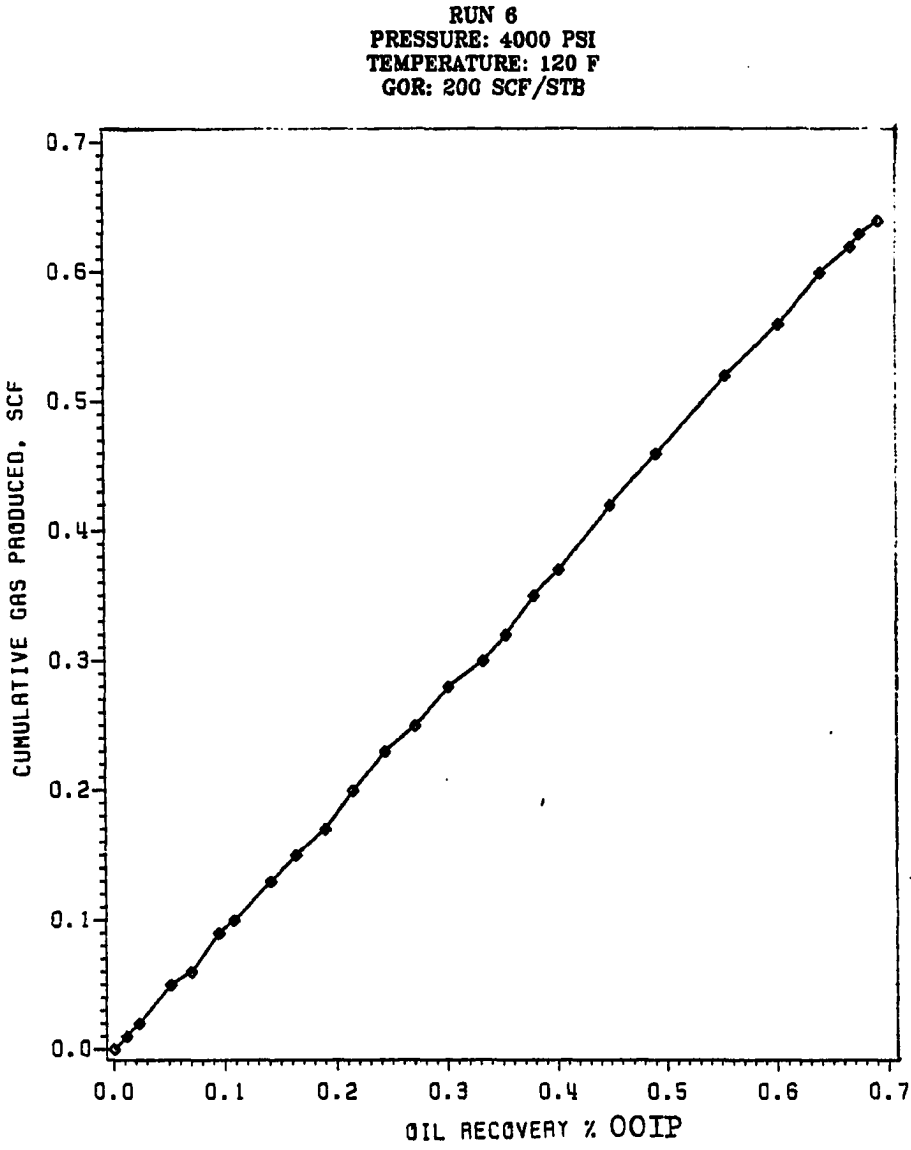

FIGURE 74
CUMULATIVE GAS PRODUCED VS OIL FRACTION RECOVERY

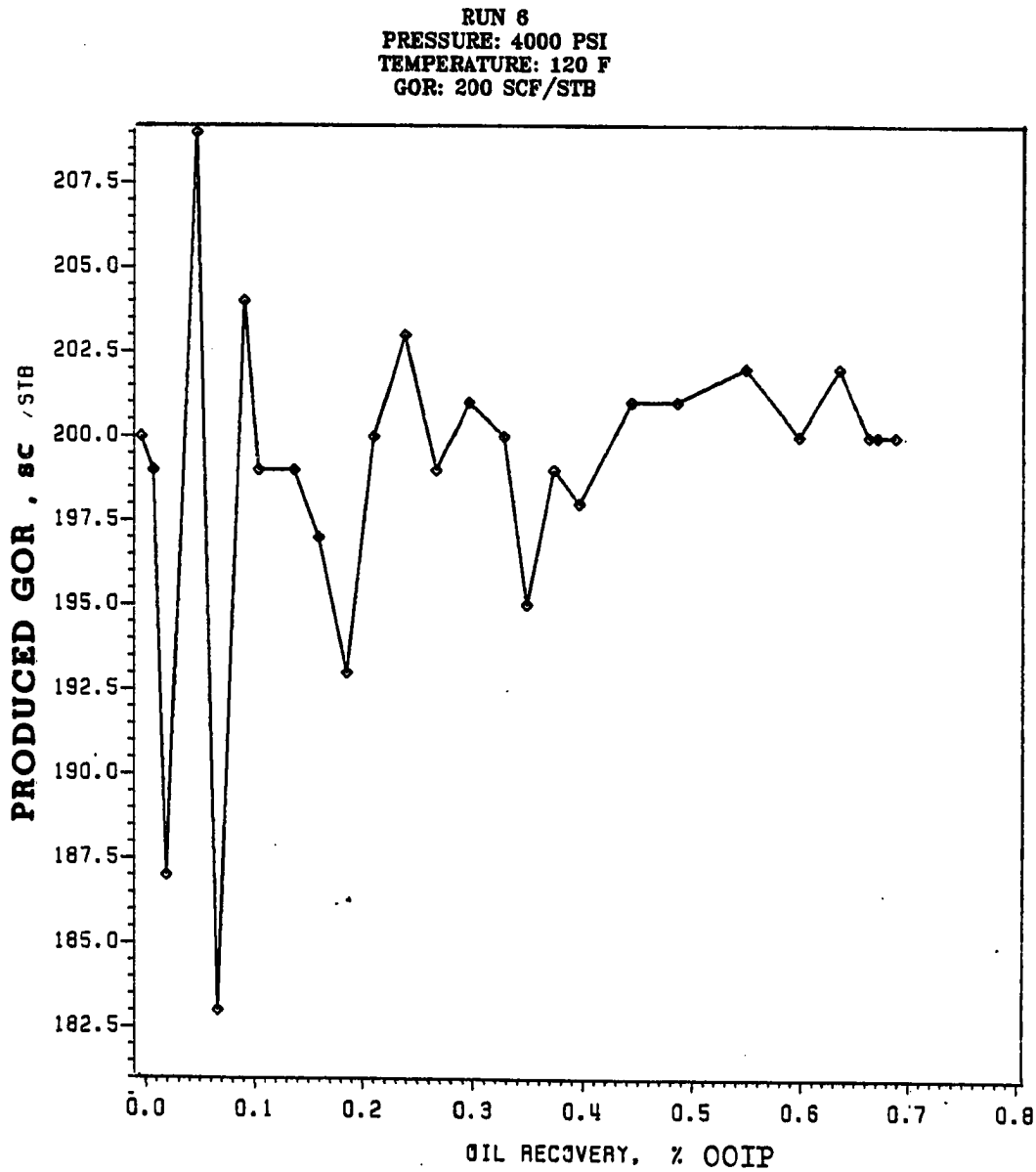

FIGURE 75
PRODUCED GOR VS OIL RECOVERY

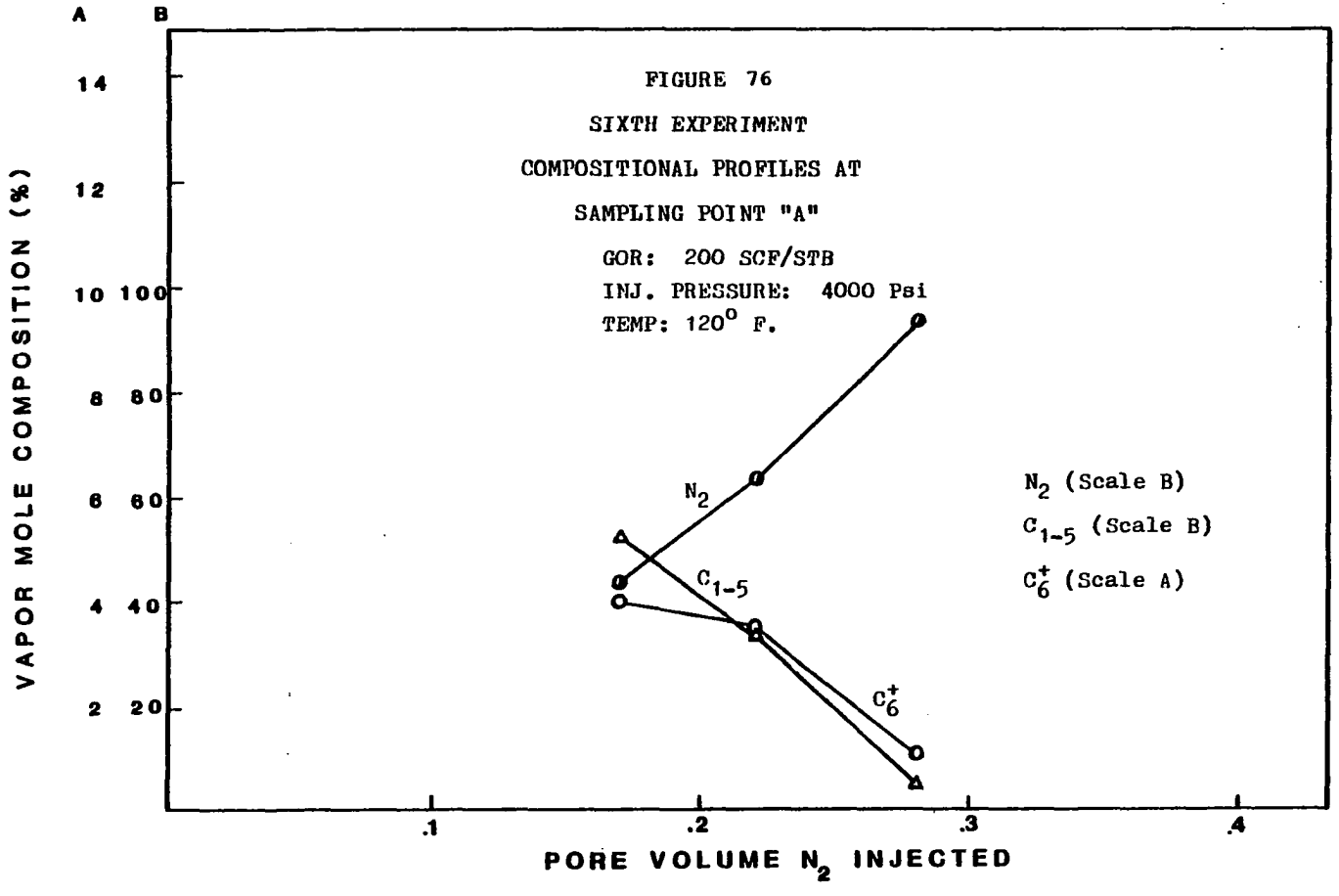

FIGURE 76

SIXTH EXPERIMENT

COMPOSITIONAL PROFILES AT

SAMPLING POINT "A"

GOR: 200 SCF/STB

INJ. PRESSURE: 4000 Psi

TEMP: 120° F.

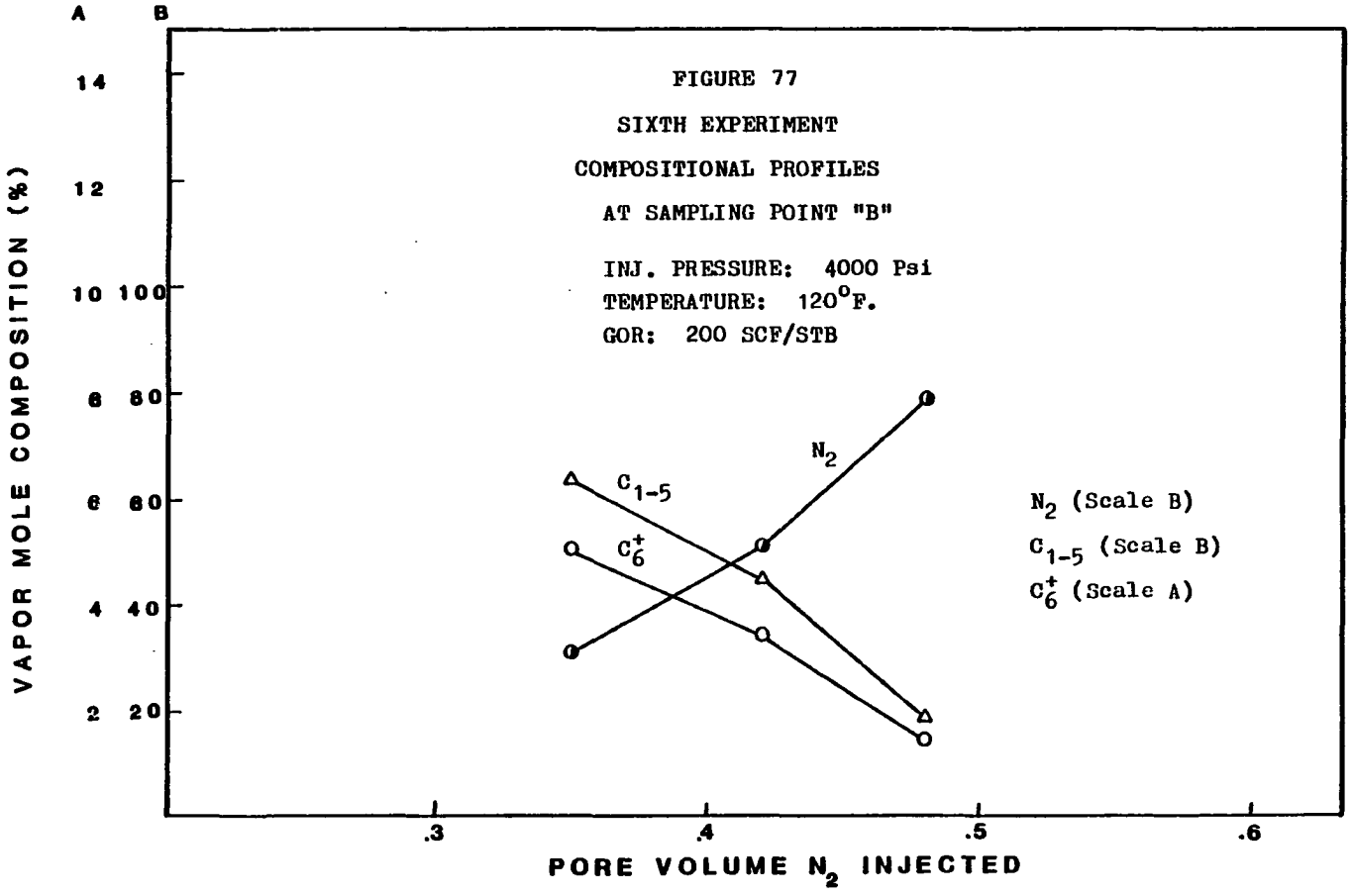

FIGURE 77

SIXTH EXPERIMENT

COMPOSITIONAL PROFILES

AT SAMPLING POINT "B"

INJ. PRESSURE: 4000 Psi
TEMPERATURE: 120°F.
GOR: 200 SCF/STB

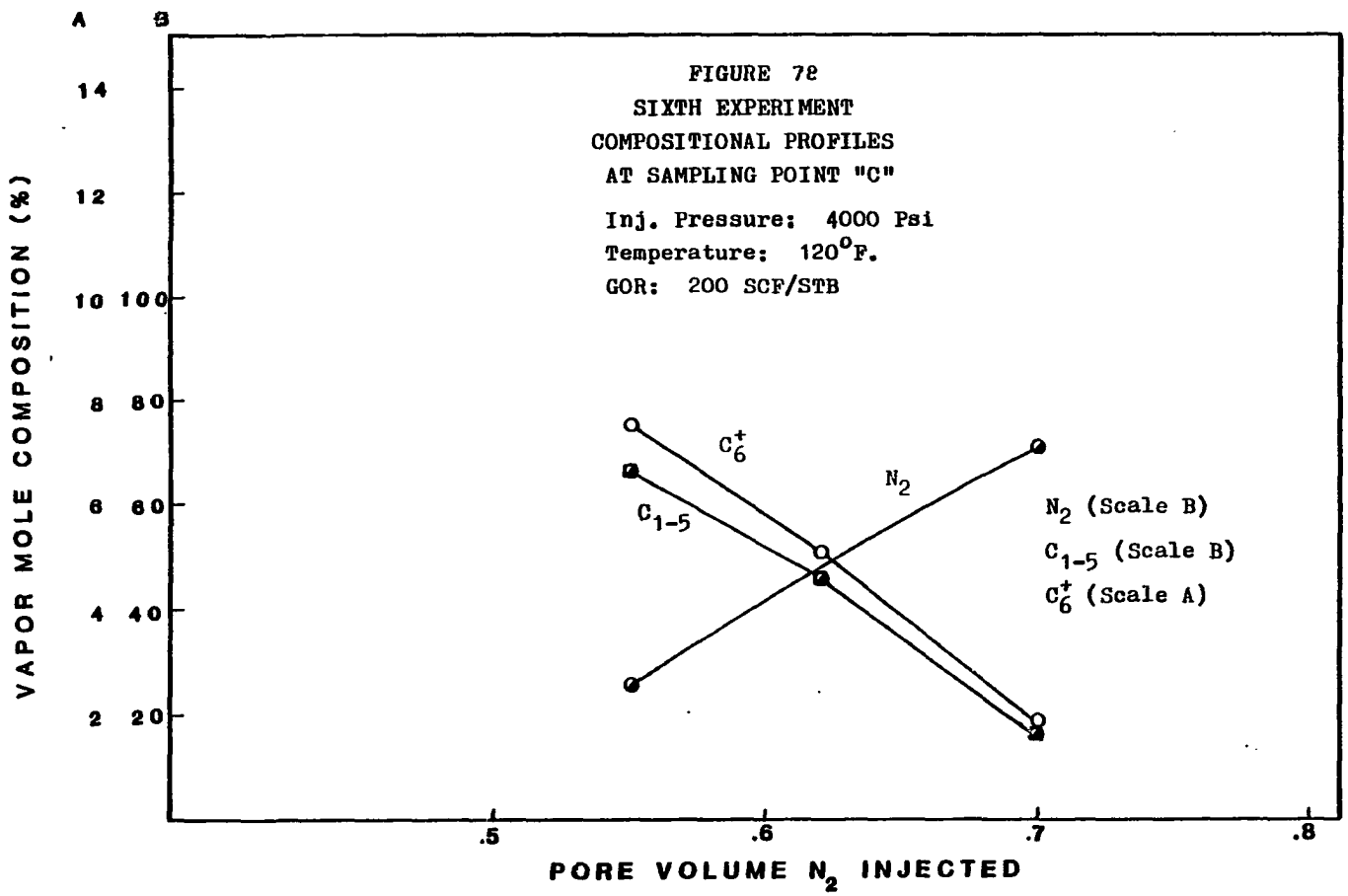

FIGURE 78
SIXTH EXPERIMENT
COMPOSITIONAL PROFILES
AT SAMPLING POINT "C"

Inj. Pressure: 4000 Psi
Temperature: 120°F.
GOR: 200 SCF/STB

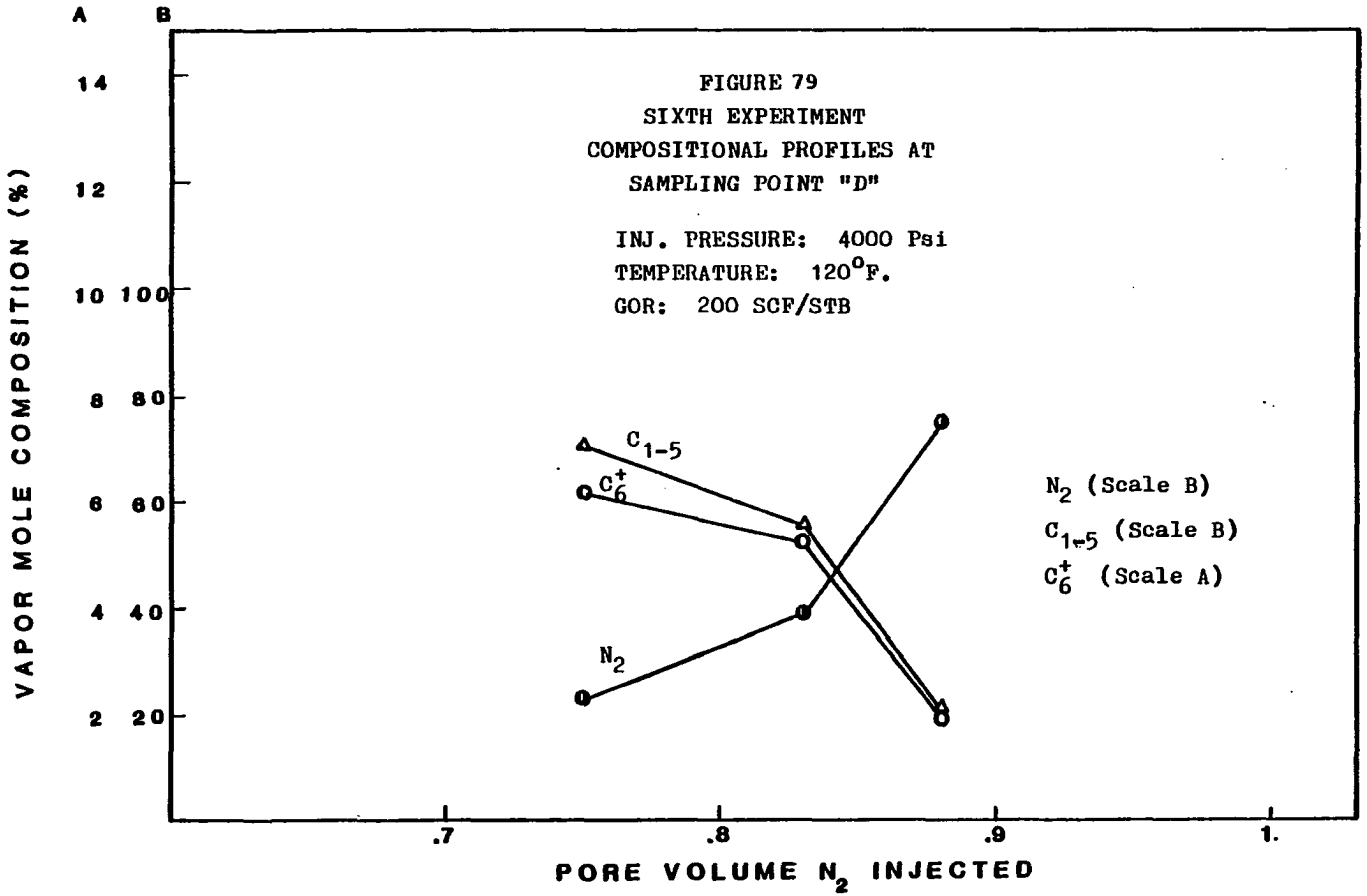

FIGURE 79
SIXTH EXPERIMENT
COMPOSITIONAL PROFILES AT
SAMPLING POINT "D"

INJ. PRESSURE: 4000 Psi
TEMPERATURE: 120°F.
GOR: 200 SCF/STB

The parameters and conditions for this test are given hereunder:

Barometric Pressure	29.1 Hg.
Room Temperature.	74°F.
Reservoir physical model temperature	120°F.
Solution Gas-Oil Ratio.	575 SCF/STB
Crude Oil Saturation.	25% PV
Water Saturation.	75% PV
Stock Tank Oil in Place	203.71 cc
Oil Gravity	42.4° API
Volumetric Flow	.85 cc/min
Front Advance Velocity.	.12 cm/sec
Formation Volumetric Factor	1.29 Bbl/STB

No problem during the test was reported.

Production history curves for the regular waterflooding performed in this study are shown in Figures 80 and 81. The water recovery and performance compare very well with traditional values of waterflooding referred to the literature. This recovery also agrees with recovery reported by Ahmed (1) in cold conditions.

The test #8 was designed to observe how the temperature would affect the tertiary recovery with a low saturation of oil and free water in the reservoir.

Samples of vapor were very difficult to obtain at the pre-established times during the injection because only water was obtained at those times at the sampling points. The

TABLE 16

WATERFLOODING DATA - EXPERIMENT #7

TIME (MIN)	CUM. OIL PROD. (CC)	WATER VOLUME (CC)	PRESSURE INLET (PSIG)	OUTLET (PSI)	TEMP. (°F.)	WATER LEVEL (CC)	CUM. GAS (SCF)
0	0	0	6000	2000	120	1950	.0
43	40	52	4750	2000	121	1898	.14
59	60	77	4750	2000	120	1873	.22
93	95	123	4750	2040	121	1827	.34
122	120	155	4725	2080	120	1795	.43
138	140	181	4710	2050	120	1769	.51
167	174	224	4675	2000	120	1726	.63
196	200	257	4725	2000	120	1693	.72
208	220	283	4750	2000	118	1667	.80
240	255	324	4800	2000	118	1626	.92
298	310	399	5000	2000	118	1551	1.12
239	350	451.80	5000	2000	118	1498.2	1.27
412	400	516	5000	2000	118	1434	1.45
470	435	561	5000	2000	120	1389	1.57
480	440	567	5250	2040	121	1383	1.59
498	445	574	5250	2040	120	1376	1.61
527	449	579	5000	2010	121	1371	1.62
530	449.5				BREAKTHROUGH		

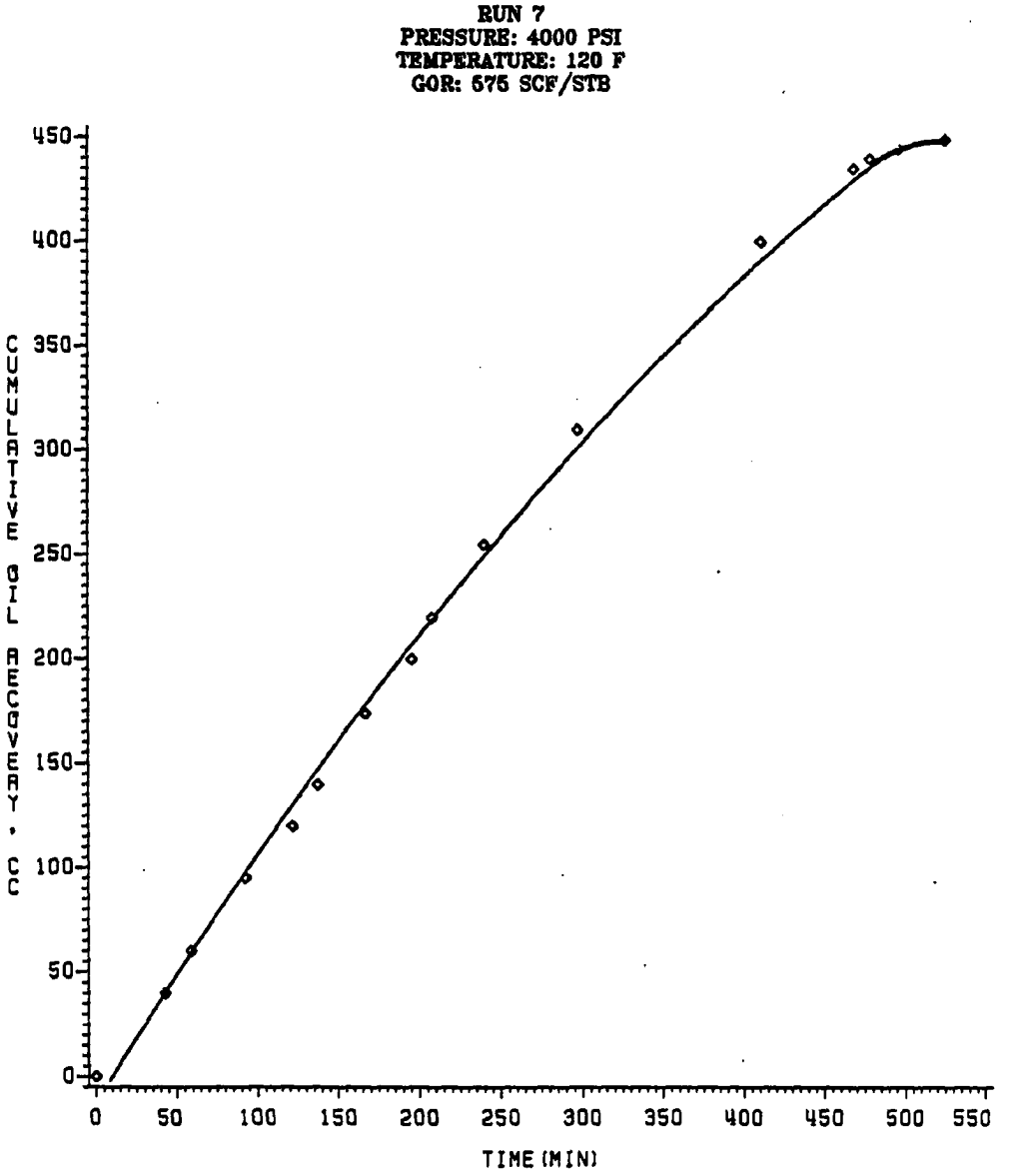

FIGURE 80
CUMULATIVE OIL RECOVERY VS TIME

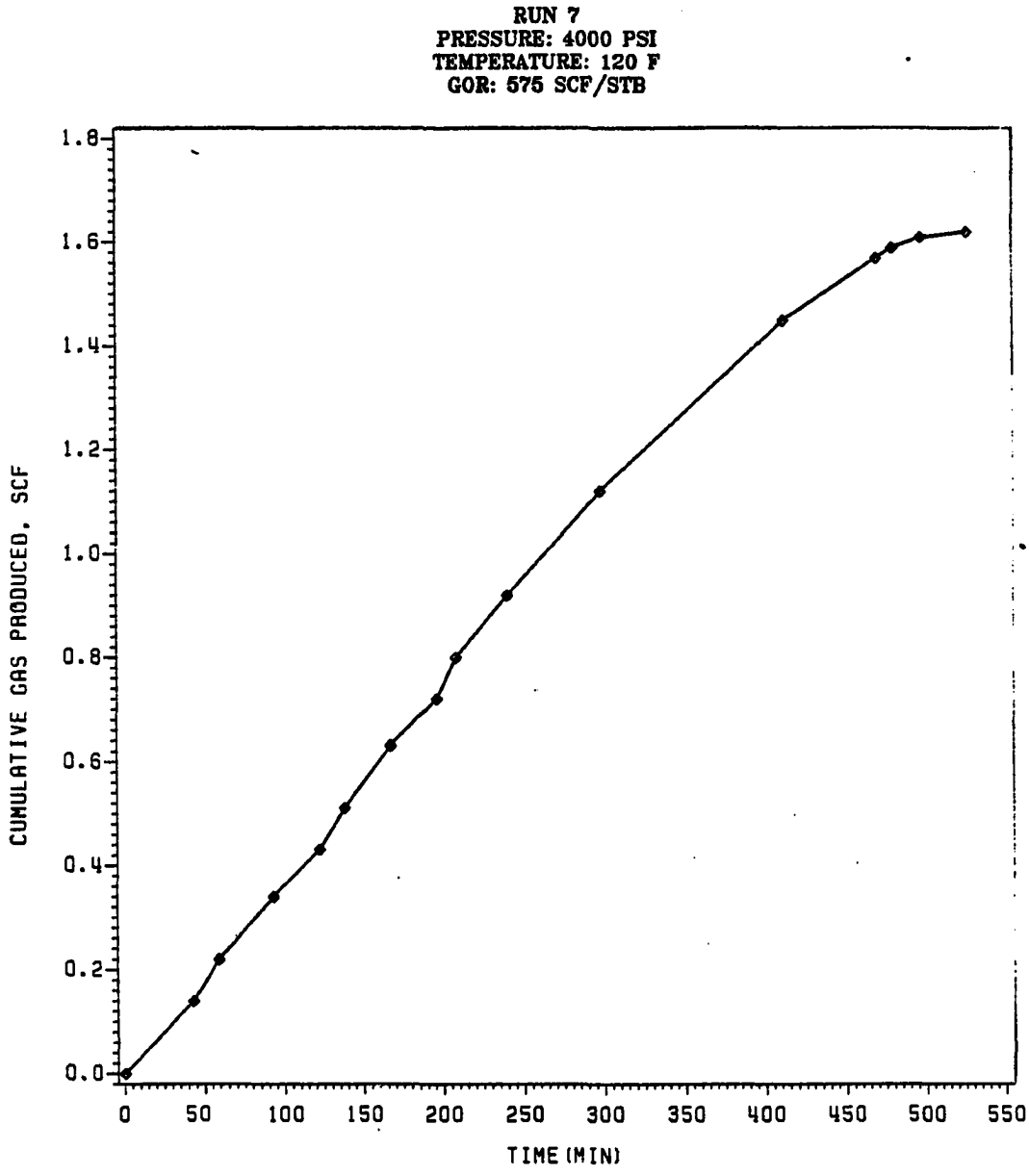

FIGURE 81
CUMULATIVE GAS PRODUCED VS TIME

samples that were possible to analyze did not show any compositional change.

No conclusion of merit can be done on recovery and miscibility depending on oil saturation and temperature. Production history is shown in Figure 82.

B-9. Ninth Experiment

The last test, experiment #9, was a special one. A 10% PV propane slug driven by high-pressure nitrogen injection was used to recovery crude oil with 200 SCF/STB dissolved in. The production data obtained from this experiment is presented in Table 18. The parameter values and other conditions are given below:

Barometric Pressure	28.6" Hg.
Room Temperature.	71°F.
Reservoir Temperature	120°F.
Propane slug.	10% PV
Solution Gas-Oil Ratio.	200 SCF/STB
Crude Oil Saturation.	79% PV
Water Saturation.	21% PV
Stock Tank Oil.	747.27 cc.
Oil Gravity	42.4° API
Formation Volume.	1.1 Bbl/STB
Front Advance Velocity.	0.0837 cm/sec.

This test was designed with the purpose to initiate this type of enhance oil recovery method at Oklahoma University and determine its potential in order to continue future

TABLE 17

NITROGEN FLOODING AFTER WATERFLOODING
EXPERIMENT #8

TIME (MIN)	CUMULATIVE OIL PROD. (CC)	CUMUL-ATIVE GAS (SCF)	TEMPERATURES (°F) (1)	(2)	(3)	(4)	OUTLET PRESSURE (PSIG)
0	0	0	120	120	120	118	2000
25	6	0.02	120	120	118	118	2000
56	10	0.035	120	120	118	118	2000
100	14	0.05	120	118	118	118	2000
125	16	0.058	120	120	120	120	2000
150	18	0.065	121	120	121	120	2000
201	20.8	.075	122	120	122	120	2000

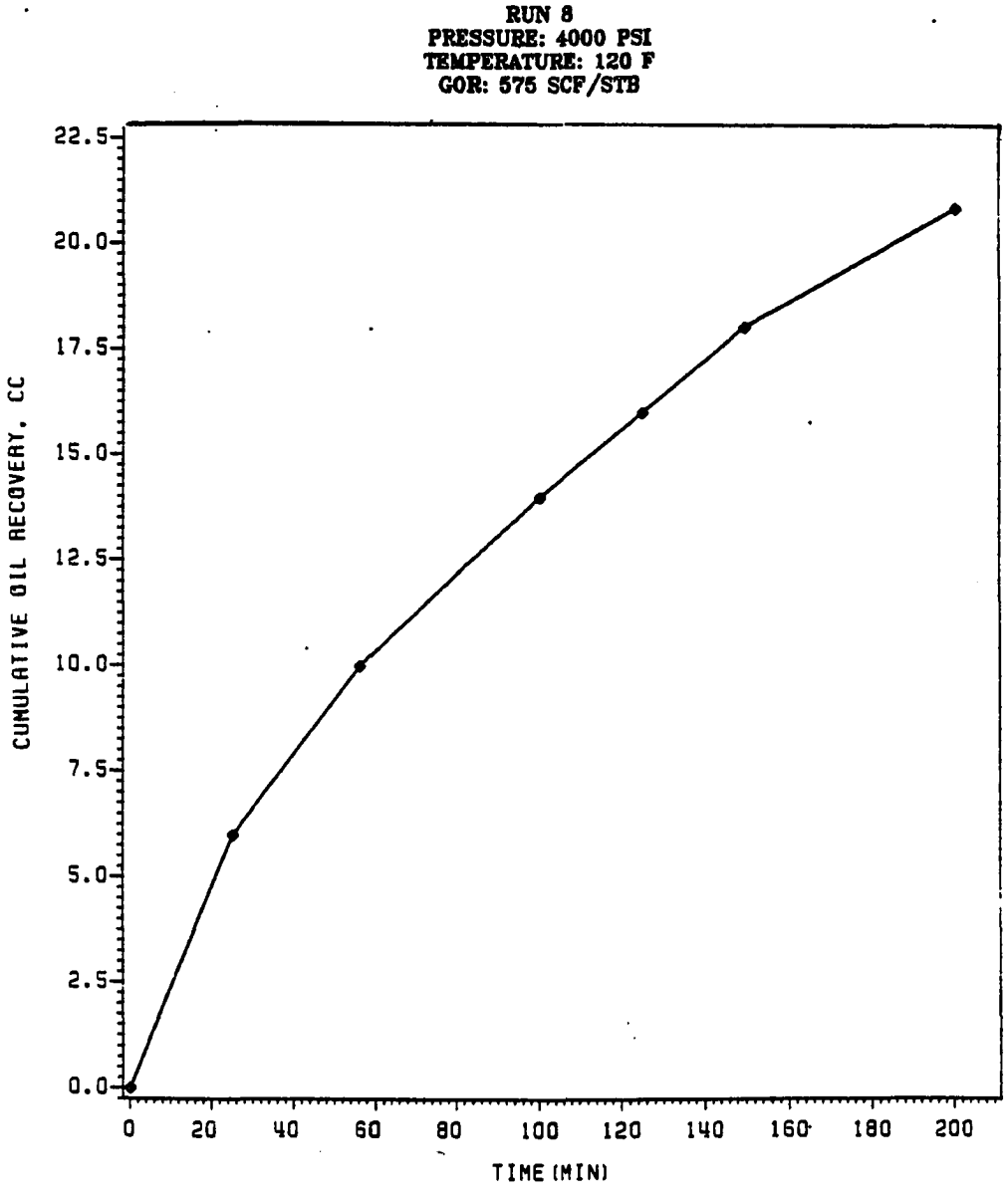

FIGURE 82
CUMULATIVE OIL RECOVERY VS TIME

TABLE 18

PROPANE SLUG DRIVEN BY HIGH PRESSURE NITROGEN INJECTION--EXPERIMENT #9
Injection Pressure: 4000 PSIG

TIME (MIN)	CUMULATIVE OIL PROD. (CC)	CUMUL. GAS (SCF)	TEMPERATURES (°F) (1)	(2)	(3)	(4)	OUTLET PRESSURE (PSIG)
0	0	0	120	118	118	118	2000
20	18	0.02	122	120	118	118	2000
24	22	0.03	118	117	119	119	2000
31	30	0.04	120	120	119	118	2000
41	40	0.05	119	118	119	118	2000
95	100	.13	119	118	119	118	2000
140	135	.17	120	121	120	120	2000
280	282	.31	120	120	120	120	2000
350	342	.39	120	121	121	120	2000
430	430	.50	120	120	120	120	2000
580	535	.65	118	118	119	119	2000
750	660	.83	120	120	121	121	2000
758	662	.835	121	120	121	120	2000
765	665	.84	120	118	120	118	2005
770	667	1.9	119	118	120	119	2000

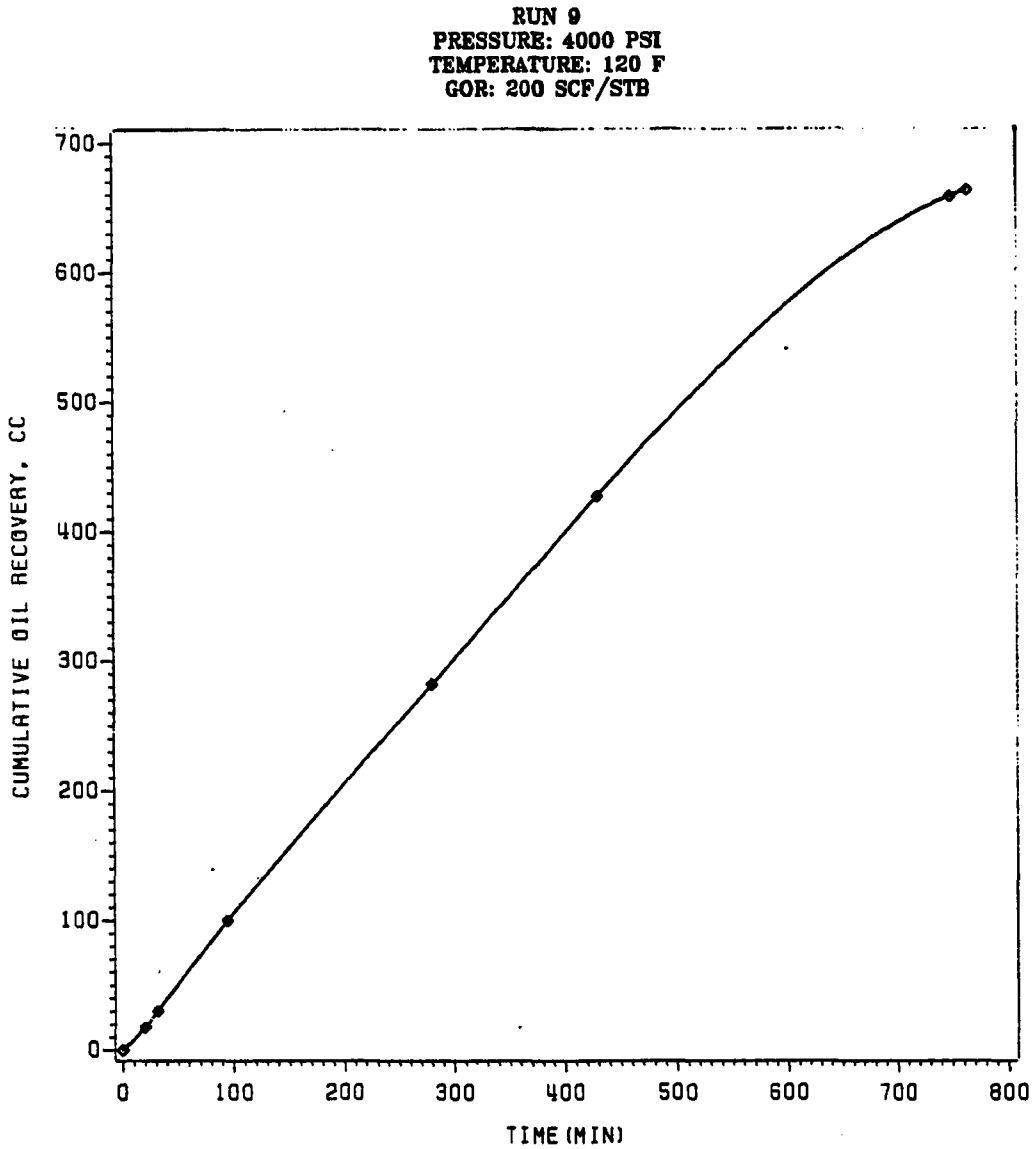

FIGURE 83
CUMULATIVE OIL RECOVERY VS TIME

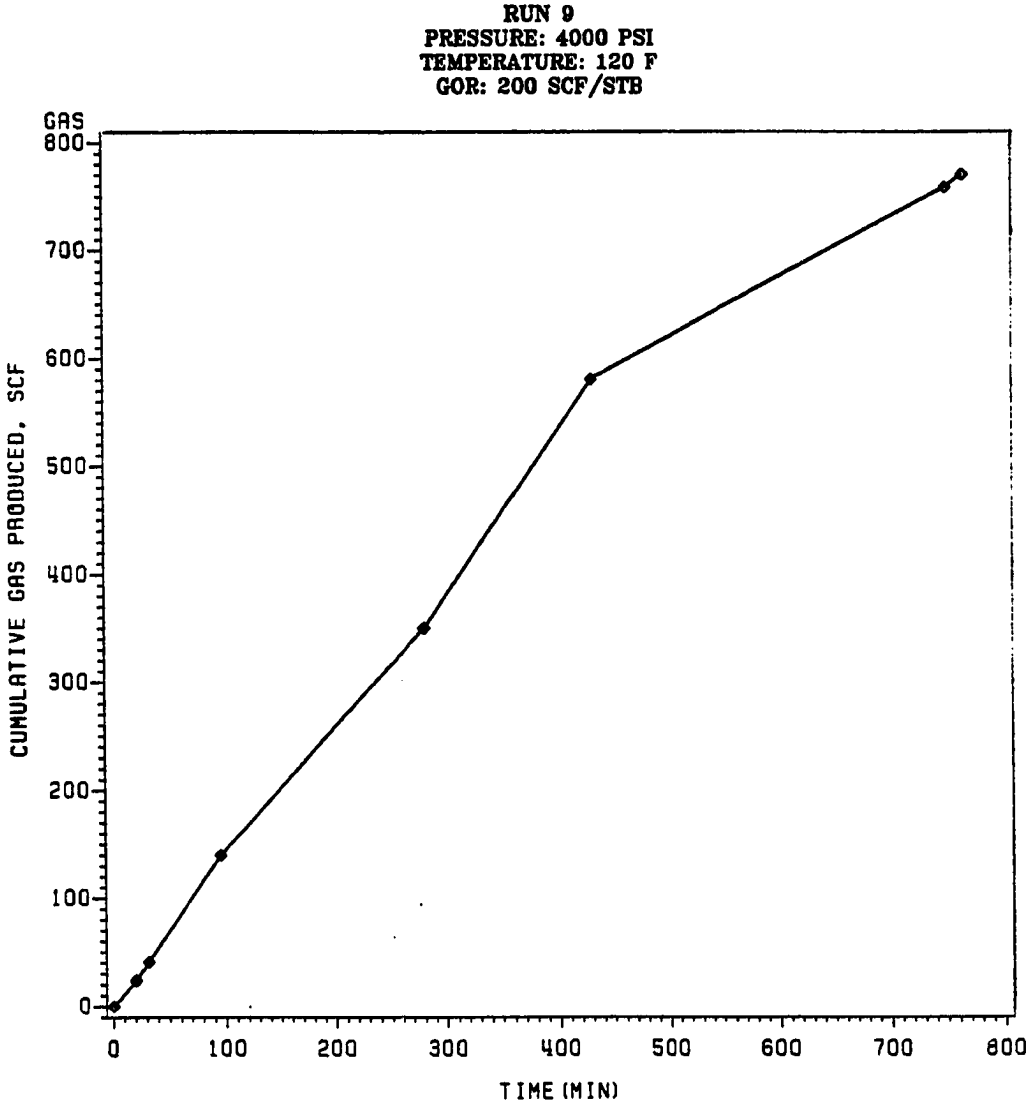

FIGURE 84
CUMULATIVE GAS PRODUCED VS TIME

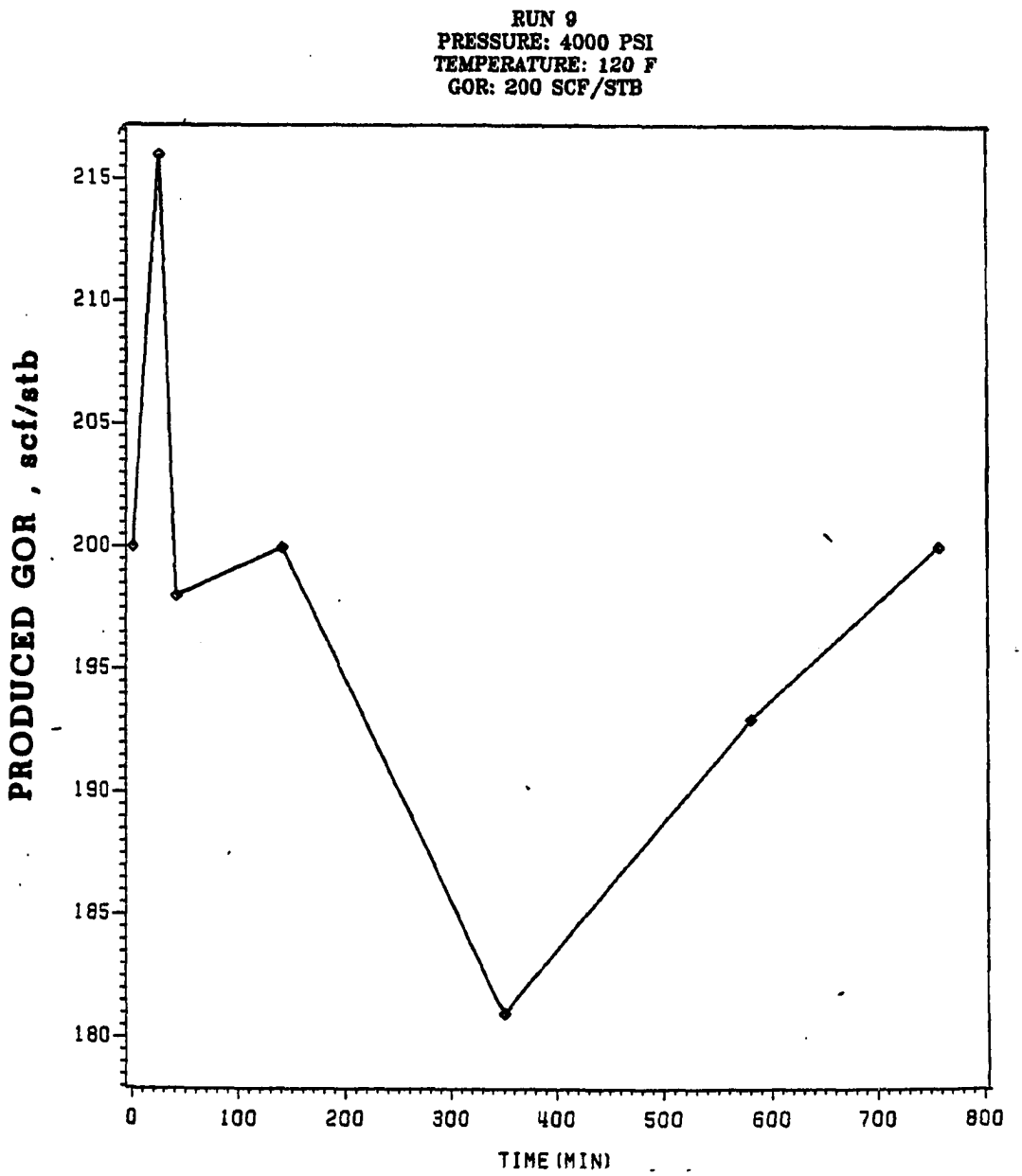

Figure 85
PRODUCED GOR VS OIL RECOVERY

work oriented in this direction.

Production history curves are presented in Figures 83 to 85. The upward curvature of the crude oil production curve suggested that the effectiveness of the displacement is reducing with distance. Maybe a deterioration of the propane slug would be a first speculation to explain the curvature, also this would explain not having 100% of crude oil recovery. The only work about nitrogen-driven propane slugs reported in the technical literature so far was made by Crawford et al. They used Seminole Crude Oil of 34.5° API gravity at 112°F. with no gas in solution using a 40 ft. long sand pack. This core was an unconsolidated sand. The coiled sandpack was immersed in a constant temperature oil bath to simulate the reservoir temperature. They reported higher recovery at breakthrough than this study test, and about the same recovery using only 4.5% PV and of propane slug.

C. Discussion of Results

C-1. High-pressure Nitrogen Displacement Process

The experimental results discussed hereunder are of prime importance in this study. The main purposes of these experiments were as follows:

1. To determine if the heating system built especially to keep constant temperature in the reservoir physical model would be suitable.

2. To determine if the heat transfer mathematical model written and prepared especially for this investigation

would be suitable in predicting temperature distribution within the reservoir physical model which will be consequently used as a tool to specify heat capacity of the heater units.

3. Determination of repeatability of the data obtained from experiments performed by using the reservoir physical model available at the University of Oklahoma.

4. To study the efficiency of crude oil recovery and understanding the mechanisms taking place within the reservoir model during high pressure nitrogen injection under different conditions of temperature and gas-oil ratio in solution.

5. To perform a high-pressure nitrogen displacement after waterflooding the model to study the efficiency of this type of process.

6. To perform an experiment of oil recovery by propane slug driven by high-pressure nitrogen injection to initiate this type of process at the existing laboratory facility of the University of Oklahoma.

The first two objectives of this study were met satisfactorily by the designed heating system. Tests #5, 6, 7, 8 and 9, were run under hot condition and temperatures are recorded in Tables 12 to 18 which show very clearly that the heating system was suitable to keep constant temperature at the reservoir model. The results showed that the heat transfer mathematical model is a practical tool to select the proper heater units according to a specific working temperature.

In this study the maximum temperature used was 120°F. Results from the experiments performed in this study at cold condition (70°F) compare fairly well with the results reported by Ahmed (1), which shows clearly that experimental repeatibility was obtained and the third purpose of this study was accomplished. Both results are shown in Tables 5 and 6.

The study of efficiency of crude oil recovery and the understanding of the mechanisms taking place within the reservoir model under different temperatures and GORs in solution require more detailed discussion. To start the discussion of this matter it is necessary to state that the building up of miscibility process by injecting N_2 at high-pressure is so complex that many interpretations can be made when this physical phenomenon is analyzed. There are several important variables involved in the process of building up miscibility in a displacement of this type. The parameters of major interest to this investigation are as follows: Interface mass transfer; relative permeability of the displacing and displaced phases; amount of hydrocarbon gas dissolved in crude oil; initial crude oil saturation; initial crude oil composition; presence of immobile or mobile water; gravity; continuity and homogeneity of the porous medium; injection pressure and temperature.

As mentioned earlier in this chapter, injection pressure was selected as a fixed variable because miscibility pressure or pressure effects on miscibility for a specific

crude oil is a very well recognized fact in the technical literature (1,30,47,50). Other independent variables were: temperature, gas-oil ratio in solution, water saturation, initial oil saturation and initial crude oil composition. For all practical purposes the rate of advance of the displacement front was considered constant in all tests. Actually the results from all the tests summarized in Table 19 suggest that the rate of advance of the displacement front in light crude oil displacements increases slightly with the increase in temperature and gas-oil ratio in solution. The main reason behind this behavior could be the improvement of crude oil viscosity by the increase of temperature.

At this point it is convenient to repeat that no direct control or determination of relative permeabilities were made during the nitrogen displacement process. The effect of gravity was theoretically reduced by using a very slim core with a diameter of 0.435 inches. The effect of possible spots of heterogeneities, along the core was theoretically minimized by using a long core with a length of 125 feet.

The evaluation of the production history curves, ternary diagrams, compositional profiles and the curves for intensive properties of liquid and vapor in all the tests in this study showed consistently that three zones exist in the displacement of light crude oil by high-pressure nitrogen injection. This pattern was observed in all the displacements regardless of miscible or immiscible condition.

In all the experiments with pure N_2 injection, even though with the most favorable conditions for miscibility these three zones were observed. The zones observed in these experiments were as follows:

a. A virgin zone or the zone which leads the displacement.
b. The second zone which is a two-phase flowing zone, and
c. The third zone which is a single phase flowing zone.

The virgin zone was identified in the experiments by analyzing the results obtained from produced fluids, gas and liquid. The produced GOR was almost constant in all the displacement process until nitrogen breakthrough after which the curve increased sharply. The original GOR in solution was almost similar to the produced GOR and the API gravity of the recovered crude oil matches quite well with the original oil which saturated the system. These facts lead to postulate that the leading zone in this type of displacement is a virgin zone with only one phase, crude oil. No compositional changes were identified in this zone. Consequently, there is no mass transfer in this leading zone. Since water saturation in this leading zone is immobile water, crude oil flows at maximum relative permeability. Recombinations of produced gas and oil were performed and the saturation pressures obtained were similar to the saturation pressures of the crude oil before the test.

The second zone identified in this study was a two-phase flowing zone. This zone is the result of immiscibility of nitrogen and crude oil at the first contact. The length of this zone normally was observed to be large because of the fact that relative permeability to the vapor phase is greater than the relative permeability to the liquid phase. Hence, the vapor phase has greater mobility than the liquid phase in this zone. This determines that vapor phase moves ahead contacting the fresh oil. In this zone the gas saturation progressively increases until no liquid phase is flowing.

This second zone is the most important zone in understanding the mechanisms involved in building up miscibility. The miscible bank may or may not be developed in the second zone. The displacement is basically immiscible until the miscible bank is created. Consequently, the amount of reservoir fluid that is immiscibly displaced is primarily a function of the concentration of intermediate components in the original crude oil compared with the concentration of intermediate components that the crude oil would have at the critical point in a ternary diagram. That implies that significant length of the model is displaced immiscibly from the experimental results obtained in this study. The miscibility distance was found to range between 72 and 96 feet when miscibility was achieved (Table #19). The miscibility distance was observed to decrease with increasing temperature and GOR at constant injection pressure of N_2.

The oil at the leading edge of this second zone has the same composition as the oil in the virgin zone and the gas is in thermodynamic equilibrium with the oil. After this region, both oil and gas change in composition. As it was observed from the analysis of compositional profiles from the tests performed in this study, the maximum concentration of intermediate components are present at the leading edge in the second zone. Those intermediate components have been stripped from the crude oil. Since the maximum concentration of intermediate components are present at the leading edge of the second zone, a miscible bank is very likely to develop at this leading edge if any miscibility is obtained at all. The rate of concentration of intermediate component and amount of them at one specific time is governed by vaporization. The shape of compositional profile curves from test #2 to 6 suggest that the vaporization is very strong at the beginning of the process in the leading edge of the second zone.

Behind the leading edge, the slopes of the compositional profile then decrease because of reduction in vaporization rate during the advance of the displacement process until vaporization is reduced to zero. At this point the compositional profiles show a zero slope indicative of miscibility between the displacing and displaced phase. This phenomenon suggested that providing more intermediate components in the first portion of the reservoir model would sharply reduce the

immiscible displacement length and increase displacement efficiency. On the other hand, the original composition of the crude oil is a key factor which affects the efficiency of the process.

The varying compositional profiles during N_2 displacement indicates that the building up of the miscible bank is a dynamic process which requires the inert gas, N_2, to be enriched by changing the crude oil composition by interphase mass transfer. This basic mechanism of vaporization is explained in Appendix G. Basically the way this mechanism works can be explained briefly in a step-wise manner by using a ternary diagram as shown in Figure G1 (Appendix G). For simplicity, a complex multicomponent system nitrogen-hydrocarbons is represented arbitrarily in a ternary diagram by three pseudo-components: N_2, C_{1-5}, C_6+. As pure nitrogen comes in contact with crude oil, the three pseudo-components will establish an equilibrium point R_1. The vapor phase and liquid phase compositions at this point are represented by G_1 and L_1 respectively. The equilibrium composition R_1 lies in two-phase region in the diagram. Due to the high mobility of the gas phase, gas (G_1) moves ahead to contact fresh oil stripping C_{1-5} component from the oil and equilibrium is reestablished at point R_2 having gas and liquid phase compositions G_2 and L_2 respectively. The process continues repeating itself as the gas G_n goes ahead to contact fresh oil till the critical composition is reached. At this point, the

the intensive properties become equal and surface tension is zero and the displacement process becomes miscible. As mentioned before a miscible bank is created at the leading edge of the second zone where a maximum concentration of intermediate components are present.

The experiments performed in this study show that the size of a miscible bank is a function of temperature and gas-oil ratio in solution. When the temperature increases, the size of the miscible bank increases and when the GOR in solution increases the size of miscible bank is also increased at constant injection pressure. These results related to miscible bank size could be justified by kinetic theory of gases. According to kinetic theory, molecules and atoms of any gaseous substance are in constant state of motion at all temperatures above absolute zero. This is true to a lesser extent in liquids in which the molecules both vibrate and move around. The motion of gas molecules and the vibration of liquid molecules increases as temperature increases. In this case the rate of vaporization of intermediate components increases.

It is obvious that when gas-oil ratio in solution increases, the concentration of intermediate components increases since more intermediate components are available in crude oil. The size of the miscible bank is directly affected by both temperature and GOR in solution according to the results of this study. This observation is at one

constant pressure as indicated in this study. When the pressure increases, the size of miscible bank is found decreased substantially due to retrograde vaporization (1).

At this point of the discussion, the vaporization process is the most important mechanism that accounts for building up of miscibility. The formation of a rich gas slug at the leading edge of the second zone is basically a mass transfer of intermediates components from the displaced phase (crude oil) to the displacing phase (nitrogen) by vaporization. Other than this primary mechanism, there are secondary mechanisms which play important roles in the effectiveness of crude oil recovery by nitrogen injection. The results analyzed in this study show that the following other mechanisms should also be considered:

1) Increasing the density of the displacing phase,
2) Decreasing the density of the displaced phase,
3) Increasing the viscosity of the displacing phase,
4) Decreasing the viscosity of the displaced phase,
5) Reducing the surface tension in the system, and
6) Improving the mutual solubility of both phases at the leading edge of the second zone.

Changes in density, viscosity and surface tension during this high-pressure nitrogen injection were observed by computing those properties by using available correlations at the technical literature by means of a program "PROPERT" written especially for this study and presented in Appendix H.

Calculated liquid and vapor densities are shown in Figures 32-35, 51, 64 and 65. From these figures it is obvious that in the leading edge of the second zone, the most important changes in intensive properties of liquid and vapor phases take place. A decrease in liquid density and increase in vapor density is observed as the displacement advances. This will continue until liquid and vapor densities converge to the same value. At this point a rich gas slug is formed and the displacement becomes miscible.

Behind the rich gas slug liquid density increases and vapor phase densities decreases very sharply due to the stripping process that crude oil has undergone. The variation of densities in the liquid and vapor phases are the results of two combined mechanisms as stated hereunder:

1) At the leading edge of the second zone where the development of miscible bank is in progress, there is a mutual phase transfer between liquid and vapor.

2) Behind the leading edge of the second zone, a stripping process takes place as explained formerly, by using ternary diagram (Appendix G).

The changes in viscosities and densities of the liquid and vapor during high-pressure N_2 injection are shown in figures 32 to 39, 51 to 52, and 64 to 65.
The change in viscosity also reflects the phenomenon of vaporization taking place during the displacing process. By examining the liquid and vapor viscosity curves, the following

observations were made:

1. At the leading edge of the second zone, the liquid viscosity decreases and vapor viscosity increases as displacement process advances, both liquid and vapor densities converge at a point when the critical composition is reached and the displacement process becomes miscible

2. Behind the leading edge of the second zone, where the stripping process is under way, the liquid viscosity increases and vapor viscosity decreases.

It is evident that mobility ratio improves because of changes of viscosities of both phases at the leading edge of the second zone, consequently, the displacement becomes more effective. The viscous fingering is reduced as a consequence of reduced mobility ratio. This secondary mechanism is important because it causes an improvement in the displacement until the miscibility is achieved.

Theoretically, surface tension reaches zero when miscibility is achieved. According to the results obtained in this study a significant reduction of the surface tension was achieved during the displacement processes, but it never reached zero as evident from the calculations. From these results it is possible to say that no perfect miscibility was achieved during any displacement test performed in this study. This means that after theoretical miscibility is achieved, the crude oil was not recovered totally and some residual oil was left in the reservoir model.

The surface tension increases behind the leading edge of the second zone as the displacement process advances as shown in Figures 40 and 65A. This is in agreement with the primary mechanism of vaporization that takes place during high-pressure nitrogen injection.

The third zone is a single phase flowing zone where pure nitrogen is moving with maximum relative permeability because only residual oil is present. The beginning of the third zone is detected from the compositional profiles at the point where nitrogen composition increases sharply and hydrocarbon components are reduced drastically.

C-2. Effect of Temperature and Gas-Oil Ratio on High Pressure Nitrogen Injection

Experiments 1 to 6 were basically performed with the purpose of studying the effects of gas-oil ratio in solution and temperature on crude oil recovery at breakthrough in displacements with high pressure nitrogen injection. An additional purpose for these tests was to establish repeatibility in order to determine validity of the reservoir physical model used in this study and in previous research (1).

The results of all the experiments performed in this study are summarized in Table 16. The overall effect of gas-oil in solution on crude oil recovery is illustrated in figures 86 and 87. It is convenient to mention at this point that no research concerning gas-oil in solution and temperature effects on nitrogen injection process have yet been reported in the technical literature.

From the interpretation of the results shown in Figure 87, the following observations can be pointed out.

a) The initial amount of gas dissolved in the crude oil in a high pressure nitrogen injection displacement process affects the crude oil recovery of breakthrough.

b) Definitely, there is not a linear relationship between gas-oil ratio in solution and crude oil recovery.

c) The shape and general tendency of the curves seem to be characteristic for these experiments. The type of curve is similar when temperature is fixed higher and the GOR is the manipulated variable.

From the results it can be proposed that the higher the amount of gas in solution in a crude oil, the higher the recovery at breakthrough at one specific temperature. The effect of GOR in solution on crude oil recovery is even more clear when Figure 86 is analyzed. This figure shows crude oil recovery as a function of temperature using GOR in solution as parameter. The response observed in this figure could be explained by the position that the recombined crude oil has in a ternary diagram depending on its concentration of intermediate components (C_{1-5}). Since the natural gas is a source of intermediate components, the higher amount of gas dissolved in the crude oil, the closer to the critical point the crude oil will be.

In a ternary diagram (Appendix G) an increase in GOR in solution necessary would move the point representing the

crude oil to the right. Consequently, the displacing nitrogen would need less contacts to develop miscibility. Hence, the distance to develop miscibility would be shorter and crude oil recovery higher. The results obtained in this study shows that crude oil recovery increases with GOR in solution increases.

Results obtained in this work compare fairly well with values obtained by Ahmed (1). As it is shown in Table 2 and Figures 86 and 87, his results agree fairly with the recovery obtained in this study under the same conditions. The previous researcher (1) concentrated his study on determining pressure effects on miscibility and crude oil recovery, but also he made a test using dead oil without gas in solution. He reported a crude oil recovery of 59% of the original oil in place. This value can be considered high when it is compared with the value obtained by extrapolation of the results obtained in this work presented in Figure 81. The extrapolated value at zero GOR is 55% OOIP at 70°F and the value of crude oil recovery is 57% OOIP when temperature was 120°F. Also, Crawford et al obtained experimentally a crude oil recovery of 55% of OOIP at 112°F., 3000 PSI and displacing a crude oil of 34.5° API gravity by nitrogen.

The high results of Ahmed (1) (see Figure 87) could be the result of not having a temperature control system during his experiments. Since he could not keep constant temperature, it is possible that the higher value of oil recovery

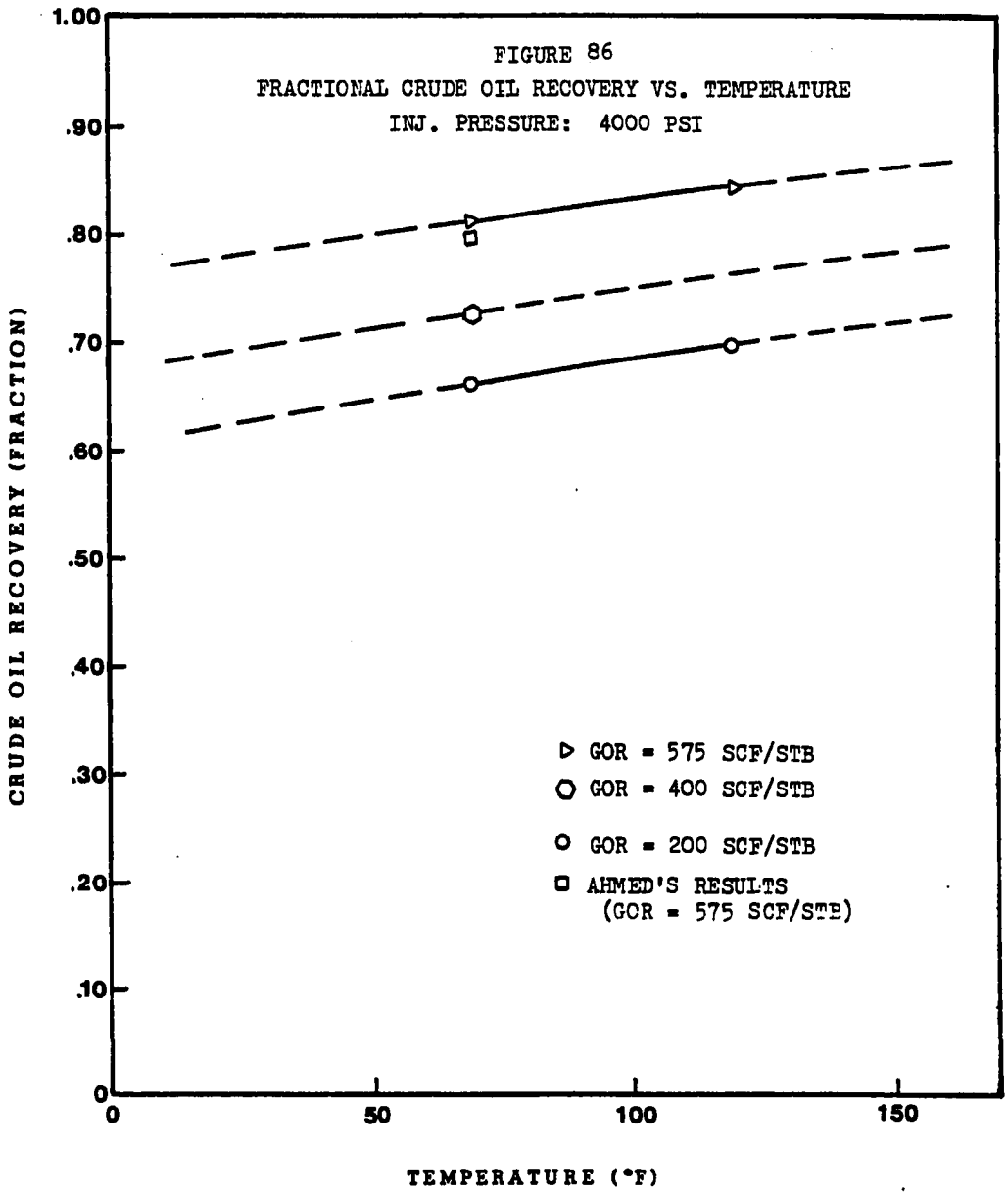
FIGURE 86
FRACTIONAL CRUDE OIL RECOVERY VS. TEMPERATURE
INJ. PRESSURE: 4000 PSI
CRUDE OIL RECOVERY (FRACTION)
1.00
.90
.80
.70
.60
.50
.40
.30
.20
.10
0
0
50
100
150
TEMPERATURE (°F)
GOR = 575 SCF/STB
GOR = 400 SCF/STB
GOR = 200 SCF/STB
AHMED'S RESULTS
(GOR = 575 SCF/STB)

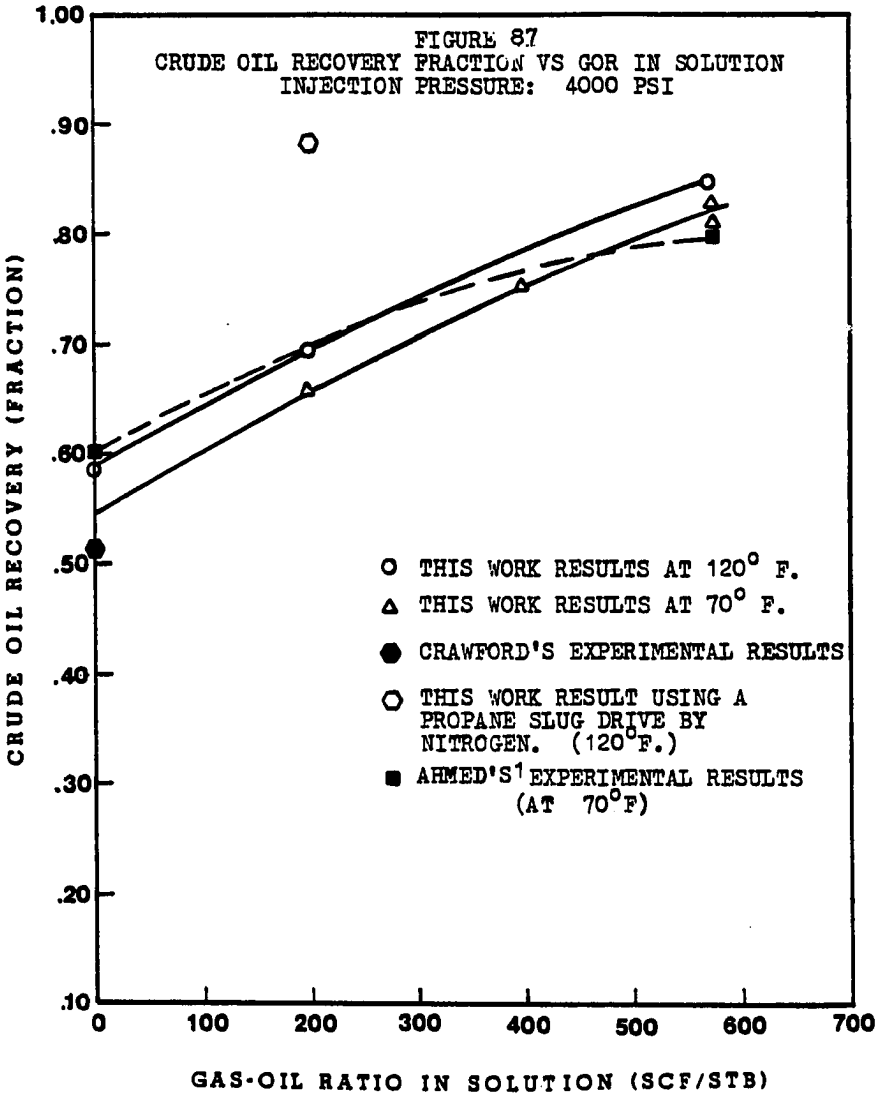
FIGURE 87
CRUDE OIL RECOVERY FRACTION VS GOR IN SOLUTION
INJECTION PRESSURE: 4000 PSI
CRUDE OIL RECOVERY (FRACTION)
1.00
.90
.80
.70
.60
.50
.40
.30
.20
.10
0
100
200
300
400
500
600
700
GAS-OIL RATIO IN SOLUTION (SCF/STB)
THIS WORK RESULTS AT 120° F.
THIS WORK RESULTS AT 70° F.
CRAWFORD'S EXPERIMENTAL RESULTS
THIS WORK RESULT USING A PROPANE SLUG DRIVE BY NITROGEN. (120°F.)
AHMED'S[1] EXPERIMENTAL RESULTS (AT 70°F)

reported by him was due to higher temperature or other parameter during the run.

To study the effects of temperature on high-pressure nitrogen injection process were used two different temperatures (70°F and 120°F) in the experiments performed in this study. Figures 86 and 87 show the effect of temperature on this displacement process.

The tests where temperature was the unique independent variable showed that increases in temperature produces increases in crude oil recovery at breakthrough. As it can be observed in Figure 87, increments in temperature for different GOR's in solution seem to follow a pattern creating a family of curves that characterize the effect of temperature on crude oil recovery in nitrogen displacement. The only conclusion that might have merit from Figures 86 and 87 is that a general increase in crude oil recovery occurs for increase in temperature and GOR in solution.

An initial reaction was to make a linear correlation through the data points with the assumption that at higher temperature the recovery will be higher. For instance, to recover 100% of crude oil in the reservoir physical model, it would be necessary, by extrapolating the upper curve in Figure 86, to increase temperature to 360°F when using a GOR in solution of 575 SCF/STB. The increase in temperature would be greater for lower GOR in solution. However, there appears to be no basis for assuming a linear relation between

temperature and crude oil recovery beyond the range of temperatures used in this study. With this limitation in mind, and by using the Statistical Analysis System package (SAS) available at Oklahoma University, a multiple regression equation was obtained to predict crude oil recovery with both temperature and GOR in solution as predictors.
The resulting equation is:

$$R = 0.5546756 + 0.00053705T + 0.00041454\ GOR \qquad (1)$$

where:

R = crude oil recovery, % OOIP

T = temperature, °F

GOR = gas-oil ratio in solution, SCF/STB.

Equation (1) predicts crude oil recovery when the injection pressure is 4000 PSI. The correlation coefficient for equation (1) is .99590. That means that it is very precise to predict recovery for the reservoir physical model. The SAS computer program and other statistical information is given in the Appendix I.

The results obtained in this study, crude oil recovery showed to depend on temperature and gas-oil ratio in solution. The results obtained by Ahmed (1) strongly support that recovery was a function of pressure. Since that was very clear, all the results obtained in this study were put together with Ahmed's (1) results (Table 20) to produce a multiple regression equation to predict crude oil recovery using as predictors the variables temperature, pressure and gas-oil ratio in the reservoir physical model used in this study. This

proposed correlation would apply only for this model and for the type of oil used in these experiments. The resulting equation is the following:

$$R = -0.164 + 0.0294 \sqrt{T} + 0.0001198\ P + 0.000338\ GOR \qquad (2)$$

Where:

R = crude oil recovery % OOIP

T = temperature, °F

GOR = Gas-oil ratio in solution, SCF/STB

P = Injection pressure, psi

Standard deviation of R about regression line is S = 0.05672. In order to obtain equation (2), the statistical Minitab package was used. This package is available in the computer VAX system at the Oklahoma University. In Table 21 is given the output of the computer. In this table the actual values or observed values of R are compared with predicted values of R and the residuals are shown. For instance, the R from the test #3 of this study was 84.5% and its predicted value using equation (2) was 83.18%. The difference of 1.32% is given under residual. This equation has a coefficient of determination of 77.3 percent. That means that the efficiency of predicating values by the equation (2) is only 77.3%. The correlation coefficient is 83.8% which is a good one. This value could be improved by gathering more data in the reservoir physical model used in these studies.

The increase in crude oil recovery with increase in temperature in high-pressure nitrogen displacement could be explained by Molecular Theory and Thermodynamics. Molecular

TABLE 19

SUMMARY OF EXPERIMENTS

(High Pressure N_2 Injection)

OIL GRAVITY 42.4° API

TEST	TEMP. °F	GOR	S_O	S_W	FVF	STOIP	RECOVERY	TYPE	PRESSURE
1.	72	575	77.0	23	1.29	689.92	83%	MISCIBLE	VARIABLE
2.	69.5	575	76.38	23.62	1.29	621.75	81.1%	MISCIBLE	4000
3.	70.5	400	78.	22	1.2	762.50	75.4%	MISCIBLE	4000
4.	69.5	200	77.	23	1.1	809.00	66.0%	INMISCIBLE	4000
5.	120	575	80.2	19.8	1.29	647.28	84.5%	MISCIBLE	4000
6.	120	200	80.88	19.12	1.1	738.18	69.4%	INMISCIBLE	4000
7.	120	575	80.2	19.8	1.29	652.71	68.8	INMISCIBLE	VARIABLE
8.	120	575	25.0	75.0	1.29	203.71	10.2	INMISCIBLE	4000
9.	120	200	79.0	21.0	1.1	747.27	88.9	MISCIBLE	4000

TABLE 20

DATA SET USED TO PROPOSED EQUATIONS (1) & (2)

TEMPERATURE (T)	RECOVERY (R)	PRESSURE (P)	GAS-OIL RATIO (GOR)
72.000	0.830000	5000.00	575.
69.500	0.811000	4000.00	575.
70.500	0.755000	4000.00	400.
69.800	0.660000	4000.00	200.
120.000	0.845000	4000.00	575.
120.000	0.694000	4000.00	200.
70.000	0.800000	4000.00	575.
70.000	0.860000	5000.00	575.
70.000	0.540000	3000.00	575.
70.000	0.720000	3700.00	575.
70.000	0.590000	5000.00	0.

TABLE 21

MULTIPLE REGRESSION OUTPUT FOR PREDICTING RECOVERY (C_1) FROM: TEMPERATURE (C_6), INJECTION PRESSURE (C_3) AND GAS OIL RATIO (C_4) - STATISTICAL PACKAGE: MINITAB

Regress C_2 on 3 predictors in C_6, C_3, and C_4

The regression equation is:

$Y = -0.164 + 0.0294 X_1 + 0.0001 X_2 + 0.0003 X_3$

	COLUMN	COEFFICIENT	ST. DEV. OF COEF.	T-RATIO = COEF/S.D.
	--	-0.1640	0.2281	-0.72
x1	C6	0.02936	0.0175	1.68
x2	C3	0.00011988	0.00003039	3.94
x3	C4	0.00033860	0.00008991	3.77

The St. Dev. of Y about regression line is:
S = 0.05672
with (11- 4) = 7 degrees of freedom

R-squared = 77.3 percent
R-squared = 67.6 percent, adjusted for D.F.

Analysis of Variance:

Due to	DF	SS	MS=SS/DF
Regression	3	0.076827	0.025609
Residual	7	0.022523	0.003218
Total	10	0.099350	

Further analysis of Variance
SS explained by each variable when entered in the order given

Due to	DF	SS
Regression	3	0.076827
C6	1	0.002087
C3	1	0.029106
C4	1	0.045635

ROW	x1 C6	Y C2	Pred. Y Value	St. Dev. Pred. Y	Residual	St Res.
1	8.5	0.8300	0.8792	0.0354	-0.0492	-1.11
2	8.3	0.8110	0.7549	0.0222	0.0222	1.07
3	8.4	0.7550	0.6974	0.0204	00.0576	1.09
4	8.4	0.6600	0.6285	0.0312	0.0315	0.66
5	11.0	0.8450	0.8318	0.0433	00.0132	0.36
6	11.0	0.6940	0.7048	0.0436	-0.0108	-0.30
7	8.4	0.8000	0.7558	0.0220	0.0442	0.84
8	8.4	0.8600	0.8757	0.0355	-0.0355	-0.35
9	8.4	0.5400	0.6359	0.0395	-0.0959	-2.35R
10	8.4	0.7200	0.7199	0.0247	0.0001	0.00
11	8.4	0.5900	0.6810	0.0452	-0.0310	-0.91

R denotes an Obs. with a large St. Res.

Durbin-Watson Statistic = 1.59

(x-Prime x) inverse

	0	1	2	3
0	16.17609			
1	-0.97369	0.09519		
2	-0.00151	0.00002	0.00000	
3	-0.00274	0.00007	0.00000	0.00000

activity increases with temperature, producing more interaction between phases. This increase in interaction is translated into a faster vaporization process during the nitrogen displacing crude oil as it can be seen in Figures 18-9 to 18-99 of the Reference (22), the equilibrium constants increase with temperature. That means theoretically, that miscibility can be obtained faster because vaporization is greater at higher temperature. On the other hand, liquid viscosity is a strong function of temperature. An increase in temperature will produce a strong decrease in liquid viscosity. This decrease in viscosity improves the liquid mobility, especially in the virgin zone. The viscosity decrease in the liquid phase in the second zone will promote miscibility in the leading edge of this zone.

The relative permeabilities for both liquid and vapor phases are functions of temperature also. Poston et al (71) reported that both K_{ro} and K_{rw} curves increase with temperature. Sinnokrot et al (71) reported that K_{ro} curve increases with temperature but K_{rw} decreases. From those authors it is clear that at least K_{ro} curve increase with temperature.

To summarize, any significant increase of temperature helps the heavy ends in the reservoir fluids to be more volatile in contact with nitrogen.

C-3. N_2 Injection as a Tertiary Recovery Method After Waterflooding

A regular waterflood was performed in this study. The results are in agreement with the traditional values of crude

oil recovery by waterflooding in the technical literature. Also the crude oil recovery agrees with results reported by the previous researcher (1) who made his run at cold conditions. The only observation of merit that can be done at this point is that the range of temperature used in this study for hot conditon seems to be not enough to cause a significant difference in crude oil recovery. The crude oil recovery at hot conditions resulted in this work was slightly higher than the value reported by Ahmed (1) at cold conditions. A comparative conclusion with Ahmed's (1) results may not be justified because he used an intermittent water injection by means of a high-pressure mercury pump. This pump produces an intermittent injection with very long down periods, so, the slightly higher crude oil recovery obtained in the waterflooding in this study may be a effect of constant rate and higher temperature.

The results obtained from the test where nitrogen injection was injected after waterflooding suggests that when there are low saturation of crude oil and free water in the reservoir physical model the efficiency of the nitrogen as displacing phase seems to be inefficient. Also the results of this test suggest that there must be a minimum oil saturation at which nitrogen injection is efficient. However no conclusion of merit can be done on crude oil recovery and miscibility depending on oil saturation and temperature. The crude oil recovery at hot condition obtained in this study

was even lower than reported by Ahmed (1) at cold conditions. The test #8 only shows that discontinuous oil phase with mobile water saturation is inefficient when it is displaced by nitrogen injection at breakthrough under laboratory conditions.

No effects of temperature on crude oil recovery was shown in the response of this experiment, if it is compared with the previous researcher (1) data run under cold conditions. The early breakthrough of nitrogen may be explained by this: nitrogen may follow the viscous fingers already developed and established during the waterflooding. If nitrogen goes through those preferential paths it does not have chance to get in touch with residual oil very much, consequently the mass transfer of intermediate components from the residual oil to the vapor phase by vaporization process is limited, so the most important mechanism in high-pressure nitrogen injection is reduced to a minimum.

C-4.
Crude Oil Recovery by Propane Slug Driven by High-Pressure Nitrogen Injection

The results obtained by using a propane slug driven by high-pressure nitrogen injection suggest very strongly that the process was fully miscible from the very beginning of the displacement. The high recovery, 88% OOIP, indicates that crude oil recovery by propane slug-driven by high-pressure nitrogen injection would be a more efficient method, especially if it is compared with the first six tests performed

in this study and results reported by Ahmed (1). Taking into consideration the gas dissolved for this test was 200 SCF/STB which was supposed to bear a crude oil recovery around 70%, the difference is very significant.

Analysis of crude oil recovery and production history curves suggest that the effectiveness of the displacement is reduced with distance. Maybe a deterioration of the propane slug with distance would be first speculation to explain the curvature of the cumulative crude oil production versus time, also this would explain not having 100% of crude oil recovery.

Crawford et al (10) reported about the same crude oil recovery using a propane slug of 4.5% PV. The test performed in this study used a propane slug of 10%PV. The difference between Crawford et al (10) results and those reported in this study could be explained because the reservoir physical model used in this study reflected much closer an actual reservoir than Crawford's model. They saturated their model with 100% oil with no gas dissolved and the sandpack was unconsolidated sand. Their conditions were more ideal and this would be the difference. In order to make serious comparisons in the future between both studies, it will be necessary to conduct more tests of this type on this reservoir physical model. However, the results reported by Crawford et al (10) propane slug driven by nitrogen suggest that the same results in crude oil recovery could be obtained by using a smaller propane slug. The results reported by Koch and

Slobod (58) using propane slugs driven by lean natural gas also suggest that smaller propane slugs could yield the same crude oil recovery.

CHAPTER V

CONCLUSIONS AND RECOMMENDATIONS

A. Conclusions

As a result of the research conducted in this study, the following conclusions were made for the subject experimental conditions:

1. By comparison with the previous researcher's (1) data (tests 1 and 2), the results of this study showed high validity of the data obtained by using the reservoir physical model available at the University of Oklahoma.

2. A heat transfer Mathematical Model was developed to simulate temperature distribution in the reservoir physical model and to specify equipment to build a system to control temperature in the laboratory.

3. A two-phase flowing zone was generated in each of the first six high-pressure nitrogen displacement processes (tests 1 to 6), regardless of the fact that some of them were conducted under ideal conditions for generating miscibility. This fact suggests that initial composition of the displacing fluid would be a key factor for earlier miscibility and higher recovery.

4. When the temperature was isolated as the unique independent variable in the high-pressure displacement process, the crude oil recovery increased as temperature increased.

5. When the gas-oil ratio in solution was isolated as the unique independent variable in the high-pressure displacement process, the crude oil recovery increased as gas-oil ratio in solution increased.

6. Two multiple regression equations with high coefficient of determination were developed to predict crude oil recovery in the reservoir physical model used in this study or similar laboratory models. The first equation is able to predict crude oil recovery as a function of temperature and gas-oil ratio in solution when injection pressure is constant at 4000 PSI. The second equation is able to predict crude oil recovery using as predictors temperature, GOR in solution and injection pressure.

7. Effect of temperature on high pressure nitrogen displacement process used as tertiary recovery after waterflooding seems to be not significant.

8. Recovery of discontinuous oil phase with high saturation of mobile water seem to be inefficient when it is displaced by high-pressure nitrogen injection.

9. The size of the generated miscible bank slightly increases with increases in temperature and GOR in solution.

10. Miscible distance slightly decreases with increases in temperature and GOR in solution.

11. Laboratory results obtained in this study (experiment #9) strongly suggests that high recovery might be expected from nitrogen-driven propane slugs.

12. Results obtained in this study (experiment #1) suggested that variations of the nitrogen injection pressure above the miscible pressure does not affect significantly the final crude oil recovery.

B. Recommendations

Based on the experimental results of this research, the author would recommend for future investigations to be conducted at the University of Oklahoma, the following:

1. To continue the nitrogen-driven propane slugs displacement processes investigation, to fully determine the effect of slug size, injection pressure, temperature and oil gravity on crude oil recovery.

2. Since one of the practical applications of a regular high-pressure nitrogen injection is tertiary recovery in reservoirs after waterflooding, the process might be studied to fully understand the effect of crude oil saturation and high mobile water saturation on crude oil recovery. The temperature effect on this process is also very important.

3. Investigate the effect of temperature, injection pressure and gas-oil-ratio on recovery of different API gravity oils to develop more general equations to predict recovery.

4. Conduct investigations similar to this study and the previous one using other reservoir physical models designed as a scale model in order to obtain information representative of a particular reservoir under study.

5. Investigate the effect of pre-enrichment of nitro-

gen with intermediate hydrocarbon to achieve early miscibility in the displacement process.

6. Investigate the importance and magnitude of capillary pressure, gravity, relative permeability, diffusion and dispersion in a high-pressure nitrogen displacement process.

7. Develop a compositional mathematical model to simulate the high-pressure nitrogen displacement process.

8. Use a liquid and vapor chromatograph to obtain experimental values of liquid composition and equilibrium constant.

NOMENCLAUTRE

b = Constant characteristic of a particular hydrocarbon

C_i = ith component in a hydrocarbon mixture, mole fraction

B.P = Bubble point pressure, psi

GOR = Gas-oil ratio, SCF/STB

K = Permeability, md

K_i = Equilibrium vaporization ratio for component i

L = Reservoir Path length, ft

M_{wi} = Molecular weight of ith component

N_2 = Nitrogen

P = Absolute Pressure of the system, psi

P_{ci} = Critical Pressure of the ith component, psi

P_{chi} = Parachor of ith component

P^k = Convergence pressure, psi

P_r = Pseudo-reduced pressure, dimensionless

P.V = Pore Volume, fraction

T = Absolute temperature, °F

T_{ci} = Critical temperature of ith component, psi

T_r = Pseudo-reduced pressure, dimensionless

U_1 = Viscosity of gas mixture at atmospheric pressure

U_1^* = Viscosity of component ith at atmospheric pressure, Cp.

V_i = Specific Volume of ith component, ft^3/lb

$V_{C6}+$ = Specific volume of hexane and heavier, ft^3/lb

V_{ci} = Critical volume of ith component, $ft^3/lb\text{-}mole$

X_i = Mole Fraction of ith component in liquid phase

Y_i = Mole Fraction of ith component in vapor phase

ρ_V = Vapor density, lb/ft^3

ρ_L = Liquid density, lb/ft^3

σ = Surface tension, dynes/cm

μ_V = Vapor viscosity, Cp

μ_L = Liquid viscosity, Cp

BIBLIOGRAPHY

1. Ahmed, T. H., "An Experimental Study of Crude Oil Recovery by High Pressure Nitrogen Injections." A Ph.D. Dissertation, The University of Oklahoma, (1980).

2. Alonso, M. et al., "A Laboratory Investigation of the Enriched Gas Displacement Process in Vertical Models," THE JOURNAL OF CANADIAN PETROLEUM. (January-March, 1973).

3. Bashbush, Jose L., "A Method to Determine K-Values from Laboratory Data and its Applications." SPE PAPER #10127. (1981).

4. Batycky, J. P. et al., "Miscible and Immiscible Displacement Studies on Carbonate Reservoir Cores." THE JOURNAL OF CANADIAN PETROLEUM. (January-March, 1981). pp. 104, 111.

5. Bernard, George G., Holm, L. W., and Harvey, C. P., "Use of Surfactant to Reduce CO_2 Mobility in Oil Displacement." SPEJ. (August, 1980) pp. 281-292.

6. Besseren, George J. et al., "An Efficient Phase Behavior Package for Use in Compositional Reservoir Simulation Studies." SPE PAPER #8288.

7. Brown, G. G.; Katz, D. L.; Oberfell, G. G. and Allen, R. C., "Natural Gasoline and the Volatile Hydrocarbons." N.G.A.A. Tulsa, Oklahoma. (1948).

8. Blackwell, R. J.; Rayne, J. R. and Torry, W. M., "Factors Influencing the Efficiency of Miscible Displacement." TRANS., AIME (1959) 216, 1-8.

9. Calvin, W. James and Vogel, L. J., "An Evaluation of Nitrogen Injection as a Method of Increasing Gas Cap Reserves and Accelerating Depletion--Ryckman Creek Field, Uinto County, Wyoming." SPE PAPER #8384. (1979).

10. Carlisle, Larry E. and Crawford, Paul B., "Oil Recovery by Nitrogen-Driven Propane Slugs." PETROLEUM ENGINEER INTERNATIONAL. (December, 1981), pp. 86, 94.

11. Carr, N. L.,; Kobayashi, R. and Burrows, D. B., "Viscosity of Hydrocarbon Gases Under Pressure." TRANS. AIME (1954). p. 201.

12. Chowdhry, M.A., "Study of Oil Vaporization and Miscible

Displacement During High Pressure Injection of Various Gases." Master Science Thesis, the University of Oklahoma. (1978).

13. Clark, N.J. et al. "Miscible Drive - its Theory and Application in Oil and Gas Operations." JOURNAL OF PETROLEUM TECHNOLOGY. (June, 1958).

14. Clark, Norman J. "Practical Application of Oil and Gas Equilibrium Calculations." JOURNAL OF PETROLEUM TECHNOLOGY. (January, 1962) pp. 491-501.

15. Clark, Norman J. "Theoretical Aspects of Oil and Gas Equilibrium Calculations". JOURNAL OF PETROLEUM TECHNOLOGY. (April, 1962).

16. Clancy, J.P. et al. "How Nitrogen is Produced and Used for Enhanced Recovery". WORLD OIL. (Oct., 1981) pp. 233-244.

17. Cook, Alton B. et al. "The Role of Vaporization in High Percentage Oil Recovery by Pressure Maintenance". JOURNAL OF PETROLEUM TECHNOLOGY. (February, 1967). pp. 245-250.

18. Cook, Alton B. et al. "Realistic K Values of C_7^+ Hydrocarbons for Calculating Oil Vaporization During Gas Cycling at High Pressures". JOURNAL OF PETROLEUM TECHNOLOGY. (July, 1969) pp. 901,915.

19. Crawford, P.B. "West Texas Oils Respond to Nitrogen-Driven CO_2. DRILL BIT. (December, 1979) pp.62-65.

20. Donohoe, Charles W.; Buchanan, Robert D. "Economic Evaluation of Cycling Gas-Condensate Reservoirs with Nitrogen". JOURNAL OF PETROLEUM TECHNOLOGY. (February, 1981) pp. 263-270.

21. Eckles, Wesley W., Jr.; Prihoada, Clarence and Holden, W.W. "Unique Enhanced Oil and Gas Recovery Project for very High Pressure Wilcox Sands Uses Cryogenic Nitrogen and Methane Mixture". SPE PAPER # 9415. Paper presented at the 55th Annual Fall Technical Conference and Exhibition of SPE held in Dallas, Texas. (September, 1980).

22. Engineering Data Book, compiled and Edited by Gas Processors Association. Ninth Edition, 1972.

23. Greenwalt, Wayne A. "A Field Test of Nitrogen WAG Injectivity". JOURNAL OF PETROLEUM TECHNOLOGY (February, 1982) pp. 266,272.

24. Habermann, B. "The Efficiency of Miscible Displacement as a Function of Mobility Ratio". PETROLEUM TRANSACTIONS, AIME Vol. 264 (1960) pp. 264-272.

25. Hardy, Jay H. and Robertson, Nelson. "Miscible Displacement by High Pressure Gas at Block 31". PETROLEUM ENGINEER. (November, 1975).

26. Hause, R.W. "Where EOR Stand Today", PETROLEUM ENGINEERING INTERNATIONAL. (November, 1981) pp. 55-72.

27. Hendricks, David R. "Gas Chromatography". Florida Gas Transmission Company, Zachary, Louisiana.

28. Herning, F. and Zipperer, L. "Calculation of the Viscosity of Technical Gas Mixtures for the Viscosity of the Individual Gases", GAS U. WASSERFOCH. (1936), v. 79, p. 69.

29. Holm, L.W. and Josendal V.A. "Mechanism of Oil Displacement by Carbon Dioxide", JOURNAL OF PETROLEUM TECHNOLOGY. (December, 1974).

30. Hutchinson, C.A., Jr. and Braum, Philip H. "Phase Relation of Miscible Displacement in Oil Recovery," AICh. E. JOURNAL, (March, 1961), pp. 64-72.

31. Jenks, Loren H. et al. "A Field Test of the Gas-Driven Liquid Propane Method of Oil Recovery", PETROLEUM TRANSACTIONS, AIME, Vol. 210 (1957) pp.34-39.

32. Kamath, K.I. et al. "The Role of Temperature in CO_2 Flooding", DOE ENERGY TECH. CENTER. Paper presented at the 5th Symposium of EOR, Tulsa, Oklahoma (August, 1979).

33. Katz, D.L.; Monroe, R.R. and Trainer, R.R. "Surface Tension of Crude Oils Containing Dissolved Gases", PETROLEUM TECHNOLOGY. (September, 1943).

34. Katz, Donald L. HANDBOOK OF NATURAL GAS ENGINEERING ENGINEERING. McGraw Hill Book Company, Inc. New York, N.Y. (1959).

35. Kays, Wm. M. CONVECTIVE HEAT AND MASS TRANSFER, McGraw Hill Book Company, New York, N.Y. (1966).

36. Koch, H.H., Jr.; Hutchinson, C.A., Jr. "Miscible Displacements of Reservoir Oil Using Flue Gas", PETROLEUM TRANSACTIONS AIME Vol. 213 (1958)pp.7-10.

37. Lacey, James L. et al. "Miscible Fluid Displacement in Porous Media", PETROLEUM TRANSACTIONS, AIME, Vol. 213, (1958).

38. Lenoir,J.M. and White, G.A. "Predicting Convergence Pressure," PETROLEUM REFINER, (March, 1958) pp. 173, 181.

39. Lohrenz, J., B.G. and Clark, C.R. "Calculating Viscosity of Reservoir Fluids from their Composition", J. PET. TECH. (October, 1964) pp. 1171-1176.

40. McLeod, W.R. Ph.D Thesis, University of Oklahoma (1968).

41. Menzie, D.E. and Nielsen, R.F. "A Study of Vaporization of Crude Oil by CO_2 Repressuring," J. PETRO. TECH. (November, 1963).

42. Metcalfe, R.S. et al. "A Multicell Equilibrium Separation Model for the Study of Multiple Contact Miscibility in Rich-Gas Drives", SOCIETY OF PETROLEUM ENGINEERS JOURNAL. (June, 1973).

43. Miller, James M. and Harmon, Richard L. ELEMENTARY THEORY OF GAS CHROMATOGRAPHY, Prepared and published by GOW-MAC Instrument Co. Madison, N.J., U.S.A. (February, 1977).

44. Moses, Phillip L. and Wilson Keith. "Phase Equilibrium Considerations in Utilizing Nitrogen for Improved Recovery from Retrograde Condensate Reservoirs", JOURNAL OF PETROLEUM TECHNOLOGY. (February, 1981) pp. 256-261.

45. O'Leary, J.P.; Murray, T.M.; Guillary, T.; Grieve, C.; Reece, M.C.; Nugent, M.; Perkins, T.; Crawford, P.B. "Nitrogen-Driven CO_2 Slugs Reduce Costs", PETROLEUM ENGINEER INTERNATIONAL (May, 1979).

46. Perkins, T.K. and Johnston, O.C. "A Review of Diffusion and Dispersion in Porous Media", SOCIETY OF PETROLEUM ENGINEERS JOURNAL. (March, 1963) pp. 70, 84.

47. Peterson, A.V. "Optimal Recovery Experiments with N_2 and CO_2", PETROLEUM ENGINEER. (November, 1978).

48. Power, Harry H. "Relative Propulsive Efficiencies of Air and Natural Gas in Pressure Drive Operations",

PETROLEUM TRANSACTIONS, AIME Vol. 82 (1929).

49. Rathmell, J.J.; Stalkup, F.I. and Hasinger, R.C. "A Laboratory Investigation of Miscible Displacement by Carbon Dioxide", SPE PAPER #3483.

50. Robinson, Donald B. and Peng-Joo Ng. "Capability of the Peng-Robinson Programs", HYDROCARBON PROCESSING. (April, 1978). pp. 95.98.

51. Rushing, M.D. "High Pressure Air Injection", PETROLEUM ENGINEERING. (November, 1976).

52. Rushing, M.D.; Thomason, B.C.; Reynolds, B. and Crawford, P.B. "High Pressure Nitrogen or Air May Be Used for Miscible Displacement in Deep, Hot Oil Reservoirs", SPE PAPER #6445. (April, 1977).

53. Rushing, M.D.; Thomason, B.C. et al. "Miscible Displacement by High Pressure Nitrogen Injection," 24th Annual Southwestern Petroleum Short Course, Ass. Mtg. Procc. (1977).

54. Slobod, R.L. and Koch, H.A., Jr. "High Pressure Gas Injection - Mechanism of Recovery Increase". API Drilling and Prod. Practice. (1973).

55. Soo Gun Oh and Slattery, J.C. "Interfacial Tension Required for Significant Displacement of Residual Oil", SPEJ. (April, 1979) pp. 83-96.

56. Standing, M.B. and Katz, D.L. "Density of Natural Gases", TRANS. (AIME) (1942).

57. Standing, M.B. "Volumetric and Phase Behavior of Oil Hydrocarbon Systems", Reinhold Publishing Corporation. New York, N.Y. (1952).

58. Starling, Kenneth E. FLUID THERMODYNAMIC PROPERTIES FOR LIGHT PETROLEUM SYSTEMS. Gulf Publication Company. Houston, Texas. (1977).

59. Starling, Kenneth E. and Fish, Larry W. "A Mixture Thermodynamic Properties Computer Program". Technical Report ORO-4944-2. School of Chemical Engineering and Materials Science. The University of Oklahoma, Norman, Ok. (December, 1975).

60. Sutton, Carl. CHROMATOGRAPHY AND GPA, Seventh Chromatography School, University of Southwestern Louisiana, Lafayette, Lousisiana. (December, 1977)

61. Sugden, J. CHEM. SOC., Vol. 125, (1924).

62. Taber, J.J., "Dynamic and Static Forces Required to Remove a Discontinuous Oil Phase from Porous Media Containing both Oil and Water," SOCIETY OF PETROLEUM ENGINEERS JOURNAL, (March, 1969), pp. 3, 12.

63. Tiffin, David L. and Yelling, William F., "Effects of Mobile Water on Multiple Contact Miscible Gas Displacements," SPE/DOE PAPER #10687, (1982).

64. Van Poollen, H. K. and Associates, Inc. FUNDAMENTALS OF ENHANCED OIL RECOVERY. Pennwell Publishing Co., Tulsa, Oklahoma (1980), pp. 114-131, 146-151.

65. Vogel, John L. and Yarborough, Lyman, "The Effect of Nitrogen on the Phase Behavior and Physical Properties of Fluids," SPE PAPER #8815. This paper was presented at the First Symposium on Enhanced Oil Recovery at Tulsa, Oklahoma, (April, 1980).

66. Whorton, L. P. and Kieschnick, W. R., Jr., "Oil Recovery by High Pressure Gas Injection," OIL AND GAS JOURNAL, (April 6, 1950).

67. Wiemer, R. F., "LPG-Gas Injection Recovery Process Burkett Unit, Greenwood County, Kansas." JOURNAL OF PETROLEUM TECHNOLOGY, (October, 1963), pp. 1067-1072.

68. Wilson, Keith, "Enhanced-Recovery by Inert Gas Processes Compared." OIL AND GAS JOURNAL (July 31, 1978), pp. 162-166.

69. Wilson, A.; Maddox, R.N. and Erbar, J.H., "C_6^+ Fractions Affect Phase Behavior." OIL & GAS JOURNAL, (August, 1978), pp. 76-81.

70. Weinbrandt, R. M. et al., "The Effect of Temperature on Relative and Absolute Permeability of Sandstones," SPEJ, Oct. 1975.

71. Yarbrough, L. and Smith, L.R., "Solvent and Driving Gas Compositions for Miscible Slug Displacement." SOC. PET. ENG. J., (September, 1970), pp. 298-310.

APPENDIX A

CALIBRATION OF THE LDG MINIPUMP

CALIBRATION OF THE LDG MINIPUMP

A1: DESCRIPTION:

The LDG minipump model 396 (duplex) is a reciprocating plunger, positive displacement type pump. It is designed to produce liquid flow in precise quantities against pressure up to 6,000 PSIG. The duplex version consists of two pump bodies. The pump has two manual micrometer dial controls to fix the stroke length of the pump. Adjustment of the flow rate may be made while the pump is shutdown.

A2: CALIBRATION:

Since the flow rate is proportional to the motor speed and stroke length it was necessary to perform a test to obtain data to determine relationships between micrometric dial position and the flow rate. The performance data for the minipump is given in table A1 and the calibration curve is shown in figure A1.

TABLE A1

Performance Data for the LDG Minipump

TIME (SEC)	RECOVERY VOLUME (MIN) RATE	LDG MINIPUMP DIAL SETTING
0	-	0
480	10	10
960	20	10
206	10	20
412	20	20
979	70	30
1116	80	30
1437	110	35
1555	120	35
1699	130	35
330	30	40
440	40	40
550	50	40
177	20	50
145	20	60
327	45	60

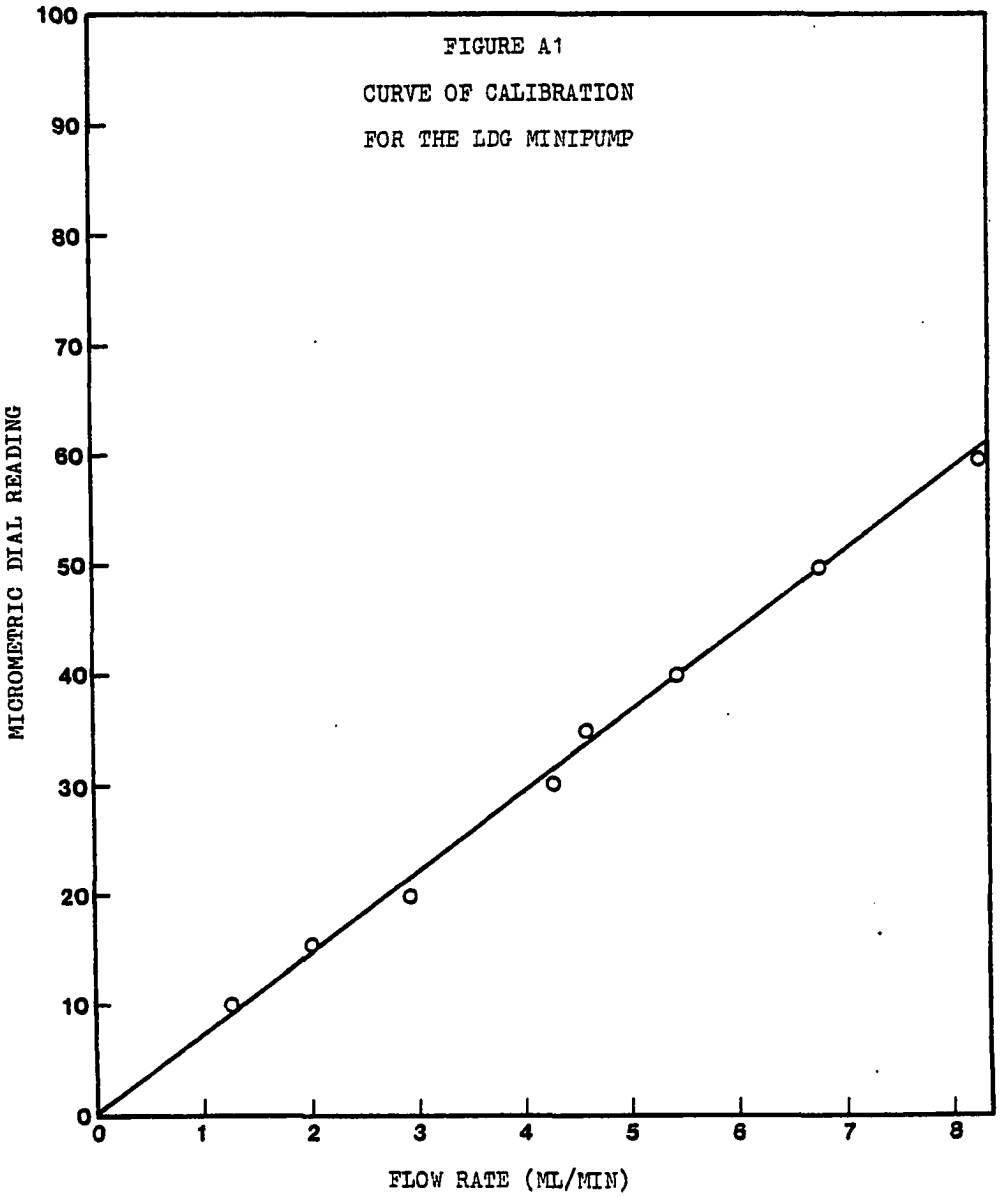
FIGURE A1
CURVE OF CALIBRATION
FOR THE LDG MINIPUMP
MICROMETRIC DIAL READING
FLOW RATE (ML/MIN)
0
10
20
30
40
50
60
70
80
90
100
0
1
2
3
4
5
6
7
8

APPENDIX B

LISTING OF COMPUTER PROGRAM AND SUBROUTINES USED IN THIS STUDY TO SIMULATE HEAT TRANSFER IN THE RESERVOIR PHYSICAL MODEL AND WITH LISTING OF A SAMPLE OUTPUT

```
$JOB
C**** USR=(CALCOCER./BIN/GUS)
      DIMENSION DELTP(200),DELTT(200),TPIPE(200),TTUBE(200),
     1 DELTME(200)
      DIMENSION QREQ(2),HC(200),QR(200),QRAR(200),UN(200),UNO(200),
     1 QRAP(200),HCO(200),QLOST(200),QLOSP(200),QLOSA(200),QLSTOT(200)
      REAL PIE,LPIPE,LTUBE,KSAND,KGAS,KSTEEL,MASSP,MASST,MASSC,LOTUBE
      REAL MASSA,NUAIR,NUSSLT
      DIMENSION QSUPLY(2),QRAR1(200),UN1(200),HC1(200),QLOSTP(200)
      READ(5,100) TPIP,TTUB,TFLAME,TAMB,AFLAME,FFP,FFT,DELTM
100   FORMAT(10F8.0)
      READ(5,100) RHOST,RHOS,RHOG,SPHST,SPHS,SPHG,KSTEEL,KSAND,KGAS
      AF = AFLAME
      READ(5,100) ALFST,ALFSND,ALFGAS,DOP,DIP,DOT,DIT,LPIPE,LTUBE,
     1 RHOA
      READ(5,110) NOPT,HITCAP,QCFM,TAIR
110   FORMAT(I8,8F8.0)
      TAIRF = TAIR-460.0
      IF(TAIRF.GT.32.0.AND.TAIRF.LE.100.0)NUAIR=0.162E-03
      IF(TAIRF.GT.100.0.AND.TAIRF.LE.200.0)NUAIR=0.2055E-03
      IF(TAIRF.GT.200.0.AND.TAIRF.LE.300.0)NUAIR=0.273E-03
      IF(TAIRF.GT.300.0.AND.TAIRF.LE.400.0)NUAIR=0.342E-03
      IF(TAIRF.GT.400.0.AND.TAIRF.LE.500.0)NUAIR=0.416E-03
      IF(TAIRF.GT.500.0.AND.TAIRF.LE.800.0)NUAIR=0.548E-03
CCCCCCCCCCCCCCCCCCCCCCCCCCCCCCCCCCCCCCCCCCCCCCCCCCCCCCCCCCCCCCCCCCCC
C                                                                  C
C                                                                  C
C          NOPT        = CONTROL VARIABLE FOR USING                C
C                        CONVECTIVE OR RADIATIVE HEAT TRANSFER     C
C                        DEPENDING ON THE HEATER TYPE.             C
C                                                                  C
C          HITCAP      = TOTAL HEAT CAPACITY OF THE RECOMMENDED    C
C                        HEATER.
C                                                                  C
C          QCFM        = RATE OF AIR BLOWN BY THE HEATER           C
C                        IN CFM.
C                                                                  C
C          NUAIR   = KINEMATIC VISCOSITY OF AIR IN SQ. FT./SEC.    C
C                                                                  C
C          VAIR    = VELOCITY OF AIR IN FT./SEC.                   C
C                                                                  C
C          HCAR    = CONVECTIVE HEAT TRANSFER COEFFICIENT OF AIR   C
C                                                                  C
C          TRAIR   = TEMPERATURE OF AIR AT RADIUS 'RPIPE' IN DEG.F C
C                                                                  C
C          TAIR    = TEMPERATURE OF AIR AT THE CEN. OF PIPE IN DF  C
CCCCCCCCCCCCCCCCCCCCCCCCCCCCCCCCCCCCCCCCCCCCCCCCCCCCCCCCCCCCCCCCCCCC
      DPIPE = 15.0/12.0
      LOTUBE = 5.0
      DTUBE = 0.45/12.0
      FPT=1.0
      DELTME(1) = DELTM
      PIE   = 3.1415927
      TPIPE(1)=TPIP
      QLOSP(1)=0.0
      QLOST(1)=0.0
      QLOSTP(1)=0.0
      QLOSA(1) =0.0
      TTUBE(1)=TTUB
      APIPE = PIE*DPIPE*LPIPE
```

```
      ATUBE = PIE*DTUBE*LTUBE
      AOTUBE= PIE*DTUBE*LDTUBE
      AOT=PIE*DDT*LTUBE
      SIGMA = 0.1714E-08
      VOLP   = PIE*((DDP**2.0)-(DIP**2.0))*LPIPE/4.0
      VOLT   = PIE*((DOT**2.0)-(DIT**2.0))*LTUBE/4.0
      MASSP = RHOST*VOLP
      MASST = RHOST*VOLT
      FR  = 0.72
      LLP =0
      TOTLOS = 0.0
      DO 10 I=1,51,1
      JM=I
      GO TO (120,130), NOPT
120   CONTINUE
      LLP = LLP+1
      QDOTRT=AF*FFT*SIGMA*((TFLAME**4.0)-(TTUBE(I)**4.0))*0.01-
     1QLOST(I)-QLOSA(I)-QLOSTP(I)
      QDOTRP=AF*FFP*SIGMA*((TFLAME**4.0)-(TPIPE(I)**4.0))*0.01 -
     1QLOSP(I)
      DELTP(I)=(QDOTRP)/(MASSP*SPHST)
      DELTT(I)=(QDOTRT)/(MASST*SPHST)
      TPIPE(I+1)=TPIPE(I)+DELTP(I)
      TTUBE(I+1)=TTUBE(I)+DELTT(I)
130   CONTINUE
      IF(TTUBE(I).GT.575.0)GO TO 301
      LLP=LLP+1
      VAIR = DDPM*4.0/(PIE*DPIPE*DPIPE*60.0)
      REYNO = (VAIR*DPIPE)/NUAIR
      IF(REYNO.GT.2300.0)GO TO 150
      CONST = 0.229
      EN    = 0.632
      HCAR  = KGAS*CONST*(REYNO**EN)
      GO TO 160
150   CONTINUE
      NUSSLT=0.023*(1.0+(DPIPE/LPIPE)**0.7)*(REYNO**0.8)*(PR**0.33)
      HCAR = NUSSLT*KGAS/DPIPE
160   CONTINUE
      RPIPE = DPIPE/2.0
      DTDX  = 3.0
      IF(TAIRF.GT.400.0) DTDX=4.50
      TRAIR = TAIR-VAIR*DTDX*(RPIPE**2.0)*0.75/(4.0*ALFGAS)
      GO TO 302
301   CONTINUE
      HCAR = 0.0
      TRAIR = TPIPE(I)
      VAIR = 0.0
      REYNO = 0.0
302   CONTINUE
      GO TO(190,200), NOPT
200   CONTINUE
      IF(TPIPE(I).GT.TTUBE(I))QLOSTP(I)=0.0
      QDOTRT=HCAR*AOT*(TAIR-TTUBE(I))*0.01-QLOST(I)-QLOSTP(I)-QLOSA(I)
      QDOTRP=HCAR*APIPE*(TRAIR-TPIPE(I))*0.01-QLOSP(I)
      DELTP(I)=QDOTRP/(MASSP*SPHST)
      DELTT(I)=QDOTRT/(MASST*SPHST)
      TPIPE(I+1)=TPIPE(I)+DELTP(I)
      TTUBE(I+1)=TTUBE(I)+DELTT(I)
190   CONTINUE
      AOP  = PIE*DDP*LPIPE
```

```
91          AOT = PIE*DOT*(LTUBE-LOTUBE)
92          GRAR(I) = 3.16*10E6*(DCP**3.0)*(TPIPE(I)-TAMB)
93          GRAR1(I)=3.16*10E06*(DOT**3.0)*(TTUBE(I)-TAMB)
94          UN(I) = 0.152*(GRAR(I)**0.281)
95          UN1(I)=0.152*(GRAR1(I)**0.281)
96          HC(I) = UN(I)*KGAS/DUP
97          HC1(I)=UN1(I)*KGAS/DOT
98          QLOSP(I+1) = HC(I)*AOP*(TPIPE(I+1)-TAMB)*0.01
99          IF(TTUBE(I).GT.574.0.AND.NOPT.GT.1) GO TO 170
100         QLOST(I+1)=0.0
101         GO TO 180
102   170   CONTINUE
103         QLOST(I+1)=HC1(I)*AOT*(TTUBE(I+1)-((TPIPE(I+1)+TTUBE(I+1))/2.0)
        1)*0.01
104   180   CONTINUE
      C FOR HEAT TRANSFER FROM THE TUBE AT THE ENDS OUTSIDE THE PIPE
105         PR = 0.72
106         GR(I) = 3.1*10E6*(LOTUBE**3.0)*(TTUBE(I)-TAMB)
107         GRAP(I) = (GR(I)*PR)
108         VOLTUBE=PIE*((DOT**2.0)/4.0)*(LTUBE-8.0)
109         UNO(I) = 0.55*(GRAP(I)**0.25)
110         HCO(I) = UNO(I)*KGAS/LOTUBE
111         MASSA=QCFM*RHOA*60.0
112         AOT=PIE*DOT*(LTUBE-LOTUBE)
113        VOLTM=((PIE*(DPIPE**2.0))/4.0 - AOT)
114         IF(NOPT.EQ.1)MASSA=VOLTM*4.0*RHOG
115         QLOSTP(I+1)=ATUBE*FFT*SIGMA*((TTUBE(I+1)**4.0)-(TPIPE(I+1)**4.0
        1))*0.01
      C  TOTAL HEAT LOSS FROM THE SYSTEM = QLSTOT
116         QLSTOT(I) = QLOSP(I)+QLOST(I)+QLOSA(I)
117         DELTME(I+1) = DELTME(I)+0.01
118         QLOSA(I+1) = AOTUBE*(SIGMA*(TTUBE(I)**4.-(TAMB**4.))*0.01)
119         IF(I.GT.1)GO TO 57
120         WRITE(6,51)
121   51    FORMAT(1H1,9X,'TPIPE',9X,'TTUBE',9X,'TIME',10X,'HEAT LOSS',6X,/)
122         WRITE(6,66)
123   66    FORMAT(//9X,'DEG. F',10X,'DEG. F',10X,'HRS.',12X,'BTU',6X,//)
124   57    CONTINUE
125         WRITE(6,52)TPIPE(I),TTUBE(I),DELTME(I),QLSTOT(I)
126   52    FORMAT(/,5X,3F12.4,F16.4,//)
127         TOTLOS = TOTLOS+QLSTOT(I)
128   10    CONTINUE
129         IF(NOPT.GT.1) GO TO 303
130         QSUPLY(1)=TOTLOS + MASSP*SPHST*(TPIPE(25)-TPIPE(1))+MASSA*SPHG*
        1 LLP*0.01*(TAIR-TAMB)+MASST*SPHST*(TTUBE(25)-TTUBE(1))
131         GO TO 304
132   303   CONTINUE
133         QSUPLY(1)=TOTLOS + MASSP*SPHST*(TPIPE(50)-TPIPE(1)) +
        1 MASST*SPHST*(TTUBE(50)-TTUBE(1))
134         QSUPLY(2)= MASSA*SPHG*LLP*0.01*(TAIR-TAMB)
135         IF(QSUPLY(1).GT.QSUPLY(2))QSUPLY(1)=QSUPLY(2)
136   304   CONTINUE
137         WRITE(6,53)QSUPLY(1),QSUPLY(2)
138   53    FORMAT(//,5X,'TOTAL HEAT REQUIRED TO BE SUPPLIED INITIALLY=',
        12X,F14.3,'BTU',1X,//,5X,'HEAT SUPPLIED BY THE HEATER FOR HALF
        1HOUR = ',2X,F14.3,'BTU',1X,//)
139         CALL SSUPLI(TPIPE,TTUBE,QSUPLY,DELTF,DELTT,QLOSP,QLOST,QLOSA,
        1QLSTOT,QLOSTP,DELTME,PIE,DIT,RHOS,SPHS,KSAND,AF,TFLAME,HITCAP,
        1NOPT,HCAR,TAIR,TRAIR,QCFM)
140         STOP
```

```
141          END

142          SUBROUTINE SSUPLI(TPIPE,TTUBE,QSUPLY,DELTP,DELTT,QLOSP,QLCST,
           1 QLCSA,QLSTCT,QLCSTP,DELTME,PIE,DIT,RHCS,SPHS,KSAND,AF,TFLAME,
           1 HITCAP,NCPT,HCAR,TAIR,TRAIR,GCFM)
143          DIMENSION DELTP(200),DELTT(200),TPIPE(200),TTUBE(200),
           1 DELTME(200),QGAINC(200),TSAND(200)
144          DIMENSION GREQ(2),HC(200),GR(200),GRAR(200),UN(200),UNC(200),
           1 GRAP(200),HCC(200),QLCST(200),QLOSP(200),QLOSA(200),QLSTCT(200)
145          REAL PIE,LPIPE,LTUBE,KSAND,KGAS,KSTEEL,MASSP,MASST,MASSC,LCTUBE
146          REAL MASSA
147          DIMENSION QSUPLY(2),GRAR1(200),UN1(200),HC1(200),QLOSTP(200)
148          DPIPE = 15.0/12.0
149          LOTUBE = 5.0
150          DTUBE = 0.45/12.0
151          FPT=1.0
152          DELTME(1) = 0.01
153          DATA DOP,DIP,DOT,LPIPE,LTUBE,RHOA/1.285,1.25,0.04,22.0,125.0,
           10.071/
154          DATA RHOST,SPHST,KSTEEL/490.0,0.11,26.2/
155          DATA FFP,FFT,TAMB/0.60,0.32,532.0/
156          DATA KGAS,SPHG/0.0154,0.248/
157          PIE   = 3.1415927
158          TPIPE(1)=535.0
159          AIPIP=PIE*DIP*DIP/4.0
160          QLOSP(1)=0.0
161          QLCST(1)=0.0
162          QLOSTP(1)=0.0
163          QLOSA(1) =0.0
164          TTUBE(1)=535.0
165          APIPE = PIE*DPIPE*LPIPE
166          ATUBE = PIE*DTUBE*LTUBE
167          AOTUBE= PIE*DTUBE*LOTUBE
168          SIGMA = 0.1714E-08
169          VOLP   = PIE*((DOP**2.0)-(DIP**2.0))*LPIPE/4.0
170          VOLT   = PIE*((DOT**2.0)-(DIT**2.0))*LTUBE/4.0
171          VC=24.0/3600.0
172          MASSP = RHOST*VOLP
173          MASST = RHOST*VOLT
174          TSAND(51)=515.0
175    36    CONTINUE
176          DO 10 I=51,150,1
177          JM=I
178          TEMPL=VC*(I-50)*0.01*3600.0
179          VOLC=PIE*(DIT**2.0)*TEMPL/4.0
180          MASSC=RHCS*VOLC
181          QGAINC(I)=(KSAND*PIE*DIT*TEMPL*(TTUBE(I)-TSAND(I))/(DIT/2.))*(
           10.01)
182          DELTS=QGAINC(I)/(MASSC*SPHS)
183          TSAND(I+1)=TSAND(I)+DELTS
184          IF(NCPT.GT.1)GO TO 110
185          QDOTRT=AF*FFT*SIGMA*((TFLAME**4.0)-(TTUBE(I)**4.0))*0.01-
           1QLCST(I)-QLCSA(I)-QLCSTP(I) -QGAINC(I)
186          QDOTRP=AF*FFP*SIGMA*((TFLAME**4.0)-(TPIPE(I)**4.0))*0.01 -
           1QLOSP(I)
187          GO TO 120
188   110    CONTINUE
189          AOT = ATUBE
190          QDOTRT=HCAR*AOT*(TAIR-TTUBE(I))*0.01-QLOST(I)-QLOSTP(I)-QLCSA(I)
191          QDOTRT = QDOTRT-QGAINC(I)
```

```
192            QDCTRP=HCAR*AIPIP*(TRAIR-TPIPE(I))*0.01-QLOSP(I)
193    120     CONTINUE
194            DELTP(I)=(QDCTRP)/(MASSP*SPHST)
195            DELTT(I)=(QDCTRT)/(MASST*SPHST)
196            TPIPE(I+1)=TPIPE(I)+DELTP(I)
197            TTUBE(I+1)=TTUBE(I)+DELTT(I)
198            AOP  = PIE*DOP*LPIPE
199            AOT = PIE*DOT*(LTUBE-LOTUBE)
200            GRAR(I) = 3.16*10E6*(DOP**3.0)*(TPIPE(I)-TAMB)
201            GRAR1(I)=3.16*10E06*(DOT**3.0)*(TTUBE(I)-TAMB)
202            UN(I) = 0.152*(GRAR(I)**0.281)
203            UN1(I)=0.152*(GRAR1(I)**0.281)
204            HC(I) = UN(I)*KGAS/DOP
205            HC1(I)=UN1(I)*KGAS/DOT
206            QLOSP(I+1) = HC(I)*AOP*(TPIPE(I+1)-TAMB)*0.01
207            QLOST(I+1)=HC1(I)*AOT*(TTUBE(I+1)-((TPIPE(I+1)+TTUBE(I+1))/2.0)
          1)*0.01
      C FOR HEAT TRANSFER FROM THE TUBE AT THE ENDS OUTSIDE THE PIPE
208            PR = 0.72
209            GR(I) = 3.1*10E6*(LOTUBE**3.0)*(TTUBE(I)-TAMB)
210            GRAP(I) = (GR(I)*PR)
211            VOLTBE=PIE*((DOT**2.0)/4.0)*(LTUBE-5.0)
212            UNC(I) = 0.55*(GRAP(I)**0.25)
213            HCC(I) = UNC(I)*KGAS/LOTUBE
214            MASSA=(PIE*(DIP**2.)*LPIPE/4.0 - VOLTBE)*RHOA
215           QLOSA(I+1)=PIE*DOT*LOTUBE*SIGMA*(TTUBE(I)**4.0-TAMB**4.0)*0.01
216            QLOSTP(I+1)=ATUBE*FPT*SIGMA*((TTUBE(I+1)**4.0)-(TPIPE(I+1)**4.0
          1))*0.01
      C  TOTAL HEAT LOSS FROM THE SYSTEM = QLSTOT
217            QLSTOT(I) = QLOSP(I)+QLOST(I)+QLOSA(I)+QLOSTP(I)
218            DELTME(I+1) = DELTME(I)+0.01
219            IF(I.LT.150)GO TO 70
220            IF(TSANC(150).LT.560.0) GO TO 65
221            GO TO 70
222    65      AF=1.8*AF
223            GO TO 36
224    70      CONTINUE
225            IF(I.GT.51)GO TO 57
226            WRITE(6,56)
227    56      FORMAT(1H1,12X,'TEMPERATURE RESPONSE OF THE PIPE AND TUBES
          1 DURING FIRST HOUR OF CRUDE INJECTION',6X,//)
228            WRITE(6,51)
229    51      FORMAT(9X,'TPIPE',14X,'TTUBE',14X,'TIME',17X,'HEAT LOSS',10X,
          1'TSANDSTONE',4X,'AIR FLOW RATE',/)
230            WRITE(6,58)
231    58      FORMAT(9X,'DEG. R',12X,'DEG. R',13X,'HRS',18X,'BTU',18X,'DEG. R
          1',9X,'CFM',1X,//)
232    57      CONTINUE
233            WRITE(6,52)TPIPE(I),TTUBE(I),DELTME(I),QLSTOT(I),TSANC(I),QCFM
234    52      FORMAT(/,5X,F12.4,6X,F12.4,6X,F12.4,6X,F16.4,6X,F12.4,3X,F12.4,
          12X,//)
235    10      CONTINUE
236            TOTLOS = QLSTOT(100)*100.0
237            QSUPLY(1) = TOTLOS + MASSP*SPHST*(TPIPE(100)-TAMB)+MASSA*SPHG*
          1 (TAIR-TAMB)+MASST*SPHST*(TTUBE(100)-TAMB)
238            IF(QSUPLY(1).GT.HITCAP)GO TO 210
239            GO TO 220
240    210     HITCAP=QSUPLY(1)*1.25
241            GO TO 36
242    220     CONTINUE
```

```
243          WRITE(6,53)QSUPLY(1)
244    53    FORMAT(//,5X,'TOTAL HEAT REQUIRED TO BE SUPPLIED DURING
            1FIRST HOUR OF CRUDE INJECTION=',2X,F14.3,'BTU',1X,//)
245          RETURN
246          END

     $EXEC
```

TPIPE	TTUBE	TIME	HEAT LOSS
DEG. R	DEG. R	HRS.	BTU
535.0000	535.0000	0.0100	0.0000
535.7336	535.1340	0.0200	1.3196
536.4463	535.2625	0.0300	1.6671
537.1497	535.3906	0.0400	2.0246
537.8438	535.5166	0.0500	2.3914
538.5286	535.6465	0.0600	2.7658
539.2941	535.7742	0.0700	3.1463
539.8704	535.9016	0.0800	3.5317
540.5273	536.0291	0.0900	3.9211
541.1748	536.1563	0.1000	4.3133
541.8130	536.2832	0.1100	4.7077
542.4419	536.4102	0.1200	5.1036
543.0618	536.5369	0.1300	5.5005

543.6724	536.6633	0.1400	5.8578
544.2739	536.7858	0.1500	6.2950
544.8665	536.9160	0.1600	6.6917
545.4500	537.0420	0.1700	7.0875
546.0247	537.1680	0.1800	7.4821
546.5906	537.2937	0.1900	7.8753
547.1477	537.4152	0.2000	8.2666
547.6963	537.5447	0.2100	8.6559
548.2363	537.6699	0.2200	9.0429
548.7678	537.7949	0.2300	9.4275
549.2910	537.9199	0.2400	9.8094
549.8059	538.0447	0.2500	10.1885
550.3125	538.1692	0.2600	10.5645
550.8110	538.2937	0.2700	10.9375
551.3015	538.4180	0.2800	11.3072

551.7842	538.5420	0.2900	11.6736
552.2590	538.6660	0.3000	12.0366
552.7261	538.7858	0.3100	12.3960
553.1855	538.9133	0.3200	12.7518
553.6375	539.0369	0.3300	13.1039
554.0818	539.1602	0.3400	13.4522
554.5188	539.2832	0.3500	13.7966
554.9487	539.4063	0.3600	14.1374
555.3716	539.5291	0.3700	14.4743
555.7874	539.6516	0.3800	14.8073
556.1960	539.7742	0.3900	15.1362
556.5979	539.8965	0.4000	15.4612
556.9932	540.0186	0.4100	15.7823
557.3816	540.1406	0.4200	16.0993
557.7634	540.2625	0.4300	16.4123

558.1389	540.3840	0.4400	16.7213
558.5081	540.5056	0.4500	17.0264
558.8708	540.6270	0.4600	17.3274
559.2275	540.7480	0.4700	17.6245
559.5781	540.8691	0.4800	17.9176
559.9226	540.9500	0.4900	18.2066
560.2612	541.1108	0.5000	18.4917
560.5940	541.2314	0.5100	18.7728

TOTAL HEAT REQUIRED TO BE SUPPLIED INITIALLY= 2618.3818TU

HEAT SUPPLIED BY THE HEATER FOR HALF HOUR = 11638.1708TU

TEMPERATURE RESPONSE OF THE PIPE AND TUBES DURING FIRST HOUR OF CRUDE INJECTION

TPIPE DEG. R	TTUBE DEG. R	TIME HRS	HEAT LOSS BTU	TSARCSTONE DEG. R	AIR FLOW MA CFM
540.5040	541.2314	0.5100	18.7726	515.0000	200.0000
540.3752	549.0132	0.5200	19.9425	543.7415	200.0000
560.1575	560.5173	0.5300	20.1457	549.5176	200.0000
555.4419	565.1936	0.5400	19.8536	550.3724	200.0000
559.7288	569.7717	0.5500	21.1612	565.7800	200.0000
559.5173	572.8169	0.5600	22.0072	570.1565	200.0000
559.3083	574.8864	0.5700	22.5266	573.6713	200.0000
559.1016	576.0037	0.5800	22.8443	574.5727	200.0000
558.8970	576.8862	0.5900	23.0027	576.1899	200.0000
558.6943	577.3743	0.6000	23.0272	576.9526	200.0000
558.4937	577.6649	0.6100	22.8441	577.4146	200.0000
558.2952	577.7574	0.6200	22.9665	577.6775	200.0000
558.0988	577.6263	0.6300	22.8959	577.8091	200.0000

587.9041	577.8433	0.6400	22.7546	577.8242	200.0000
587.7114	577.7666	0.6500	22.6773	577.8420	200.0000
587.5200	577.7241	0.6600	22.5526	577.7922	200.0000
587.3320	577.6348	0.6700	22.4235	577.7172	200.0000
587.1490	577.5344	0.6800	22.2915	577.6267	200.0000
586.9600	577.4270	0.6900	22.1552	577.5254	200.0000
586.7769	577.3152	0.7000	22.0263	577.4175	200.0000
586.5958	577.2009	0.7100	21.8937	577.3022	200.0000
586.4158	577.0852	0.7200	21.7619	577.1909	200.0000
586.2380	576.9688	0.7300	21.6318	577.0750	200.0000
586.0620	576.8523	0.7400	21.5014	576.9585	200.0000
585.8877	576.7363	0.7500	21.3725	576.8420	200.0000
585.7161	576.6211	0.7600	21.2456	576.7261	200.0000
585.5462	576.5063	0.7700	21.1202	576.6108	200.0000
585.3780	576.3928	0.7800	20.9968	576.4963	200.0000

555.2073	574.2206	0.7700	20.8721	574.3220	200.0000
555.0413	574.1662	0.8000	20.7515	574.2700	200.0000
554.8770	574.0574	0.8100	20.6318	574.1584	200.0000
554.7141	573.9480	0.8200	20.5118	574.0479	200.0000
554.5530	573.8394	0.8300	20.3926	573.9382	200.0000
554.3933	573.7319	0.8400	20.2747	573.8298	200.0000
554.2351	573.6255	0.8500	20.1581	573.7224	200.0000
554.0786	573.5200	0.8600	20.0428	573.6162	200.0000
553.9236	573.4155	0.8700	19.9289	573.5107	200.0000
553.7700	573.3122	0.8800	19.8163	573.4063	200.0000
553.6179	573.2100	0.8900	19.7046	573.3032	200.0000
553.4673	573.1086	0.9000	19.6190	573.2009	200.0000
553.3181	573.0083	0.9100	19.5081	573.0996	200.0000
553.1704	572.9089	0.9200	19.3996	572.9995	200.0000
553.0240	572.8105	0.9300	19.2922	572.9001	200.0000

552.8789	574.7131	0.9400	19.1620	574.4018	200.0000
552.7324	574.6167	0.9500	19.0900	574.7046	200.0000
552.5930	574.5212	0.9600	18.9652	574.6342	200.0000
552.4521	574.4268	0.9700	18.8246	574.5127	200.0000
552.3125	574.3330	0.9800	18.7010	574.4182	200.0000
552.1741	574.2405	0.9900	18.4636	574.3247	200.0000
552.0371	574.1484	1.0000	18.3173	574.2324	200.0000
551.9014	574.0576	1.0100	18.2021	574.1404	200.0000
551.7668	573.9678	1.0200	18.4679	574.0496	200.0000
551.6335	573.8784	1.0300	18.3140	573.9595	200.0000
551.5015	573.7900	1.0400	18.2228	573.8706	200.0000
551.3706	573.7024	1.0500	18.1216	573.7822	200.0000
551.2410	573.6160	1.0600	18.0418	573.6948	200.0000
551.1125	573.5300	1.0700	17.9527	573.5084	200.0000
550.9854	573.4451	1.0800	17.8246	573.5225	200.0000

550.8594	573.3668	1.0900	17.7772	573.4375	200.0000
550.7346	573.2773	1.1000	17.6918	573.3535	200.0000
550.6108	573.1940	1.1100	17.6067	573.2700	200.0000
550.4883	573.1130	1.1200	17.5226	573.1879	200.0000
550.3667	573.0320	1.1300	17.4394	573.1057	200.0000
550.2463	572.9517	1.1400	17.3571	573.0249	200.0000
550.1272	572.8721	1.1500	17.2758	572.9446	200.0000
550.0090	572.7932	1.1600	17.1953	572.8650	200.0000
549.8918	572.7151	1.1700	17.1157	572.7861	200.0000
549.7759	572.6377	1.1800	17.0369	572.7083	200.0000
549.6609	572.5613	1.1900	16.9592	572.6309	200.0000
549.5468	572.4854	1.2000	16.8821	572.5544	200.0000
549.4338	572.4102	1.2100	16.8059	572.4785	200.0000
549.3220	572.3354	1.2200	16.7306	572.4036	200.0000
549.2112	572.2617	1.2300	16.6561	572.3289	200.0000

549.1013	572.1067	1.2400	16.5824	572.2251	200.0000
548.9924	572.1162	1.2500	16.5056	572.1924	200.0000
548.8645	572.0447	1.2600	16.4375	572.1099	200.0000
548.7776	571.9734	1.2700	16.3662	572.0383	200.0000
548.6716	571.9031	1.2800	16.2987	571.9670	200.0000
548.5464	571.8323	1.2900	16.2256	571.9967	200.0000
548.4022	571.7639	1.3000	16.1567	571.8271	200.0000
548.3389	571.6956	1.3100	16.0884	571.7570	200.0000
548.2566	571.6274	1.3200	16.0102	571.6891	200.0000
548.1550	571.5463	1.3300	15.9536	571.6213	200.0000
548.0344	571.4934	1.3400	15.8877	571.5544	200.0000
547.9548	571.4278	1.3500	15.8222	571.4878	200.0000
547.8360	571.3618	1.3600	15.7578	571.4216	200.0000
547.7581	571.2971	1.3700	15.6934	571.3560	200.0000
547.6409	571.2327	1.3800	15.6310	571.2915	200.0000

547.5647	571.1689	1.3900	15.5673	571.1171	200.0000
547.4652	571.1087	1.4060	15.5052	571.1033	200.0000
547.3748	571.0422	1.4100	15.4436	571.1001	200.0000
547.2810	570.9810	1.4200	15.3630	571.0376	200.0000
547.1880	570.9194	1.4300	15.3128	570.9783	200.0000
547.0959	570.8584	1.4400	15.2633	570.9141	200.0000
547.0046	570.7981	1.4500	15.2044	570.8539	200.0000
546.9141	570.7383	1.4600	15.1461	570.7927	200.0000
546.8242	570.6787	1.4700	15.0884	570.7329	200.0000
546.7354	570.6199	1.4800	15.0313	570.6733	200.0000
546.6472	570.5615	1.4900	14.9746	570.6147	200.0000
546.5598	570.5039	1.5000	14.9191	570.5564	200.0000

TOTAL HEAT REQUIRED TO BE SUPPLIED DURING FIRST HOUR OF CRUDE INJECTION= 3618.3840BTU

STATEMENTS EXECUTED= 7644

CORE USAGE OBJECT CODE= 14760 BYTES.ARRAY AREA= 25624 BYTES.TOTAL AREA AVAILABLE= 112240 BYTES

DIAGNOSTICS NUMBER OF ERRORS= 0. NUMBER OF WARNINGS= 0. NUMBER OF EXTENSIONS= 0

APPENDIX C

SYMBOLS USED IN THE HEAT TRANSFER SIMULATION COMPUTER PROGRAM

SYMBOLS USED IN THE HEAT TRANSFER SIMULATION COMPUTER PROGRAM

DELTP - Change in Pipe temperature.

DELTT - Change in tube temperature.

TPIPE - Current pipe temperature in ^{o}R.

TTUBE - Current tube temperature in ^{o}R.

DELTME - Increment of time in hours.

Hc - Heat transfer coefficient outside the pipe.

GRAR - Grashof number.

UN - Nusselt number outside the pipe.

QLOST - Heat lost from the tube.

PR - Prandtl number.

VOLTBE - Volume of the tube.

MASSA - Mass of air.

AOT - Area of tube.

QLSTOT - Total heat loss (current).

QLOSA - Heat lost to the air.

TOTLOS - Total heat loss (summation).

QSUPLY - Heat supplied.

HCAR - Convective heat transfer coefficient of air.

RHOST - Density of Steel.

RHOG - Density of air.

RHOS - Density of core.

SPHST - Specific heat of steel.

SPHS - Specific heat of core.

SPHG - Specific heat of gas.

KSTEEL - Thermal conductivity of steel.

KGAS - Thermal conductivity of gas.

KSAND - Thermal conductivity of core.

ALFST - Thermal diffusivity coefficient of steel.

ALFSND - Thermal diffusivity coefficient of air.

DOP - Outside diameter of pipe.

DIP - Inside diameter of pipe.

DOT - Outside diameter of tube.

DIT - Inside diameter of tube.

QCFM - Air flow in cubic feet per minute.

QLOST Heat loss from tube to pipe.

AF,AFLAME - Surface area of flame front.

REYNO - Reynold's number.

NUSSLT - Nusselt number.

QDOTRT - Heat loss/gain from tube by radiation.

QDOTRP - Heat loss/gain from pipe by radiation.

DTDX - Temperature gradient over the length of tube.

NOPT - Control variable for using convective or radiative heat transfer depending on the heater type.

HITCAP - Total heat capacity of the recommended heater.

QCFM - Rate of air blown by the heater in cfm.

NUAIR - Kinematic viscosity of air in Sq. ft./sec.

VAIR - Velocity of air in FT./Sec.

HCAR - Convective heat transfer coefficient of air.

TRAIR - Temperature of air at radius "Rpipe" in Deg. R.

TAIR - Temperature of air at the cen. of pipe in OR.

APPENDIX D.

CALIBRATION OF THE REFRACTOMETER

CALIBRATION OF THE REFRACTOMETER

In order to clean the model by using a miscible displacement it was necessary to prepare a refractometric curve with the purpose of obtaining the fraction composition from the mixture of naphtha - crude oil at different times in the displacement process.

From an optical point of view, two different types of naphtha were used in the cleaning process. For the first one, naphtha-1, 11 refractive indices were obtained. The results of the calibration are presented in figure D1.

For naphtha-2, a total of four samples were analyzed. The resultsof calibration are presented in figure D2.

An "ABBE" refractometer available at Oklahoma University was used in this experiment.

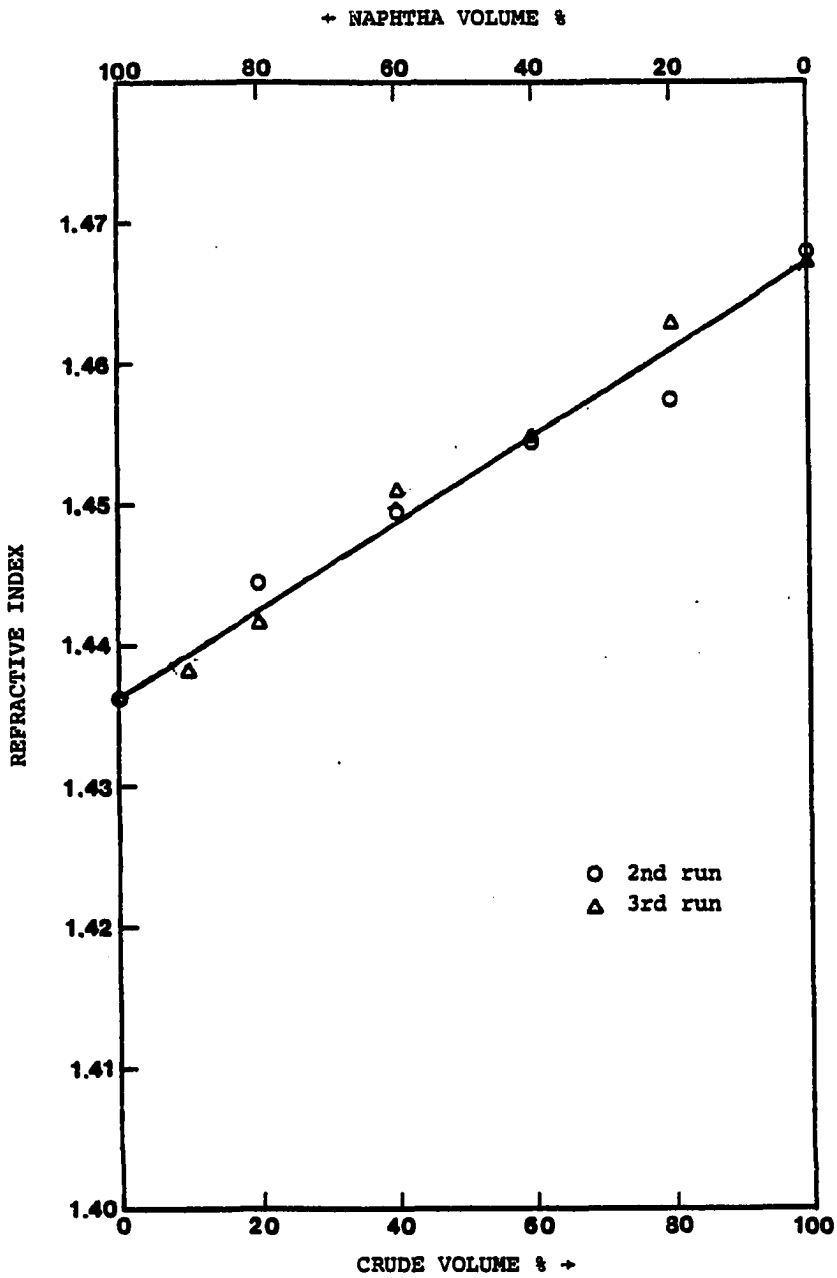

Figure D1: Refractometric Curve for Naptha 1-Crude

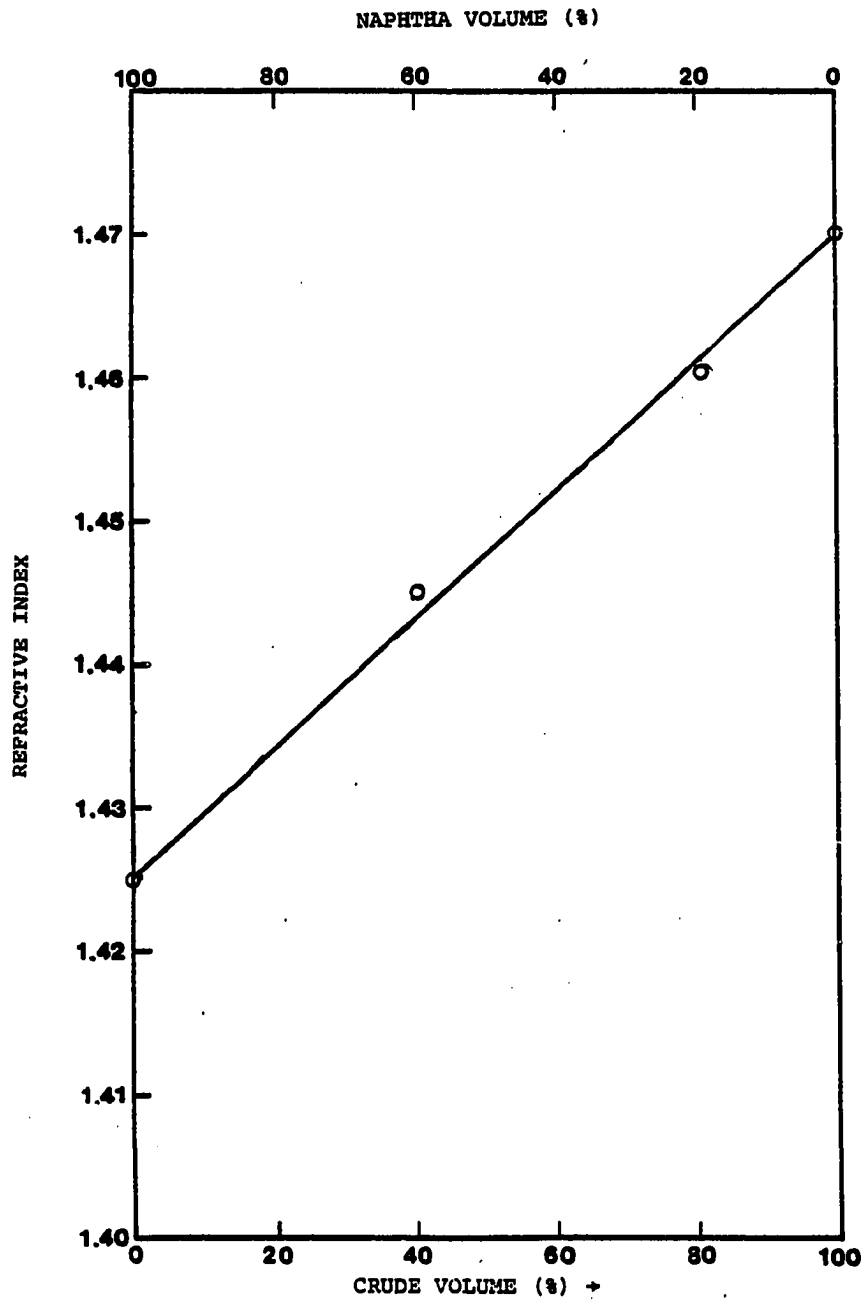

Figure D2: Refractometric Curve for Naphtha 2 - Crude

APPENDIX E

DETERMINATION OF ABSOLUTE PERMEABILITY OF THE RESERVOIR PHYSICAL MODEL

DETERMINATION OF ABSOLUTE PERMEABILITY OF THE RESERVOIR PHYSICAL MODEL

PERMEABILITY MEASUREMENTS

The absolute permeability of the pore medium of the reservoir physical model was determined from flow test data. Nitrogen was displaced at different rates through the model. Each reading was taken after steady conditions were obtained for each pressure and flow. The average time for each reading was 24 hours. Table E1 shows the results obtained by displacing N_2.

N_2 was used as the flowing fluid for the following reasons:

a) Steady state flow is quickly obtained, which allows rapid determination in a long core;

b) Nitrogen does not alter the mineral constituents of the rock; and,

c) 100% saturation to the flowing fluid is easily obtained.

Specific instructions for permeability measurements may be found in the API Code no. 27. The pressure differential was measured by suitable manometer. The flow volume was obtained with a high precision gas meter.

Nitrogen permeability is calculated from a suitable form of Darcy's equation.

For linear fluid flow:

$$k = \frac{2q_2\mu L P_2}{A(P_1^2 - P_2^2)} \quad \text{or} \quad k = \frac{q_m \mu L}{A \Delta P} \quad \ldots.(1)$$

Where:

k = permeability, Darcy's

q_2 = flow rate at exit conditions, cc/sec

q_m = flow rate at mean conditions, $\frac{P_1 + P_2}{2}$, cc/sec

μ = gas viscosity at test temperature, cp.

L = sample length, cm

A = Core area, cm^2

P = pressure differential across sample, atm

P_1 = inlet pressure, atm (absolute)

P_2 = exit pressure, atm (absolute)

Based on this equation a computer program to calculate apparent absolute permeability was obtained. The listing of the program and result are given above in this appendix.

DISCUSSION

In order to obtain the absolute permeability of a rock from gas flow tests, it is necessary that an anomaly caused by the nature of a gas be accounted for. This was recognized by Klinkenberg and is known as the Klinkenberg effect or connection. This principle states that permea-

bility to gas is a function of the mean free path of the molecules, and therefore dependent on the mean pressure at which the test is performed. This is expressed by equation:

$$k_a = k_L \left(1 + \frac{b}{\bar{P}}\right) \quad \ldots\ldots\ldots\ldots\ldots (2)$$

Where:

k_a = apparent absolute permeability (measure at pressure P)

k_L = true absolute permeability of the core or equivalent liquid permeability.

b = a constant dependent on pore size which increases in value as pore size decreases.

$\bar{P}$ = mean pressure

In equation (2) when:

$$\bar{P} \rightarrow \infty \qquad \frac{k_L b}{P} \rightarrow 0$$

Then:

$$k_a \rightarrow k_L$$

Figure E1 shows the plotting of equation (2). The resultant absolute permeability was 910 md.

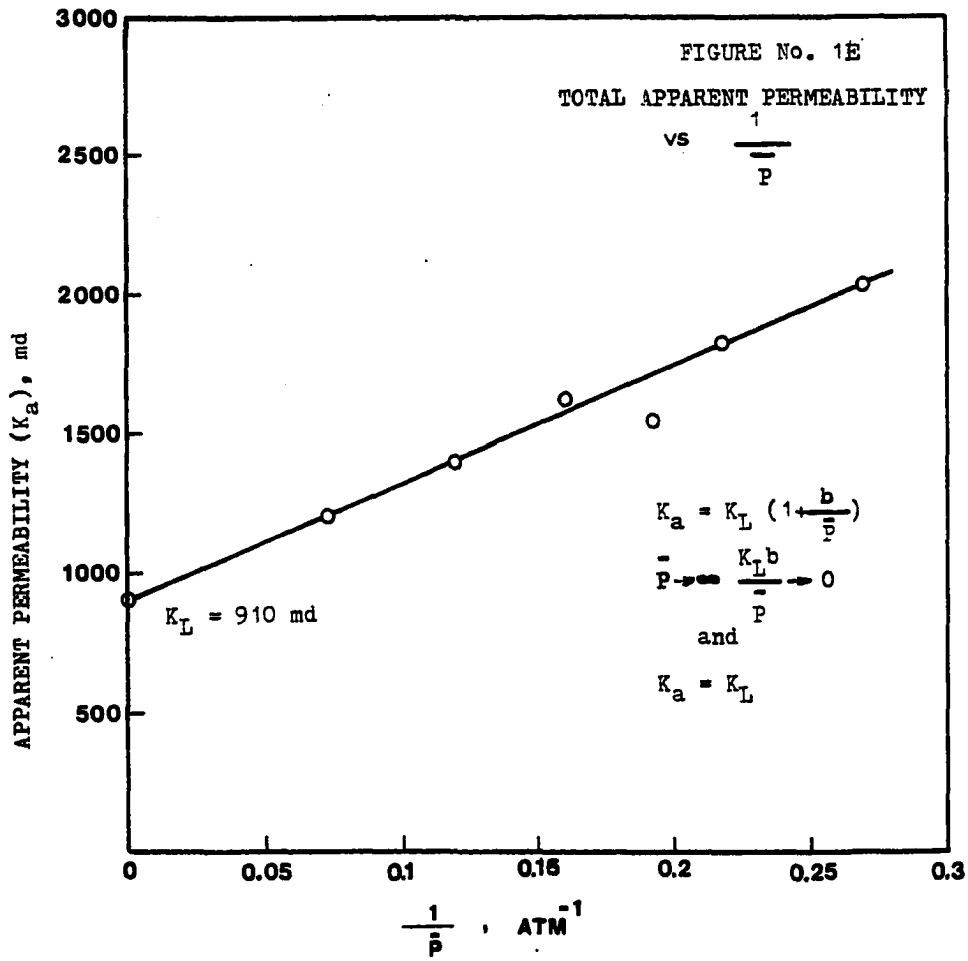
FIGURE No. 1E
TOTAL APPARENT PERMEABILITY
vs $\frac{1}{\bar{P}}$
$K_a = K_L (1 + \frac{b}{\bar{P}})$
$\bar{P} \to \infty \quad \frac{K_L b}{\bar{P}} \to 0$
and
$K_a = K_L$
K_L = 910 md
APPARENT PERMEABILITY (K_a), md
3000
2500
2000
1500
1000
500
0
0.05
0.1
0.15
0.2
0.25
0.3
$\frac{1}{\bar{P}}$, ATM^{-1}

```
$JOB
      REAL EP1,EP2,P3,EPBAR,EPPBAR,K,KK,G2
      DIMENSION EP1(100),EP2(100),Q2(100),EK(100),EKK(100),DELTP(100),
     1EPBAR(100),EPPBAR(100)
      READ(5,100) NJ,EL,ATUBE
100   FORMAT(I4,7F8.0)
      DO 10 J=1,NJ
      READ(5,200) EP1(J),EP2(J),Q2(J)
200   FORMAT(10F8.0)
10    CONTINUE
      VISGAS = 0.0182
      DO 20 M=1,NJ
      EK(M)=2.*Q2(M)*VISGAS*EL*EP2(M)/(ATUBE*(EP1(M)**2.0-EP2(M)**2.0
     1))
      EKK(M)=EK(M)*1000.0
      DELTP(M) = EP1(M)-1.0
      EPBAR(M)  = EP2(M)+DELTP(M)/2.0
      EPPBAR(M) = 1/EPBAR(M)
20    CONTINUE
      WRITE(6,500)
500   FORMAT(1H1,6X,'PERMEABILITY',6X,'1/PBAR',6X,'FLOW RATE',6X,
     1'BAR. PRESSURE',4X,'INLET PRESSURE',/)
      WRITE(6,600)
600   FORMAT(10X,'MIL. DARCY',7X,'1/ATM',10X,'CC/SEC',12X,'ATM',
     112X,'ATM',//)
      DO 30 JM=1,NJ
      WRITE(6,700) EKK(JM),EPPBAR(JM),Q2(JM),EP2(JM),EP1(JM)
700   FORMAT(6X,F9.3,2X,F10.4,4X,F10.4,6X,F10.4,6X,F10.4,//)
30   CONTINUE
      STOP
      END

$EXEC
```

TABLE E1

Nitrogen Displacements to Obtain Absolute Permeability Data.

Nitrogen Viscosity = 0.0182 Cp.

Core Length = 3810 CM

Area = 1.0261 Cm^2

Standard pressure: 29.08" Hg.

Temperature: 70° F.

cc/sec	P_1 (PSIg)	P_2 (atm) Hg
363.65	382.77	29.08"
156.84	224.1	29.08"
97.02	164.6	29.08"
60.00	135.70	29.08"
47.50	111.42	29.08"
37.61	91.89	29.08"

APPENDIX F

CALCULATION OF EQUILIBRIUM RATIO (K) DATA BY THE METHOD OF CONVERGENCE PRESSURE (Pk)

CALCULATION OF EQUILIBRIUM RATIO (K) DATA BY THE METHOD OF CONVERGENCE PRESSURE (Pk)

The equilibrium ratio k of each component in a system is a function of the system pressure, temperature and composition. One way to represent the parameter composition in a system is using the concept of convergence pressure. The convergence pressure is, in general, the critical pressure of a system at a given temperature. At a specific temperature all the k-values of all the components of the system converge to unit when the system pressure reaches the convergence pressure, Pk.

If K-values are obtained by using the convergence pressure method, the liquid composition Xi of the system can be calculated from the vapor composition Yi measured experimentally in the laboratory by means of the gas chromatograph. The method to obtain convergence pressure, Pk, used in this work was proposed by The Gas Processors-Suppliers Association (22). This method has the following steps:

Step 1: Assume a convergence pressure.

Step 2: Obtain K-values from appropriate charts based on convergence pressure, temperature and pressure of the system.

Step 3: Calculate the liquid composition Xi by using the equation $K_i = Yi/X_i$. The vapor composition Yi is known.

Step 4: Identify the lightest hydrocarbon component. In this case it is Nitrogen (N_2) and make the calculation in Step 5 omitting this lightest component.

Step 5: "Calculate the weight average critical temperature and critical pressure for the remaining heavier components to form a pseudo binary system."

Step 6: Using values obtained in Step 5, locate the critical point of the system in figure 18-5 of reference . Make an approximation by drawing the critical locus of the binary system consisting of the light component (N_2) and pseudo-heavy component.

Step 7: Read the convergence pressure (ordinate) at the temperature (abscisa) of the system.

Step 8: Compare the convergence pressure read in Step 7 with convergence pressure assumed in Step 1. If they check within an acceptable tolerance, the calculated liquid composition Xi is correct. Otherwise, the procedure has to be repeated until $P_{k_{assume}} \simeq P_{k_{calculated}}$.

In order to use this method, the computer program "CALC" was written. The computer program calculates the liquid composition Xi, weight average temperature, tc, and weight average pressure, Pc. The remaining steps 6, 7 and 8

are made by hand. A listing of the computer program "CALC" is given in this appendix. Also, samples of K-values obtained by using the method described here is presented in tables F1 to F9.

In order to compare results with previous researcher the K-values for heaviest fraction were estimated by using the method presented by Clark (15).

```
$JOB
      CHARACTER*2 A(9)
      DIMENSION X(9),R(9),TC(9),PC(9),CK(9),B(9),Y(9),XM(9),TCXM(9),
     *PCXM(9)
      DATA (Y(I),I=1,9)/.875,.061,.021,.023,.0035,.0045,.0015,.0015,.085
     */
      DATA (CK(I),I=2,9)/1.65,.8,.74,.47,.44,.22,.18,.118/
      DATA (B(I),I=1,9)/552.05,808.,1415.,1792.,2045.,2129.,2375.,2473.,
     *4428./
      DATA (R(I),I=1,9)/28.016,16.068,30.068,44.096,58.12,58.12,72.124,
     *72.124,214.5/
      DATA(TC(I),I=1,9)/227.,344.,550.,666.,733.,766.,830.,847.,1270./
      DATA (PC(I),I=1,9)/492.,673.,709.,618.,530.,551.,462.,485.,255./
      READ(5,17)(A(I),I=1,9)
   17 FORMAT(9A2)
      ACC1= 0.
      ACC2= 0.
      ACC3= 0.
      DO 25 I=2,9
      X(I)=Y(I)/ CK(I)
      XM(I)=X(I)*R(I)
      TCXM(I)= TC(I)*XM(I)
      PCXM(I)=PC(I)*XM(I)
   25 CONTINUE
      WRITE(6,95)
      WRITE(6,30)A(1),R(1),B(1),TC(1),PC(1),Y(1)
      DO 45 I=2,9
      WRITE(6,27) A(I),R(I),B(I),TC(I),PC(I),Y(I),CK(I),X(I),XM(I),
     *TCXM(I),PCXM(I)
   45 CONTINUE
      DO 35 I=2,9
      ACC1 =ACC1 + XM(I)
      ACC2= ACC2 + TCXM(I)
      ACC3= ACC3 + PCXM(I)
   35 CONTINUE
      WTC=ACC2/ACC1
      WPC=ACC3/ACC1
      WRITE(6,29) ACC1,ACC2,ACC3,WTC,WPC
      WRITE(6,95)
      STOP
   27 FORMAT(8X,A2,F8.3,F8.2,2F5.0,F6.3,3F7.3,2F10.3//)
   30 FORMAT(8X,A2,F8.3,F8.2,2F5.0,F6.3//)
   29 FORMAT(51X,3F11.3//62X,2F9.3)
   95 FORMAT('1'////////////////)
      END

$EXEC
```

TABLE F1

CALCULATION OF EQUILIBRIUM RATIO (K) DATA

Sampling Point A
Pk= 7500 psi
Experiment # 2 Cum N2 Inj. = .15 p.v.

Comp.	MWi.	b	Tc	Pc	Yi	Ki	Xi	xiMWi	TcXiMWi	PcXiMWi
N2	28.016	552.05	227.	492.	0.523	-	0.153	-	-	-
C1	16.068	808.00	344.	673.	0.301	1.340	0.225	3.609	1241.600	2429.060
C2	30.068	1415.00	550.	709.	0.061	0.810	0.075	2.264	1245.408	1605.444
C3	44.096	1792.00	666.	618.	0.035	0.620	0.056	2.489	1657.866	1538.381
C4	58.120	2045.00	733.	530.	0.022	0.520	0.042	2.459	1802.390	1303.229
C4	58.120	2129.00	766.	551.	0.023	0.440	0.052	3.038	2327.177	1673.987
C5	72.124	2375.00	830.	462.	0.006	0.360	0.017	1.202	997.715	555.354
C5	72.124	2473.00	847.	485.	0.010	0.300	0.035	2.524	2138.115	1224.304
C6	214.500	4428.00	1270.	255.	0.019	0.055	0.345	74.100	94106.930	18895.490
								91.686	105517.100	29225.240
									1150.849	318.752

TABLE F 2

CALCULATION OF EQUILIBRIUM RATIO (K) DATA

Sampling Point A

Pk= 7500 psi

Experiment # 2

Cum. N2 Inj. = .17 p.v.

Comp.	MWi	b	Tc	Pc	Yi	Ki	Xi	XiMWi	Tc XiMWi	PcXiMWi
N2	28.016	552.05	227.	492.	0.719	-	0.139	-	-	-
C1	16.068	808.00	344.	673.	0.181	1.700	0.106	1.711	588.504	1151.347
C2	30.068	1415.00	550.	709.	0.042	0.800	0.052	1.579	868.213	1119.206
C3	44.096	1792.00	666.	618.	0.024	0.590	0.041	1.794	1194.627	1108.528
C4	58.120	2045.00	733.	530.	0.004	0.480	0.008	0.484	355.016	256.697
C4	58.120	2129.00	766.	551.	0.012	0.400	0.030	1.744	1335.597	960.723
C5	72.124	2375.00	830.	462.	0.004	0.320	0.012	0.902	748.286	416.516
C5	72.124	2473.00	847.	485.	0.005	0.280	0.018	1.288	1090.875	624.645
C6	214.500	4428.00	1270.	255.	0.010	0.016	0.594	127.359	161746.300	32476.640
								136.860	167927.400	38114.290
									1227.003	278.491

TABLE F 3

CALCULATION OF EQUILIBRIUM RATIO (K) DATA

Sampling Point B
Pk= 5000 psi

Experiment # 2
Cum. N2 Inj. = .30 p.v.

Comp.	MWi	b	Tc	Pc	Yi	Ki	Xi	XiMWi	TcXiMWi	PcXiMWi
N2	28.016	552.05	227.	492.	0.332	-	0.121	-	-	-
C1	16.068	808.00	344.	673.	0.451	1.610	0.280	4.501	1548.355	3029.196
C2	30.068	1415.00	550.	709.	0.081	0.840	0.096	2.899	1594.676	2055.682
C3	44.096	1792.00	666.	618.	0.061	0.580	0.105	4.638	3088.695	2866.087
C4	58.120	2045.00	733.	530.	0.012	0.430	0.028	1.622	1188.891	859.635
C4	58.120	2129.00	766.	551.	0.014	0.390	0.036	2.086	1598.150	1149.583
C5	72.124	2375.00	830.	462.	0.006	0.270	0.022	1.603	1330.287	740.473
C5	72.124	2473.00	847.	485.	0.005	0.250	0.020	1.442	1221.780	699.602
C6	214.500	4428.00	1270.	255.	0.038	0.130	0.292	62.700	79628.930	15988.490
								81.492	91199.750	27388.740
									1119.130	336.093

TABLE F 4

CALCULATION OF EQUILIBRIUM RATIO (K) DATA

Sampling Point C — Cum. N2 Inj. = .55 p.v.

Pk= 5000 psi — Experiment # 2

Comp.	MWi	b	Tc	Pc	Yi	Ki	Xi	XiMWi	TcXiMWi	PcXiMWi
N2	28.016	552.05	227.	492.	0.270	-	0.106	-	-	-
C1	16.068	808.00	344.	673.	0.402	1.650	0.244	3.915	1346.673	2634.625
C2	30.068	1415.00	550.	709.	0.134	0.800	0.167	5.036	2770.013	3570.799
C3	44.096	1792.00	666.	618.	0.095	0.720	0.132	5.818	3874.936	3595.661
C4	58.120	2045.00	733.	530.	0.016	0.380	0.042	2.447	1793.766	1296.993
C4	58.120	2129.00	766.	551.	0.016	0.330	0.048	2.818	2158.541	1552.684
C5	72.124	2375.00	830.	462.	0.008	0.215	0.037	2.684	2227.457	1239.862
C5	72.124	2473.00	847.	485.	0.009	0.180	0.050	3.606	3054.450	1749.006
C6	214.500	4428.00	1270.	255.	0.051	0.293	0.174	37.336	47416.920	9520.719
								63.660	64642.750	25160.330
									1015.430	395.227

TABLE F 5

CALCULATION OF EQUILIBRIUM RATIO(K) DATA

Sampling Point C

Pk= 6000 psi

Experiment # 2

Cum N2 Inj.= .65 p.v.

Comp.	MWi	b	Tc	Pc	Yi	Ki	Xi	XiMWi	TcXiMWi	PcXiMWi
N2	28.016	552.05	227.	492.	0.530	-	0.173	-	-	-
C1	16.068	808.00	344.	673.	0.272	1.650	0.165	2.649	911.182	1782.632
C2	30.068	1415.00	550.	709.	0.060	0.790	0.076	2.284	1256.003	1619.103
C3	44.096	1792.00	666.	618.	0.060	0.660	0.091	4.009	2669.811	2477.392
C4	58.120	2045.00	733.	530.	0.011	0.348	0.032	1.637	1346.613	973.677
C4	58.120	2129.00	766.	551.	0.012	0.300	0.040	2.325	1780.796	1280.964
C5	72.124	2375.00	830.	462.	0.005	0.200	0.025	1.803	1496.572	833.031
C5	72.124	2473.00	847.	485.	0.008	0.170	0.047	3.394	2874.777	1646.124
C6	214.500	4428.00	1270.	255.	0.042	0.120	0.351	75.326	95664.060	19208.140
								93.626	107999.700	29821.060
									1153.519	318.511

TABLE F 6

CALCULATION OF EQUILIBRIUM RATIO (K) DATA

Sampling Point C
Pk= 7000 psi

Experiment # 2
Cum. N2 Inj. = .72 p.v.

Comp.	MWi	b	Tc	Pc	Yi	Ki	Xi	XiMWi	TcXiMWi	PcXiMWi
N2	28.016	552.05	227.	492.	0.809	-	0.232	-	-	-
C1	16.068	808.00	344.	673.	0.114	1.700	0.067	1.078	370.660	725.158
C2	30.068	1415.00	550.	709.	0.010	0.780	0.013	0.385	212.018	273.310
C3	44.096	1792.00	666.	618.	0.045	0.600	0.075	3.307	2202.594	2043.849
C4	58.120	2045.00	733.	530.	0.002	0.340	0.006	0.342	250.600	181.198
C4	58.120	2129.00	766.	551.	0.002	0.280	0.007	0.415	317.999	228.744
C5	72.124	2375.00	830.	462.	0.000	0.190	0.000	0.000	0.000	0.000
C5	72.124	2473.00	847.	485.	0.000	0.160	0.000	0.000	0.000	0.000
C6	214.500	4428.00	1270.	255.	0.018	0.030	0.600	128.700	163448.900	32818.480
								134.227	166802.700	36270.740
									1242.690	270.219

TABLE F 7

CALCULATION OF EQUILIBRIUM RATIO (K) DATA

Sampling Point D

Pk= 4000 psi

Experiment # 2
Cum. N2 Inj. = .90 p.v.

Comp	MWi	b	Tc	Pc	Yi	Ki	Xi	XiMWi	TcXiMWi	PcXiMWi
N2	28.016	552.05	227.	492.	0.875	-	0.154	-	-	-
C1	16.068	808.00	344.	673.	0.061	1.650	0.037	0.594	204.346	399.781
C2	30.068	1415.00	550.	709.	0.021	0.800	0.026	0.789	434.106	559.603
C3	44.096	1792.00	666.	618.	0.023	0.740	0.031	1.371	912.786	847.000
C4	58.120	2045.00	733.	530.	0.004	0.470	0.007	0.433	317.248	229.388
C4	58.120	2129.00	766.	551.	0.005	0.440	0.010	0.594	455.317	327.519
C5	72.124	2375.00	830.	462.	0.002	0.220	0.007	0.492	408.156	227.190
C5	72.124	2473.00	847.	485.	0.002	0.180	0.008	0.601	509.075	291.501
C6	214.500	4428.00	1270.	255.	0.085	0.118	0.720	154.513	196231.000	39400.730
								159.387	199472.000	42282.710
									1251.499	265.284

TABLE F 8

CALCULATION OF EQUILIBRIUM RATIO (K) DATA

Sampling Point B — Cum.N2 Inj. = .42 p.v.

Pk= 6000 psi — Experiment # 4

Comp.	MWi	b	Tc	Pc	Yi	Ki	Xi	XiMWi	TcXiMWi	PcXiMWi
N2	28.016	552.05	227.	492.	0.645	-	0.442	-	-	-
C1	16.068	808.00	344.	673.	0.200	1.850	0.108	1.737	597.555	1169.054
C2	30.068	1415.00	550.	709.	0.062	0.820	0.076	2.273	1250.388	1611.864
C3	44.096	1792.00	666.	618.	0.031	0.580	0.053	2.357	1569.665	1456.536
C4	58.120	2045.00	733.	530.	0.008	0.410	0.021	1.205	883.210	638.610
C4	58.120	2129.00	766.	551.	0.002	0.370	0.004	0.236	180.486	129.827
C5	72.124	2375.00	830.	462.	0.008	0.260	0.031	2.219	1841.936	1025.270
C5	72.124	2473.00	847.	465.	0.006	0.240	0.025	1.803	1527.225	874.503
C6	214.500	4428.00	1270.	255.	0.032	0.134	0.240	51.377	65249.090	13101.190
								63.207	73059.500	20006.850
									1156.501	316.527

TABLE F 9

CALCULATION OF EQUILIBRIUM RATIO (K) DATA

Sampling Point C — Experiment # 4

Pk= 7000 psi — Cum.N2 Inj. = .70 p.v.

Comp.	MWi	b	Tc	Pc	Yi	Ki	Xi	XiMWi	TcXiMWi	PcXiMWi
N2	28.016	552.05	227.	492.	0.805	-	0.631	-	-	-
C1	16.068	808.00	344.	673.	0.135	1.700	0.079	1.276	438.939	858.739
C2	30.068	1415.00	550.	709.	0.030	0.780	0.038	1.156	636.053	819.931
C3	44.096	1792.00	666.	618.	0.010	0.600	0.017	0.735	489.465	454.188
C4	58.120	2045.00	733.	530.	0.001	0.340	0.003	0.171	125.300	90.599
C4	58.120	2129.00	766.	551.	0.000	0.280	0.000	0.000	0.000	0.000
C5	72.124	2375.00	830.	462.	0.000	0.190	0.000	0.000	0.000	0.000
C5	72.124	2473.00	847.	485.	0.000	0.160	0.000	0.000	0.000	0.000
C6	214.500	4428.00	1270.	255.	0.019	0.082	0.232	49.701	63120.520	12673.800
								53.040	64810.270	14897.250
									1221.924	280.871

APPENDIX G

ENRICHMENT PROCESS AND MISCIBILITY GENERATION WHEN NITROGEN IS INJECTED AT HIGH PRESSURE IN A LIGHT CRUDE OIL RESERVOIR

ENRICHMENT PROCESS AND MISCIBILITY GENERATION WHEN NITROGEN IS INJECTED AT HIGH PRESSURE IN A LIGHT CRUDE OIL RESERVOIR

Many researchers (1,36,47,51 and 52) have investigated the process of achieving miscibility of nitrogen with hydrocarbons with a high content of intermediate components (C_2-C_6) during multiple contact under high pressure N_2 injection. They have confirmed the applicability of the nitrogen injection in enhanced oil recovery processes.

The accepted general idea is that the composition of the injected gas is not critical for reaching miscibility for a particular reservoir fluid. The miscibility mainly depends on the reservoir fluid composition, especially the concentration of intermediate fraction in the crude oil. Injected gas basically is the agent by which intermediates can create a miscible displacement.

The high pressure nitrogen-oil system phase relation during multiple contact of gas and oil to reach miscibility is illustrated by a ternary diagram, shown in Figure G-1. The process can be explained step by step as follows: When N_2 is injected into the oil reservoir, the hydrocarbon component and N_2 establish an equilibrium point R1. This equilibrium point

represents two phases (liquid and vapor). The gas composition at R1 is G1 and the liquid composition is L1. Because of the high mobility of the gas phase, this moves ahead to contact new oil and again equilibrium is reached at point R2. This process repeats itself until the critical point C is reached. At the critical point differentiation of phases is impossible because intensive properties as viscosity and density are equals. At this point, when interfacial tension is zero then miscibility is accomplished. The injection pressure, temperature and composition of the crude oil play an important role in determining the number of steps to reach miscibility. The higher the pressure, the lower the number of steps required to reach miscibility, and the higher the content of intermediate fractions in the crude oil, the lower the number of steps required to reach miscibility. If the composition of the original crude oil at reservoir conditions fall out of the miscibility region shown in the ternary diagram (figure G-1), then the displacement process by nitrogen is basically inmiscible displacement or in other words, the miscibility is impossible by a multi-contact mechanism. On the other hand, the residual oil at a location as nitrogen continuously moves through to evaporate intermediates undergoes an inverse process. Its intermediates are stripped by vaporization and transfer to the gas phase. The process can be illustrated by using the ternary diagram shown in Figure G-2.

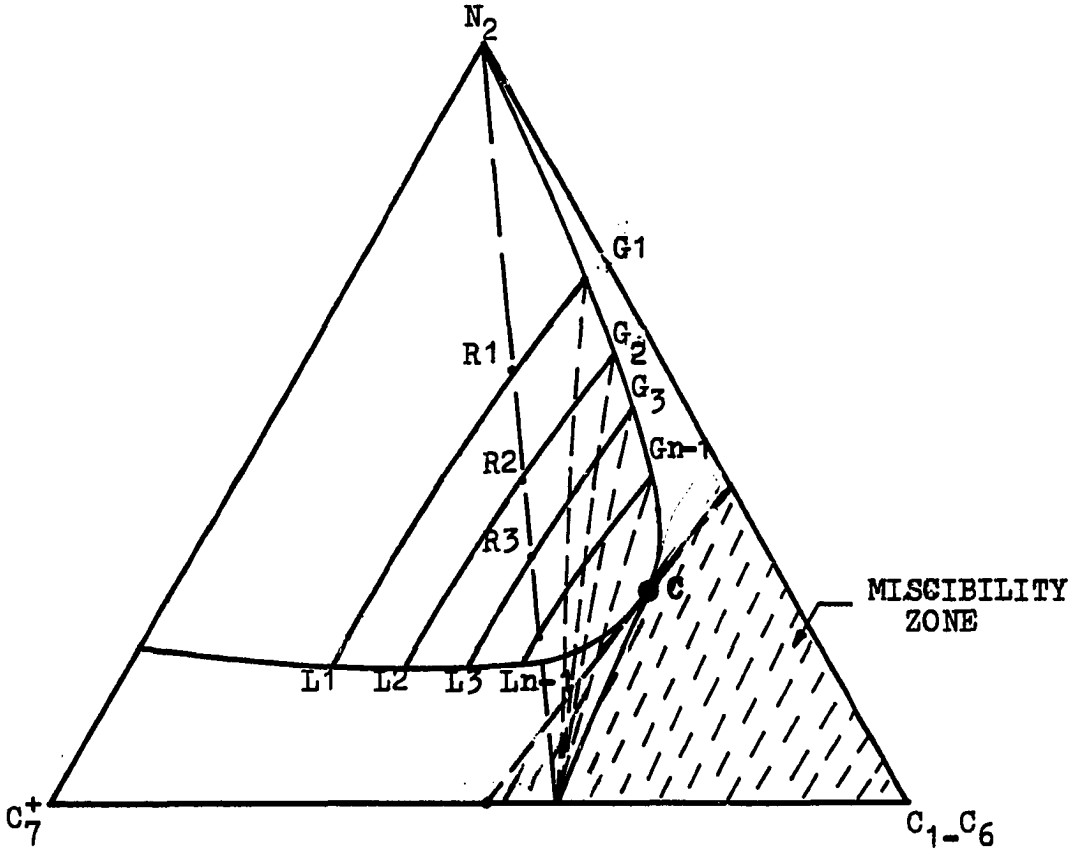

FIGURE G-1

TERNARY PHASE DIAGRAM ILLUSTRATING COMPOSITIONAL CHANGES IN A NITROGEN-MULTI-HYDROCARBONS SYSTEM AT PRESSURE "P" AND TEMPERATURE "T".

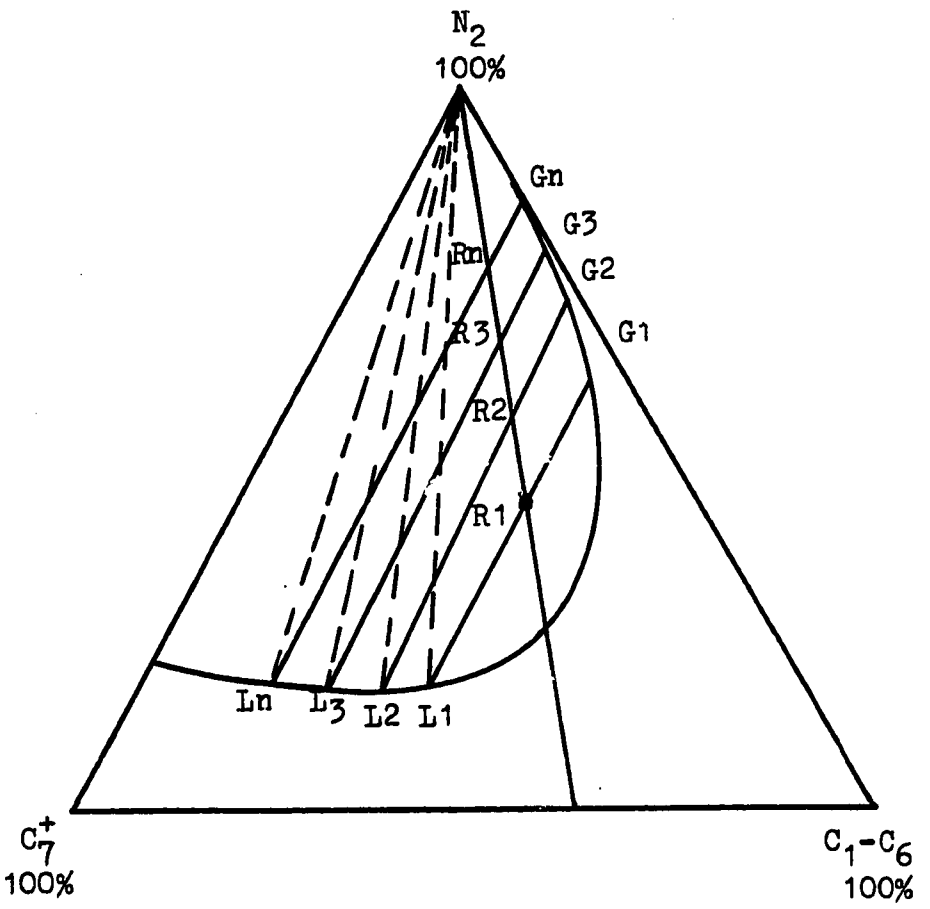

FIGURE G-2 TERNARY DIAGRAM REPRESENTING THE STRIPPING OF INTERMEDIATES BY N_2 FROM THE CRUDE OIL AT ONE LOCATION.

APPENDIX H

CORRELATIONS TO CALCULATE VAPOR AND LIQUID HYDROCARBON MIXTURE PROPERTIES AND LISTING OF THE COMPUTER PROGRAM "PROPERT"

CORRELATIONS TO CALCULATE VAPOR AND LIQUID HYDROCARBON MIXTURE PROPERTIES AND LISTING OF THE COMPUTER PROGRAM "PROPERT"

A computer program to calculate liquid and vapor hydrocarbon mixture properties by using molal composition was written specially for this study. The computer program "PROPERT" is based on correlations and equations available at the technical literature. A complete listing of the computer program "PROPERT" is presented in this appendix. Also, samples of the computer program output are given in this appendix in Tables H-1 to H-49.

The most widely used correlations to calculate viscosities, densities, molecular weight and surface tension of hydrocarbon mixtures were used to prepare the computer program "PROPERT".

The following correlations and equation were used in this study:

<u>Liquid Hydrocarbon Properties Calculations</u>

1. Density of hydrocarbon mixtures were calculated using the Standing (50) correlation.
2. Molecular weight of hydrocarbon mixtures were calculated by using the method developed by McLeod (52).

3. Viscosity of hydrocarbon mixtures were calculated by using correlation proposed by Lohrenz et al (57).

Gas Hydrocarbon Properties Calculations

1. Density of hydrocarbon mixtures were calculated by using the conventional law of corresponding states. The gas deviation factor for natural gas was correlated by using pseudo-reduced properties and the correlation by Brown el at (49).
2. Viscosity of hydrocarbon mixtures were obtained by using correlation proposed by Herning and Zipperer (35) at atmospheric pressure and the temperature of interest. The correlation by Carr et al (11) were used to obtain viscosity at desired pressure.
3. The molecular weight of the hydrocarbon mixtures were calculated from molecular weights of individual components in the mixture (MW_i) and vapor molal composition (Yi).

Surface Tension

The surface tension between liquid and vapor during high-pressure nitrogen displacements were estimated by the method proposed by Katz et al (53). The method is based on the parachor and equation proposed by Sugdeon (54).

All the correlations used in preparing the computer program "PROPERT" were suggested by Chowdhry (12) and used by Ahmed (1) in his work. Details of correlations are given at Tarek's work and at the references.

```
      $JOB
 1          IMPLICIT REAL (8-H,M-Z)
 2          CHARACTER*3 ACOMPS
 3          DIMENSION M(9),Y(9),X(9),ML(9),VL(9),U(9),PCC(9),PROXV(9),
           1TCC(9),BEE(9),PC(9),TC(9),TB(9),ACOMPS(9),PRONY(9),SIGMAK(9)
 4          DIMENSION PROXT(9),PROXP(9),ZAM(9),X1(9),Y1(9),X2(9),VC(9)
 5          DIMENSION UG(9),VISCG(9),VISCG1(9),VISCL(9),VISCL1(9)
 6          DIMENSION MYTC(9),PYTC(9),PROMX(9),PROMXV(9)
 7          DIMENSION XY(9),XRCM(9),YRCM(9)
 8          READ(5,99) (ACOMPS(I),I=1,9)
 9    99    FORMAT(9A3)
10          READ(5,100) Z,TABS,PABS
11   100    FORMAT(10F8.0)
12          R=10.72
13          IK=9
14          DO 10 I=1,IK
15          READ(5,100) M(I),Y(I)
16   10     CONTINUE
17          SUM=0.0
     C DENSITY OF THE VAPOR PHASE= RHOV
     C AVERAGE MOLECULAR WEIGHT = MBAR
18          DO 20 J=1,IK
19          PRONY(J)=M(J)*Y(J)
20          MBAR=PRONY(J) + SUM
21          SUM = MBAR
22   20     CONTINUE
23   11     FORMAT(//,10X,A3,4X,6F14.8)
24          RHOV = MBAR*PABS/(Z*R*TABS)
25          CALL QUID(RHOL,X,ML,VL,ACOMPS,PROMX,PROMXV,SUMXM,SUMXMV)
26          WRITE(6,200)
27   200    FORMAT(1H1,10X,'GAS DENSITY',5X,'LIQUID DENSITY',2X,/)
28          WRITE(6,201)
29   201    FORMAT(15X,'LB/CUFT.',8X,'LB/CUFT.',2X,//)
30          WRITE(6,202) RHOV,RHOL
31   202    FORMAT(10X,F12.9,8X,F12.9,4X,////)
32          CALL SURTEN(SIGMA,RHOL,RHOV,X,Y,M,ML,ACOMPS,X1,Y1)
33          SUM1=0.0
34          SUM2=0.0
35          SUM3=0.0
36          DO 21 I=1,IK
37          READ(5,100)PC(I),TC(I),TB(I)
38          COP=PC(I)
39          TOP=TC(I)
40          BEE(I)=(ALOG10(COP)-ALOG10(14.7))*(TB(I)+TC(I))/(TC(I)-TB(I))
41          PCC(I)=PC(I)
42          TCC(I)=TC(I)
43          MYTC(I)=Y(I)*TC(I)
44          PYTC(I)=Y(I)*PC(I)
45          SUM1=MYTC(I)+SUM1
46          SUM2=PYTC(I)+SUM2
47          SUM3=PRONY(I)+SUM3
48   21     CONTINUE
49          WRITE(6,571)
50   571    FORMAT(1H1,26X,'TABLE - I',//)
51          WRITE(6,561)
52   561    FORMAT(12X,'COMP.',8X,'Y(I)',7X,'M(I)',6X,'Y(I)TC(I)',
           16X,'Y(I)PC(I)',///////)
53          DO 562 IJI=1,IK
54          WRITE(6,563)ACOMPS(IJI),Y(IJI),M(IJI),PRONY(IJI),MYTC(IJI),
           1PYTC(IJI)
```

```
562     CONTINUE
563     FORMAT(12X,A3,4X,F12.8,3X,F10.3,5X,F12.4,6X,F12.4,4X,F12.6,//)
        WRITE(6,564)SUM1,SUM2,SUM3
564     FORMAT(10X,'SUMMATION Y(I)TC(I) = ',2X,F12.4,//,10X,'SUMMATION
       1PC(I)Y(I) =',2X,F12.4,//,10X,'SUMMATION Y(I)M(I) =',3X,F12.4,//)
        WRITE(6,572)
572     FORMAT(1H1,26X,'TABLE -II',//)
        WRITE(6,122)
122     FORMAT(10X,'FOLLOWING ARE THE LISTING OF COMPOSITION,
       1FRACTION X(I), ML(I), X(I)ML(I), VL(I), X(I)M(I)VL(I)',/////)
        DO 521 I=1,IK
        WRITE(6,11)ACOMPS(I),X(I),ML(I),PROMX(I),VL(I),PROMXV(I)
521     CONTINUE
        WRITE(6,573)SUMXM,SUMXMV
573     FORMAT(////,10X,'SUMMATION M(I)X(I) =',3X,F12.4,//,10X,
       1'SUMMATICN M(I)X(I)V(I) =',3X,F12.4,/)
        DATA U/0.0176,0.0108,0.0102,0.0082,0.0077,.0079,0.0065,.0067,
       13.0/
        SOM = 0.0
        SOM1 = 0.0
        DATA UG/0.0176,0.0108,0.0102,0.0082,0.0077,.0079,0.0065,.0067,
       10.005/
        DO 30 JL = 1,IK
        JIL = JL
        VISCG(JL)=Y(JL)*UG(JL)*(M(JL)**0.5)
        VISCG1(JL)=Y(JL)*(M(JL)**0.5)
        NEEM = Y(JL)*UG(JL)*(M(JL)**0.5) + SOM
        DEEN = Y(JL)*(M(JL)**0.5) + SOM1
        SOM = NEEM
        SOM1 = DEEN
30      CONTINUE
        UL = NEEM/DEEN
        WRITE(6,575)
575     FORMAT(1H1,26X,'TABLE - III',//)
        WRITE(6,129)
129     FORMAT(10X,'LISTING OF COMPOSITION, MOL. FRAC. YI,MOL. WT.,
       1YI(ROOT(MI)), UG(YI)(ROOT(MI))',//)
        WRITE(6,574)DEEN,NEEM
574     FORMAT(/,12X,'SUM UI(ROOT(MI) =',2X,F12.5,//,12X,'SUM UIYI(ROOT
       1(MI) =',2X,F12.5,//////)
        DO 522 JJK=1,IK
        WRITE(6,11)ACOMPS(JJK),Y(JJK),M(JJK),VISCG1(JJK),VISCG(JJK)
522     CONTINUE
C UL= VISCOSITY OF GAS MIXTURE AT THE ATMOSPHERIC PRESSURE IN CP
        SOM = 0.0
        SOM1 = 0.0
        II=IK-1
        DO 40 JK=1,IK
        JKL=JK
        VISCL(JK)=X(JK)*U(JK)*(ML(JK)**0.5)
        VISCL1(JK)=X(JK)*(ML(JK)**0.5)
        NOM=X(JK)*U(JK)*(ML(JK)**0.5) + SOM
        DON = X(JK)*(ML(JK)**0.5) + SOM1
        SOM = NOM
        SOM1 = DON
40      CONTINUE
        ULL = NOM/DON
        SOOM = 0.0
        DO 62 IJK=1,IK
        X2(IJK)=X(IJK)
```

```
107          X1(IJK)=X(IJK)
108          Y1(IJK)=Y(IJK)
109    62    CONTINUE
110          DATA VC/3.125,6.173,4.926,4.545,4.386,4.346,4.31,4.28,3.551/
111          DO 50 JI=1,II
112          PROXV(JI)=X2(JI)*VC(JI)
113          DENO = PROXV(JI) + SOOM
114          SOOM = DENO
115    50    CONTINUE
116          PROXV(9) = X2(9)*VC(9)
117          WRITE(6,576)
118    576   FORMAT(1H1,26X,'TABLE - IV',//)
119          WRITE(6,123)
120    123   FORMAT(10X,'FOLLOWING ARE THE LISTING OF COMPOSITION,
            1,FRACTION X, CRIT. VCL. VC. XIVC(I), XI(ROOT(MI), XU(ROOT(MI),
            1XIMI',//////)
121          DO 321 JJI=1,IK
122          WRITE(6,11)ACOMPS(JJI),X2(JJI),VC(JJI),PROXV(JJI),VISCL(JJI)
            1,VISCL1(JJI),PROMX(JJI)
123    321   CONTINUE
124          DENO = DENO + X2(9)*VC(9)
125          RHOR = RHOL/DENO
126          WRITE(6,577)DON,NON,DENO,SUMXM
127    577   FORMAT(//,9X,'SUM X(RT. M)=',2X,F12.4,/,9X,'SUM XU(RT. M)=',2X,
            1F12.6,/,9X,'SUM XI(VC(I)=',2X,F12.6,/,9X,'SUM XM=',2X,F12.6,//)
128          WRITE(6,203)
129    203   FORMAT(1H1,10X,'SURFACE TENSION',3X,
            1'VISCOSITY OF GAS MIX.',3X,'VISCOSITY OF LIQ.',3X,'REDUCED
            1DENSITY',/)
130          WRITE(6,204)
131    204   FORMAT(15X,'(SIGMA)',12X,'CP',16X,'CP',8X,//)
132          WRITE(6,205)SIGMA,UL,ULL,RHOR
133    205   FORMAT(10X,E15.7,5X,F12.4,5X,F12.4,12X,F12.4,5X,//)
134          WRITE(6,216)
135    216   FORMAT(1H1,5X,'CONST. CHAR. OF HC',6X,/)
136          WRITE(6,217)
137    217   FORMAT(8X,'(B-VALUE)',//)
138          DO 22 J=1,IK
139          WRITE(6,218)BEE(J)
140    218   FORMAT(8X,F16.8,/)
141    22    CONTINUE
       C
       C ESTIMATION OF MIXTURE VISCOSITY PARAMETER 'E'
       C
142          SUM1 = 0.0
143          SUM2 = 0.0
144          SUM3 = 0.0
145          DO 60 JJ=1,II
146          PROXT(JJ)=X(JJ)*TCC(JJ)
147          NUM1 = X(JJ)*TCC(JJ) + SUM1
148          SUM1 = NUM1
149          DEN1 = X(JJ)*M(JJ) + SUM2
150          SUM2 = DEN1
151          PROXP(JJ)=X(JJ)*PCC(JJ)
152          DEN2 = X(JJ)*PCC(JJ)+SUM3
153          SUM3 = DEN2
154    60    CONTINUE
155          A=1./6.
156          B=0.5
157          C=2.0/3.0
```

```
158            PROXT(9) = X(9)*TCC(9)
159            PROXP(9) = X(9)*PCC(9)
160            WRITE(6,583)
161    583     FORMAT(//,26X,'TABLE - VI',//)
162            WRITE(6,241)
163    241     FORMAT(10X,'FOLLOWING LISTINGS ARE COMPOSITION,CRITICAL TEMP
           1ERATURE,CRIT. PRESSURE,PRODUCT OF X*TCC AND X*PCC RESPECTIVELY'
           1,//)
164            DO 421 JIJ=1,IK
165            WRITE(6,11)ACOMPS(JIJ),TCC(JIJ),PCC(JIJ),PROXT(JIJ),PROXP(JIJ)
166    421      CONTINUE
167            NUUM1 = (NUM1+X(9)*TCC(9))**A
168            DEEN1 = (DEN1+X(9)*M(9))**B
169            DEEN2 = (DEN2+X(9)*PCC(9))**C
170            DEEN = (DEEN1)*(DEEN2)
171            E = NUUM1/DEEN
       C
       C SOLVING FOR LIQUID VISCOSITY AT PREVAILING PRESSURE AND TEMPERATURE.
       C
172            UPREV = (ABS(0.1023+0.023364*RHOR+0.058533*(RHOR**2.0)-
           10.40758*(RHOR**3.0)+0.009332*(RHOR**4.0))**4.0-10.E-04)/E
           1+ULL
       C
       C CALCULATION OF WEGHTED AVERAGE CRITICAL TEMP. AND PRESS. 'TECEE' &
       C 'PECEE'
173            DO 70 IJ=1,IK
174            JJI=IJ
175            ZAM(IJ)=Y(IJ)/X(IJ)
176    70      CONTINUE
177            SOM1=0.0
178            SOM2=0.0
179            SOM3=0.0
180            SOM4=0.0
181            DO 80 JK=1,II
182            NOM1 = X(JK)*M(JK)*TCC(JK) + SOM1
183            SOM1 = NOM1
184            DEN1 = X(JK)*M(JK) + SOM2
185            SOM2 = DEN1
186            NOM2 = X(JK)*M(JK)*PCC(JK) + SOM3
187            SOM3 = NOM2
188            DEN2 = X(JK)*M(JK) + SOM4
189            SOM4 = DEN2
190    80      CONTINUE
191            NOOM1 = NOM1 + X(9)*M(9)*TCC(9)
192            DEEN1 = DEN1 + X(9)*M(9)
193            TECEE = NOOM1/DEEN1
194            NOOM2 = NOM2 + X(9)*M(9)*PCC(9)
195            DEEN2 = DEN2 + X(9)*M(9)
196            PECEE = NOOM2/DEEN2
197            WRITE(6,206)
198    206     FORMAT(1H1,10X,'MIX. VISC. PARAMETER',3X,'LIQ. VISC. AT PREVA
           1ILING PRESSURE',3X,'WT. AVG. CRIT. TEMP.',3X,'WT. AVG. CRIT. PRESS
           1.',/)
199            WRITE(6,207)
200    207     FORMAT(16X,'E',20X,'CP',28X,'F',18X,'PSI',//)
201            WRITE(6,208) E,UPREV,TECEE,PECEE
202    208     FORMAT(10X,F12.5,12X,E15.7,28X,F12.4,14X,F12.6,//)
203            STOP
204            END
       C
```

```
C FOLLOWING SUBROUTINES WILL CALCULATE SURFACE TENSION & LIQ. DENSITY
C
      SUBROUTINE SURTEN(SIGMA,RHOL,RHOV,X,Y,M,ML,ACOMPS,X1,Y1)
      IMPLICIT REAL (B-H,M-Z)
      CHARACTER*3 ACOMPS
      DIMENSION PCH(9),X(9),Y(9),M(9),ML(9),ACOMPS(9)
      DIMENSION X1(9),Y1(9),SIGMAK(9),XY(9),XROM(9),YROM(9)
      IK=9
      DO 10 I=1,IK
      X1(I)=X(I)
      Y1(I)=Y(I)
      READ(5,100) PCH(I)
10    CONTINUE
100   FORMAT(10F8.0)
      RHOL=RHOL*0.016019
      RHOV=RHOV*0.016019
      NOOM = 0.0
      DOON = 0.0
      DO 27 JIK=1,IK
      NOOM = ML(JIK)*X1(JIK) + NOOM
      DOON = M(JIK)*Y1(JIK) + DOON
27    CONTINUE
      M2 = NOOM
      MV = DOON
      SUM=0.0
      DO 20 J=1,IK
      XY(J)=X(J)*Y(J)
      XROM(J)=X(J)*RHOL/M2
      YROM(J)=Y(J)*RHOV/MV
      SIGMAK(J) = PCH(J)*((X1(J)*RHOL/M2)-(Y1(J)*RHOV/MV))
      SIGMAQ    = SIGMAK(J) + SUM
      SUM = SIGMAQ
20    CONTINUE
      WRITE(6,581)
581   FORMAT(1H1,26X,'TABLE - V',//)
      WRITE(6,111)
111   FORMAT(10X,'COMPSN', 16X,'PRODUCT OF *LIQ., VAPOR DENSITY
     1', 'XI(RHOL/ML)',5X,'YI(RHOV/MV)',2X,'PARACHOR',2X,'(*)-(5)]PCH',
     1//////)
      DO 222 I=1,IK
      WRITE(6,11)ACOMPS(I),XY(I),XROM(I),YROM(I),PCH(I),SIGMAK(I)
222   CONTINUE
      WRITE(6,582)SIGMAQ
582   FORMAT(12X,////,'SUM LAST COLUMN =',2X,F14.6,//)
11    FORMAT(10X,A3,5X,F14.6,8X,F16.4,6X,F12.4,5X,F14.6,5X,F14.6,//)
      SIGMA = (SIGMAQ)**4.0
      RETURN
      END

      SUBROUTINE QUID(RHOL,X,ML,VL,ACOMPS,PROMX,PROMXV,SUMXM,SUMXMV)
      IMPLICIT REAL (B-H,M-Z)
      CHARACTER*3 ACOMPS
      DIMENSION X(9),ML(9),ACOMPS(9),VL(9),PROMX(9),PROMXV(9)
      IK=9
      DO 10 I=1,IK
      READ(5,100) ML(I),X(I),VL(I)
10    CONTINUE
100   FORMAT(3F8.0)
      SUM1 = 0.0
```

```
259          SUM2 = 0.0
260          II = IK-1
261          DO 20 J=1,IK
262          PROMX(J)=X(J)*ML(J)
263          PROMXV(J)=X(J)*ML(J)*VL(J)
264          MBAR1 = X(J)*ML(J) + SUM1
265          MBAR2 = X(J)*ML(J)*VL(J) + SUM2
266          SUM1 = MBAR1
267          SUM2 = MBAR2
268    20    CONTINUE
269          NUM = MBAR1
270          DEN = MBAR2
       C X(6) AND ML(6) REPRESENT XC6+ AND MC6+ I.E. MOL. FRAC. AND MOL. WT.
       C OF HEXANE AND HEAVIER COMPONENT RESPECTIVELY.
271          SUMXM=NUM
272          SUMXMV=DEN
273          RHOL = NUM/DEN
274          RETURN
275          END

       $EXEC
```

TABLE H-1

GAS DENSITY

SAMPLING POINT = A
Cum. N2 Inj. = .17 p.v.

Experiment # 2

Comp.	Yi	MWi	YiMWi	YiTci	YiPci
N1	0.52300000	28.016	14.6524	118.7210	257.420400
C1	0.30099990	16.068	4.8365	103.3032	202.603100
C2	0.06100000	30.068	1.8341	33.5012	43.206290
C3	0.03500000	44.096	1.5434	23.3100	21.608990
C4N	0.02200000	58.120	1.2786	16.8366	12.115390
C4I	0.02300000	58.120	1.3368	16.8981	12.169300
C5N	0.00600000	72.124	0.4327	5.0736	2.937000
C5I	0.01000000	72.124	0.7212	8.2980	4.830000
C6+	0.01900000	128.000	2.4320	20.3870	6.346000

SUMMATION Y(I)TC(I) = 346.3279

SUMMATION PC(I)Y(I) = 563.2356

SUMMATION Y(I)M(I) = 29.0677

Gas Density = 20.694 Lb/Cuft

TABLE H-2

LIQUID DENSITY

SAMPLING POINT = A

Cum. N2 Inj. = .17 p.v.

Experiment # 2

Comp.	Xi	MWi	Xi MWi	Sp. Volume Vi, Cuft/Lb	XiMWiVi
N2	0.15299990	28.01600000	4.28644800	0.01980000	0.08487165
C1	0.22500000	16.06799000	3.61529800	0.05350000	0.19341840
C2	0.07498999	30.06799000	2.25509800	0.04300000	0.09696919
C3	0.05600000	44.09599000	2.46937500	0.03160000	0.07803226
C4N	0.04200000	58.11999000	2.44103900	0.02750000	0.06712854
C4I	0.05200000	58.11999000	3.02223900	0.02700000	0.08160043
C5N	0.01700000	72.12399000	1.22610700	0.02540000	0.03114313
C5I	0.03500000	72.12399000	2.52433900	0.02500000	0.06310844
C6+	0.34500000	214.50000000	74.00250000	0.01976000	1.46228800
			95.8424		2.158

Stock Tank Density= 44.4 Lb/Cuft

Density at Current Conditions = 45.7 Lb/Cuft

TABLE II-3

GAS VISCOSITY

SAMPLING POINT = A
Cum. N2 Inj.= .17 p.v.

Experiment # 2

Comp.	Yi	MWi	Yi $MWi^{1/2}$	$Ui^{*}YiMWi^{1/2}$
N1	0.52300000	28.01600000	2.76824500	0.04872112
C1	0.30099990	16.06799000	1.20655500	0.01303080
C2	0.06100000	30.06799000	0.33448910	0.00341179
C3	0.03500000	44.09599000	0.23241680	0.00190582
C4N	0.02200000	58.11999000	0.16772010	0.00129145
C4I	0.02300000	58.11999000	0.17534380	0.00138522
C5N	0.00600000	72.12399000	0.05095551	0.00033121
C5I	0.01000000	72.12399000	0.08492583	0.00056900
C6+	0.01900000	128.00000000	0.21496040	0.00107480
			5.23561	0.07172

Mixture Atmospheric Viscosity=U^{*}= .0137 cp

Mixture Viscosity at current Conditions = U = .028 cp

TABLE F-4

LIQUID VISCOSITY

SAMPLING POINT = A
Cum. N2 Inj. = .17 p.v.

Experiment # 2

Comp.	Xi	Critical Volume Vci, grm/cm^3	XiVci	XiUiMWi$^{1/2}$	XiMWi$^{1/2}$	XiMWi
N2	0.15299990	3.12500000	0.47812490	0.01425303	0.80983120	4.28644800
C1	0.22508000	6.17300000	1.38892400	0.00974063	0.90191020	3.61529800
C2	0.07499999	4.92599900	0.36944990	0.00419482	0.41125700	2.25509800
C3	0.05600000	4.54500000	0.25451990	0.00304931	0.37186690	2.46937500
C4N	0.04200000	4.38599900	0.18421190	0.00246549	0.32019310	2.44103900
C4I	0.05200000	4.34599900	0.22599190	0.00313179	0.39642950	3.02223900
C5N	0.01700000	4.31000000	0.07326996	0.00093843	0.14437380	1.22610700
C5I	0.03500000	4.27999900	0.14979990	0.00199151	0.29724040	2.52433900
C6+	0.34500000	3.55099900	1.22509400	15.15841000	8.05280600	74.00250000
			4.34938	15.1981	8.7059	95.84

Liquid Viscosity = 1.59353 cp

TABLE H-5

SURFACE TENSION

SAMPLING POINT = A

Cum. N2 Inj. = .17 p.v.

Experiment # 2

Comp.	(1) XiYi	(2) $Xi\rho_L/M_l$	(3) $Yi\,\rho_V/M_v$	(4) Parachor Pchi	(5) ((2)-(3))*(4))
N2	0.080019	0.0011	0.0060	41.000000	-0.197994
C1	0.067725	0.0017	0.0034	77.000000	-0.135751
C2	0.004575	0.0006	0.0007	108.000000	-0.015022
C3	0.001960	0.0004	0.0004	150.300000	0.002469
C4N	0.000924	0.0003	0.0003	190.000000	0.011550
C4I	0.001196	0.0004	0.0003	181.500000	0.022433
C5N	0.000102	0.0001	0.0001	232.000000	0.013394
C5I	0.000350	0.0003	0.0001	225.000000	0.032781
C6+	0.006555	0.0026	0.0002	349.000000	0.817920
					0.55172

SURFACE TENSION = 0.09269 Dynes/cm.

TABLE II-6

LIQUID DENSITY

SAMPLING POINT= A
Cum. N2 Inj. =.22 p.v.

Experiment # 2

Comp.	Xi	MWi	XiMWi	Sp. Volume Vi, Cuft/lb	XiMWiVi
N2	0.13999990	28.01600000	3.92224000	0.01980000	0.07766032
C1	0.10600000	16.06799000	1.70320700	0.05350000	0.09112155
C2	0.05200000	30.06799000	1.56353400	0.04300000	0.06723195
C3	0.04100000	44.09599000	1.80793500	0.03160000	0.05713077
C4N	0.00800000	58.11999000	0.46495990	0.02750000	0.01278640
C4I	0.03000000	58.11999000	1.74359900	0.02700000	0.04707719
C5N	0.01200000	72.12399000	0.86548770	0.02540000	0.02198339
C5I	0.01800000	72.12399000	1.29823100	0.02500000	0.03245578
C6+	0.59399990	214.50000000	127.41290000	0.01976000	2.51768000
			140.782		2.9251

Stock Tank Density= 48.12 Lb/Cuft

Density at Current Conditions= 49.22 Lb/Cuft

TABLE H-6A

GAS DENSITY

SAMPLING POINT = A
Cum. N2 Inj.= .22 p.v.

Experiment # 2

Comp.	Yi	MWi	YiMWi	YiTci	YiPci
N1	0.71899990	28.016	20.1435	163.2130	353.891600
C1	0.18099990	16.068	2.9083	62.1192	121.831100
C2	0.04200000	30.068	1.2629	23.0664	29.748590
C3	0.02400000	44.096	1.0583	15.9840	14.817590
C4N	0.00400000	58.120	0.2325	3.0612	2.202800
C4I	0.01200000	58.120	0.6974	8.8164	6.349199
C5N	0.00400000	72.124	0.2885	3.3824	1.958000
C5I	0.00500000	72.124	0.3606	4.1490	2.414999
C6+	0.01000000	128.000	1.2800	10.7300	3.340000

SUMMATION Y(I)TC(I) = 294.5208

SUMMATION PC(I)Y(I) = 536.5527

SUMMATION Y(I)M(I) = 28.2319

GAS DENSITY = 20.099 Lb/Cuft

TABLE H-7

GAS VISCOSITY

SAMPLING POINT= A
Cum. N2 Inj.=.22 p.v.

Experiment # 2

Comp.	Yi	MWi	$YiMWi^{1/2}$	$U^*_i YiMWi^{1/2}$
N2	0.71899990	28.01600000	3.80567600	0.06697989
C1	0.18099998	16.06799000	0.72553658	0.00703579
C2	0.04200000	30.06799000	0.23030400	0.00234910
C3	0.02400000	44.09599000	0.15937140	0.00130685
C4N	0.00400000	58.11999000	0.03049459	0.00023481
C4I	0.01200000	58.11899000	0.09148371	0.00072272
C5N	0.00400000	72.12399000	0.03397034	0.00022081
C5I	0.00500000	72.12399000	0.04246291	0.00020450
C6+	0.01000000	128.00000000	0.11313700	0.00056569
			5.233243	0.08055

Mixture Atmospheric Viscosity= U^*= 0.154 cp.
Mixture Viscosity at Current Conditions= 0.02503 cp.

TABLE H-8
LIQUID VISCOSITY

SAMPLING POINT = A
Cum. N2 Inj. = .22 p.v. Experiment # 2

Comp.	Xi	Critical Volume Vci	XiVci	$XiUiMWi^{1/2}$	$XiMWi^{1/2}$	XiMWi
N2	0.13999990	3.12500000	0.43749990	0.01304198	0.74102190	3.92224000
C1	0.10600000	6.17300000	0.65433800	0.00458892	0.42489980	1.70320700
C2	0.05200000	4.92599900	0.25615190	0.00290841	0.28513830	1.56353400
C3	0.04100000	4.54500000	0.18634490	0.00223253	0.27225970	1.80793500
C4N	0.00800000	4.38599900	0.03508800	0.00046962	0.06098918	0.46495990
C4I	0.03000000	4.34599900	0.13037990	0.00180680	0.22870930	1.74359900
C5N	0.01200000	4.31000000	0.05172000	0.00066242	0.10191090	0.86548770
C5I	0.01800000	4.27999900	0.07703996	0.00102421	0.15286640	1.29823100
C6+	0.59399990	3.55099900	2.10929200	26.09883000	8.69961500	127.41290000
			3.9378	26.1255	10.9674	140.2821

Liquid Viscosity= 2.22 cp.

TABLE H-9

SURFACE TENSION

SAMPLING POINT = A

Cum. N2 Inj.= .22 p.v. Experiment # 2

Comp.	(1) XiYi	(2) $Yi\rho v/M_l$	(3) $Yi\rho v/Mv$	(4) Parachor Pchi	(5) ((2)-(3))*(4))
N1	0.100660	0.0008	0.0082	41.000000	-0.304759
C1	0.019186	0.0006	0.0021	77.000000	-0.114247
C2	0.002184	0.0003	0.0005	108.000000	-0.020976
C3	0.000984	0.0002	0.0003	150.300000	-0.007391
C4N	0.000032	0.0000	0.0000	190.600000	-0.000343
C4I	0.000360	0.0002	0.0001	181.500000	0.004980
C5N	0.000048	0.0001	0.0000	232.000000	0.004663
C5I	0.000090	0.0001	0.0001	225.000000	0.009349
C6+	0.005940	0.0033	0.0001	349.000000	1.095476
					0.666751

Surface Tension = 0.1976305

TABLE H-10

GAS DENSITY

SAMPLING POINT = A

Cum. N2 Inj.= .28 p.v. Experiment # 2

Comp.	Yi	MWi	YiMWi	YiTci	YiPci
N1	0.86799990	28.016	24.3179	197.0360	427.229400
C1	0.07200003	16.068	1.1569	24.7104	48.463210
C2	0.02800000	30.068	0.8419	15.3776	19.832390
C3	0.01100000	44.096	0.4851	7.3260	6.791398
C4N	0.00200000	58.120	0.1162	1.5306	1.101399
C4I	0.00500000	58.120	0.2906	3.6735	2.645499
C5N	0.00100000	72.124	0.0721	0.8456	0.489500
C5I	0.00100000	72.124	0.0721	0.8298	0.483000
C6+	0.01200000	128.000	1.5360	12.8760	4.007998

SUMMATION Y(I)TC(I) = 264.2053

SUMMATION PC(I)Y(I) = 511.0427 GAS DENSITY= 20.566 Lb/cuft

SUMMATION Y(I)M(I) = 28.8888

TABLE H-11

LIQUID DENSITY

SAMPLING POINT = A
CUM. N2 INJ.= .28 p.v.

Experiment # 2

Comp.	Xi	MWi	XiMWi	Sp. Volume Vi, Cuft/Lb	XiMWiVi
N1	0.17199990	28.01600000	4.81875200	0.01980000	0.09541124
C1	0.04500000	16.06799000	0.72305970	0.05350000	0.03868369
C2	0.03500000	30.06799000	1.05237900	0.04300000	0.04525232
C3	0.01800000	44.09599000	0.79372780	0.03160000	0.02508179
C4N	0.00400000	58.11999000	0.23247990	0.02750000	0.00639320
C4I	0.01000000	58.11999000	0.58120000	0.02700000	0.01569240
C5N	0.00300000	72.12399000	0.21637190	0.02540000	0.00549585
C5I	0.00300000	72.12399000	0.21637190	0.02500000	0.00540930
C6+	0.70999990	214.50000000	152.29490000	0.01976000	3.00934800
			160.92		3.2468

Stock Tank Density = 49.56 Lb/Cuft

Density at Current Conditions= 50.72 Lb/Cuft

TABLE II -12
GAS VISCOSITY

SAMPLING POINT = A
Cum. N2 Inj.= .28 p.v.

Experiment #2

Comp.	Yi	MWi	$YiMWi^{1/2}$	$U_i^*YiMWi^{1/2}$
N1	0.86799990	28.01600000	4.59433500	0.08086026
C1	0.07200003	16.06799000	0.28861130	0.00311700
C2	0.02600000	30.06799000	0.15353590	0.00156607
C3	0.01100000	44.09599000	0.07304525	0.00059897
C4N	0.00200000	58.11999000	0.01524729	0.00011740
C4I	0.00500000	58.11999000	0.03811822	0.00030113
C5N	0.00100000	72.12399000	0.00849258	0.00005520
C5I	0.00100000	72.12399000	0.00849258	0.00005690
C6+	0.01200000	128.00000000	0.13576440	0.00067882
			5.31564	0.08735

Mixture Atmospheric Viscosity= 0.0164 cp.

Mixture Viscosity at Current Conditions= 0.02665 cp.

TABLE II-13

LIQUID VISCOSITY

SAMPLING POINT= A

Cum. N2. Inj. = .28 p.v. Experiment # 2

Comp.	Xi	Critical Volume Vci, gm/cm^3	XiVci	XiUi MWi$^{1/2}$	XiMWi$^{1/2}$	XiMWi
N1	0.17199990	3.12500000	0.53749990	0.01602301	0.91039840	4.81875200
C1	0.04500000	6.17300000	0.27778500	0.00194813	0.10038200	0.72305970
C2	0.03500000	4.92599900	0.17240990	0.00195758	0.19191990	1.05237900
C3	0.01800000	4.54500000	0.08181000	0.00098013	0.11952860	0.79372780
C4N	0.00400000	4.38599900	0.01754400	0.00023481	0.03049459	0.23247990
C4I	0.01000000	4.34599900	0.04346000	0.00060227	0.07623643	0.58120000
C5N	0.00300000	4.31000000	0.01293000	0.00016561	0.02547775	0.21637190
C5I	0.00300000	4.27999900	0.01284000	0.00017070	0.02547775	0.21637190
C6+	0.70999990	3.55099900	2.52120800	31.19557000	10.39853000	152.29490000
			3.67748	31.2176	11.9584	160.929

Liquid Viscosity= 2.457 cp.

TABLE H-14

SURFACE TENSION

SAMPLING POINT = B
Cum. N2 Inj.= .42 p.v.

Experiment # 2

Comp.	(1) XiYi	(2) $Xi\rho_L/Ml$	(3) $Yi\rho_V/Mv$	(4) Parachor Pchi	(5) ((2)-(3))*(4))
N1	0.149296	0.0008	0.0099	41.000000	-0.371070
C1	0.003240	0.0002	0.0008	77.000000	-0.046131
C2	0.000980	0.0002	0.0003	108.000000	-0.015837
C3	0.000198	0.0001	0.0001	150.300000	-0.005507
C4N	0.000008	0.0000	0.0000	190.000000	-0.000584
C4I	0.000050	0.0000	0.0001	181.500000	-0.001395
C5N	0.000003	0.0000	0.0000	232.000000	0.000788
C5I	0.000003	0.0000	0.0000	225.000000	0.000764
C6+	0.008520	0.0035	0.0001	349.000000	1.174790
					0.735818

Surface Tension = 0.2931 Dynes/cm

TABLE H-15

GAS DENSITY

SAMPLING POINT = B

Cum. N2 Inj.= .35 p.v. Experiment # 2

Comp.	Yi	MWi	YiMWi	YiTci	YiPci
N1	0.33200000	28.016	9.3013	75.3640	163.410300
C1	0.45099990	16.068	7.2467	154.7832	303.568100
C2	0.08099997	30.068	2.4355	44.4852	57.372260
C3	0.06100000	44.096	2.6899	40.6260	37.661390
C4N	0.01200000	58.120	0.6974	9.1836	6.608398
C4I	0.01400000	58.120	0.8137	10.2858	7.407400
C5N	0.00600000	72.124	0.4327	5.0736	2.937000
C5I	0.00500000	72.124	0.3606	4.1490	2.414999
C6+	0.03800000	128.000	4.8640	40.7740	12.691990

SUMMATION Y(I)TC(I) = 384.7239

SUMMATION PC(I)Y(I) = 594.0708

SUMMATION Y(I)M(I) = 28.8418

Gas Density = 20.533 Lb/Cuft

TABLE H-16

LIQUID DENSITY

SAMPLING POINT = B

Cum. N2 Inj. = .35 p.v. EXPERIMENT # 2

Comp.	Xi	MWi	XiMWi	Sp. Volume Vi, Cuft/Lb	XiMWiVi
N1	0.12099990	28.01600000	3.38993600	0.01980000	0.06712073
C1	0.27999990	16.06799000	4.49903600	0.05350000	0.24069840
C2	0.09600002	30.06799000	2.88652700	0.04300000	0.12412060
C3	0.10500000	44.09599000	4.63007900	0.03160000	0.14631040
C4N	0.02800000	58.11999000	1.62735900	0.02750000	0.04475238
C4I	0.03600000	58.11999000	2.09231900	0.02700000	0.05649262
C5N	0.02200000	72.12399000	1.58672700	0.02540000	0.04030287
C5I	0.02000000	72.12399000	1.44247900	0.02500000	0.03606198
C6+	0.29199990	214.50000000	62.63398000	0.01976000	1.23764700
			84.7084		1.9935

Stock Tank Density = 42.532 Lb/Cuft

Density at Current Conditions= 43.732 Lb/Cuft

TABLE H-17

GAS VISCOSITY

SAMPLING POINT = P

Cum. N2 Inj.=.35 p.v. Experiment # 2

Comp.	Yi	MWi	$Y_iMW_i^{1/2}$	$U_i^*Y_iMW^{1/2}$
N1	0.33200000	28.01600000	1.75728000	0.03092814
C1	0.45099990	16.06799000	1.80782700	0.01952454
C2	0.08099997	30.06799000	0.44415750	0.00453041
C3	0.06100000	44.09599000	0.40506920	0.00332157
C4N	0.01200000	58.11999000	0.09148371	0.00070442
C4I	0.01400000	58.11999000	0.10673090	0.00084317
C5N	0.00600000	72.12399000	0.05095551	0.00033121
C5I	0.00500000	72.12399000	0.04246291	0.00028450
C6+	0.03800000	128.00000000	0.42992080	0.00214960
			5.13588	0.08735

Mixture Atmospheric Viscosity = U^* = 0.122 cp.

Mixture Viscosity at Current Conditions= 0.0345 cp.

TABLE H-18

LIQUID VISCOSITY

SAMPLING POINT = B

Cum..N2 Inj. = .35 p.v. Experiment # 2

Comp.	Xi	Critical Volume Vci, gm/cm^3	XiVci	XiUiMWi$^{1/2}$	XiMW$^{1/2}$	XiMWi
N1	0.12099990	3.12500000	0.37812490	0.01127200	0.64045470	3.38993600
C1	0.27999990	6.17300000	1.72843900	0.01212167	1.12237600	4.49903600
C2	0.09600002	4.52599900	0.47289600	0.00536937	0.52640920	2.88652700
C3	0.10500000	4.54500000	0.47722500	0.00571745	0.69725060	4.63007900
C4N	0.02800000	4.38599500	0.12280790	0.00164366	0.21346210	1.62735980
C4I	0.03600000	4.34599500	0.15645590	0.00216816	0.27445120	2.09231900
C5N	0.02200000	4.31000000	0.09481996	0.00121444	0.18683680	1.58672700
C5I	0.02000000	4.27999900	0.08559996	0.00113801	0.16985160	1.44247900
C6+	0.29199990	3.55099900	1.03689000	12.82973000	4.27657700	62.63398000
			4.5532	12.8703	8.677	84.788

Liquid Viscosity= 1.3436 cp.

TABLE H-19

SURFACE TENSION

SAMPLING POINT = B
Cum. N2 Inj. = .35 p.v.

Experiment # 2

Comp.	(1) X_iY_i	(2) $X_i\rho_L/M_L$	(3) $Y_i\rho_V/M_V$	(4) Parachor Pchi	(5) ((2)-(3))*(4))
N1	0.040172	0.0010	0.0038	41.000000	-0.115374
C1	0.126280	0.0022	0.0051	77.000000	-0.222797
C2	0.007776	0.0008	0.0009	108.000000	-0.016454
C3	0.006405	0.0008	0.0007	150.300000	0.022254
C4N	0.000336	0.0002	0.0001	190.000000	0.016747
C4I	0.000504	0.0003	0.0002	181.500000	0.023526
C5N	0.000132	0.0002	0.0001	232.000000	0.025139
C5I	0.000100	0.0002	0.0001	225.000000	0.023330
C6+	0.011096	0.0023	0.0004	349.000000	0.667644
					0.424014

Surface Tension = 0.032323 Dines/cm

TABLE H-20

GAS DENSITY

SAMPLING POINT = B

Cum. N2 Inj. = .42 p.v. Experiment # 2

Comp..	Yi	MWi	YiMWi	YiTci	YiPci
N1	0.60699990	28.016	17.0057	137.7890	298.765100
C1	0.22100000	16.068	3.5510	75.8472	148.755100
C2	0.07499999	30.068	2.2551	41.1900	53.122480
C3	0.05100000	44.096	2.2489	33.9660	31.487380
C4N	0.00800000	58.120	0.4650	6.1224	4.405600
C4I	0.00800000	58.120	0.4650	5.8776	4.232801
C5N	0.00200000	72.124	0.1442	1.6912	0.979000
C5I	0.00200000	72.124	0.1442	1.6596	0.966000
C6+	0.02800000	128.000	3.5840	30.0440	9.352000

SUMMATION Y(I)TC(I) = 334.1863

SUMMATION PC(I)Y(I) = 552.0645

SUMMATION Y(I)M(I) = 29.8631

Gas Density = 46.358 Lb/Cuft

TABLE H-21

LIQUID DENSITY

SAMPLING POINT = B

Cum. N2 Inj.= .42 p.v. Experiment # 2

Comp.	Xi	MWi	XiMWi	Sp. Volume Vi, Cuft/Lb	XiMWiVi
N1	0.22000000	28.01600000	6.16352100	0.01980000	0.12203770
C1	0.11900000	16.06799000	1.91209100	0.05350000	0.10229680
C2	0.09100002	30.06799000	2.73618700	0.04300000	0.11765600
C3	0.08800000	44.09599000	3.88044600	0.03160000	0.12262200
C4N	0.02000000	58.11999000	1.16239900	0.02750000	0.03196598
C4I	0.02200000	58.11999000	1.27863900	0.02700000	0.03452327
C5N	0.00800000	72.12399000	0.57699200	0.02540000	0.01465560
C5I	0.00800000	72.12399000	0.57699200	0.02500000	0.01442480
C6+	0.42400000	214.50000000	90.94799000	0.01976000	1.79713200
			109.2352		2.3573

Stock Tank Density = 46.3388 Lb/Cuft

Density at current Conditions= 47.458 Lb/Cuft

TABLE H-22

GAS VISCOSITY

SAMPLING POINT = B

Cum. N2 Inj.= .42 p.v. Experiment # 2

Comp.	Yi	MWi	$YiMWi^{1/2}$	$U_i^* YiMWi^{1/2}$
N1	0.60699990	28.01600000	3.21285900	0.05654632
C1	0.22100000	16.06799000	0.88587620	0.00956746
C2	0.07499999	30.06799000	0.41125700	0.00419482
C3	0.05100000	44.09599000	0.33866440	0.00277705
C4N	0.00800000	58.11999000	0.06098918	0.00046962
C4I	0.00800000	58.11999000	0.06098918	0.00048181
C5N	0.00200000	72.12399000	0.01698517	0.00011040
C5I	0.00200000	72.12399000	0.01698517	0.00011380
C6+	0.02800000	128.00000000	0.31678370	0.00158392
			5.32139	0.07585

Mixture Atmospheric Viscosity= U^*= 0.0143 cp.

Mixture Viscosity at Current Conditions= U= 0.0405 cp.

TABLE H-23

LIQUID VISCOSITY

SAMPLING POINT = B

Cum. N2 Inj. = .42 p.v. Experiment # 2

Comp.	Xi	Critical Volume Vci, gm/cm^3	XiVci	XiUiMWi$^{1/2}$	XiMWi$^{1/2}$	XiMWi
N1	0.22000000	3.12500000	0.68750000	0.02049455	1.16446300	6.16352100
C1	0.11900000	6.17300000	0.73458710	0.00515171	0.47701030	1.91209100
C2	0.09100002	4.92599900	0.44826600	0.00508972	0.49899210	2.73618700
C3	0.08800000	4.54500000	0.39995990	0.00479177	0.58436220	3.88044600
C4N	0.02000000	4.38599900	0.08771998	0.00117404	0.15247290	1.16239900
C4I	0.02200000	4.34599500	0.09561199	0.00132499	0.16772010	1.27863900
C5N	0.00800000	4.31000000	0.03448001	0.00044161	0.06794065	0.57699200
C5I	0.00800000	4.27999500	0.03424000	0.00045520	0.06794065	0.57699200
C6+	0.42400000	3.55099900	1.50562300	18.62945000	6.20982600	90.94799000
			4.02798	18.6683	9.3907	109.2357

Liquid Viscosity = 1.835 cp.

TABLE II-24

SURFACE TENSION

SAMPLING POINT = B
Cum. N2 Inj. = .42 pav.

Experiment # 2

Comp.	(1) XiYi	(2) $Xi\rho_l/M_l$	(3) $Yi\rho_v/Mv$	(4) Parachor Pchi	(5) ((2)-(3))*(4))
N1	0.133540	0.0015	0.0069	41.000000	-0.222529
C1	0.026299	0.0008	0.0025	77.000000	-0.131804
C2	0.006825	0.0006	0.0009	108.000000	-0.025591
C3	0.004488	0.0006	0.0006	150.300000	0.002460
C4N	0.000160	0.0001	0.0001	190.000000	0.008488
C4I	0.000176	0.0001	0.0001	181.500000	0.010575
C5N	0.000016	0.0001	0.0000	232.000000	0.007321
C5I	0.000016	0.0001	0.0000	225.000000	0.007100
C6+	0.011872	0.0029	0.0003	349.000000	0.894118
					0.550137

Surface Tension = 0.09159 Dines/cm

TABLE H-25
GAS DENSITY

SAMPLING POINT = C
Cum. N2 Inj. = .55 p.v. Experiment # 2

Comp.	Yi	MWi	YiMWi	YiTci	YiPci
N1	0.26959990	28.016	7.5643	61.2900	132.893900
C1	0.40200000	16.068	6.4593	137.9664	270.586100
C2	0.13400000	30.068	4.0291	73.5928	94.912200
C3	0.09500003	44.096	4.1891	63.2700	58.652990
C4N	0.01600000	58.120	0.9299	12.2448	8.811198
C4I	0.01600000	58.120	0.9299	11.7552	8.465601
C5N	0.00800000	72.124	0.5770	6.7648	3.916000
C5I	0.00900000	72.124	0.6491	7.4682	4.346999
C6+	0.05100000	128.000	6.5280	54.7230	17.033990

SUMMATION Y(I)TC(I) = 429.0742
SUMMATION PC(I)Y(I) = 599.6182
SUMMATION Y(I)M(I) = 31.8558

Gas Density = 22.673 lb/Cuft

TABLE H-26

LIQUID DENSITY

SAMPLING POINT = C

Cum. N2 Inj. = .55 p.v. Experiment # 2

Comp.	Xi	MWi	XiMWi	Sp. Volume Vi, Cuft/Lb	XiMWiVi
N1	0.10600000	28.01600000	2.96969600	0.01980000	0.05879998
C1	0.24400000	16.06799000	3.92059000	0.05350000	0.20975150
C2	0.16699990	30.06799000	5.02135400	0.04300000	0.21591820
C3	0.13200000	44.09599000	5.82067200	0.03160000	0.18393310
C4N	0.04200000	58.11999000	2.44103900	0.02750000	0.06712854
C4I	0.04800000	58.11999000	2.78975900	0.02700000	0.07532346
C5N	0.03700000	72.12399000	2.66858700	0.02540000	0.06778210
C5I	0.05000000	72.12399000	3.60619900	0.02500000	0.09015495
C6+	0.17400000	214.50000000	37.32299000	0.01976000	0.73750240
			66.5608		1.7063

STOCK TANK DENSITY = 39.009 Lb/Cuft

Density at Current Conditions= 40.30 Lb/Cuft

TABLE H-27
GAS VISCOSITY

SAMPLING POINT = C
Cum. N2 Inj.= .55 p.v. Experiment # 2

Comp.	Yi	MWi	$Y_iMW_i^{1/2}$	$U_i^*Y_iMW_i^{1/2}$
N1	0.26999990	28.01600000	1.42911300	0.02515240
C1	0.40200000	16.06799000	1.61141200	0.01740325
C2	0.13400000	30.06799000	0.73477940	0.00749475
C3	0.09500003	44.09599000	0.63084580	0.00517293
C4N	0.01600000	58.11999000	0.12197620	0.00093923
C4I	0.01600000	58.11999000	0.12197820	0.00096363
C5N	0.00800000	72.12399000	0.06794065	0.00044161
C5I	0.00900000	72.12399000	0.07643324	0.00051210
C6+	0.05100000	128.00000000	0.57699900	0.00288499
			5.37148	0.06066

Mixture Atmospheric Viscosity= U^*= 0.0113 cp.

Mixture Viscosity at Current Conditions= U = 0.02812 cp.

TABLE H-28

LIQUID VISCOSITY

SAMPLING POINT # C

Cum. N2 Inj.= .55 p.v. Experiment # 2

Comp.	Xi	Critical Volume Vci, gm/cm^3	XiVci	XiUiMWi$^{1/2}$	XiMWi$^{1/2}$	XiMWi
NI	0.10000000	3.12500000	0.33125000	0.00987465	0.56105950	2.96969600
C1	0.24400000	6.17300000	1.50621100	0.01056317	0.97807150	3.92059000
C2	0.16699990	4.92599900	0.82264190	0.00934047	0.91573250	5.02135400
C3	0.13200000	4.54500000	0.59994010	0.00718766	0.87654360	5.82067200
C4N	0.04200000	4.38599900	0.18421190	0.00246549	0.32019310	2.44103900
C4I	0.04800000	4.34599900	0.20860790	0.00289089	0.36593500	2.78975900
C5N	0.03700000	4.31000000	0.15946990	0.00204247	0.31422560	2.66858700
C5I	0.05000000	4.27999900	0.21399990	0.00284502	0.42462920	3.60619900
C6+	0.17400000	3.55099900	0.61787390	7.64511700	2.54837200	37.32299000
			4.6442	7.6923	7.3048	66.5608

Liquid Viscosity = 0.905 cp.

TABLE H-29

SURFACE TENSION

SAMPLING POINT = C
Cum. N2 Inj. = .55 p.v.

Experiment # 2

Comp.	(1) XiYi	(2) $Xi\,\rho_L/M_l$	(3) $Yi\,\rho_v/Mv$	(4) Parachor Pchi	(5) ((2)-(3))*(4))
N1	0.028620	0.0010	0.0031	41.000000	-0.085447
C1	0.098088	0.0023	0.0046	77.000000	-0.176630
C2	0.022378	0.0016	0.0015	108.000000	0.004279
C3	0.012540	0.0012	0.0011	150.300000	0.023418
C4N	0.000672	0.0004	0.0002	190.000000	0.040248
C4I	0.000768	0.0005	0.0002	181.500000	0.048671
C5N	0.000296	0.0003	0.0001	232.000000	0.059421
C5I	0.000450	0.0005	0.0001	225.000000	0.082523
C6+	0.008874	0.0016	0.0006	349.000000	0.367117
					0.36360

Surface Tension = 0.01747 Dynes/cm

TABLE H-30

GAS DENSITY

SAMPLING POINT = C

Cum. N2 Injj. = .62 p.v. Experiment # 2

Comp.	Yi	MWi	YiMWi	YiTci	YiPci
N1	0.52959990	28.016	14.8485	120.3100	260.865700
C1	0.27200000	16.068	4.3705	93.3504	183.083200
C2	0.06000000	30.068	1.8041	32.9520	42.498000
C3	0.06000000	44.096	2.6458	39.9600	37.043990
C4N	0.01100000	58.120	0.6393	8.4183	6.057699
C4I	0.01200000	58.120	0.6974	8.8164	6.349199
C5N	0.00500000	72.124	0.3606	4.2280	2.447499
C5I	0.00800000	72.124	0.5770	6.6384	3.864000
C6+	0.04200000	128.000	5.3760	45.0660	14.027990

SUMMATION Y(I)TC(I) = 359.7385

SUMMATION PC(I)Y(I) = 556.2361 Gas Density = 22.29 Lb/Cuft

SUMMATION Y(I)M(I) = 31.3191

TABLE H-31

LIQUID DENSITY

SAMPLING POINT = C

Cum. N2 Inj. = .62 p.v. Experiment # 2

Comp	Xi	MWi	XiMWi	Sp. Volume Vi, Cuft/Lb	XiMWiVi
N1	0.17299990	28.01600000	4.84676800	0.01980000	0.09596598
C1	0.16500000	16.06799000	2.65121800	0.05350000	0.14184030
C2	0.07599998	30.06799000	2.28516500	0.04300000	0.09826213
C3	0.09100002	44.09599000	4.01273500	0.03160000	0.12680230
C4N	0.03200000	58.11999000	1.85983900	0.02750000	0.05114558
C4I	0.04000000	58.11999000	2.32479900	0.02700000	0.06276953
C5N	0.02500000	72.12399000	1.80309900	0.02540000	0.04579873
C5I	0.04700000	72.12399000	3.38982600	0.02500000	0.08474565
C6+	0.35100000	214.50000000	75.28948000	0.01976000	1.48771900
			98.4629		2.950

Stock Tank Density = 44.856 Lb/Cuft

Density at Current Conditions = 46.056 Lb/Cuft

TABLE H-32
GAS VISCOSITY

SAMPLING POINT = C

Cum. N2 Injs. = .62 p.v. Experiment #2

Comp.	Yi	MWi	$Y_iMW_i^{1/2}$	$U_i^*Y_iMW_i^{1/2}$
N1	0.52999990	28.01600000	2.80529600	0.04937322
C1	0.27200000	16.06799000	1.09030900	0.01177534
C2	0.06000000	30.06799000	0.32900570	0.00335586
C3	0.06000000	44.09599000	0.39842870	0.00326712
C4N	0.01100000	58.11999000	0.08386010	0.00064572
C4I	0.01200000	58.11999000	0.09148371	0.00072272
C5N	0.00500000	72.12399000	0.04246291	0.00027601
C5I	0.00800000	72.12399000	0.06794065	0.00045520
C6+	0.04200000	128.00000000	0.47517570	0.00237588
			5.3839	0.07225

Mixture Atmospheric Viscosity=U^*= 0.0134 cp.

Mixture Viscosity at Current Conditions = U = 0.0469 cp.

TABLE H-33

LIQUID VISCOSITY

SAMPLING POINT = C

Cum. N2 Inj. = .62 p.v. Experiment # 2

Comp.	Xi	Critical Vol. Vci, gm/cm^3	XiVci	XiUiMW$^{1/2}$	XiMWi$^{1/2}$	XiMWi
N1	0.17299990	3.12500000	0.54062490	0.01611616	0.91569130	4.84676800
C1	0.16500000	6.17300000	1.01854500	0.00714313	0.66140080	2.65121800
C2	0.07599998	4.52599900	0.37437580	0.00425075	0.41674040	2.28516500
C3	0.09100002	4.54500000	0.41359500	0.00495512	0.60428380	4.01273500
C4N	0.03200000	4.38599900	0.14035190	0.00187846	0.24395660	1.85983900
C4I	0.04000000	4.34599900	0.17383990	0.00240907	0.30494580	2.32479900
C5N	0.02500000	4.31000000	0.10774990	0.00138004	0.21231450	1.80309900
C5I	0.04700000	4.27999900	0.20115990	0.00267431	0.39915140	3.38982600
C6+	0.35100000	3.55099900	1.24640000	15.42203000	5.14068100	75.28948000
			4.21664	15.4628	8.8992	98.462

Liquid Viscosity= 1.5852 cp.

TABLE H-34

SURFACE TENSION

SAMPLING POINT = C

Cum. N2 Inj. = .62 p.v. Experiment # 2

Comp.	(1) XiYi	(2) $Xi\rho_L/M_l$	(3) $Yi\rho_v/Mv$	(4) Parachor Pchi	(5) ((2)-(3))*(4))
N1	0.091690	0.0013	0.0060	41.000000	-0.196057
C1	0.044880	0.0012	0.0031	77.000000	-0.146138
C2	0.004560	0.0006	0.0007	108.000000	-0.014001
C3	0.005460	0.0007	0.0007	150.300000	-0.003032
C4N	0.000352	0.0002	0.0001	190.000000	0.020535
C4I	0.000480	0.0003	0.0001	181.500000	0.028143
C5N	0.000125	0.0002	0.0001	232.000000	0.029098
C5I	0.000376	0.0003	0.0001	225.000000	0.056646
C6+	0.014742	0.0026	0.0005	349.000000	0.726804
					0.501997

Surface Tension = 0.063504 Dynes/cm

TABLE H -35
GAS DENSITY

SAMPLING POINT = C
Cum. N2 Inj. = .70 p.v. Experiment # 2

Comp.	Yi	MWi	YiMWi	YiTci	YiPci
N1	0.80900000	28.016	22.6649	183.6430	398.189600
C1	0.11400000	16.068	1.8318	39.1248	76.733410
C2	0.01000000	30.068	0.3007	5.4920	7.083001
C3	0.04500000	44.096	1.9843	29.9700	27.782980
C4N	0.00200000	58.120	0.1162	1.5306	1.101399
C4I	0.00200000	58.120	0.1162	1.4694	1.058200
C5N	0.00000000	72.124	0.0000	0.0000	0.000000
C5I	0.00000000	72.124	0.0000	0.0000	0.000000
C6+	0.01800000	128.000	2.3040	19.3140	6.011999

SUMMATION Y(I)TC(I) = 280.5435
SUMMATION PC(I)Y(I) = 517.9602
SUMMATION Y(I)M(I) = 29.3181

Gas Density = 20.8721 Lb/Cuft

TABLE H-36

LIQUID DENSITY

SAMPLING POINT = C

Cum. N2 Inj. = .70 p.v. Experiment # 2

Comp.	Xi	MWi	XiMWi	Sp. Volume Vi, Cuft/Lb	XiMWiVi
N1	0.23199990	28.01600000	6.49971200	0.01980000	0.12869420
C1	0.06699997	16.06799000	1.07655400	0.05350000	0.05759566
C2	0.01300000	30.06799000	0.39088380	0.04300000	0.01680800
C3	0.07499959	44.09599000	3.30719800	0.03160000	0.10450740
C4N	0.00600000	58.11999000	0.34872000	0.02750000	0.00958980
C4I	0.00700000	58.11999000	0.40683990	0.02700000	0.01098467
C5N	0.00000000	72.12399000	0.00000000	0.02540000	0.00000000
C5I	0.00000000	72.12399000	0.00000000	0.02500000	0.00000000
C6+	0.60000000	214.50000000	128.69990000	0.01976000	2.54311100
			140.7299		2.8713

Stock Tank Density = 49.01275 Lb/Cuft

Density at Current Conditions= 50.212 Lb/Cuft

TABLE H-37
GAS VISCOSITY

SAMPLING POINT = C
Cum. N2 Inj. = .70 p.v. Experiment # 2

Comp.	Yi	MWi	$YiMWi^{1/2}$	$U_i^*YiMWi^{1/2}$
N1	0.80900000	28.01600000	4.28204800	0.07536399
C1	0.11400000	16.06799000	0.45696780	0.00493525
C2	0.01000000	30.06799000	0.05483430	0.00055931
C3	0.04500000	44.09599000	0.29882160	0.00245034
C4N	0.00200000	58.11999000	0.01524729	0.00011740
C4I	0.00200000	58.11999000	0.01524729	0.00012045
C5N	0.00000000	72.12399000	0.00000000	0.00000000
C5I	0.00000000	72.12399000	0.00000000	0.00000000
C6+	0.01800000	128.00000000	0.20364670	0.00101823
			5.32681	0.08456

Mixture Atmospheric Viscosity = U^* = 0.0159 cp.
Mixture Viscosity at Current Conditions= U = 0.06042 cp.

TABLE H-38

LIQUID VISCOSITY

SAMPLING POINT = C

Cum. N2 Inj. = .70 p.v. Experiment # 2

Comp.	Xi	Critical Volume Vi, gm/cm^3	XiVci	XiUiMwi$^{1/2}$	XiMWi$^{1/2}$	XiMWi
N1	0.23199990	3.12500000	0.72499990	0.02161242	1.22797800	6.49971200
C1	0.06699997	6.17300000	0.41359080	0.00290054	0.26856860	1.07655400
C2	0.01300000	4.92599900	0.06403798	0.00072710	0.07128453	0.39088380
C3	0.07499999	4.54500000	0.34087490	0.00408389	0.49803590	3.30719800
C4N	0.00600000	4.38599900	0.02631600	0.00035221	0.04574189	0.34872000
C4I	0.00700000	4.34599900	0.03042199	0.00042159	0.05336552	0.40683990
C5N	0.00000000	4.31000000	0.00000000	0.00000000	0.00000000	0.00000000
C5I	0.00000000	4.27999900	0.00000000	0.00000000	0.00000000	0.00000000
C6+	0.60000000	3.55099900	2.13059900	26.36245000	8.78749000	128.69990000
			3.73083	26.39254	10.1525	140.7299

Liquid Viscosity = 2.207 cp.

TABLE II-39

SURFACE TENSION

SAMPLING POINT = C
Cum. N2 Inj. = .70 p.v.

Experiment # 2

Comp.	(1) XiYi	(2) $Xi\rho_L/M_l$	(3) $Yi\rho_v/Mv$	(4) Parachor Pchi	(5) ((2)-(3))*(4))
N1	0.187688	0.0013	0.0092	41.000000	-0.325209
C1	0.007638	0.0004	0.0013	77.000000	-0.071327
C2	0.000130	0.0001	0.0001	108.000000	-0.004484
C3	0.003375	0.0004	0.0005	150.300000	-0.014245
C4N	0.000012	0.0000	0.0000	190.000000	0.002026
C4I	0.000014	0.0000	0.0000	181.500000	0.002948
C5N	0.000000	0.0000	0.0000	232.000000	0.000000
C5I	0.000000	0.0000	0.0000	225.000000	0.000000
C6+	0.010800	0.0033	0.0002	349.000000	1.096603
					0.68631

Surface Tension = .22186 Dines/ cm

TABLE H-40

GAS DENSITY

SAMPLING POINT = A

Cum. N2 Inj. = .22 p.v. Experiment # 3

Comp.	Yi	MWi	YMWi	YiTci	YiPci
N1	0.75999990	28.016	21.2922	172.5200	374.071700
C1	0.13800000	16.068	2.2174	47.3616	92.887810
C2	0.04900000	30.068	1.4733	26.9108	34.706690
C3	0.03000000	44.096	1.3229	19.9800	18.521980
C4N	0.00100000	58.120	0.0581	0.7653	0.550700
C4I	0.00800000	58.120	0.4650	5.8776	4.232801
C5N	0.00200000	72.124	0.1442	1.6912	0.979000
C5I	0.00100000	72.124	0.0721	0.8298	0.483000
C6+	0.01800000	128.000	2.3040	19.3140	6.011999

SUMMATION Y(I)TC(I) = 295.2495

SUMMATION PC(I)Y(I) = 532.4448

SUMMATION Y(I)M(I) = 29.3491

Gas Density = 20.894 Lb/Cuft

TABLE H-41

LIQUID DENSITY

SAMPLING POINT = A

Cum. N2 Inj. = .22 p.v. Experiment # 3

Comp.	Xi	MWi	XiMWi	Sp. Volume Vi, Cuft/Lb	XiMWiVi
N2	0.26069990	28.01600000	7.31217600	0.01980000	0.14478100
C1	0.08099997	16.06799000	1.30150600	0.05350000	0.06963056
C2	0.06100000	30.06799000	1.83414700	0.04300000	0.07886833
C3	0.05100000	44.09599000	2.24889400	0.03160000	0.07106507
C4N	0.00200000	58.11999000	0.11623990	0.02750000	0.00319660
C4I	0.02000000	58.11999000	1.16239900	0.02700000	0.03138478
C5N	0.00500000	72.12399000	0.36061980	0.02540000	0.00915974
C5I	0.00500000	72.12399000	0.36061980	0.02500000	0.00901549
C6+	0.51399990	214.50000000	110.25290000	0.01976000	2.17859800
			124.9496		2.5957

Stock Tank Density = 48.137 Lb/Cuft

Density at Current Conditions = 49.317 Lb/Cuft

TABLE H-42

GAS VISCOSITY

SAMPLING POINT = A

Cum. N2 Inj. = .22 p.v. Experiment # 3

Comp.	Yi	MWi	$Y_iMW_i^{1/2}$	$U_i^*Y_iM_{wi}^{1/2}$
N2	0.75999990	28.01600000	4.02269000	0.07079929
C1	0.13800000	16.06799000	0.55317150	0.00597425
C2	0.04900000	30.06799000	0.26868790	0.00274062
C3	0.03000000	44.09599000	0.19921430	0.00163356
C4N	0.00100000	58.11999000	0.00762364	0.00005870
C4I	0.00800000	58.11999000	0.06098918	0.00046181
C5N	0.00200000	72.12399000	0.01698517	0.00011040
C5I	0.00100000	72.12399000	0.00849258	0.00005690
C6+	0.01800000	128.00000000	0.20364670	0.00101823
			5.34150	0.08287

Mixture Atmospheric Viscosity = 0.0155 cp

Mixture Viscosity at Current Conditions= 0.02519 cp.

TABLE H-43

LIQUID VISCOSITY

SAMPLING POINT = A

Cum. N2 Inj. = .22 p. v.

Experiment # 3

Comp	Xi	Critical Volume Vci, gm/cm^3	XiVci	XiUiMWi$^{1/2}$	XiMWi$^{1/2}$	XiMWi
N2	0.26099990	3.12500000	0.81562460	0.02431397	1.38147600	7.31217600
C1	0.08099997	6.17300000	0.50001280	0.00350663	0.32468740	1.30150600
C2	0.06100000	4.92599900	0.30048590	0.00341179	0.33448910	1.83414700
C3	0.05100000	4.54500000	0.23179490	0.00277705	0.33866440	2.24889400
C4N	0.00200000	4.38599900	0.00877200	0.00011740	0.01524729	0.11623990
C4I	0.02000000	4.34599500	0.08691996	0.00120454	0.15247290	1.16239900
C5N	0.00500000	4.31000000	0.02155000	0.00027601	0.04246291	0.36061980
C5I	0.00500000	4.27999900	0.02139999	0.00028450	0.04246291	0.36061980
C6+	0.51399990	3.55099900	1.82521300	22.58384000	7.52795000	110.25290000
			3.84177	22.619	10.1599	124.9495

Liquid Viscosity = 2.073 cp.

TABLE H-44

SURFACE TENSION

SAMPLING POINT = A

Cum. N2 Inj. = .22 p.v. Experiment # 3

Comp.	(1) XiYi	(2) $Xi\rho_L/M_l$	(3) $Yi\rho_V/Mv$	(4) Parachor Pchi	(5) ((2)-(3))*(4))
N1	0.198360	0.0016	0.0087	41.000000	-0.289325
C1	0.011178	0.0005	0.0016	77.000000	-0.082694
C2	0.002989	0.0004	0.0006	108.000000	-0.019696
C3	0.001530	0.0003	0.0003	150.300000	-0.004118
C4N	0.000002	0.0000	0.0000	190.000000	0.000178
C4I	0.000160	0.0001	0.0001	181.500000	0.005843
C5N	0.000010	0.0000	0.0000	232.000000	0.001867
C5I	0.000005	0.0000	0.0000	225.000000	0.004377
C6+	0.009252	0.0032	0.0002	349.000000	1.035412
					0.65184

Surface Tension = 0.1805 Dynes/cm

TABLE H-45

GAS DENSITY

SAMPLING POINT = B

Cum. N2 Inj. = .35 p.v.

Experiment # 3

Comp.	Yi	MWi	YiMWi	YiTci	YiPci
N1	0.26999990	28.016	7.5643	61.2900	132.893900
C1	0.44800000	16.068	7.1955	153.7536	301.546800
C2	0.09899998	30.068	2.9767	54.3708	70.121670
C3	0.07860001	44.096	3.4395	51.9480	48.157190
C4N	0.00800000	58.120	0.4650	6.1224	4.406400
C4I	0.00600000	58.120	0.3487	4.4002	3.174601
C5N	0.01200000	72.124	0.8655	10.1472	5.873999
C5I	0.00800000	72.124	0.5770	6.6384	3.064000
C6+	0.07099990	128.000	9.0880	76.1830	23.713980

SUMMATION Y(I)TC(I) = 424.8606

SUMMATION PC(I)Y(I) = 593.7527

SUMMATION Y(I)M(I) = 32.5231

Gas Density = 23.1544 Lb/Cuft

TABLE B-46

LIQUID DENSITY

SAMPLING POINT = B

Cum. N2 Inj. = .35 p.v. Experiment # 3

Comp.	Xi	MWi	XiMWi	Sp. Volume Vci, Cuft/Lb	XiMWiVci
N1	0.07999998	28.01600000	2.24127900	0.01900000	0.04437733
C1	0.27799990	16.06799000	4.46690100	0.05350000	0.23097920
C2	0.11799990	30.06799008	3.54802200	0.04300000	0.15256490
C3	0.13400008	44.09599000	5.90006300	0.03160000	0.18672000
C4N	0.01900000	58.11999000	1.10427900	0.02750000	0.03036760
C4I	0.01600000	58.11999000	0.92991980	0.02700000	0.02510783
C5N	0.04400000	72.12399000	3.17345500	0.02540000	0.08060875
C5I	0.03200000	72.12399000	2.30798700	0.02500000	0.05769917
C6+	0.27799990	214.50080000	59.63099000	0.01976000	1.17830800
			83.3116		1.9947

Stock Tank Density = 41.7658 Lb/Cuft

Density at Current Conditions = 42.865 Lb/Cuft

TABLE H-47
GAS VISCOSITY

SAMPLING POINT = B
Cum. N2 Injection = .35 p.v. Experiment # 3

Comp.	Yi	MWi	$Y_iMW_i^{1/2}$	$U_i^*Y_iMW_i^{1/2}$
N2	0.26999990	28.01600000	1.42911300	0.02515240
C1	0.44800000	16.06799000	1.79588300	0.01939467
C2	0.09899998	30.06799000	0.54285930	0.00553716
C3	0.07800001	44.09599000	0.51795750	0.00424725
C4N	0.00800000	58.11999000	0.06098918	0.00046962
C4I	0.00600000	58.11959000	0.04574189	0.00036136
C5N	0.01200000	72.12399000	0.10191090	0.00066242
C5I	0.00800000	72.12399000	0.06794065	0.00046520
C6+	0.07099998	128.00000000	0.60327300	0.00401636
			5.36558	0.06030

Mixture Atmospheric Viscosity $= U^* = 0.0112$ cp.
Mixture Viscosity at Current Conditions $= U = 0.0169$ cp.

TABLE H-48

LIQUID VISCOSITY

SAMPLING POINT = B
Cum. N2 Inj.= .35 p.v.

Experiment # 3

Comp.	Xi	Vci, Cm/cm^3	XiVci	XiUiMWi$^{1/2}$	XiMWi$^{1/2}$	XiMWi
N1	0.07999998	3.12500000	0.24999990	0.00745256	0.42344100	2.24127900
C1	0.27799990	6.17300000	1.71609400	0.01203509	1.11435900	4.46690100
C2	0.11799990	4.92599900	0.58126770	0.00659985	0.64704440	3.54802200
C3	0.13400000	4.54500000	0.60903000	0.00729656	0.88982440	5.90886300
C4N	0.01900000	4.38599900	0.08333397	0.00111534	0.14484920	1.10427900
C4I	0.01600000	4.34599900	0.06953597	0.00096363	0.12197820	0.92991980
C5N	0.04400000	4.31000000	0.18963990	0.00242888	0.37367360	3.17345500
C5I	0.03200000	4.27999900	0.13695990	0.00182081	0.27176260	2.30796700
C6+	0.27799990	3.55099900	0.98717780	12.21461000	4.07153700	59.63099000
			4.62303	12.2543	8.0585	83.31164

Liquid Viscosity = 1.368 cp.

TABLE II-49

SURFACE TENSION

SAMPLING POINT = B
Cum. N2 Inj. = .35 p.v.

Experiment # 3

Comp.	(1) X_iY_i	(2) $X_i \rho_L/M_l$	(3) $Y_i \rho_V/M_v$	(4) Parachor P_{chi}	(5) ((2)-(3))*(4))
N1	0.021600	0.0006	0.0031	41.000000	-0.099907
C1	0.124544	0.0022	0.0051	77.000000	-0.221506
C2	0.011682	0.0009	0.0011	108.000000	-0.019595
C3	0.010452	0.0011	0.0009	150.300000	0.028039
C4N	0.000152	0.0002	0.0001	190.000000	0.011656
C4I	0.000096	0.0001	0.0001	181.500000	0.010901
C5N	0.000520	0.0004	0.0001	232.000000	0.050227
C5I	0.000256	0.0003	0.0001	225.000000	0.037293
C6+	0.019738	0.0022	0.0008	349.000000	0.496558
					0.29366

Surface Tension = 0.07437 Dynes /cm

APPENDIX "I"

LISTING AND RESULTS OF "SAS" COMPUTER PROGRAM FOR MULTIPLE REGRESSION ANALYSIS

```
1                                   S T A T I S T I C A L   A N A L Y S I S   S Y S T E M

NOTE: THE JOB SLCAL HAS BEEN RUN UNDER RELEASE 79.6 OF SAS AT THE UNIVERSITY OF OKLAHOMA (00646).

NOTE: SAS OPTIONS SPECIFIED ARE:
       SORT=4


1            DATA;
2            INPUT T P GOR REC;
3            CARDS;

NOTE: DATA SET WORK.DATA1 HAS 6 OBSERVATIONS AND 4 VARIABLES. 529 OBS/TRK.
NOTE: THE DATA STATEMENT USED 0.04 SECONDS AND 60K.

10           PROC GLM;
11           MODEL REC=T GOR;

NOTE: THE PROCEDURE GLM USED 0.14 SECONDS AND 198K AND PRINTED PAGE 1.

12           PROC PRINT;

NOTE: THE PROCEDURE PRINT USED 0.10 SECONDS AND 120K AND PRINTED PAGE 2.

13           PROC GPLOT;
14           PLOT REC*T;

NOTE: THE PROCEDURE GPLOT USED 0.32 SECONDS AND 294K.

NOTE: SAS USED 294K MEMORY.

NOTE: SAS INSTITUTE INC.
      SAS CIRCLE
      BOX 8000
      CARY, N.C. 27511-8000
```

S T A T I S T I C A L A N A L Y S I S S Y S T E M

GENERAL LINEAR MODELS PROCEDURE

DEPENDENT VARIABLE: REC

SOURCE	DF	SUM OF SQUARES	MEAN SQUARE	F VALUE	PR > F	R-SQUARE	C.V.
MODEL	2	0.02866646	0.01433323	181.91	0.0007	0.991822	1.1591
ERROR	3	0.00023638	0.00007879		STD DEV		REC MEAN
CORRECTED TOTAL	5	0.02890283			0.00887652		0.76583333

SOURCE	DF	TYPE I SS	F VALUE	PR > F	DF	TYPE IV SS	F VALUE	PR > F
T	1	0.00007271	0.92	0.4076	1	0.00092922	11.79	0.0414
GOR	1	0.02859374	362.90	0.0003	1	0.02859374	362.90	0.0003

PARAMETER	ESTIMATE	T FOR H0: PARAMETER=0	PR > |T|	STD ERROR OF ESTIMATE
INTERCEPT	0.54467756	30.72	0.0001	0.01773170
T	0.00053705	3.43	0.0414	0.00015639
GOR	0.00041454	19.05	0.0003	0.00002176